Spring 2020

Theraputic Strategies for Altering the Trajectory of Neurocognitive Impairments in HIV-1 Associated Neurocognitive Disorders in the Post-Cart Era

Kristen Addie McLaurin

THERAPUTIC STRATEGIES FOR ALTERING THE TRAJECTORY OF NEUROCOGNITIVE IMPAIRMENTS IN HIV-1 ASSOCIATED NEUROCOGNITIVE DISORDERS IN THE POST-CART ERA

By:

Kristen Addie McLaurin

Bachelor of Arts
Winthrop University, 2014

Master of Arts
University of South Carolina, 2016

Submitted in Partial Fulfillment of the Requirements

For the Degree of Doctor of Philosophy in

Experimental Psychology

College of Arts and Sciences

University of South Carolina

2020

Accepted by:

Charles F. Mactutus, Major Professor

Rosemarie M. Booze, Committee Member

Amanda J. Fairchild, Committee Member

Edsel A. Pena, Committee Member

Cheryl L. Addy, Vice Provost and Dean of the Graduate School

DEDICATION

To my parents: Thank you for always encouraging me to dream big, reach for the stars, and pursue my passion. Thank you for always reminding me to persevere, no matter what obstacles stood in my way. But most importantly, thank you for your endless love and support.

ACKNOWLEDGEMENTS

I sincerely thank my mentor, Dr. Charles F. Mactutus, for his encouragement, commitment and support throughout my graduate career. You have modeled the attributes necessary to pursue high caliber research, and have always reminded me to always seek the truth and ask meaningful questions. I appreciate the countless spectacular opportunities for growth as both a scientist and an individual; opportunities which have been vital to helping me achieve my goals. Thank you for believing in me, even when I didn't believe in myself.

I would also like to thank Dr. Rosemarie M. Booze for her mentorship and dedication to providing opportunities to expand and deepen my understanding of neuroanatomy. You exemplify the qualities of the female scientist I aspire to be. Additionally, I would like to thank Dr. Amanda J. Fairchild for her guidance and mentorship in advanced quantitative techniques. I am grateful for the opportunity to learn how to explore causal mechanisms and conduct simulations, pushing the bounardies of analytic techniques commonly used in neuroscience. I would also like to thank Dr. Edsel A. Pena for providing guidance as a member of my committees throughout my graduate studies. I also thank Dr. Steven Harrod for his valuable support. Thank you all for being influential role models for my career as a scientist.

Furthermore, I appreciate Dr. Hailong Li's commitment and considerable contribution to the neuroanatomical work presented herein. I would like to thank the undergraduate and post-baccalaureate trainees throughout the years, including Elizabeth

M. Balog, Anna K. Cook, Iris K. Dayton, Maddison R. Gassman, Abbie L. Lafond, Alexis F. League, and Victor A. Madormo. Additionally, I appreciate the support from members of the laboratory, past and present, including Dr. Landhing M. Moran, Dr. Sarah J. Bertrand, Adam R. Denton, Jessica M. Illenberger, and Alex Steiner.

This work was supported in part by grants from NIH (National Institute on Drug Abuse, DA013137; Eunice Kennedy Shriver National Institute of Child Health and Human Development, HD043680; National Institute of Mental Health, MH106392; National Institutes of Neurological Disorders and Stroke, NS100624) and the interdisciplinary research training program supported by the University of South Carolina Behavioral-Biomedical Interface Program.

ABSTRACT

The marked increase in life expectancy for individuals with human immunodeficiency virus type 1 (HIV-1), following the great success of combination antiretroviral therapy (cART), necessitates an investigation of the progression of HIV-1 associated neurocognitive disorders (HAND), and associated neural mechanisms, across the functional lifespan. Furthermore, given the persistence of HAND in the post-cART era, there remains a critical need to develop adjunctive therapeutics targeting the neural mechanisms underlying HAND. Thus, the guiding hypothesis for the present study was threefold. First, that there will be a differential progression of NCI in HIV-1 Tg and control animals. Second, that synaptodendritic dysfunction will mechanistically underlie NCI and progress throughout the early lifespan. Third, that the altered developmental trajectory of NCI, as a function of the HIV-1 transgene, will be restored with SE, targeting synaptodendritic dysfunction. Neurocognitive and neuroanatomical assessments were utilized to critically test these hypotheses.

The HIV-1 transgenic (Tg) rat, resembling HIV-1 seropositive individuals on lifelong cART, exhibits age-related progressive neurocognitive impairments in the absence of sensory or motor system deficits and comorbidities. Independent of biological sex, the HIV-1 Tg rat exhibits a differential progression of long-term episodic memory, temporal processing, stimulus-reinforcement learning, sustained attention, and flexibility and inhibition. Synaptic dysfunction in pyramidal neurons from layers II-III of the medial

prefrontal cortex (mPFC) were characterized by alterations in dendritic branching complexity, synaptic connectivity and dendritic spine morphology.

Critically testing the therapeutic efficacy of SE in the HIV-1 Tg rat revealed an innovative therapeutic approach for the prevention of NCI in HAND; a therapeutic that, at least partially, restores the developmental trajectory of neurocognitive function. Mechanistically, SE remodels neuronal circuitry at the synaptic level, evidenced by profound long-term modifications in neuronal morphology and dendritic spines in pyramidal neurons from layers II-III of the mPFC.

A longitudinal experimental design was subsequently utilized to assess the progression of synaptic function from postnatal day (PD) 30 to PD 180. Prominent developmental alterations in regressive (i.e., pruning) processes, as well as synaptic function, were observed, independent of biological sex, in pyramidal neurons from layers II-III of the mPFC in the HIV-1 Tg rat, supporting a key neural mechanism underlying HAND. Taken together, the present studies have defined HAND as a neurodegenerative disease characterized by age-related, progressive neurocognitive impairments and synaptic dysfunction; a disease which can be modified by therapeutics (i.e., SE) that mechanistically target synaptic dysfunction.

TABLE OF CONTENTS

LIST OF FIGURES

LIST OF ABBREVIATIONS

AD..... Alzheimer's disease

ANOVA .....Analysis of Variance

ASR..... Auditory Startle Response

cART..... Combination Antiretroviral Therapy

CI.....Confidence Interval

CNS..... Central Nervous System

DA.....Dopamine

DAI .....Daidzein

DAT ..... Dopamine Transporter

DFA..... Discriminant Function Analysis

dlPFC .....Dorsolateral Prefrontal Cortex

ER ..... Estrogen Receptors

GABA ..... γ-aminobutyric Acid

Gap-PPI..... Gap Prepulse Inhibition

HAND .....HIV-1 Associated Neurocognitive Disorders

HIV-1 ..... Human Immunodeficiency Virus Type 1

IACUC .....Institutional Animal Care and Use Committee

IC.....Inferior Colliculus

ISI.....Interstimulus Interval

ITI .....Intertrial Interval

LC .....Locus Coeruleus

Levodopa.....L-DOPA

LGP .....Lateral Globus Pallidus

LQ ..... Liquiritigenin

MAO-A ..... Monoamine Oxidase A

mPCR..... Multiplex PCR

mPFC ..... Medial Prefrontal Cortex

MSN..... Medium Spiny Neurons

Nac .....Nucleus Accumbens

NAcc ..... Nucleus Accumbens Core Subregion

NCI..... Neurocognitive Impairments

NE ..... Norepinephrine

NIH ..... National Institutes of Health

oPFC ..... Orbital Prefrontal Cortex

PD ..... Postnatal Day

PET .....Positron Emission Tomography

PFC .....Prefrontal Cortex

PHE.....Progressive HIV-1 Encephalopathy

PHIV .....Pediatric HIV-1

PnC.....Pontine Reticular Nucleus

PPI.....Prepulse Inhibition

PPTg..... Pedunculopontine Tegmental Nucleus

PSD .....Postsynaptic Density

pTH ..... Phosphorylated Tyrosine Hydroxylase

PVP ..... Polyvinylpyrrolidone

SC..... Superior Colliculus

SE..... S-Equol

SEM .....Standard Error of the Mean

Tg .....Transgenic

VTA .....Ventral Tegmental Area

η_p^2.....Partial Eta Squared

CHAPTER 1

INTRODUCTION

HUMAN IMMUNODEFICIENCY VIRUS TYPE-1 (HIV-1)

HIV-1 remains a human health pandemic, afflicting approximately 37.9 million individuals worldwide (UNAIDS, 2019). The great success of combination antiretroviral therapy (cART) has dramatically increased the life expectancy for HIV-1 seropositive individuals, leading to an increased prevalence (i.e., 30-50%) of older individuals (> 50 years of age) living with HIV-1 (UNAIDS, 2013); a prevalence that is expected to reach approximately 73% by 2030 (Smit et al., 2015). In the post-cART era, milder forms of neurocognitive impairments (NCI) have become a hallmark of the disease, afflicting between 40-70% of HIV-1 seropositive individuals (Letendre et al., 2010; McArthur et al., 2010; Heaton et al., 2011). Cross-sectional studies have provided a wealth of knowledge on HIV-1 associated neurocognitive disorders (HAND), characterized by deficits in higher-order cognitive processes (e.g., attention, working memory, executive function: Cysique et al., 2004; Heaton et al., 2011). However, extrapolating cross-sectional findings to age-related disease progression is inferentially fraught (Kraemer, 2000), heralding an examination of the progression of HAND using a longitudinal experimental design. To date, however, there has been no extant *in vivo* biological system available to provide a truly longitudinal study of HAND.

BIOLOGICAL SYSTEMS TO MODEL NCI IN HIV-1

In a seminal paper, Reid et al. (2001) reported the development of the HIV-1 transgenic (Tg) rat, which contains a *gag-pol*-deleted HIV-1 provirus regulated by the viral promotor. The highest levels of transgene (located on chromosome 2 and 9) expression were observed in the lymph nodes, spleen, kidney, and thymus (Reid et al., 2001). Clinical manifestations, including neurological abnormalities (i.e., circling behavior, hind-limb

paralysis), skin lesions, cataract formation, and relatively early wasting (i.e, between 5 to 9 months of age) were also observed in the original derivation of the HIV-1 Tg rat (Reid et al., 2001).

The contemporary HIV-1 Tg phenotype, however, is a healthier derivation than those originally described. Similar growth rates (Peng et al., 2010; Moran et al., 2012; Moran et al., 2013a; Roscoe et al., 2014) and a longer lifespan (i.e., 50% of HIV-1 Tg rats survive through 21 months of age; Peng et al., 2010) have been reported in the current derivation of the HIV-1 Tg rat. Viral proteins are expressed in the non-infectious HIV-1 Tg rat constitutively throughout development (Peng et al., 2010; Abbondanzo & Chang, 2014), resembling HIV-1 seropositive individuals on cART. Cross-sectional studies have promoted the HIV-1 Tg rat as an advantageous model for NCI, reporting alterations in temporal processing (e.g., Moran et al., 2013a; McLaurin et al., 2017a; McLaurin et al., 2017b), sustained attention (e.g., Moran et al., 2014a), learning (Moran et al., 2014a; Vigorito et al., 2007), and memory (Repunte-Canonigo et al., 2014). The neural mechanisms underlying NCI in the HIV-1 Tg rat also support its utility as an advantageous model in the post-cART era, with reports of neurotransmitter alterations (e.g., Sinharay et al., 2017; Javadi-Paydar et al., 2017), synaptic dysfunction (e.g., Roscoe et al., 2014; McLaurin et al., 2018a) and neuroinflammation (e.g., Royal et al., 2012).

A longitudinal assessment of NCIs for the progression of HAND, and associated neural mechanisms, in the HIV-1 Tg rat, however, remains a critical knowledge gap. Understanding the progression of neurocognitive impairment, and the effect of biological sex in this progression, heralds an opportunity for the development of an advantageous

model of progressive NCI in HIV-1 and establishes fundamental groundwork for the development of neurorestorative treatments.

SELECTIVE ESTROGEN RECEPTOR BETA AGONISTS (SERBAs)

Estrogen receptors (ER), which belong to the nuclear receptor family of transcription factors, are classified into two primary subtypes, including ERα (Jensen, 1962), and ERβ (Kuiper et al., 1996). Although both ERα and ERβ bind to 17β-estradiol with high affinity (Kuiper et al., 1996) and share structural characteristics (e.g., near-identical DNA-binding domain (96%), Kuiper et al., 1996), significant differences in tissue distribution and biological effects have been observed (e.g., Kuiper et al., 1997). Specifically, ERα is predominant in reproductive organs (e.g., uterus, mammary glands), skeletal muscle and bone, playing a critical role in maintaining female reproductive functions (for review, Paterni et al., 2014). ERβ, however, is involved in mediating estradiol signaling in the immune and central nervous systems (for review, Paterni et al., 2014). Within the central nervous system, cells containing ERβ mRNA or immunoactivity are widely dispersed (e.g., Li et al., 1997; Shughrue et al., 1997; Zhang et al., 2002; Gonzalez et al., 2007), and observed in brain regions (e.g., prefrontal cortex, ventral tegmental area, hippocampus) commonly associated with HAND (e.g., Maki et al., 2009; Israel et al., 2019).

Phytoestrogens, which exhibit a higher affinity for ERβ than ERα (e.g., Kuiper et al., 1998; Mueller et al., 2004), are plant-derived compounds that are structurally similar to 17β-estradiol (Glazier & Bowman, 2001). Isoflavones, including genistein, daidzein (DAI), and glycitein, are one class of phytoestrogens commonly found in soy products (Murphy, 1982; Setchell, 1998). Equol is an active metabolite produced by gut microbiota

following the ingestion of the soy derived phytoestrogen DAI (Setchell et al., 1984). S-Equol (SE), the only enantiomer produced by humans (Setchell et al., 2005), exhibits neuroprotective effects via its selective affinity for ERβ (Setchell et al., 2005; Bertrand et al., 2015). Furthermore, when SE crosses the blood-brain-barrier it distributes most significantly to the prefrontal cortex (Lund et al., 2001); a brain region associated with higher-order cognitive functioning. Most critically, however, the translational relevance of SE is evidenced by its progression into clinical trials for Alzheimer's disease (AD; Ausio Pharmaceuticls; NCT03101085), another progressive, neurodegenerative disorder.

SE has been implicated as a potential adjunctive therapeutic for HAND in both *in vitro* (Bertrand et al., 2015) and *in vivo* (Moran et al., 2019; McLaurin et al., 2019a) studies. In primary neuronal cell cultures, pretreatment with SE prevented synapse loss induced by the HIV-1 viral protein, Tat (Bertrand et al., 2015). Precursors to SE, including daidzein (DAI) and liquiritigenin (LQ), which also selectively target ERβ (DAI: Casanova et al., 1999 ; LQ: Mersereau et al., 2008), similarly prevented Tat induced neuronal apoptosis (Adams et al., 2012) and restored synaptodendritic injury (Bertrand et al., 2014). Cross-sectional *in vivo* studies have further supported the utility of SE as a neuroprotective and/or neurorestorative therapeutic for HAND in ovariectomized HIV-1 Tg animals (Moran et al., 2019; McLaurin et al., 2019a). There remains, however, a critical need to utilize a longitudinal experimental design to assess whether SE is able to alter the trajectory of NCI and its mechanism of action.

EXPERIMENTAL QUESTIONS

The overarching aims of the present study are threefold. First, to establish the progression of NCI, and associated neural mechanisms, across the functional lifespan

(Chapters 2-4). Second, to assess the utility of SE as a therapeutic strategy to alter the trajectory of NCI in the post-cART era (Chapters 5-6). Third, to examine the progression of synaptic dysfunction using a longitudinal experimental design (Chapter 7).

The guiding hypothesis for the present study was threefold. First, that there will be a differential progression of NCI in HIV-1 Tg vs. control animals. Second, synaptodendritic dysfunction will mechanistically underlie NCI. Third, that the altered developmental trajectory of NCI, as a function of the HIV-1 transgene, will be restored with SE, targeting synaptodendritic dysfunction.

CHAPTER 2

PROGRESSION OF TEMPORAL PROCESSING DEFICITS IN THE HIV-1 TRANSGENIC RAT[1]

[1] KA McLaurin, RM Booze, CF Mactutus. 2016. *Scientific Reports.* 6: 32831. Reprinted here with permission of publisher.

INTRODUCTION

Despite the success of cART in diminishing the prevalence of progressive HIV-1 encephalopathy (PHE), high rates of chronic neurological impairment are still being reported in HIV-1 seropositive children (Franklin et al., 2005; Paramesparan, 2010; Smith & Wilkins, 2015; Crowell et al., 2014). Approximately 3.2 million children (≤15 years of age; Centers for Disease Control and Prevention, 2013) are currently living with HIV-1, however, neurocognitive deficits in HIV-1 seropositive children, including disease progression, are poorly understood (Crowell, 2014). The HIV-1 Tg rat may be used to model the effects of long-term HIV-1 viral exposure on the development and progression of chronic neurological deficits observed in children perinatally infected with HIV-1 (Vigorito et al., 2015). The HIV-1 Tg rat, originally developed by Reid *et al.,* (2001), is non-infectious, expresses 7 of the 9 HIV-1 genes, and exhibits many clinical phenotypes (i.e. cataracts, low body weight) seen in HIV-1 seropositive individuals on cART (Peng et al., 2010). Therefore, a longitudinal analysis of temporal processing deficits, a potential underlying dimension of neurocognitive impairment in HIV-1, may provide insight into the effect of long-term HIV-1 viral protein exposure on the development of chronic neurologic impairment in HIV-1 seropositive children.

Deficits in temporal processing, caused by HIV-1, may manifest prior to early symptoms of impairment in higher level cognitive processes (Castello et al., 1998; Fitting et al., 2008a; Minassian et al., 2013; Moran et al., 2013a). Temporal processing deficits are commonly assessed using translational experimental paradigms, including prepulse inhibition (PPI) of the auditory startle response (ASR; Hoffman & Searle, 1965; Ison & Hammond, 1971). PPI involves two stimuli: a punctate prestimulus or prepulse (i.e. a light

or a tone) and a startle stimulus (Hoffman & Ison, 1980). Presentation of a prepulse 30-500 msec prior to the startle stimulus, causes dramatic reductions in the ASR (Hoffman & Ison, 1980; Fitch et al., 2008). Specifically, the degree to which the ASR is inhibited by the prepulse is dependent upon the interstimulus interval (ISI), the time interval between the prepulse and the startle stimulus. Use of PPI of the ASR, a behavioral approach, may elucidate the underlying mechanisms of more complex neurological processes (Hoffman & Ison, 1980).

Alterations in temporal processing observed in the HIV-1 Tg rat have been observed in multiple preclinical models of HIV-1, as well as HIV-1 seropositive humans. Specifically, deficits in temporal processing have been observed in Sprague-Dawley rats stereotaxically injected with the HIV-1 viral proteins Tat and gp120. Neonatal (postnatal day (PD) 1) intrahippocampal Tat injections flattened the ISI function in auditory PPI, causing a shift in maximum peak inhibition (Fitting et al., 2006a; Fitting et al., 2008a). A shift in the maximal peak inhibition for auditory PPI was also reported in 9-month old male and female Sprague-Dawley rats neonatally (PD 1) injected with gp120 (Fitting et al., 2006b). Temporal processing deficits have also been observed in SIV and FIV positive animals (Huitron-Resendiz et al., 2004; Phipps et al., 2000; Prospero-Garcia, 1999; Raymond et al., 1998), as well as HIV-1 seropositive individuals meeting criteria for HAND (Minassian et al., 2013).

Analyses in the HIV-1 Tg rat have provided additional evidence that temporal processing deficits may be a potential underlying dimension of neurocognitive impairment in HIV-1. Cross-modal PPI was conducted in HIV-1 Tg and control rats between two and six months (Moran et al., 2013a). HIV-1 Tg animals, in comparison to control animals,

exhibited significant alterations in the development of temporal processing, evidenced by a relative insensitivity to the manipulation of ISI on both visual and auditory prepulse trials and a lack of perceptual sharpening with age (Moran et al., 2013a). The generalizability of temporal processing deficits in the HIV-1 Tg rat, assessed using cross-modal PPI, were extended to animals at a more advanced age (i.e., 9-10 months of age; McLaurin et al., 2016a). HIV-1 Tg animals exhibited a relative insensitivity to the manipulation of ISI in both auditory and visual PPI (McLaurin et al., 2016a). Consistent observations of temporal processing deficits regardless of the agent (i.e., single proteins, HIV, SIV, FIV, and the HIV-1 Tg rat) used to study neurocognitive deficits provide ample evidence for the critical importance of understanding the progression of these deficits using a longitudinal experimental design, as in the present study.

Lesioning (i.e., Leitner & Cohen, 1985) and electrical stimulation studies (i.e., Li et al., 1998; Li & Yeomans, 2000) suggest that PPI of the ASR is mediated through a well-defined serial circuit. Excitatory input from the auditory pathway relays information the inferior colliculus (IC), while input from the visual or tactile pathway relays information to the superior colliculus (SC). From the SC, sensory input subsequently activates the pedunculopontine tegmental nucleus (PPTg), triggering a cholinergic projection to the caudal pontine reticular nucleus (PnC) mediating PPI of the ASR (Fendt et al., 1994; Fendt et al., 2001; Koch et al., 1993; Koch & Schnitzler, 1997). Activation of the PnC is relayed to motor neurons causing a startle response. Additionally, previous studies have established the hierarchical regulation of PPI, commonly abbreviated as the "CSPP circuitry," which is comprised of both sequential and parallel neural connections (Koch et al., 1993; Koch & Schnitzler, 1997).

Gap prepulse inhibition (gap-PPI) is another translational experimental paradigm for sensorimotor 'gating' that may be used to study temporal processing deficits (Leitner et al., 1993). Specifically, in gap-PPI the absence of a background stimulus (relative to the presentation of an added stimulus) serves as the punctate prestimulus. Significant reductions in startle amplitude have been observed when a gap in background noise occurs between 30 and 200 msec prior to the startling stimulus (Ison et al., 1998). Analyses of gap-PPI in HIV-1 Tg rat at an advanced age (i.e. 9-10 months of age) revealed a differential sensitivity to the manipulation of ISI. Specifically, control animals exhibited maximal inhibition at the 50 msec ISI, while HIV-1 Tg animals displayed a rightward shift, to maximal inhibition at the 100 msec ISI (McLaurin et al., 2016a). Additionally, gap-PPI has been used as an innovative paradigm for studies of tinnitus in animals, including guinea pigs (Dehmel et al., 2012), mice (Ison et al., 1998) and rats (Turner et al., 2006; Turner & Parrish, 2008; Sun et al., 2014), providing proof-of concept for the utility of gap-PPI as a translational diagnostic tool for tinnitus in humans. Subsequently, the gap startle paradigm was employed in adults with tinnitus offering new insight into the underlying neural mechanisms involved in tinnitus (Fournier & Hebert, 2013). Use of the gap-PPI experimental paradigms in HIV-1 seropositive children, therefore, may not only serve as a screening tool for chronic neurological impairment in pediatric HIV-1, but may also offer insight into the underlying neural mechanisms implicated in HIV-1.

Modeling the progression of neurocognitive deficits in the HIV-1 Tg rat is fundamental to the advancement of our knowledge of pediatric HIV-1 as well as to the long-term viral protein exposure present in successful cART-treated individuals with HAND. Thus, the aims of the present study were threefold. First, using a longitudinal

experimental design, establish the progression of temporal processing deficits using the gap-PPI experimental paradigm in the HIV-1 Tg rat. All animals were tested at 30 day intervals beginning at PD 30. Second, to investigate the role of sex in the progression of temporal processing deficits in HIV-1; both male and female animals were integral to the experimental design. Thirdly, to assess the ability of gap-PPI to correctly classify animals in regard to their genotype based on measures of prepulse inhibition and temporal sensitivity. Progression of temporal processing deficits in the HIV-1 Tg rat affords a relatively untapped opportunity to increase our mechanistic understanding of the role of long-term exposure to HIV-1 viral proteins, such as seen in pediatric HIV-1 (PHIV), in the development of chronic neurological impairment, as well as suggest an innovative clinical diagnostic screening tool.

METHODS

Progression of temporal processing deficits in the HIV-1 Tg rat was assessed using a longitudinal analysis of gap-PPI. Alterations in the development of temporal processing were explored using a 2(genotype) x 2(sex) x 6(age) x 6(ISI) mixed factor design. A discriminant function analysis was conducted to determine the diagnostic accuracy, and potential translational relevance, of gap-PPI.

Animals

A longitudinal analysis of gap-PPI was conducted using intact Fischer (F344/N; Harlan Laboratories Inc., Indianapolis, IN) rats (Male HIV-1 Tg, *n*=26*;* Female HIV-1 Tg, *n*=22; Male Control, *n*=20; Female Control, *n*=19). Animals were tested for gap-PPI beginning at PD 30 and retested every thirty days at PD 60, PD 90, PD 120, PD 150, and PD 180. Animals were delivered to the facility between PD 7 and PD 9 over the course of

four months. All animals were housed with their biological dam until PD 21 when animals were weaned and separated by sex. Subsequently animals were pair- or group-housed with animals of the same sex throughout experimentation. Rodent food (Pro-Lab Rat, Mouse, Hamster Chow #3000) and water were provided *ad libitum* through 60 days of age. Subsequently, all animals were under food restriction (85% body weight) due to their participation in a subsequently conducted signal detection task.

Animals were maintained according to the National Institutes of Health (NIH) guidelines in AAALAC-accredited facilities. The targeted environmental conditions for the animal facility were 21° ± 2° C, 50% ± 10% relative humidity and a 12-h light:12-h dark cycle with lights on at 0700 h (EST). The Institutional Animal Care and Use Committee (IACUC) of the University of South Carolina approved the project protocol as consistent with federal assurance (# A3049-01).

Apparatus

The startle platform (SR-Lab Startle Reflex System, San Diego Instruments, Inc., San Diego, CA) was enclosed in a 10 cm-thick double-walled, 81×81×116-cm isolation cabinet (external dimensions) (Industrial Acoustic Company, INC., Bronx, NY), instead of the 1.9 cm thick ABS plastic or laminate cabinets offered with this system. Sound attenuation of 30dB (A) was provided in the isolation chamber relative to the external environment. An ambient sound level of 22dB (A) was presented in the chamber without any stimuli presented. The high-frequency loudspeaker of the SR-Lab system (Radio Shack model#40-1278B), mounted inside the chamber 30 cm above the Plexiglas animal test cylinder, delivered all auditory stimuli (frequency range of 5k-16k Hz). The animal's response to the auditory stimulus produced deflection of the test cylinder, which was

converted into analog signals by a piezoelectric accelerometer integral to the bottom of the cylinder. The response signals were digitized (12 bit A to D) and saved to a hard disk. Response sensitivities were calibrated using a SR-LAB Startle Calibration System. Sound levels were measured and calibrated with a sound level meter (Kjaer Bruel 2203) with the microphone placed inside the Plexiglas cylinder.

Behavioral Assessments

Gap-Prepulse Inhibition Test

Intact Fischer rats (Male HIV-1 Tg, *n*=26*;* Female HIV-1 Tg, *n*=22; Male Control, *n*=20; Female Control, *n*=19) were tested for gap-PPI of the ASR beginning at PD 30. A 20-min test session began with a 5-min acclimation period in the dark with 70 dB(A) background white noise, followed by six pulse-only ASR trials, used for habituation, with a 10s intertrial interval (ITI). Thirty-six trials were presented using 6-trial blocks interdigitated using a Latin Square experimental design. Animals were tested with a 20-msec gap in white noise preceding a startle stimulus presented at ISIs of 30, 50,100, and 200 msec. Two control trials, the 0 and 4000 msec ISI trials, were included to provide a reference ASR within gap-PPI. The startle stimulus intensity was 100 dB (A) (20 msec duration) measured inside the test cylinder. Mean peak ASR amplitude values were collected for analysis. All test sessions were conducted in the dark. Because it is well known that many stimulus parameters may influence the dependent measure of startle response amplitude, e.g., duration, intensity, frequency, etc., we choose (and held constant) stimulus parameters for robust prepulse inhibition, but that also would permit detection of increases or decreases in responding. We manipulated the fundamental factor that operationally defines prepulse inhibition, the ISI.

Statistical Analyses

Data were analyzed using analysis of variance (ANOVA) techniques (SPSS Statistics 20, IBM Corp., Somers, NY). Planned orthogonal contrasts The Greenhouse-Geisser *df* correction factor (Greenhouse & Geisser, 1959) and were used for potential violations of sphericity of within-subjects variables (Winer, 1971). Regression analyses and graphs were completed using GraphPad Prism 5 (GraphPad Software, Inc., La Jolla, CA). An alpha level of $p \leq 0.05$ was considered significant for all statistical tests.

The area of inflection of the ASR amplitude response curve, illustrated in Figure 2.1 (i.e., shaded gray area), was calculated for each animal at every testing session as a measure of prepulse inhibition. A three-way mixed factor ANOVA was performed on the mean area of peak inflection where genotype (HIV-1 Tg vs. control) and sex (male vs. female) served as the between-subjects factor. Age served as the within-subjects factor.

The ISI indexing the point of peak inflection for prepulse inhibition, as illustrated in Figure 2.1, was also determined for each animal at every testing session. Specifically, a five-way mixed-factor ANOVA was performed on mean peak ASR amplitude for the 0-4000 msec ISIs as a measure of temporal sensitivity. Genotype (HIV-1 Tg vs. control) and sex (male vs. female) served as the between-subjects factor, while age, ISI, and trial served as the within-subjects factors.

The diagnostic accuracy of gap-PPI, i.e., the ability of the observed measures in gap-PPI correctly identified animals in regard to their genotype (HIV-1 Tg vs. Control) was determined with a discriminant function analysis (DFA). Prepulse inhibition measurements (i.e., slope for the area of peak inflection, area of peak inflection at each test session) and temporal sensitivity (i.e., age at which a shift in maximum inhibition was

observed) were included in the analysis. Slope for the area of peak inflection was calculated for each animal using the best-fit polynominal function.

RESULTS

HIV-1 Tg rats exhibited a profound alteration in the progression of temporal processing assessed using prepulse inhibition.

The progression of PPI, assessed using mean area of the amplitude inflection, was altered in HIV-1 Tg animals in comparison to control animals (Figure 2.2). PPI for control animals was best fit using a first-order polynomial (R^2: 0.99). In contrast, the best fit for HIV-1 Tg animals was a one-phase association (R^2: 0.96). Control animals exhibited a significant development of temporal processing across age, while HIV-1 Tg animals failed to exhibit any significant progression of temporal processing after PD 90. The overall ANOVA on mean area of the amplitude inflection confirmed these observations, as revealed by a significant age x genotype interaction [$F(5,415)=6.3$, $p_{GG} \leq 0.001$, $\eta_p^2=0.07$] with a prominent linear component [$F(1,83)=19.0$, $p \leq 0.001$, $\eta_p^2=0.19$] as well as an age x sex interaction [$F(5,415) =2.6$, $p_{GG} \leq 0.034$, $\eta_p^2=0.03$], also with a prominent linear component [$F(1,83)=9.0$, $p \leq 0.001$, $\eta_p^2=0.10$]. Significant main effects of age [$F(5,415) =21.0$, $p_{GG} \leq 0.001$, $\eta_p^2=0.20$] and sex [$F(1, 83) =19.4$, $p \leq 0.001$, $\eta_p^2=0.19$] were also present.

Complementary results were obtained by conducting separate analyses of each genotype, illustrated in Figure 2.2. A first-order polynomial was the best fit for both male and female control animals (Male R^2: 0.99; Female R^2: 0.95), indicating an increase in PPI across age. However, there was a significant difference in the rate of increase in PPI [$F(1,230)=4.3$, $p_{GG} \leq 0.04$]. The rate of temporal processing development was significantly greater in male control animals (β_1: 2820) in comparison to female control animals (β_1:

1824). The overall ANOVA for control animals confirmed these observations, as revealed by significant main effects of age [$F(5,185)=20.8$, $p_{GG}\leq 0.001$, $\eta_p^2=0.36$] and sex [$F(1,37)=10.6$, $p\leq 0.001$, $\eta_p^2=0.22$]. In contrast, a one-phase association appeared to be the best fit function for both male and female HIV-1 Tg animals (Male R^2: 0.92; Female R^2: 0.82). No significant differences in PPI were observed on PD 30. However, at PD 60 and all subsequent test dates, male HIV-1 Tg animals exhibited significantly greater PPI in comparison to female HIV-1 Tg animals. The overall ANOVA for HIV-1 Tg animals confirmed these observations, as revealed by significant main effects of age [$F(5,230)=5.8$, $p_{GG}\leq 0.001$, $\eta_p^2=0.11$] and sex [$F(1,46)=11.4$, $p\leq 0.002$, $\eta_p^2=0.20$]. Female HIV-1 Tg animals, therefore, may be more susceptible to the consequences of long-term HIV-1 viral protein exposure in comparison to male HIV-1 Tg animals. However, regardless of sex, PPI provided little, if any, compelling evidence for normal development of temporal processing in the HIV-1 Tg rat.

HIV-1 Tg animals displayed a differential sensitivity to the manipulation of ISI.

HIV-1 Tg animals displayed a differential sensitivity to the manipulation of ISI, as illustrated in Figure 2.3. A shift in maximal inhibition (from 30 msec to 50 msec) occurred in both the HIV-1 Tg and control animals; however, the shift occurred significantly earlier in the HIV-1 Tg animals. In the control group, a first-order polynomial (R^2: 0.97) suggested peak inhibition was observed at the 30 msec ISI during the first three test periods (PD 30, PD 60 and PD 90), but that rightward shift to the 50 msec ISI occurred during the latter three test periods (PD 120, PD 150 and PD 180). In contrast, the HIV-1 Tg group, well described with a one-phase association (R^2: 0.99), displayed peak inhibition at 30 msec during the first testing period (PD 30), but displayed a rightward shift during all later testing

periods. The overall ANOVA revealed significant three ways interactions: genotype x age x ISI interaction [$F(25,2050)=11.1$, $p_{GG}\leq 0.001$, $\eta_p^2=0.12$] and genotype x age x sex interaction [$F(5,410)=4.5$, $p_{GG}\leq 0.001$, $\eta_p^2=0.05$], and an age x ISI x sex interaction [$F(25,2050)=4.4$, $p_{GG}\leq 0.001$, $\eta_p^2=0.05$]. Second order interactions were also confirmed including: a genotype x age interaction [$F(5,410)=54.4$, $p_{GG}\leq 0.001$, $\eta_p^2=0.40$], an age x ISI interaction [$F(25,2050)=26.3$, $p_{GG}\leq 0.01$, $\eta_p^2=0.24$], an age x sex interaction [$F(5,410)=10.2$, $p_{GG}\leq 0.001$, $\eta_p^2=0.11$], an ISI x genotype interaction [$F(5,410)=7.1$, $p_{GG}\leq 0.001$, $\eta_p^2=0.08$] and an ISI x sex interaction [$F(5,410)=23.3$, $p_{GG}\leq 0.001$, $\eta_p^2=0.22$]. Significant main effects of age [$F(5,410)=68.3$, $p_{GG}\leq 0.001$, $\eta_p^2=0.45$], ISI [$F(5,410)=164.9$, $p_{GG}\leq 0.001$, $\eta_p^2=0.67$], genotype [$F(1,82)=100.7$, $p\leq 0.001$, $\eta_p^2=0.55$], and sex [$F(1,82)=40.6$, $p\leq 0.001$, $\eta_p^2=0.33$] were also noted. Clearly, there was a significantly greater effect of age on the variation of response amplitude by ISI for HIV-1 Tg animals in comparison to control animals.

Analyses of each genotype were conducted to further examine differences in the progression of temporal processing (Figure 2.3). A first-order polynomial was a well-described fit for male control animals (R^2: 0.98), while a one-phase association provided a well-described fit for female control animals (R^2: 0.99). Specifically, female control animals exhibited a shift in maximal inhibition from 30 msec to 50 msec significantly earlier than male control animals. The overall ANOVA for control animals revealed an age x ISI x sex interaction [$F(25,900)=2.9$, $p_{GG}\leq 0.001$, $\eta_p^2=0.08$], an age x ISI interaction [$F(25,900)=23.3$, $p_{GG}\leq 0.001$, $\eta_p^2=.39$], an age x sex interaction [$F(5,180)=7.2$, $p_{GG}\leq 0.001$, $\eta_p^2=0.17$], and an ISI x sex interaction [$F(5,180)=12.6$, $p_{GG}\leq 0.001$, $\eta_p^2=0.26$]. A significant main effect of age [$F(5,180)=62.8$, $p_{GG}\leq 0.001$, $\eta_p^2=0.64$], ISI [$F(5,180)=111.4$,

$p_{GG} \leq 0.001$, $\eta_p^2 = 0.76$], and sex [$F(1,36) = 16.0$, $p \leq 0.001$, $\eta_p^2 = 0.31$] were also revealed. In contrast, a one-phase association provided a well-described fit for both female and male HIV-1 Tg animals (R^2: 0.99) suggesting that the shift in maximal inhibition from 30 msec to 50 msec was not dependent upon sex in the presence of the HIV-1 transgene. The overall ANOVA for the HIV-1 Tg group did not reveal a significant age x sex interaction [$F(5,230) = 1.7$, $p_{GG} \leq 0.146$, $\eta_p^2 = 0.04$], nor a main effect of age [$F(5,230) = 1.4$, $p_{GG} \leq 0.246$, $\eta_p^2 = 0.03$], confirming these observations. Most notably, therefore, regardless of sex, HIV-1 Tg animals exhibited a significantly earlier shift in maximal inhibition, indicating a differential sensitivity to the manipulation of ISI.

Longitudinal gap-PPI can accurately diagnose the presence of the HIV-1 Transgene.

Progression of temporal processing, assessed using gap-PPI, was further analyzed using a DFA to determine the potential utility of gap-PPI as a diagnostic screening tool for chronic neurological impairment associated with the HIV-1 transgene. Transgene presence was best predicted using measures of PPI (i.e., mean area of the peak inflection) and measures of temporal sensitivity (i.e., cumulative frequency), as illustrated in Figure 2.4. The stepwise DFA selected four variables (slope of area of the peak inflection, area of the peak inflection at PD 180 and cumulative frequency at PD 60 and PD 180) that maximally separated the HIV-1 Tg and control animals (canonical correlation of 0.80). Animals were correctly diagnosed for the presence of the HIV-1 transgene with 90.8% accuracy (F approximation of Wilks' λ of 0.368, $F(4, 82) = 35.2$, $p \leq 0.001$).

DISCUSSION

Prominent temporal processing deficits in the HIV-1 Tg rat were detected using the gap-PPI experimental paradigm. The developmental trajectory of PPI, assessed using the

gap-PPI experimental paradigm, was altered in the HIV-1 Tg rat relative to control animals, regardless of sex, from 30 to 180 days of age. Additionally, female HIV-1 Tg animals exhibited significantly less PPI in comparison to male HIV-1 Tg animals. A differential sensitivity to the manipulation of ISI was also observed in the HIV-1 Tg rat, regardless of sex. Animals were correctly classified (90.8%) for the presence of the genotype (HIV-1 Tg or control) using measures of PPI and temporal sensitivity. Temporal processing deficits observed in the HIV-1 Tg rat resemble those reported in HIV-1 seropositive individuals, providing insight into the effect of long-term exposure to HIV-1 viral proteins and the potential for development of a diagnostic screening tool for chronic neurological impairment.

HIV-1 Tg rats displayed a differential development of PPI, assessed using the gap-PPI experimental paradigm, in a longitudinal experimental design. A one-phase association was the best fit for HIV-1 Tg animals, while a first-order polynomial was the best fit for control animals. No statistical differences in temporal processing between the HIV-1 Tg and control groups were observed at PD 30. However, significant differences in the progression of temporal processing, assessed using PPI, were exhibited at subsequent testing sessions. Specifically, control animals displayed a linear increase in PPI from PD 30 to PD 180. In contrast, HIV-1 Tg animals only exhibited a significant increase in PPI from PD 30 to PD 90, after which point a plateau in temporal processing was observed. To our knowledge, the present study is the first to investigate the progression of temporal processing deficits using gap-PPI in the HIV-1 Tg rat, which is vital for the development of an extant model for HIV-1.

Sex differences in the progression of temporal processing deficits, assessed using PPI, provide fundamental information for our understanding of the long-term effect of HIV-1 viral protein exposure in PHIV. Both female HIV-1 Tg and control animals displayed significantly less PPI, in comparison to male HIV-1 Tg and control animals, consistent with previous observations in healthy individuals (Abel et al., 1998; Ornitz et al., 1991; Kumari et al., 2004). Regardless of sex, however, HIV-1 Tg animals exhibited significant alterations in temporal processing, assessed using PPI; alterations which were more profound in female HIV-1 Tg animals in comparison to male HIV-1 Tg animals. Sex differences in the HIV-1 Tg rat expand on differences observed in HIV-1 seropositive individuals. Recent studies have reported significantly greater neurological impairment in HIV-1 seropositive women, in comparison to HIV-1 seropositive women (Royal et al., 2016; Hestad et al., 2012). The effect of sex on the progression of neurocognitive impairments in HIV-1 seropositive individuals has been relatively understudied; the need for longitudinal study is critical (Maki et al., 2015).

A differential sensitivity to the manipulation of ISI was evidenced by a shift in the point of maximal inhibition. Both HIV-1 Tg and control animals displayed maximal inhibition at the 30 msec ISI on PD 30. However, HIV-1 Tg animals display a rightward shift in peak inhibition, from 30 msec to 50 msec, at PD 60. Notably, no sex differences were observed in the HIV-1 Tg animals. The point of maximal peak inhibition in control animals shifts from 30 msec to 50 msec at PD 120. Female control animals exhibited a significantly earlier shift in maximal inhibition in comparison to male control animals. Results of differential sensitivity to the manipulation of ISI in the present study extend those previously reported in the HIV-1 Tg rat (Moran et al., 2013a; McLaurin et al., 2016a)

and Sprague-Dawley rats stereotaxically injected with the HIV-1 viral proteins (Fitting et al., 2006a; Fitting et al., 2006b; Fitting et al., 2008a).

Temporal processing deficits observed using gap-PPI in the HIV-1 Tg rat may provide a novel screening tool for the diagnosis of chronic neurological impairment in PHIV. A DFA, used to evaluate the potential utility of gap-PPI, correctly identified animals in regards to their genotype (HIV-1 Tg vs. control) with 90.8% accuracy. The presence of the HIV-1 transgene was best predicted using four variables as assessments of PPI (i.e., slope of area of the peak inflection, area of the peak inflection at PD 180) and temporal sensitivity (i.e., cumulative frequency at PD 60 and PD 180). Gap-PPI was previously implicated as a novel screening tool for the diagnosis of tinnitus. Specifically, rats with noise over-expression induced tinnitus (Dehmel et al., 2012) or salicylate-induced tinnitus (Sun et al., 2014) exhibited little to no inhibition in gap-PPI studies. The gap-PPI experimental paradigm was subsequently employed in adults with tinnitus offering new insight into the neural mechanisms of tinnitus (Fournier & Hebert, 2013). Use of the gap-PPI experimental paradigms in HIV-1 seropositive humans, therefore, may not only serve as a screening tool for chronic neurological impairment in PHIV, but may also offer insight into the underlying neural mechanisms implicated in HAND.

Clinical and preclinical studies have implicated disruptions in the development of the dopamine (DA) system as an underlying factor in neurocognitive impairments observed in pediatric HIV-1 (Webb et al., 2010; Moran et al., 2013b; Lee et al., 2014; Moran et al., 2014a; Fitting et al., 2015). A case study of five HIV-1 seropositive children observed improved motor function and activity with administration of levodopa (L-DOPA), a DA agonist (Mintz, 1996). In addition, pharmacological assessments have previously been

used to examine alterations in the midbrain DAergic system in the HIV-1 Tg rat (Webb et al., 2010; Moran et al., 2013b). DAergic system dysfunction, assessed using Western blotting, was evidenced by alterations in phosphorylated tyrosine hydroxylase (pTH), dopamine transporter (DAT) mRNA, and/or monoamine oxidase A (MAO-A; Webb et al., 2010; Moran et al., 2013b). In addition, young HIV-1 Tg rats exhibit deficits in $D_{2/3}$ receptors in the dorsal striatum, assessed using [^{18}F]fallypride positron emission tomography (PET; Lee et al., 2014).

DA system dysfunction may underlie temporal processing deficits observed in the HIV-1 Tg rat, as evidenced by previous behavioral and pharmacological studies (Geyer et al., 2001; Moran et al., 2009; Zhang et al., 2000). Administration of direct (i.e., apomorphine) and indirect DA agonists (i.e., amphetamine) have been used to manipulate DA, subsequently disrupting PPI (Geyer et al., 2001). We have previously observed an insensitivity to the manipulation of ISI, assessed using crossmodal PPI, in rats administered apomorphine; results that are comparable to those observed in the HIV-1 Tg rat (Moran et al., 2009) and schizophrenic patients (Adler et al., 1982; Braff et al., 1978). Although temporal processing deficits observed in the HIV-1 Tg rat may be mediated by multiple neural systems, HIV-1 infection often affects DA system function and is associated with subsequent cognitive deficits (Di Rocco et al., 2000; Wang et al., 2004).

The potential role of oxidative stress and neuroinflammation as well as synaptodendritic injury are other potential mechanisms contributing to neurocognitive impairment in the HIV-1 Tg rat. Prior research has reported evidence of chronic immune activation in the brains of the HIV-1 Tg rat (Rao et al., 2011; Royal et al., 2012). Thus, in the absence of viral replication, a chronic, mild, neuroinflammatory microenvironment

exists in the HIV-1 Tg animals. Interestingly, the DAergic system appears to be particularly sensitive to neuroinflammatory degenerative processes (Tansey et al., 2010; Gao et al., 2008). Decifits in synaptic proteins as well as decreases in dendritic branching complexity and shifts in dendritic spine parameters have also been established (Rao et al., 2011; Roscoe et al., 2014). HAND is thought to be the result of dendritic injury (e.g., Ellis et al., 2007) and synaptic dysfunction (Gelman & Nguyen, 2010).

The interpretation of the results presented herein and the longitudinal experimental design employed deserves further consideration. Prior longitudinal assessments of temporal processing provide evidence for experienced-based improvements (Dean et al., 1990; Threlkeld et al., 2009; Friedman et al., 2004), a potential caveat for interpretation of the present study. However, assessments of gap-PPI in the present study began at PD 30, after the ontogeny of gap-PPI attains mature level (PD 28; Dean et al., 1990; Kellog et al., 1983). Although the response amplitude per se may decrease as a function of experience (Dean et al., 1990; Threlkeld et al., 2009; Friedman et al., 2004), there were no significant shifts in the ISI for peak inhibition in the amplitude response curve, which are observed in the present study as a function of age (i.e., Figure 3.3). Critically, all animals in the present study were subjected to the same experiences during early development and immediately prior to experimentation; a level of control not present in studies with humans. As previously observed (Moran et al., 2013a), the protracted development of perceptual sharpening across repeated testing, as indexed by the relative insensitivity to ISI, may reflect, in part, impaired central nervous system (CNS) plasticity in the HIV-1 Tg rat.

The use of the classical ISI approach in the gap-PPI experimental paradigm also merits further discussion. The classic approach, popularized by Ison and Hammond (1971),

relies on the manipulation of the ISI as the fundamental operationally defined factor for PPI to assess sensorimotor 'gating', i.e., a measure of temporal processing. The present study employs a constant gap duration (i.e., 20 msec) and a range of ISI values to accurately assess the response amplitude curves for gap-PPI. Temporal acuity *per se*, as may be assessed via manipulation of the stimulus parameter of gap duration (Dean et al., 1990; Threlkeld et al., 2009; Friedman et al., 2004), was not measured in the present study. Braff et al. (1978) assessed the effect of re-test on the startle reflex employing the classical ISI approach. Startle response is a relatively stable phenomenon when the classical ISI approach is employed (Braff et al., 1978), providing additional evidence that the present results are not an effect of experience. Thus, the use of a longitudinal experimental design and manipulation of ISI in gap-PPI affords an undeniable opportunity to assess the effect of age on the development of perceptual sharpening, of temporal sensitivity, which may be a critical underlying dimension for the cognitive impairments observed in HAND.

The study of early neurological deficits is vital for the development of an extant model for the progression of neurocognitive deficits in HIV-1, as well as the development of an effective treatment for PHIV. The HIV-1 Tg rat, which resembles HIV-1 seropositive individuals on cART, provides a vehicle for understanding the progression of neurological impairment using a longitudinal experimental design. HIV-1 Tg rats used in the present study displayed no significant health disparities in comparison to F344 controls (i.e. similar growth rates), consistent with our previous studies (Moran et al., 2012; Moran et al., 2013a; Roscoe et al., 2014). HIV-1 Tg animals used in the current study are a healthier derivation of those originally described (Reid et al., 2001), which displayed severe phenotypical alterations, and wasting at a relatively young age (5-9 months). In contrast, no general

wasting or pathological phenotypes were observed in the HIV-1 Tg animals used in the current study. Both HIV-1 Tg and control animals displayed similar inhibition in visual PPI suggesting that, despite the presence of cataracts in the HIV-1 Tg group, animals were able to detect the 20 msec visual stimulus presented (Moran et al., 2013a). Thus, the current HIV-1 Tg rat displays a moderate phenotype closely resembling HIV-1 seropositive children on cART, making it useful for longitudinal studies of HAND progression.

Temporal processing deficits observed in the HIV-1 Tg rat, assessed using gap-PPI, resemble temporal processing deficits commonly exhibited in HIV-1 seropositive individuals. Understanding the altered progression of temporal processing and differential sensitivity to the manipulation of ISI fills previous gaps in our knowledge about the effect of long-term exposure to HIV-1 viral proteins on neurocognitive impairment evident in PHIV and may reveal information regarding the underlying neural circuitry. Temporal processing measures suggest a diagnostic screening tool for chronic neurological impairment, as well as a venue for the development of novel therapeutics.

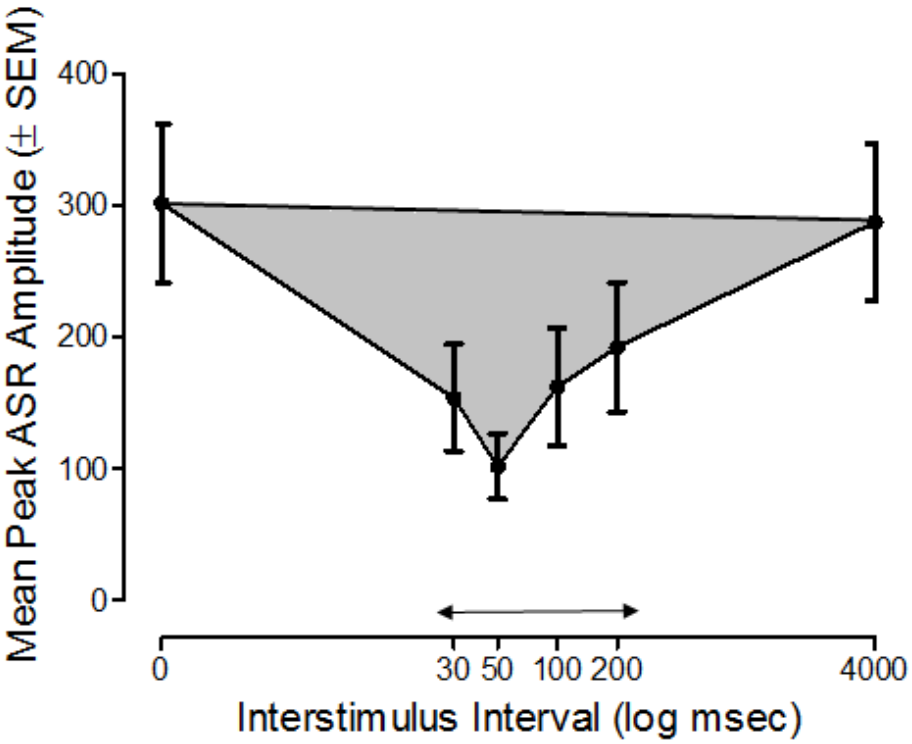

Figure 2.1 Derivation of Prepulse Inhibition. Diagram of the methodology used to derive prepulse inhibition and cumulative frequencies. PPI was derived using area of the peak inflection, which is shaded in gray. The double arrow indicates the potential shift in maximal inhibition, which occurred as a function of age.

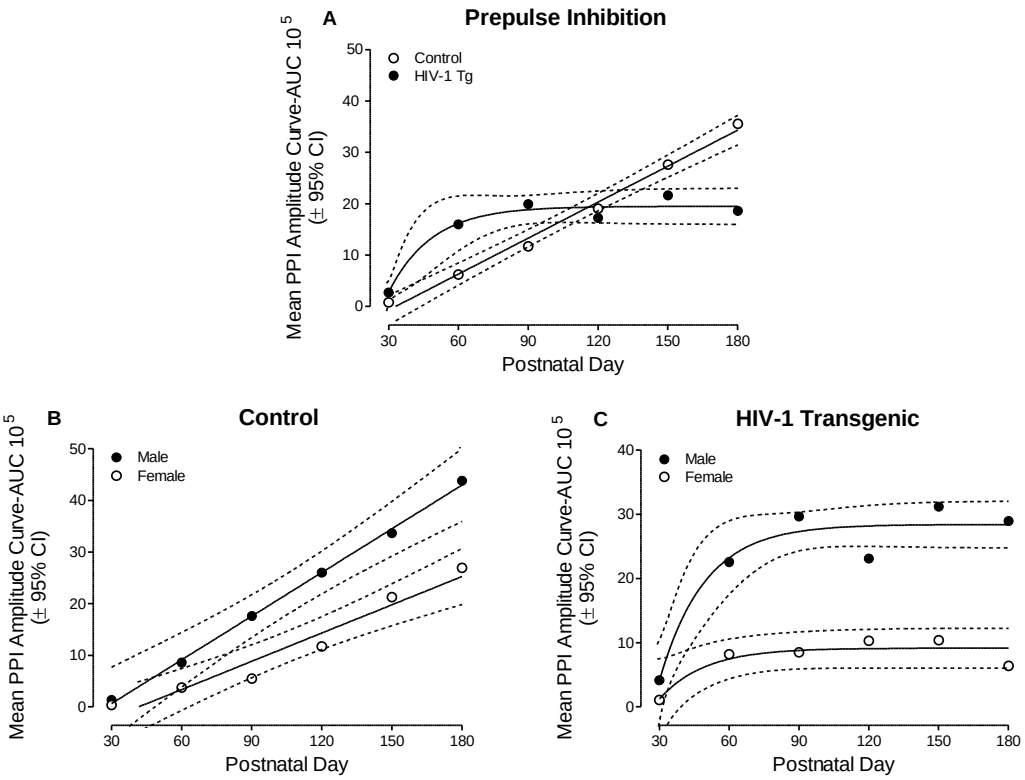

Figure 2.2 Progression of Temporal Processing: Gap-PPI. (A) PPI, assessed using mean area of the peak inflection, is illustrated as a function of genotype (HIV-1 Tg or Control) and age (± 95% CI). As age increases, control animals exhibit an linear increase in PPI. PPI for HIV-1 Tg animals, however, was best fit using a one-phase association. Although control animals develop increased PPI across age, HIV-1 Tg animals failed to exhibit an increase in PPI after PD 90. Linear regression fit (R^2): HIV-1 Tg, 0.96; Control, 0.99. **(B)** PPI for control animals is illustrated as a function of sex (Male or Female) and age (±95% CI). A first-order polynomial was fit to both male and female control animals. Although a linear increase PPI was exhibited by both male and female control animals, there was a significant difference between groups in the rate at which PPI increases [$F(1,230) = 4.3$, $p \leq 0.04$]. Linear regression fit (R^2): Male, 0.99; Female, 0.95. **(C)** PPI for HIV-1 Tg animals is illustrated as a function of sex (Male or Female) and age (±95% CI). PPI for both male and female HIV-1 Tg animals was best fit using a one-phase association. Female HIV-1 Tg animals displayed significantly less PPI than male HIV-1 Tg animals. Linear regression fit (R^2): Male, 0.92; Female, 0.82.

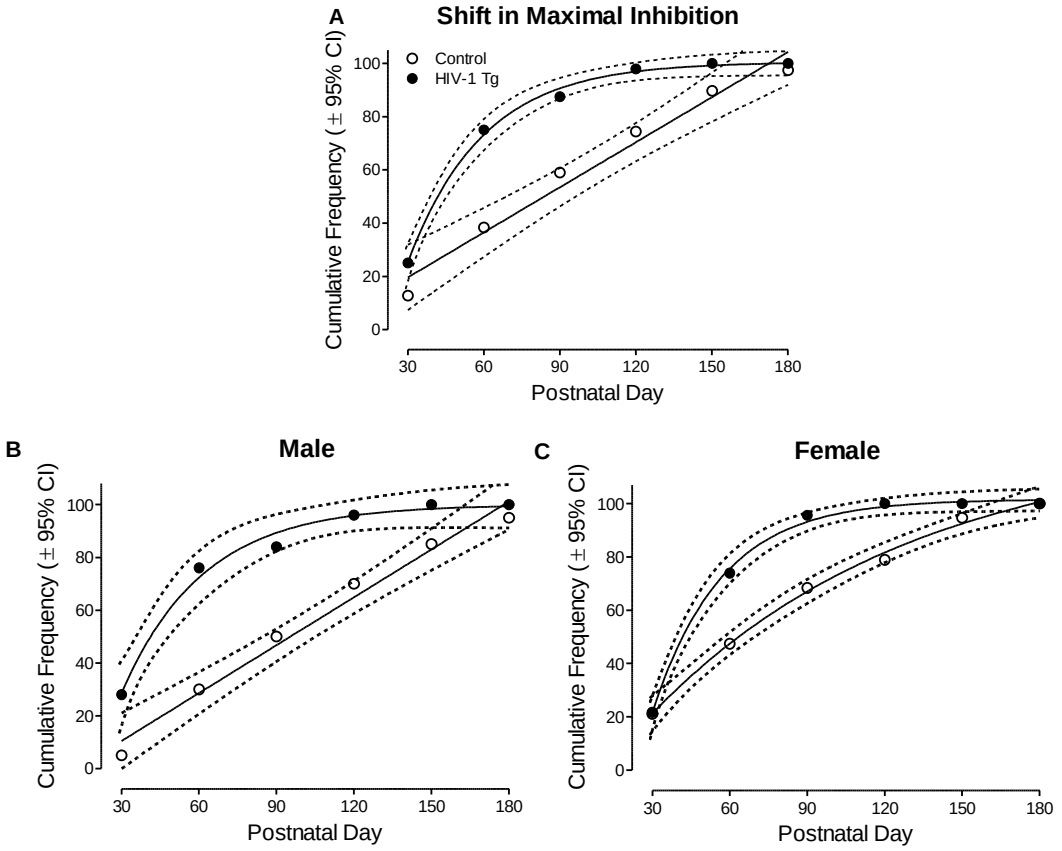

Figure 2.3 Progression of Temporal Processing: Shift in Maximal Inhibition. (A) The cumulative frequency for the shift in maximal inhibition from 30 msec to 50 msec is illustrated as a function of genotype (HIV-1 Tg or Control) and age (± 95% CI). A shift in temporal processing occurred in both the HIV-1 Tg and control animals, however, the shift occurred significantly earlier in the HIV-1 Tg animals. A one-phase association was the best fit for HIV-1 Tg animals, while a first-order polynomial was the best fit for control animals. Linear regression fit (R^2): HIV-1 Tg, 0.99; Control, 0.97. **(B)** The cumulative frequencies for the shift in maximal inhibition from 30 msec to 50 msec for control animals are illustrated as a function of sex (Male or Female) and age (± 95% CI). Female control animals, which were fit using a one-phase association, exhibited a significantly earlier shift in maximal inhibition in comparison to control animals, which were best fit using a first-order polynomial. Linear regression fit (R^2): Male, 0.98; Female, 0.99. **(C)** The cumulative frequencies for the shift in maximal inhibition from 30 msec to 50 msec for HIV-1 Tg animals are illustrated as a function of sex (Male or Female) and age (± 95% CI). A one-phase association global fit was the best fit for both male and female HIV-1 Tg animals. Sex, therefore, did not have a significant effect on sensitivity to the manipulation of ISI in HIV-1 Tg animals. Linear regression fit (R^2): 0.99.

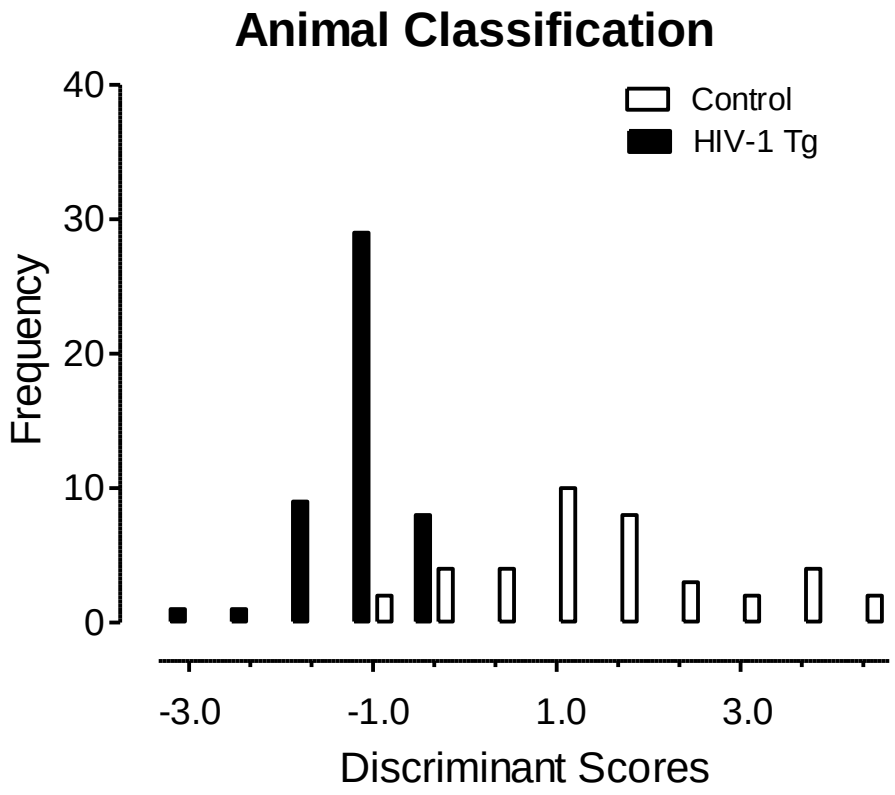

Figure 2.4 Animal Classification. Animal classification is illustrated as a function of the canonical variable representing the simplest linear function that best separated the HIV-1 Tg and control groups (canonical correlation 0.80) and correctly identified (jackknife classification) group membership with 90.8% accuracy (79.5% of controls, and 100% of HIV-1 Tg animals).

CHAPTER 3

EVOLUTION OF THE HIV-1 TRANSGENIC RAT: UTILITY IN ASSESSING THE PROGRESSION OF HIV-1 ASSOCIATED NEUROCOGNITIVE DISORDERS[2]

[2] KA McLaurin, RM Booze, CF Mactutus. 2018. *Journal of Neurovirology*. 24(2):229-245. Reprinted here with permission of publisher.

INTRODUCTION

Approximately 73% of individuals with HIV-1 will be 50 years or older by 2030 (Smit et al., 2015) due to the marked increase in life expectancy following the great success of cART. The prevalence of the most severe forms of neurocognitive impairment, including HIV-1 associated dementia, dramatically decreased following the advent of cART. However, milder forms of neurocognitive impairments, including HAND, continue to afflict between 40-70% of HIV-1 seropositive individuals (Letendre et al., 2010; McArthur et al., 2010; Heaton et al., 2011). Cross-sectional studies have demonstrated that older HIV-1 seropositive individuals are at an elevated risk for developing neurological impairments compared to older HIV-1 seronegative individuals (Sheppard et al., 2015) and younger HIV-1 seropositive individuals (Valcour et al., 2004; Fazeli et al., 2014). Extrapolating findings from cross-sectional studies to age-related disease progression, however, is inferentially fraught (Kraemer et al., 2000; Coleman, 2004). Longitudinal experimental designs, in sharp contrast, provide an opportunity to understand age-related disease progression using repeated measures across the lifespan (Kraemer et al., 2000; West et al., 2004).

In a seminal paper, Reid et al. (2001) reported the development of the HIV-1 Tg rat, which contains a *gag-pol*-deleted HIV-1 provirus regulated by the viral promotor. The highest levels of transgene (located on chromosome 2 and 9) expression were observed in the lymph nodes, spleen, kidney, and thymus (Reid et al., 2001). Clinical manifestations, including neurological abnormalities (i.e., circling behavior, hind-limb paralysis), skin lesions, cataract formation, and relatively early wasting (i.e, between 5 to 9 months of age) were also observed in the original derivation of the HIV-1 Tg rat (Reid et al., 2001).

The current derivation of the HIV-1 Tg rat, used in the present studies, is a healthier derivation than those originally described, with the transgene now limited to chromosome 9, and in the F344/N, rather than Sprague Dawley, background strain. Similar growth rates (Peng et al., 2010; Moran et al., 2012; Moran et al., 2013b; Roscoe et al., 2014) and a longer lifespan (i.e., 50% of HIV-1 Tg rats survive through 21 months of age; Peng et al., 2010) have been reported in the contemporary HIV-1 Tg phenotype. Viral proteins are expressed in the non-infectious HIV-1 Tg rat constitutively throughout development (Peng et al., 2010; Abbondanzo & Chang, 2014), resembling HIV-1 seropositive individuals on cART. There is growing acceptance and confidence that the HIV-1 Tg rat is a valuable tool to model the neurocognitive deficits observed in HAND (e.g., Vigorito et al., 2007; Lashomb et al., 2009; Moran et al., 2013a; Moran et al., 2014a; Repunte-Canonigo et al., 2014) and may provide an opportunity to assess the effect of long-term HIV-1 viral protein exposure (Vigorito et al., 2015). However, there is a critical need to determine the integrity of sensory and motor system function, which will help establish the utility of the HIV-1 Tg rat in longitudinal studies on the progression of neurocognitive deficits through advancing age.

PPI of the ASR has been promoted as a versatile experimental technique for the evaluation of sensory system function (Ison et al., 1984; Wecker et al., 1985; Crofton & Sheets, 1989) and temporal processing (e.g., Moran et al., 2013a; McLaurin et al., 2017a, McLaurin et al., 2017b). The technique, popularized by Ison and Hammond (1971), introduces a punctate prestimulus (i.e., light, tone) prior to a startling stimulus. Introduction of the prestimulus 30 to 500 msec prior to the startling stimulus produces robust inhibition of the ASR (Hoffman & Ison, 1980). The amplitude of the startle response can be used to

determine whether the subject (i.e., rat, mouse, human) is able to detect the prestimulus (Wecker et al., 1985), thus assessing the integrity of sensory system function. Additionally, manipulation of the ISI (i.e., the time between the prestimulus and startle stimulus), as in the present studies, allows for assessment of temporal processing.

Characteristics of PPI, including brevity (i.e., rodents: approximately 20-30 minutes, Fitting et al., 2006b; Moran et al., 2013a), repeatability (Braff et al., 1978; Schwarzkoph et al., 1993), and ease of administration (i.e., no prior training, no invasive procedures) make it an attractive method for the evaluation of sensory function (Ison et al., 1984; Crofton & Sheets,1989). PPI has previously been used to assess the effect of toxicant exposure on sensory system function. For example, Young and Fechter (1983) assessed the effect of neomycin treatment on auditory system function. Results indicated not only that neomycin treatment resulted in selective hearing loss, but also the sensitivity of PPI to auditory system function (Young & Fechter, 1983). Additionally, Wecker and Ison (1986) assessed the effect of inherited retinal degeneration on visual system function using PPI. Across age, animals with inherited retinal degeneration failed to exhibit robust inhibition to the visual prestimulus at any ISI, indicative of alterations in visual system function (Wecker & Ison, 1986).

Temporal processing deficits, a potential elemental dimension of neurocognitive impairment in HIV-1, have been previously observed in the HIV-1 Tg rat using cross-modal PPI (Moran et al., 2013a; McLaurin et al., 2017b; McLaurin et al., 2017c). Specifically, a within-subject assessment from two to six months of age revealed a relative insensitivity to the manipulation of ISI and a lack of perceptual sharpening with age in HIV-1 Tg animals relative to control animals (Moran et al., 2013a). Alterations in the

development of perceptual sharpening have also been reported in preweanling HIV-1 Tg animals relative to controls (McLaurin et al., 2017c). Additionally, HIV-1 Tg and control animals were assessed between nine and ten months of age, revealing the generality and relative permanence of temporal processing deficits (McLaurin et al., 2017b). Accordingly, the present study employed auditory and visual PPI to assess the integrity of the auditory and visual sensory systems and the progression of temporal processing deficits in the HIV-1 Tg rat through the majority of the animal's functional lifespan.

Locomotor activity has been recognized as a state-of-the art technique used for the assessment of gross motor movement (Pierce & Kalivas, 2007). The protocol employed in the present study used an automated monitoring system to measure the number of photocell interruptions within a test session (i.e., 60 minutes) as an index of motor behavior (Pierce & Kalivas, 2007). Assessments of locomotor activity are commonly used as a preclinical screening tool for motoric impairment in pharmacological studies (Robbins, 1977; Pierce and Kalivas, 2007). For example, Booze and Mactutus (1990) used locomotor activity as an assessment of the long-term effects of neonatal exposure to triethyl lead. No significant differences in locomotor activity were observed at testing on PD 90, suggesting that neonatal exposure to triethyl lead has no long-term effects on motor system function (Booze & Mactutus, 1990). Additionally, locomotor activity has been used to examine the effects of prenatal cocaine exposure (1 or 3 mg/kg) on locomotor and stereotyped behavior following a cocaine challenge in adulthood (Peris et al., 1992). Animals prenatally exposed to 3 mg/kg cocaine exhibited the most profound increases in locomotor and stereotyped behavior following cocaine injections in adulthood, suggesting that cocaine in utero behaviorally sensitized animals to subsequent cocaine exposure (Peris et al., 1992).

Measures of novelty and habituation can be used to assess memory, including episodic memory, in animal models (Eacott et al., 2005; Barker et al., 2007; Moran et al., 2013b; Chao et al., 2016). Habituation, one of the simplest forms of learning characterized by a decrease in response following repeated stimulation (Harris, 1943; Thompson & Spencer, 1966; Rankin et al., 2009), allows for the assessment of learning and memory in locomotor activity, both within sessions (intrasession) and between sessions (intersession; review, Leussis & Bolivar, 2006). Significant alterations in intrasession habituation have been reported in the HIV-1 Tg rat, assessed using three consecutive test sessions in locomotor activity at 6, 7, and 11 months of age (Moran et al., 2013b). Profound deficits in intrasession habituation were observed during the third test session at 7 and 11 months in HIV-1 Tg animals compared to controls, suggestive of a deficit in long-term episodic memory (Moran et al., 2013b). Alterations in intersession habituation have also been reported in neonatal Sprague-Dawley rats stereotaxically injected with Tat_{1-86}, a HIV-1 viral protein, compared to vehicle-treated controls (Moran et al., 2014b). Therefore, the present study used locomotor activity to assess the integrity of the motoric system and the progression of long-term episodic memory in the HIV-1 Tg rat through advancing age.

The aims of the present study were thus two-fold. First, to assess the integrity of sensory and motor system function through advancing age in the HIV-1 Tg rat. Determining the integrity of sensory and motor systems in the HIV-1 Tg rat through the majority of the animal's functional lifespan provides an opportunity to help establish the applicability of the HIV-1 Tg rat in longitudinal studies of the progression of HAND. Second, to establish the progression of neurocognitive deficits, including temporal processing and long-term episodic memory, in the HIV-1 Tg rat, through the majority of

the animal's functional lifespan. The factor of biological sex was an integral component of the experimental design. Understanding the progression of neurocognitive impairment, and the effect of biological sex, heralds an opportunity for the development of an advantageous model of progressive neurocognitive deficits in HIV-1 and establishes fundamental groundwork for the development of neurorestorative treatments.

METHODS

Animals

Intact male and female Fischer (F344/N; Harlan Laboratories Inc., Indianapolis, IN) HIV-1 Tg (male, *n*=37; female, *n*=33) and control rats (male, *n*=34; female, *n*=33) were sampled from a total of 37 litters (HIV-1 Tg, *N*=20 litters; control *N*=17 litters). Cross-modal PPI and locomotor activity assessments were conducted every thirty days from PD 90 to PD 180 and every sixty days from PD 240 to PD 480.

Animals, housed with their biological dam, were delivered to the animal vivarium between PD 7 and PD 9 across eleven months. Following weaning, which occurred at PD 21, animals were pair- or group-housed with animals of the same sex. Beginning at approximately PD 60, animals were placed on food restriction (Pro-Lab Rat, Mouse, Hamster Chow #3000) to maintain 85% body weight due to their participation in a concurrently conducted signal detection task. Rodent food was again provided *ad libitum* for the duration of the study following the successful completion of signal detection (PD 100-PD 277). Water was available *ad libitum* throughout the duration of the study.

Due to health issues, including significant weight loss (i.e., approximately 20%; *n*=6) or tumors (*n*=4), some animals were euthanized prior to the completion of the study. Specifically, two HIV-1 Tg animals (male *n*=1; female *n*=1) and one control animal (male,

n=1) were euthanized prior to PD 420 and an additional five HIV-1 Tg animals (male *n*=3; female *n*=2) and two control animals (male *n*=1; female *n*=1) were euthanized prior to PD 480.

Guidelines established by the NIH were used for the maintenance of animals in AAALAC-accredited facilities. The targeted environmental conditions for the animal vivarium were 21°± 2°C, 50% ± 10% relative humidity and a 12-h light:12-h dark cycle with lights on at 0700 h (EST). The project protocol, under federal assurance (# A3049-01), was approved by the IACUC of the University of South Carolina.

Cross-Modal Prepulse Inhibition

Apparatus

An isolation cabinet (external dimensions: 10 cm-thick, double-walled, 81 x 81 x 116-cm) (Industrial Acoustic Company, INC., Bronx, NY), which provided 30 db(A) of sound attenuation relative to the external environment, enclosed the startle platform (SR-Lab Startle Reflex System, San Diego Instruments, Inc., San Diego, CA), instead of the 1.9 cm thick ABS plastic or laminate cabinets offered with this system. Background noise of 70dB(A) was continuously delivered. All auditory prepulse and startle stimuli were presented using a high-frequency loudspeaker of the SR-Lab system (model#40-1278B, Radio Shack, Fort Worth, TX). A sound level meter (model #2203, Bruël & Kjaer, Norcross, GA) was used to measure and calibrate the sound levels, with the microphone placed inside the Plexiglas test cylinder. Visual prepulse stimuli were presented using a white LED light (22 lux; Light meter model #840006, Sper Scientific, Ltd, Scottsdale, AZ). The high-frequency loudspeaker of the SR-Lab system was mounted 30 cm above the Plexiglas animal test cylinder and the white LED light was affixed on the wall in front of the test cylinder. A piezoelectric accelerometer integral to the bottom of the cylinder

converted the deflection of the test cylinder, resulting from the animal's ballistic response to the auditory stimulus, into analog signals. The response signals were digitized (12 bit A to D, recorded at a rate of 2000 samples/sec) and saved to a hard disk. A SR-LAB Startle Calibration System was used to calibrate the response sensitivities.

Procedure

Cross-modal PPI, used to assess auditory and visual sensory system function and the progression of temporal processing, was conducted similar to our prior publications (e.g., Moran et al., 2013a). In brief, a 30-minute test session, beginning with a 5-min adjustment period, was conducted in the dark every 30 days from PD 90 to PD 180 and every 60 days from PD 240 to PD 480. Six pulse-only ASR trials, with a fixed 10 second ITI, were used for habituation at the beginning of the test session. An equal number of auditory (85dB(A) white noise stimulus) and visual (22 lux) prepulse trials, totaling 72 trials, were presented using a counterbalanced order (i.e., ABBA) to control for order-effects. ISIs (0, 30, 50, 100, 200, 4000 msec) were presented in 6-trial blocks according to a Latin-square design with a variable ITI (15-25 sec). All prepulse stimuli and the auditory startle stimulus (100 db(A)) had a 20 msec duration. The peak ASR amplitude values were collected for analysis.

Locomotor Activity

Apparatus

Square (40 x 40 cm) activity monitors (Hamilton Kinder, San Diego Instruments, San Diego, CA) were converted into round (~40 cm diameter) compartments using perspex inserts. Infrared photocell (32 emitter/detector pairs) interruptions were used to detect free movement; the sensitivity of the photocells was tuned by the manufacturer to maintain their sensitivity with the additional layer of perspex.

Procedure

Motor system function and long-term episodic memory impairments were assessed using locomotor activity every thirty days from PD 90 to PD 180 and every sixty days from PD 240 to PD 480. A 60-minute test session was conducted between 700 and 1200h (EST) under dim light conditions (<10 lux) in an isolated room. The number of photocell interruptions within the 60-min test session were collected for analysis.

Statistical Analysis

ANOVA statistical techniques (SPSS Statistics 24, IBM Corp., Somer, NY) were used for the analysis of all data. Individual observations were analyzed using litter means and standard errors, dependent upon biological sex, to account for the nested design (Denenberg, 1984; Wears, 2002).The mean series imputation method was used for all censored data, either due to euthanization or an equipment malfunction, which occurred in locomotor activity at PD 90 (control: n=1) and PD 150 (HIV-1 Tg: n=7; control: n=4). Potential violations of compound symmetry were precluded by the use of orthogonal decomposition of the repeated-measures factors or addressed, post-hoc, via the conservative Greenhouse-Geisser *df* correction factor (Greenhouse & Geisser, 1959). Age-dependent effects of the HIV-1 transgene were evaluated using tests of simple mains effects and specific linear contrasts (Winer, 1971). Partial eta squared (η_p^2) was used as a measure of effect size. GraphPad Prism 5 (GraphPad Software, Inc., La Jolla, CA) was used for all regression analyses and to create all graphs. For all statistical tests, significance was set at an alpha level of $p \leq 0.05$.

Specifically, for free-feeding body weight, a mixed-factor ANOVA was conducted independently for each sex. Genotype (HIV-1 Tg vs. control) served as the between-subject's factor, while age served as the within-subjects factor. The peak ASR amplitude

values, collected in cross-modal PPI, were analyzed for the assessment of the integrity of auditory and visual system function. The progression of temporal processing was examined using the area of inflection of the ASR amplitude response curve (McLaurin et al., 2016b). Locomotor activity was assessed using the total number of photocell interruptions in a 60-minute period, to establish the integrity of motoric system function, and the number of photocell interruptions in 5-minute bins, to assess intrasession habituation, as an index for long-term episodic memory. For cross-modal PPI and locomotor activity, a mixed-factor ANOVA was performed, with genotype (HIV-1 Tg vs. control) and sex (male vs. female) as the between-subject's factors. As appropriate, age, time, ISI, and trial served as the within-subjects factors.

RESULTS

Establishing the Integrity of Sensory and Motor System Function

Body Weight: Somatic Growth

Somatic growth, assessed using body weight, was examined by litter dependent upon food access (i.e., food restriction vs. *ad libitum*) and sex. Regardless of sex and/or food access, HIV-1 Tg animals weighed significantly less than control animals throughout the duration of the experiment.

Male HIV-1 Tg and control animals exhibited a linear increase in growth (Figure 3.1), with no significant differences between genotype in the rate of growth [$F(1,60)<1.0$, $p\geq0.05$], while on food restriction due to a concurrently conducted signal detection task. All male HIV-1 Tg and control animals completed the concurrently conducted signal detection task by 6 months of age (PD 180), at which point food was subsequently available *ad libitum*. During free-feeding, a one-phase association was the best fit for both HIV-1 Tg and control animals (R^2s≥0.97); however, significant differences were observed in the rate

of growth [$F(3,357)=1230$, $p\leq0.001$]. The overall ANOVA conducted on somatic growth during free-feeding confirmed these observations, revealing a significant age x genotype interaction [$F(10,310)=70.0$, $p_{GG}\leq0.001$, $\eta_p^2=0.693$] with a prominent linear component [$F(1,31)=126.4$, $p\leq0.001$, $\eta_p^2=0.803$]. Significant main effects of age [$F(10,310)=607.1$, $p_{GG}\leq0.001$, $\eta_p^2=0.951$] and genotype [$F(1,31)=381.7$, $p\leq0.001$, $\eta_p^2=0.925$] were also observed.

Female HIV-1 Tg animals displayed an increase in weight according to a one-phase association, while female control animals exhibited an increase in weight according to a second order polynomial, during food restriction (Figure 3.1). All female HIV-1 Tg and control animals completed the concurrently conducted signal detection task by approximately 9 months of age (PD 277), at which point food was subsequently available *ad libitum.* During free-feeding, a first-order polynomial was the best fit for both HIV-1 Tg and control animals ($R^2s\geq0.98$), however, significant differences were observed in the rate of growth [$F(1,252)=13.2$, $p\leq0.001$]. The rate of increase in body weight was significantly slower in HIV-1 Tg animals ($\beta_1=3.97\pm1.07$(95% CI)) relative to control animals ($\beta_1=7.16\pm1.32$(95% CI)). The overall ANOVA confirmed these observations, revealing a significant age x genotype interaction [$F(7,210)=22.8$, $p_{GG}\leq0.001$, $\eta_p^2=0.432$] with a prominent linear component [$F(1,30)=34.4$, $p\leq0.001$, $\eta_p^2=0.534$]. Significant main effects of age [$F(7,210)=224.6$, $p_{GG}\leq0.001$, $\eta_p^2=0.882$] and genotype [$F(1,30)=59.9$, $p\leq0.001$, $\eta_p^2=0.666$] were also observed.

Cross-Modal Prepulse Inhibition: Auditory System Function

Auditory PPI (Figure 3.2) provided strong evidence for the integrity of auditory system function in both HIV-1 Tg and control animals through the majority of the animal's functional lifespan. Control animals exhibited maximal inhibition at the 100 msec ISI at all

test sessions. In sharp contrast, the maximal inhibition was observed at multiple ISIs in HIV-1 Tg animals dependent upon age (i.e., PD 90: 30 msec; PD 120-PD 240: 100 msec; PD 300: 50 msec; PD 360-PD 420: 200 msec; PD 480: 50 msec). A significant increase in ASR as a function of age was observed in control animals, but not in HIV-1 Tg animals. However, both HIV-1 Tg and control animals exhibited robust inhibition to the auditory prepulse during all test sessions, suggesting the integrity of auditory system function.

The overall ANOVA conducted on the peak ASR amplitude values confirmed these observations, revealing a significant age x ISI x genotype interaction [$F(40,2440)=11.3$, $p_{GG}\leq 0.001$, $\eta_p^2=0.157$] with a prominent linear-quadratic component [$F(1,61)=52.2$, $p\leq 0.001$, $\eta_p^2=0.461$], and a significant age x ISI x sex interaction [$F(40,2440)=7.8$, $p_{GG}\leq 0.001$, $\eta_p^2=0.113$] with a prominent quadratic-quadratic component [$F(1,61)=34.1$, $p\leq 0.001$, $\eta_p^2=0.359$]. Significant two-way interactions included an age x sex interaction [$F(8,488)=10.3$, $p_{GG}\leq 0.001$, $\eta_p^2=0.144$] with a prominent quadratic component [$F(1,61)=31.6$, $p\leq 0.001$, $\eta_p^2=0.341$], a significant age x genotype interaction [$F(8,488)=14.2$, $p_{GG}\leq 0.001$, $\eta_p^2=0.188$] with a prominent linear component [$F(1,61)=42.9$, $p\leq 0.001$, $\eta_p^2=0.413$], a significant ISI x sex interaction [$F(5,305)=77.9$, $p_{GG}\leq 0.001$, $\eta_p^2=0.561$] with a prominent quadratic component [$F(1,61)=85.7$, $p\leq 0.001$, $\eta_p^2=0.584$], a significant ISI x genotype interaction [$F(5,305)=127.2$, $p_{GG}\leq 0.001$, $\eta_p^2=0.676$] with a prominent quadratic component [$F(1,61)=139.1$, $p\leq 0.001$, $\eta_p^2=0.695$], and a significant age x ISI interaction [$F(40,2440)=29.3$, $p_{GG}\leq 0.001$, $\eta_p^2=0.324$] with a prominent linear-quadratic component [$F(1,61)=113.5$, $p\leq 0.001$, $\eta_p^2=0.651$]. Significant main effects of age [$F(8,488)=42.7$, $p_{GG}\leq 0.001$, $\eta_p^2=0.412$], ISI [$F(5,305)=764.7$, $p_{GG}\leq 0.001$, $\eta_p^2=0.926$], sex [$F(1,61)=91.4$, $p\leq 0.001$, $\eta_p^2=0.600$] and genotype [$F(1,61)=124.9$, $p\leq 0.001$, $\eta_p^2=0.672$]

were also observed. Further analyses were conducted to examine the locus of these interactions.

The ASR at the point of maximal inhibition in auditory PPI was used to further examine the significant age x ISI x genotype interaction (Figure A.1). A linear increase in the ASR at the point of maximal inhibition, well-described using a global first-order polynomial, was observed across age in both HIV-1 Tg and control animals (R^2=0.70). No significant differences in the rate of increase in the ASR at the point of maximal inhibition were observed between genotypes [$F(2,14)=3.2$, $p\geq0.05$]. The ASR at the point of maximal inhibition increased at the same rate in HIV-1 Tg (β_1=0.028±0.01 (95% CI)) and control animals (β_1=0.017±0.01 (95% CI)) suggesting the integrity of the auditory system. Thus, both control and HIV-1 Tg animals displayed robust inhibition to the auditory prepulse, albeit at different ISIs, at all test sessions, suggesting the integrity of auditory system function through advancing age.

Cross-Modal Prepulse Inhibition: Visual System Function

Visual PPI revealed the integrity of visual system function in HIV-1 Tg and control animals through the majority of the animal's functional lifespan, illustrated in Figure 3.3. Control animals, but not HIV-1 Tg animals, exhibited a significant increase in ASR as a function of age. However, both HIV-1 Tg and control animals exhibited robust inhibition to the visual prepulse at the 50 msec ISI at all test sessions, suggesting the integrity of visual system function.

The overall ANOVA conducted on the peak ASR amplitude values confirmed these observations, revealing significant higher-order interactions, including an age x ISI x genotype x sex interaction with a prominent quadratic-quadratic component [$F(1,61)=5.0$,

$p \leq 0.029$, $\eta_p^2 = 0.076$], an age x genotype x sex interaction with a prominent quadratic component [$F(1,61) = 4.9$, $p \leq 0.031$, $\eta_p^2 = 0.074$], an age x ISI x genotype interaction [$F(40,2440) = 9.0$, $p_{GG} \leq 0.001$, $\eta_p^2 = 0.129$] with a prominent linear-quadratic component [$F(1,61) = 78.1$, $p \leq 0.001$, $\eta_p^2 = 0.561$], an age x ISI x sex interaction [$F(40,2440) = 4.3$, $p_{GG} \leq 0.001$, $\eta_p^2 = 0.066$] with a prominent quadratic-quadratic component [$F(1,61) = 38.6$, $p \leq 0.001$, $\eta_p^2 = 0.387$], and an ISI x sex x genotype interaction [$F(5,305) = 4.4$, $p_{GG} \leq 0.013$, $\eta_p^2 = 0.068$] with a prominent quadratic component [$F(1,61) = 6.5$, $p \leq 0.013$, $\eta_p^2 = 0.096$]. Significant two-way interactions included, an age x sex interaction [$F(8,488) = 10.8$, $p_{GG} \leq 0.001$, $\eta_p^2 = 0.151$] with a prominent quadratic component [$F(1,61) = 37.0$, $p \leq 0.001$, $\eta_p^2 = 0.377$], an age x genotype interaction [$F(8,488) = 13.4$, $p_{GG} \leq 0.001$, $\eta_p^2 = 0.180$] with a prominent linear component [$F(1,61) = 35.1$, $p \leq 0.001$, $\eta_p^2 = 0.365$], an ISI x sex interaction [$F(5,305) = 60.9$, $p_{GG} \leq 0.001$, $\eta_p^2 = 0.500$] with a prominent quadratic component [$F(1,61) = 79.2$, $p \leq 0.001$, $\eta_p^2 = 0.565$], an ISI x genotype interaction [$F(5,305) = 149.5$, $p_{GG} \leq 0.001$, $\eta_p^2 = 0.710$] with a prominent quadratic component [$F(1,61) = 190.6$, $p \leq 0.001$, $\eta_p^2 = 0.758$], and an age x ISI interaction [$F(40,2440) = 15.6$, $p_{GG} \leq 0.001$, $\eta_p^2 = 0.204$] with a prominent quadratic-quadratic component [$F(1,61) = 113.8$, $p \leq 0.001$, $\eta_p^2 = 0.651$]. Significant main effects of age [$F(8,488) = 46.9$, $p_{GG} \leq 0.001$, $\eta_p^2 = 0.435$], ISI [$F(5,305) = 658.6$, $p_{GG} \leq 0.001$, $\eta_p^2 = 0.915$], sex [$F(1,61) = 71.7$, $p \leq 0.001$, $\eta_p^2 = 0.540$] and genotype [$F(1,61) = 108.2$, $p \leq 0.001$, $\eta_p^2 = 0.640$] were also observed.

Complementary analyses of the ASR at the point of maximal inhibition (i.e., 50 msec) in visual PPI were conducted to examine the significant age x ISI x genotype interaction (Figure A.1). A linear increase in the ASR at the point of maximal inhibition was observed as a function of age in both HIV-1 Tg and control animals, well-described

using a first-order polynomial (R^2s≥0.64). Significant differences in the rate of increase between genotypes were observed [$F(1,14)=14.5$, $p\leq0.002$]. The ASR at the point of maximal inhibition increased faster in HIV-1 Tg animals ($\beta_1=0.14\pm0.03$ (95% CI)) relative to control animals ($\beta_1=0.07\pm0.03$ (95% CI)), however, both HIV-1 Tg and control animals exhibited robust inhibition (i.e., ≥55% inhibition) to the visual prestimulus at all test sessions. Thus, visual PPI provides strong evidence for the integrity of visual system function through advancing age in both HIV-1 Tg and control animals.

Locomotor Activity: Motor System Function

The mean number of photocell interruptions in a 60-minute locomotor activity test session were used to assess motoric system function through advancing age in HIV-1 Tg and control animals (Figure 3.4). A one-phase decay was the best fit for HIV-1 Tg and control animals (R^2s≥0.91), however, a significant difference was observed between the best fit function [$F(3,12)=41.1$, $p\leq0.001$]. Specifically, control animals, relative to HIV-1 Tg animals, exhibited a significantly greater mean number of photocell interruptions from PD 90 to PD 180. No significant differences in the mean number of photocell interruptions were observed between HIV-1 Tg and control animals at PD 240 or PD 300. At PD 360 and all subsequent test sessions, HIV-1 Tg animals displayed a significantly greater mean number of photocell interruptions in comparison to controls. The repeated measures ANOVA confirmed these observations, revealing a significant age x genotype interaction [$F(8,448)=20.5$, $p_{GG}\leq0.001$, $\eta_p^2=0.251$] with a prominent linear component [$F(1,61)=96.9$, $p\leq0.001$, $\eta_p^2=0.614$], and a significant age x sex interaction [$F(8,448)=2.2$, $p_{GG}\leq0.039$, $\eta_p^2=0.035$] with a prominent quadratic component [$F(1,61)=9.8$, $p\leq0.003$, $\eta_p^2=0.139$]. Significant main effects of age [$F(8,448)=102.4$, $p_{GG}\leq0.001$, $\eta_p^2=0.627$], and sex [$F(1,61)=10.5$, $p\leq0.002$, $\eta_p^2=0.147$] were also observed. Therefore, neither HIV-1 Tg nor

control animals exhibited any gross-motoric system impairments, evidenced using the mean number of photocell interruptions, suggesting the integrity of motor system function though advancing age.

Understanding the Progression of HIV-1 Associated Neurocognitive Disorders

Cross-Modal Prepulse Inhibition (Auditory): Temporal Processing

In auditory PPI, area of the inflection of the ASR response curve, a measure of PPI, was used to establish the progression of temporal processing, illustrated in Figure 3.5. HIV-1 Tg animals exhibited a profound alteration in the progression of temporal processing relative to control animals. A segmental linear regression was the best fit for both HIV-1 Tg and control animals (R^2s$\geq$0.91). However, a leftward shift in maximal PPI was observed in HIV-1 Tg animals relative to controls. Specifically, control animals exhibited a linear increase in PPI through approximately PD 300, followed by a subsequent decrease. HIV-1 Tg animals displayed a leftward shift, with maximal peak inhibition observed at approximately PD 270, followed by a subsequent decrease. The overall ANOVA confirmed these observations, revealing a significant age x genotype interaction [$F(8,488)=11.8$, $p_{GG}\leq0.001$, $\eta_p^2=0.162$] with a prominent linear component [$F(1,61)=35.2$, $p\leq0.001$, $\eta_p^2=0.366$] and a significant age x sex interaction [$F(8,488)=8.5$, $p_{GG}\leq0.001$, $\eta_p^2=0.123$] with a prominent quadratic component [$F(1,61)=31.9$, $p\leq0.001$, $\eta_p^2=0.343$]. Significant main effects of genotype [$F(1,61)=123.3$, $p\leq0.001$, $\eta_p^2=0.669$], age [$F(8,488)=35.4$, $p_{GG}\leq0.001$, $\eta_p^2=0.367$], and sex [$F(1,61)=85.1$, $p\leq0.001$, $\eta_p^2=0.583$] were also observed.

Separate analyses of each genotype were conducted to examine the locus of these interactions (Figure 3.5). A segmental linear regression was the best fit for both male and female control animals (R^2s $\geq$0.90). Both male and female control animals exhibited

maximal PPI at approximately PD 300, followed by a subsequent decrease. However, a significant difference in the rate of temporal processing development from PD 90 to PD 300 was observed [$F(1,12)=12.4$, $p\leq0.004$]. Specifically temporal processing development was significantly greater in male control animals ($\beta_1=4815\pm1645$) relative to female control animals ($\beta_1=2387\pm367.5$); no significant differences between males and females were observed in the rate of temporal processing decline [$F(1,12)=2.7$, $p\geq0.05$]. The overall ANOVA for control animals confirmed these observations, revealing a significant age x sex interaction [$F(8,256)=4.5$, $p_{GG}\leq0.001$, $\eta_p^2=0.122$] with a prominent quadratic component [$F(1,32)=16.3$, $p\leq0.001$, $\eta_p^2=0.337$]. Significant main effects of age [$F(8,256)=34.6$, $p_{GG}\leq0.001$, $\eta_p^2=0.519$] and sex [$F(1,32)=80.3$, $p\leq0.001$, $\eta_p^2=0.715$] were also observed. For HIV-1 Tg animals, a segmental linear regression, with maximal PPI at approximately PD 270, was the best fit for male HIV-1 Tg animals ($R^2=0.88$). In sharp contrast, female HIV-1 Tg animals failed to exhibit any significant development of temporal processing, best fit using a horizontal line. The overall ANOVA for HIV-1 Tg animals confirmed these observations, revealing a significant age x sex interaction [$F(8,232)=5.5$, $p_{GG}\leq0.001$, $\eta_p^2=0.160$] with a prominent quadratic component [$F(1,29)=16.7$, $p\leq0.001$, $\eta_p^2=0.366$]. Significant main effects of age [$F(8,232)=5.3$, $p_{GG}\leq0.001$, $\eta_p^2=0.154$] and sex [$F(1,29)=24.1$, $p\leq0.001$, $\eta_p^2=0.454$] were also observed. Thus, regardless of biological sex, HIV-1 Tg animals exhibited significant alterations in the development of temporal processing, albeit alterations which are more profound in female HIV-1 Tg animals.

Cross-Modal Prepulse Inhibition (Visual): Temporal Processing

In visual PPI (Figure 3.6), HIV-1 Tg rats exhibited a significant alteration in the development of temporal processing, indexed using PPI, relative to controls. A segmental

linear regression was the best fit for both HIV-1 Tg and control animals (R^2s≥0.70). HIV-1 Tg animals exhibited a significant leftward shift in maximal PPI relative to control animals. Specifically, control animals exhibited a linear increase in PPI through PD 360, followed by a subsequent decrease. In contrast, HIV-1 Tg animals displayed maximal PPI at PD 300, followed by a subsequent decrease. The overall ANOVA on mean area of the amplitude inflection curve confirmed these observations, revealing a significant age x genotype interaction with a prominent linear component [$F(1,61)=17.5$, $p\leq0.001$, $\eta_p^2=0.223$], a significant age x sex interaction [$F(8,488)=4.4$, $p_{GG}\leq0.001$, $\eta_p^2=0.068$] with a prominent linear component [$F(1,61)=16.4$, $p\leq0.001$, $\eta_p^2=0.211$], and a significant genotype x sex interaction [$F(1,61)=4.8$, $p\leq0.032$, $\eta_p^2=0.073$]. Significant main effects of genotype [$F(1,61)=23.6$, $p\leq0.001$, $\eta_p^2=0.279$], age [$F(8,488)=10.3$, $p_{GG}\leq0.001$, $\eta_p^2=0.145$] and sex [$F(1,61)=69.9$, $p\leq0.001$, $\eta_p^2=0.534$] were also observed.

Complementary analyses were conducted for each genotype to determine the locus of these interactions (Figure 3.6). A segmental linear regression provided a well-described fit for both male and female control animals (R^2s≥0.82). Male control animals exhibited a significant increase in PPI through PD 360, followed by a subsequent decrease. Female control animals, however, exhibited rightward shift, with maximal PPI observed at PD 420, followed by a subsequent decrease. Differences in the rate of temporal processing development were also observed, with female control animals exhibiting slower development ($\beta_1=626.4\pm201.2$) relative to male animals ($\beta_1=1852\pm874.8$). The overall ANOVA confirmed these observations, revealing a significant age x sex interaction [$F(8,256)=3.6$, $p_{GG}\leq0.003$, $\eta_p^2=0.102$] with a prominent linear component [$F(1,32)=16.3$, $p\leq0.001$, $\eta_p^2=0.338$]. Significant main effects of age [$F(8,256)=11.5$, $p_{GG}\leq0.001$,

η_p^2=0.264] and sex [F(1,32)=103.0, $p\leq$0.001, η_p^2=0.763] were also observed. Male and female HIV-1 Tg animals were also best fit using a segmental linear regression (R^2s$\geq$0.62). Male HIV-1 Tg animals exhibited maximal PPI at approximately PD 300, while a rightward shift, with maximal PPI at PD 420, was observed in female HIV-1 Tg rats. Biological sex altered the rate of temporal processing development in HIV-1 Tg rats, with slower development observed in female HIV-1 Tg rats (β_1=201.8±127.1) relative to male HIV-1 Tg rats (β_1=1400±1097.5). The overall ANOVA confirmed these observations, revealing a significant main effect of age with a prominent linear component [F(1,29)=13.9, $p\leq$0.001, η_p^2=0.324] and sex [F(1,29)=12.3, $p\leq$0.002, η_p^2=0.297].

Locomotor Activity: Intrasession Habituation

The progression of intrasession habituation, used to assess long-term episodic memory, is illustrated in Figure 3.7. A one-phase decay was the best fit for HIV-1 Tg and control animals at all test sessions, however, significant differences between the best fit line were observed. Specifically, at PD 90 and PD 120, control animals, compared to HIV-1 Tg animals, exhibited a greater number of mean photocell interruptions, during the latter half of the test session. In contrast, at PD 300 and all subsequent test sessions, HIV-1 Tg animals displayed a greater number of mean photocell interruptions in the latter half of the session relative to controls.

The overall ANOVA confirmed these observations, revealing a significant age x time x genotype interaction [F(88,5368)=1.6, $p_{GG}\leq$0.025, η_p^2=0.0.25] with a prominent linear-quadratic component [F(1,61)=20.5, $p\leq$0.001, η_p^2=0.252]. Significant two-way interactions included an age x genotype interaction [F(8,488)=20.5, $p_{GG}\leq$0.001, η_p^2=0.252] with a prominent linear component [F(1,61)=96.9, $p\leq$0.001, η_p^2=0.614], an age x sex interaction [F(8,488)=2.2, $p_{GG}\leq$0.039, η_p^2=0.035] with a prominent quadratic component

[$F(1,61)=9.8$, $p\leq0.003$, $\eta_p^2=0.139$], a time x genotype interaction [$F(11,671)=18.3$, $p_{GG}\leq0.001$, $\eta_p^2=0.231$] with a prominent linear component [$F(1,61)=38.4$, $p\leq0.001$, $\eta_p^2=0.386$], a time x sex interaction [$F(11,671)=5.0$, $p_{GG}\leq0.002$, $\eta_p^2=0.076$] with a prominent linear component [$F(1,61)=10.6$, $p\leq0.002$, $\eta_p^2=0.148$], and an age x time interaction [$F(88,5368)=8.6$, $p_{GG}\leq0.001$, $\eta_p^2=0.124$] with a prominent linear-linear component [$F(1,61)=221.5$, $p\leq0.001$, $\eta_p^2=0.784$]. Significant main effects of age [$F(8,488)=102.4$, $p_{GG}\leq0.001$, $\eta_p^2=0.627$], time [$F(11,671)=1408.1$, $p_{GG}\leq0.001$, $\eta_p^2=0.958$], and sex [$F(1,61)=10.5$, $p\leq0.002$, $\eta_p^2=0.147$] were also observed. Thus, HIV-1 Tg animals failed to exhibit intrasession habituation, evidenced by significantly greater activity in the latter half of the test session, through advancing age, suggesting an impairment in long-term episodic memory.

DISCUSSION

Two interrelated goals were pursued to authenticate the utility of the HIV-1 Tg rat for the study of progressive neurocognitive deficits, a sequelae of long-term HIV-1 viral protein exposure (Vigorito et al., 2015). First, the integrity of auditory and visual sensory system function, assessed using cross-modal PPI, and motoric system function, examined using locomotor activity, was established. The integrity of sensory and motor systems in the HIV-1 Tg rat confirms the utility of the HIV-1 Tg rat in longitudinal experimental designs to determine the progression of HAND. Second, the progression of neurocognitive impairments, including temporal processing and long-term episodic memory, in the HIV-1 Tg rat were evaluated; the factor of biological sex was integral to the experimental design. Regardless of sex, HIV-1 Tg animals, relative to controls, displayed significant alterations in the development of auditory and visual PPI, suggesting a deficit in temporal processing.

However, significant sex differences in the progression of temporal processing were observed, with female HIV-1 Tg animals exhibited more pronounced deficits relative to male HIV-1 Tg animals. An impairment in long-term episodic memory, evidenced by significant alterations in intrasession habituation, was also observed in HIV-1 Tg animals relative to controls. Understanding the progression of HAND heralds an opportunity for the development of an advantageous model of neurocognitive deficits in HIV-1 and establishes critical groundwork for the development of neurorestorative and/or preventative treatments.

The integrity of sensory system function through advancing age in HIV-1 Tg and control animals was assessed using cross-modal PPI. Robust inhibition to the presence of auditory and visual prepulses was observed at all test sessions, confirming the integrity of sensory system function in both HIV-1 Tg and control animals. Notably, the phenotypic cataracts observed in the HIV-1 Tg rat do not prevent the animal from detecting brightness; visual acuity, however, has not yet been systematically investigated in the HIV-1 Tg rat. Robust inhibition to auditory, visual, and tactile prepulses have been previously observed in HIV-1 Tg and control animals, albeit at younger ages (e.g., 2-6 months of age, Moran et al., 2013a; 8-10 months of age, McLaurin et al., 2017a, McLaurin et al., 2017b). The present study provides a longitudinal assessment through the majority of the animal's functional lifespan, providing strong evidence for the integrity of sensory system function in the HIV-1 Tg rat.

Motoric system function was assessed using locomotor activity in HIV-1 Tg and control animals through advancing age. From PD 90 to PD 180, control animals exhibited a significantly greater number of mean photocell interruptions during the sixty-minute test

session, consistent with previous reports of decreased motor movement in HIV-1 Tg animals early (i.e., between 3-6 months) in development (June et al., 2009). No significant differences in the number of photocell interruptions between HIV-1 Tg and control animals were observed at PD 240 or PD 300. However, beginning at PD 360, and at all subsequent test sessions, HIV-1 Tg animals exhibited a significantly greater number of mean photocell interruptions relative to control animals. Thus, neither HIV-1 Tg nor control animals displayed gross-motoric system impairments through advancing age, indicative of the integrity of motor system function.

The overall health of HIV-1 Tg and control animals through advancing age was also assessed using growth rate. HIV-1 Tg animals, regardless of sex, weighed significantly less than control animals, but exhibited steady growth through PD 480 (approximately 16 months of age). The rate of growth, however, was significantly slower in male and female HIV-1 Tg animals relative to their control counterparts. Previous observations have reported no significant differences in the rate of growth, however, observations were restricted to younger animals (e.g., Peng et al., 2010; Moran et al., 2012; Moran et al., 2013b; Moran et al., 2014a; Roscoe et al., 2014). Early adulthood food restriction, as in the present study, may have played a role in altering the growth trajectory of HIV-1 Tg animals.

It is noteworthy that the observations in the present study (i.e., growth rates, integrity of sensory system function, intact motoric system function), differ from those reported in the original derivation of the HIV-1 Tg (Sprague-Dawley) rat, with transgene expression on chromosomes 2 and 9 (Reid et al., 2001). Specifically, Reid et al. (2001) reported relatively early wasting (i.e., 5-9 months of age), hind-limb paralysis, and AIDS

related organ pathologies. However, the current derivation of the HIV-1 Tg (F344/N) rat, used in the present study, is a healthier derivation of those originally described, with transgene expression limited to chromosome 9. In the present study, HIV-1 Tg rats exhibited no alterations in sensory system function (i.e., auditory or visual) or motor system function through advancing age. The integrity of gustatory system function has also been established using both one-bottle (Peng et al., 2010) and five-bottle (Bertrand et al., 2013) sucrose taste preference tests, which revealed no significant differences between HIV-1 Tg and control animals in sucrose consumption at any concentration. Thus, the present studies provide strong evidence for the functional health of the HIV-1 Tg rat through the majority of the animal's functional lifespan, suggesting the utility of the HIV-1 Tg rat in studies of the progression of neurocognitive deficits, including temporal processing and long-term episodic memory, commonly observed in HAND.

Prominent alterations in the progression of temporal processing, indexed using the area of inflection of the ASR amplitude response curve (McLaurin et al., 2016b), were observed in HIV-1 Tg animals, regardless of sex, relative to controls using cross-modal PPI. HIV-1 Tg animals displayed a significant leftward shift in the age at which maximal PPI was observed in both auditory and visual PPI. Specifically, in auditory PPI, control animals exhibited a significant increase in PPI as a function of age through approximately PD 300, followed by a subsequent decrease. HIV-1 Tg animals, however, displayed maximal PPI at approximately PD 270, followed by a subsequent decrease. In visual PPI, control animals exhibited an increase in PPI as a function of age through PD 360, followed by a subsequent decrease. In contrast, HIV-1 Tg animals displayed a significant leftward shift, with maximal PPI observed at PD 300. The present study establishes, via longitudinal

assessment, alterations in the progression of temporal processing through the majority of the functional lifespan of the HIV-1 Tg rat.

Temporal processing deficits in the HIV-1 Tg rat may result from DAergic system dysfunction, which has been implicated as a key target of HIV-1 infection. Alterations in DA system function have previously been reported using multiple techniques in the HIV-1 Tg rat, including immunofluorescence and Western blots (Webb et al., 2010; Moran et al., 2012; Reid et al., 2016a), as well as [18F] fallypride PET (Lee et al., 2014). The serial circuitry involved in PPI, established using lesioning (e.g., Fendt et al., 1994; Leitner & Cohen, 1985) and electrical stimulation studies (Li et al., 1998; Li & Yeomans, 2000), includes the brainstem and pedunculuopontine pathways. Alterations in the DAergic inputs at multiple points within the serial circuitry mediating PPI have downstream effects, ultimately altering startle response (Koch et al., 1999). The nucleus accumbens (Nac), which receives DAergic inputs from the ventral tegmental area (VTA), may be a critical loci for the regulation of PPI (Swerdlow et al., 1992). Specifically, the medial prefrontal cortex (mPFC), which exhibits thinning in HIV-1 seropositive humans (Thompson et al., 2005), may mediate DA release from the Nac via glutamateric projections (Koch et al., 1999). Decreased DAergic activity in the prefrontal cortex (PFC) increases DA release in the Nac (Koch et al., 1999); an effect which may be mediated by the glutamateric projection from the PFC to the VTA (Taber & Fibiger, 1995).

Pharmacological and behavioral studies have also been used to establish the role of DA in PPI (review, Geyer et al., 2001). Administration of DA agonists, including apomorphine (e.g., Fitting et al., 2006b), SCH 39166 (e.g., Ellenbroek et al., 1996), sulpiride (e.g., Ellenbroek et al., 1996), and amphetamine (e.g., Mansbach et al., 1998;

Zhang et al., 2000), produced a marked decrease in PPI. Administration of apomorphine subcutaneously in Sprague-Dawley rats stereotaxically injected with gp120, a HIV-1 viral protein, produced significant alterations in PPI, evidenced by a decrease in startle response amplitude and an insensitivity to the manipulation of ISI (Fitting et al., 2006b); results which are comparable to temporal processing deficits observed in the HIV-1 Tg rat. Significant reductions in PPI were also observed following local injections of either SCH39166 or sulpiride into the mPFC (Ellenbroek et al., 1996). Examination of the neurotransmitter adenosine, which may interact with DA in the CNS (Ferré et al., 1992), provides additional evidence for the role of DA in the regulation of PPI (e.g., Hauber & Koch, 1997). Thus, DA system dysfunction in the HIV-1 Tg rat may underlie alterations in the progression of temporal processing deficits observed in the present study.

Profound alterations in the progression of intrasession habituation were observed in the HIV-1 Tg rat in comparison to control animals, suggesting an impairment in long-term episodic memory. Beginning at PD 300 and at all subsequent test sessions, HIV-1 Tg animals displayed significant deficits in intrasession habituation, evidenced by a higher level of activity during the latter half of the session; a pattern compatible with impairment in long-term episodic memory. Multiple experimental paradigms (e.g., locomotor activity, rotarod, wheel running) have revealed alterations in both intrasession habituation (Moran et al., 2013b) and intersession habituation (Chang et al., 2006; Reid et al., 2016b) in the HIV-1 Tg rat. The present study, using a longitudinal experimental design, confirmed robust alterations in intrasession habituation through the majority of the functional lifespan of the HIV-1 Tg rat.

Alterations in intrasession habituation may also result from DA system dysfunction. Multiple pharmacological studies have provided evidence for the role of DA in intrasession habituation (Carlsson, 1972; Giros et al., 1996, Wong et al., 2003). Specifically, administration of apomorphine, a DA agonist, in rats produced decreased intrasession habituation (Carlsson, 1972). DA transporter (Giros et al., 1996) and D_1 receptor knockout mice (Wong et al., 2003) also exhibited decreased intrasession habituation in locomotor activity. Additional studies are needed, however, to determine whether alterations in intrasession habituation result from the effects of increased DA on the motor system (Leussis & Bolivar, 2006). Notably, DA release may also be critical for the formation of long-term episodic memories, commonly assessed in animal models using intrasession habituation. Lisman and Grace (2005) proposed the hippocampus-VTA loop, suggesting that DA release from the hippocampus may be vital for long-term episodic memory encoding and retrieval. A pharmacological study found that infusion of a DA antagonist into the rat hippocampus prior to encoding impairs long-term memory (Bethus et al., 2010).

The assessment of sex differences was an integral component of the experimental design, addressing the need for direct comparisons of neurocognitive deficits in males and females in both clinical and preclinical studies (Maki & Martin-Thormeyer, 2009; Maki et al., 2015). The factor of biological sex may moderate the progression of neurocognitive deficits, including temporal processing, in the HIV-1 Tg rat. Female HIV-1 Tg animals, compared to male HIV-1 Tg animals, exhibited more prominent deficits in temporal processing. Specifically, in auditory PPI, female HIV-1 Tg animals failed to display any significant development in temporal processing as a function of age. In visual PPI, female

HIV-1 Tg animals, exhibited a slower development of PPI, relative to male HIV-1 Tg animals. Sex differences in the progression of temporal processing extend those reported in auditory gap-PPI, examined using an early, time-limited longitudinal experimental design (McLaurin et al., 2016b), suggesting the generality and relative permanence of these deficits. In sharp contrast, neither compelling nor consistent sex differences were observed in the progression of intrasession habituation. Thus, biological sex may selectively moderate the influence of the HIV-1 transgene on the progression of neurocognitive deficits.

The present study provides a critical foundation for future studies examining the progression of executive function and attention deficits, which are commonly altered in HIV-1 seropositive individuals (Heaton et al., 2010; Heaton et al., 2011). For example, signal detection tasks (McGaughy & Sarter, 1995), which rely on intact sensory and motoric system function, can be used to assess sustained attention, as well as more complex executive functions, including inhibition and flexibility. In signal detection, the presence or absence of a stimulus (i.e., houselight, auditory tone) indicates the response an animal must make (i.e., which lever to press) to receive a reinforcer. We have previously used the signal detection task to assess cognitive functions in the HIV-1 Tg rat, reporting significant deficits in sustained attention, flexibility and inhibition (Moran et al., 2014a). However, a systematic evaluation of the progression of sustained attention deficits, and the effect of biological sex, in the HIV-1 Tg rat is needed.

Establishing the integrity of auditory and visual system function, as well as motoric system function, suggests the utility of the HIV-1 Tg rat for examining the progression of HAND. Further, results of the present study substantiated significant alterations in the

progression of temporal processing, which may underlie executive function and attentional deficits commonly observed in the post-cART era (Heaton et al., 2010; Heaton et al., 2011). Additionally, alterations in the progression of intrasession habituation, suggestive of an impairment in long-term episodic memory, were observed. Results provide a strong foundation for future studies assessing the progression of executive function deficits, and the effect of biological sex, in the HIV-1 Tg rat using a longitudinal experimental design. Understanding the progression of HAND, heralds an opportunity for the development of an advantageous model of neurocognitive deficits in HIV-1 and establishes critical groundwork for the development of neurorestorative treatments.

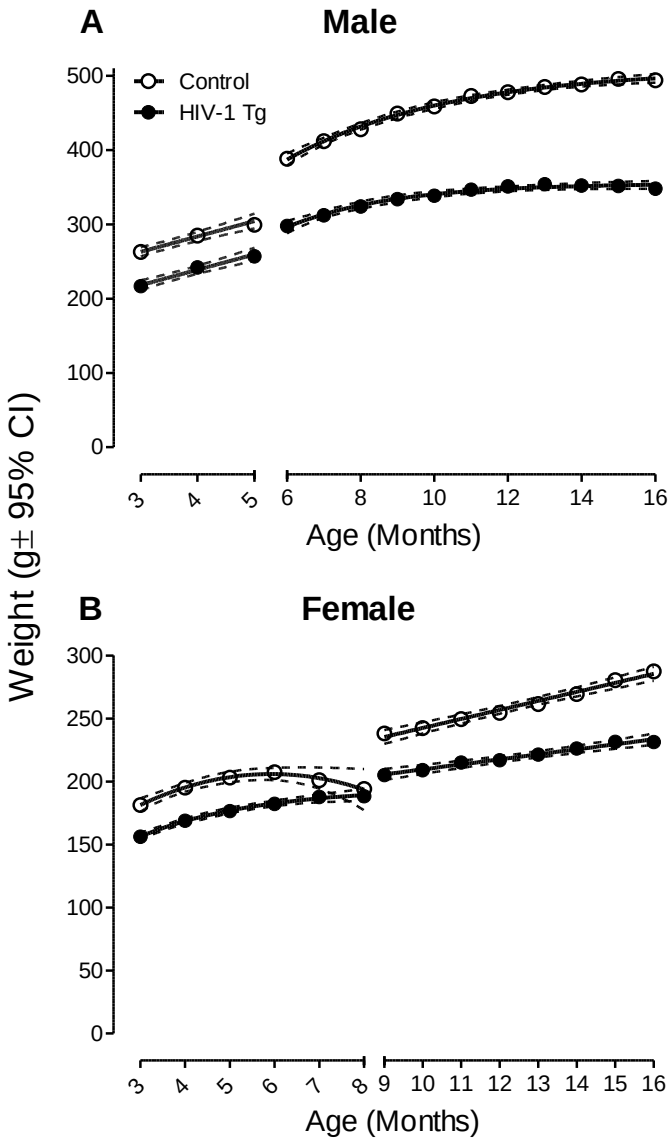

Figure 3.1 Body Weight. Mean body weight is illustrated for both males (**A**) and females (**B**) as a function of genotype (HIV-1 Tg vs. control) and age (±95% CI). HIV-1 Tg animals, regardless of sex, weighed significantly less than control animals, but exhibited steady growth through approximately 16 months of age. Notably, after a prior history of food restriction, both male and female HIV-1 Tg animals grew at a significantly slower rate relative to controls. The x-axis break at 6 months for males and 9 months for females indicates the point at which all animals were again receiving food *ad libitum.*

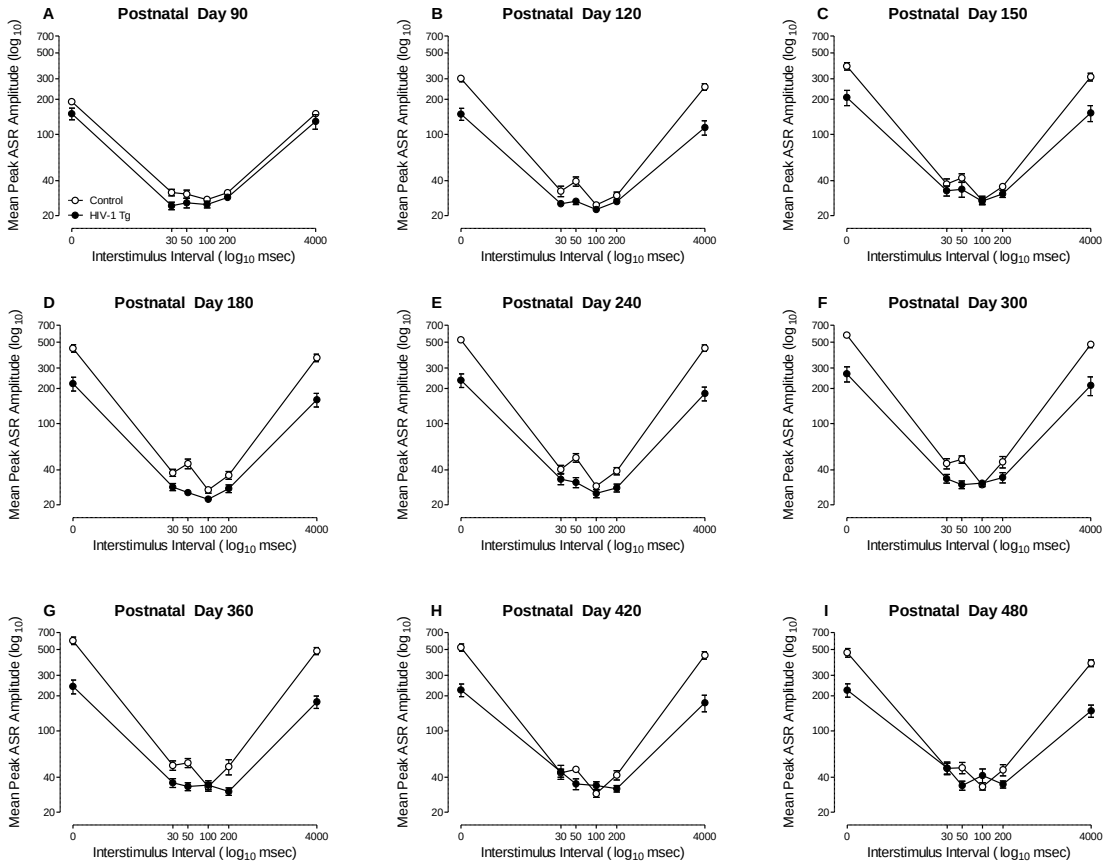

Figure 3.2 Auditory System Function. Mean peak ASR amplitude (±SEM) for auditory PPI is illustrated for all test sessions as a function of genotype (HIV-1 Tg vs. Control). Both HIV-1 Tg and control animals exhibited robust inhibition to the auditory prepulse at all ages, albeit at different ISIs, suggesting the integrity of auditory system function through the majority of the animal's functional lifespan.

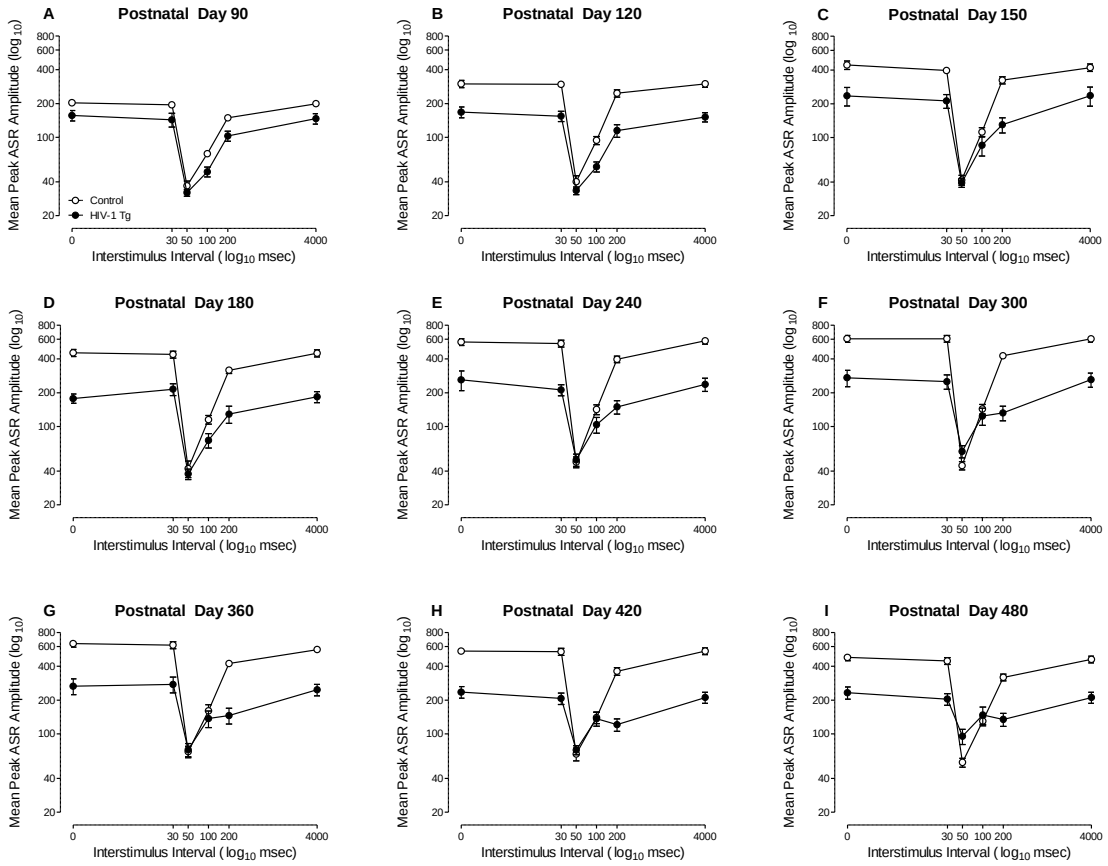

Figure 3.3 Visual System Function. Mean peak ASR amplitude (±SEM) for visual PPI is illustrated for all test sessions as a function of genotype (HIV-1 Tg vs. Control). Maximal inhibition was observed at the 50 msec ISI for both HIV-1 Tg and control animals at all test sessions. Robust inhibition to the visual prepulse was observed in both HIV-1 Tg and control animals at all assessments, suggesting the integrity of visual system function through the majority of the animal's functional lifespan.

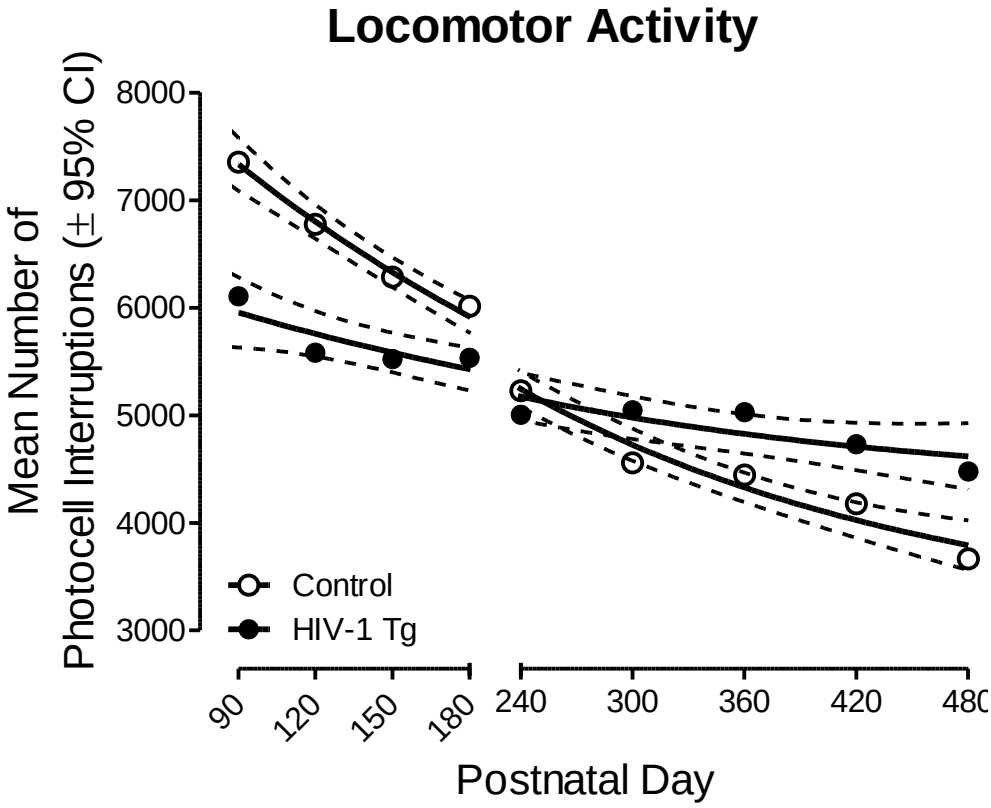

Figure 3.4 Gross-Motoric System Function. Mean number of photocell interruptions in a 60-minute locomotor activity test session are illustrated as a function of genotype (HIV-1 Tg vs. control) and age (±95% CI). A one-phase decay was the best fit for HIV-1 Tg and control animals, however, significant differences in the fit of the function were observed [$F(3,12)=41.1$, $p \leq 0.001$]. From PD 90 to PD 180, control animals exhibited a significantly greater number of mean photocell interruptions relative to HIV-1 Tg animals. However, beginning at PD 360 and all subsequent test sessions, HIV-1 Tg animals, compared to controls, displayed a significantly greater number of mean photocell interruptions. Results, therefore, suggest no gross-motoric impairments in either HIV-1 Tg or control animals through advancing age.

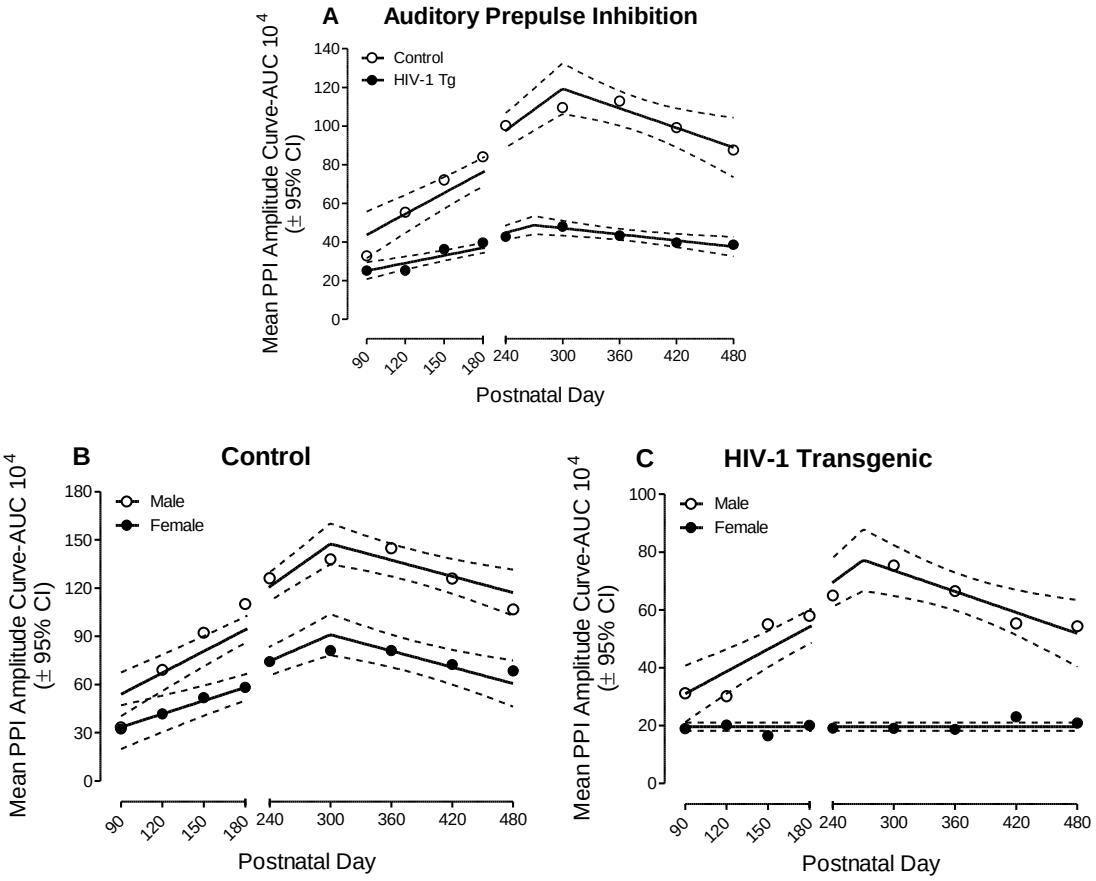

Figure 3.5 Progression of Temporal Processing: Auditory PPI. Auditory PPI, assessed using mean area of the peak inflection curve, is illustrated as a function of genotype (HIV-1 Tg vs. control) and age (±95% CI). (**A**) A segmental linear regression was the best fit for HIV-1 Tg and control animals (R^2s≥0.91). Temporal processing in control animals was well-described using a segmental linear regression, with maximal PPI observed at PD 300. In contrast, HIV-1 Tg animals displayed a prominent leftward shift, with maximal inhibition observed at approximately PD 270. (**B**) A segmental linear regression was the best fit for both male and female (R^2s ≥0.90) control animals, with maximal PPI occurring at approximately PD 300. However, female control animals exhibited a significantly slower rate of temporal processing development from PD 90 to PD 300 compared to male control animals. (**C**) A segmental linear regression, with maximal PPI at approximately PD 270, provided a well-described fit for male HIV-1 Tg animals (R^2=0.88). Female HIV-1 Tg animals, however, failed to exhibit any significant temporal processing development as a function of age, best fit using a horizontal line. Thus, regardless of sex, HIV-1 Tg animals displayed significant alterations in the progression of temporal processing, assessed using auditory PPI, compared to control animals.

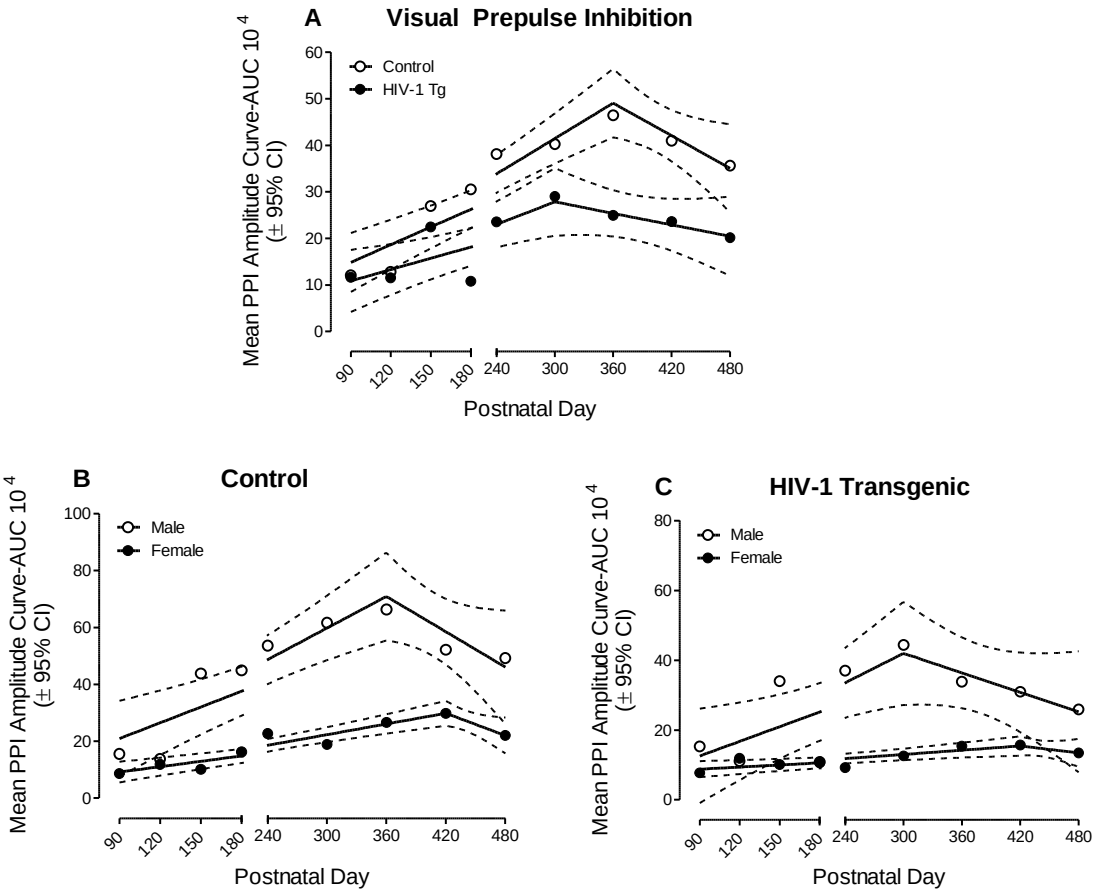

Figure 3.6 Progression of Temporal Processing: Visual PPI. Visual PPI, assessed using mean area of the peak inflection curve, is illustrated as a function of genotype (HIV-1 Tg vs. control) and age (±95% CI). (**A**) A segmental linear regression was the best fit function for both HIV-1 Tg and control animals (R^2s≥0.70), A significant leftward shift in the point of maximal inhibition was observed in HIV-1 Tg animals (PD 300) relative to control animals (PD 360). (**B**) Significant alterations in the development of temporal processing were observed in control animals dependent upon biological sex. Specifically, both male and female control animals were best fit using a segmental linear regression (R^2s ≥0.82). Male control animals exhibited a significant increase in PPI through PD 360, followed by a subsequent decrease. In contrast, a rightward shift, with maximal PPI observed at PD 420, was observed in female control animals. (**C**) Biological sex moderated the progression of temporal processing deficits in HIV-1 Tg animals. A segmental linear regression provided a well-described fit for both male and female HIV-1 Tg animals, with maximal PPI observed at PD 300 and PD 420 respectively (R^2s≥0.62). The factor of biological sex, however, altered the rate of temporal processing development in HIV-1 Tg rats, with slower development observed in female HIV-1 Tg rats relative to male HIV-1 Tg rats. HIV-1 Tg animals, regardless of sex, exhibited profound alterations in the progression of temporal processing, assessed using visual PPI, relative to control animals.

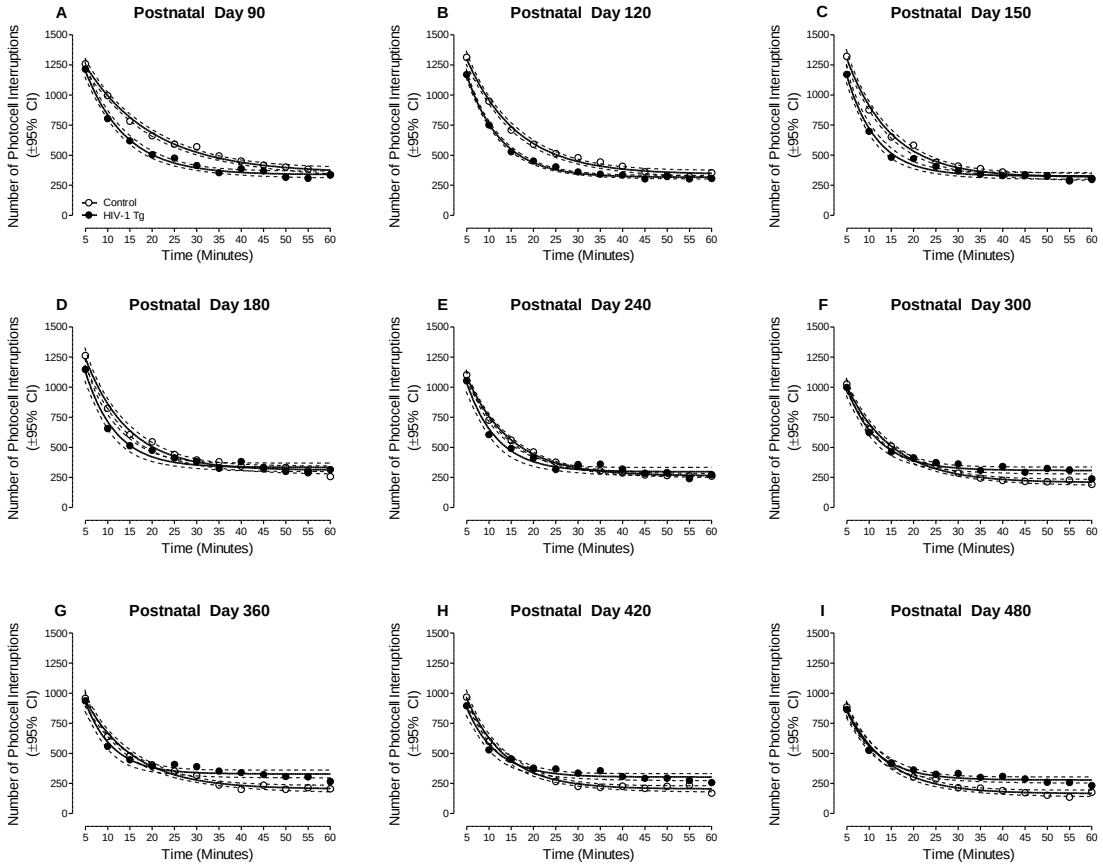

Figure 3.7 Long-Term Episodic Memory. Mean number of photocell interruptions during locomotor habituation trials across twelve 5-min trial blocks are illustrated at all test sessions as a function of genotype (HIV-1 Tg, control; ±95% CI). Significant alterations in intrasession habituation in the HIV-1 Tg rat were observed at PD 300 and all subsequent test sessions, evidenced by a higher level of activity during the latter half of the session. Alterations in intrasession habituation suggest an impairment in long-term episodic memory in HIV-1 Tg animals.

CHAPTER 4

DISRUPTION OF TIMING: NEUROHIV PROGRESSION IN THE POST-CART ERA[3]

[3] KA McLaurin, H Li, RM Booze, CF Mactutus. 2019. *Scientific Reports.* 9(1):827. Reprinted here with permission of publisher.

INTRODUCTION

HIV-1 remains a human health pandemic, with approximately 36.7 million individuals living with the disease worldwide (UNAIDS, 2017). Older individuals (>50 years of age) account for approximately 30-50% of HIV-1 seropositive individuals in high-resource countries (UNAIDS, 2013) following the great success of cART; a prevalence that is expected to reach approximately 73% by 2030 (Smit et al., 2015). In the post-cART era, milder forms of NCI have become a hallmark of HIV-1, afflicting between 40-70% of HIV-1 seropositive individuals (Letendre et al., 2010; McArthur et al., 2010; Heaton et al., 2011). Cross-sectional studies have provided a wealth of knowledge on HAND, characterized by deficits in higher-order cognitive processes (e.g., attention, working memory, executive function: Heaton et al., 2011; Cysique et al., 2004). However, extrapolating cross-sectional findings to age-related disease progression is inferentially fraught (Kraemer et al., 2000), heralding an examination of the progression of HAND using a longitudinal experimental design.

Since the seminal call for animal models of HIV-1/AIDS (WHO, 1988), there has been no extant *in vivo* animal model system available to provide a truly longitudinal study of HAND. The HIV-1 Tg rat, originally developed by Reid et al. (2001), contains a *gag-pol* deleted provirus regulated by the human viral promoter. HIV-1 Tg rats exhibit general good health through advancing age, displaying steady growth rates (Peng et al., 2010; Roscoe et al., 2014; Moran et al., 2013a), intact sensory (i.e., auditory, visual, gustatory) and motor system function (Peng et al., 2010; McLaurin et al., 2018b), and a lifespan of approximately 21 months of age (Peng et al., 2010). Cross-sectional studies have critically tested the utility of the HIV-1 Tg rat as a model for NCI; multiple laboratories have reported alterations in temporal processing (e.g., Moran et al., 2013a), sustained attention (e.g.,

Moran et al., 2014a), learning (Vigorito et al., 2007; Moran et al., 2014a), and memory (Repunte-Canonigo et al., 2014). A longitudinal assessment of NCI for the progression of HAND, and associated neural mechanisms, in the HIV-1 Tg rat, however, remains a critical knowledge gap.

Thus, in the present study, the HIV-1 Tg rat was used to establish the trajectory of NCI, in the absence of sensory or motor system deficits (McLaurin et al., 2018b) and comorbidities, across the functional lifespan. It was hypothesized that HIV-1 Tg rats, relative to F344/N controls, would display progressive, sex-dependent expression of NCI across the function lifespan; impairments that were associated with synaptic dysfunction in pyramidal neurons from layers II-III of the mPFC and/or neuroinflammatory markers in the hippocampus. A longitudinal experimental design was used to assess multiple neurocognitive domains, including learning, sustained attention, flexibility and inhibition, from approximately PD 60 through PD 600. Associated neural mechanisms, including synaptic dysfunction in the mPFC and putative markers of neuroinflammation in the hippocampus were also evaluated. The progression of HAND with age in the HIV-1 Tg rat and associated synaptic dysfunction in the mPFC affords an instrumental model system for the development of therapeutics and functional cure strategies.

METHODS

Experimental Design

The experimental design for all neurocognitive assessments and neuroanatomical assessments is illustrated in Figure 4.1.

Animals

Across 12 months, Fischer (F344/N; Harlan Laboratories Inc., Indianapolis, IN) HIV-1 Tg (*N*=20 litters) and control (*N*=17 litters) rats were received at the animal vivarium, between PD 7 and PD 9, housed with their biological dam. At approximately PD 21, animals were sampled from each litter (HIV-1 Tg: male, *n*=37, female, *n*=33; Control: male *n*=34; female, *n*=33), weaned and pair- or group-housed with animals of the same sex for the duration of experimentation.

During the original acquisition of signal detection, animals were placed on food restriction, beginning at approximately PD 60, to maintain 85% body weight. After animals successfully acquired the signal detection task (PD 100-PD 277), rodent food was again provided *ad libitum*, including during all retest assessments. HIV-1 Tg and control animals had *ad libitum* access to water throughout the duration of the study.

HIV-1 Tg and control animals were sacrificed following the successful completion of the reversal task at approximately 20 months of age to assess synaptic dysfunction in pyramidal neurons from layers II-III of the mPFC and putative markers of neuroinflammation in the hippocampus. Due to health issues, including significant weight loss (*n*=23), tumors (*n*=6), natural death (*n*=3) or other (*n*=4), some animals were euthanized prior to 20 months of age.

Recommendations in the Guide for the Care and Use of Laboratory Animals of the NIH were used for the maintenance of HIV-1 Tg and control animals in AAALAC-accredited facilities. The targeted environmental conditions for the animal vivarium were 21°± 2°C, 50% ± 10% relative humidity and a 12-h light:12-h dark cycle with lights on at

0700 h (EST). The IACUC at the University of South Carolina approved the project protocol (Federal Assurance # D16-00028).

Phase 1: Original Acquisition

Apparatus

Sixteen operant chambers, located inside sound-attenuating chambers (Med Associates, Inc., VT) were used to train animals in a signal detection task tapping sustained attention. A pellet dispenser (45 mg), located between two retractable levers, and three panel lights were located on the front wall of the operant chambers. Only the panel light located above the pellet dispenser was used in the present experiment. A house light was located at the top of the rear wall of the operant chamber. The house light, used for shaping, and central panel light, used for signal presentation during the original acquisition of signal detection and retest assessments, were incandescent (22 lux). PC and Med-PC for Windows software (V 4.1.3; Med Associates, Inc., Fairfax, VT) controlled signal presentation, lever operation, reinforcement delivery, and data collection.

Shaping

A standard shaping response protocol was used to train animals to lever-press at approximately 2 months of age, described in detail by McLaurin et al. (2017d). All animals met criteria in shaping (i.e., 60 reinforcers for 3 consecutive or 5 non-consecutive days), indicating learning the operant response, prior to beginning the signal detection task.

Signal Detection

Following successful acquisition of shaping, all HIV-1 Tg (*N*=20 litters; male, *n*=37, female, *n*=33) and control animals (*N*=17 litters; male *n*=34; female, *n*=33) were trained in a signal detection task, tapping sustained attention.

Three vigilance programs, initially described by McGaughy and Sarter (1995), were employed. In brief, animals were trained to discriminate between signal (i.e., central panel light illumination) and non-signal (i.e., no illumination) trials. In the first vigilance program, consisting of 160 trials per session, termination of the stimulus light was contingent upon a response. In the second vigilance program, consisting of 160 trials per session, the length of the stimulus light was 1 sec. Correction trials, including up to three repetitions of the trial, and force-choice trials were an integral component of the first two vigilance programs, and occurred when an animal responded incorrectly. In the third vigilance program, consisting of 162 trials per session, the length of the stimulus was manipulated (i.e., 1000, 500, 100 msec) across trials using a block randomized experimental design. Correction trials and force-choice trials were removed in the third vigilance program. During the initial acquisition, no data was censored i.e., each and every animal successfully acquired the signal detection task. A preliminary report of original acquisition, on approximately half of the animals, was presented in McLaurin et al. (2017d). Additional methodological details are presented in the Appendix B.

Phase 2: Retest Assessments

Apparatus

Throughout the retest assessments, HIV-1 Tg and control animals were assessed in the operant chambers described above.

Procedure

After the successful completion of original acquisition, HIV-1 Tg and control animals were assessed in the final vigilance program with varying signal durations every 60 days through approximately 18 months of age. Animals were given up to 60 days to

successfully complete each retest assessment and were assessed in up to 6 retest assessments.

Phase 3: 18 Month Assessment

Apparatus

At the 18 Month Assessment, HIV-1 Tg and control animals were assessed in the operant chambers described above with a minor modification. An LED light bulb (11 lux), instead of an incandescent light bulb, was used for signal presentation during the 18 month acquisition and reversal assessment due to the short (i.e., 10 msec) signal duration times.

Procedure

After the successful completion of the 6th retest assessment or at 18 months of age, HIV-1 Tg and control animals were challenged with two tasks. First, HIV-1 Tg (*N*=20 litters; male, *n*=29, female, *n*=29) and control animals (*N*=17 litters; male *n*=28; female, *n*=31) were challenged for 5-consecutive days with shorter signal durations (i.e., 1000, 100, 10 msec). Second, HIV-1 Tg (*N*=20 litters; male, *n*=18, female, *n*=29) and control animals (*N*=17 litters; male *n*=27; female, *n*=28) were assessed in a reversal task, tapping flexibility and inhibition. Response contingencies were reversed from those originally learned in the signal detection task. Animals were given up to 60 days to successfully complete the reversal assessment or were sacrificed at approximately 20 months of age after 45 days in the task.

Phase 4: Neuroanatomical Assessments

Synaptic Dysfunction

Preparation of Tissue. Animals were deeply anesthetized using sevoflurane (Abbot Laboratories, North Chicago, IL) and transcardially perfused using methodology adapted from Roscoe et al. (2014).

DiOlistic Labeling. A DiOlisitc labeling technique, originally described by Seabold et al. (2010), was used to visualize pyramidal neurons from layers II-III of the mPFC. Methodology for the preparation of DiOlistic cartridges, preparation of Tefzel tubing, and DiOlistic labeling is described in detailed by McLaurin et al. (2018a).

Pyramidal Neuron Dendritic Analysis and Spine Quantification. Pyramidal neurons from layers II-III of the mPFC, located approximately 3.7 mm to 2.2 mm anterior to Bregma (Paxinos & Watson, 2014), were analyzed. Z-stack images were obtained using methodology previously reported (Roscoe et al., 2014) on three to four pyramidal neurons from each animal [Control: *N*=17 litters, male, *n*=31, female, *n*=30; HIV-1 Tg: *N*=20 litters, male, *n*=35, female, *n*=33].

The AutoNeuron and AutoSpine extension modules, available in Neurolucida 360 (MicroBrightfield, Williston, VT), were used for the analysis of spine parameters. Selection criteria, including continuous dendritic staining, low background/dye clusters, and minimal diffusion of the DiI dye into the extracellular space, were used for spine analysis. Based on the selection criteria, one neuron from each animal was chosen for the analysis of spine parameters. Neurons not meeting the selection criteria were not included in the analysis, yielding Control, *N*=16 litters, male, *n=26,* female, *n*=20, and HIV-1 Tg *N*=19 litters, male, *n=28*, female, *n*=27.

Spine Parameters. An observer-assisted automatic classification of dendritic spines (i.e., thin, mushroom, stubby) was conducted using an algorithm in Neurolucida 360 (Rodriguez et al., 2008). The number of segments at each branch order, an assessment of dendritic branching complexity, was examined for branch orders 1 through 10. A Sholl analysis was conducted to evaluate neuronal complexity (i.e., the number of intersections

at each successive radii) and dendritic spine connectivity (i.e., the number of dendritic spines between each successive radii). Some animals were excluded due to processing errors, yielding Control, *N*=16 litters, male, *n*=21, female, *n*=18, and HIV-1 Tg *N*=17 litters, male, *n=26,* female, *n*=23. Subsequently, dendritic spine morphology was assessed using three parameters, including backbone length (µm), head diameter (µm), and volume (μm^3). Spine parameters were defined using well-accepted previously published results (i.e., backbone length, 0.1 to 4.1 µm: Ruszczycki et al., 2012; head diameter, 0 to 0.825 µm: Konur et al., 2003; volume, 0.05 to 0.5 μm^3: Hering & Sheng, 2001).

Neuroinflammatory Markers

The selection of the hippocampus for the assessment of neuroinflammation was based on the publication of Fitting et al. (2008b; 2010), which displayed frank cell loss in the hippocampus from viral protein exposure, maximizing the likelihood of detecting neuroinflammation.

Total RNA isolation and cDNA synthesis. Total RNA was isolated from 30 mg of hippocampal tissue using RNeasy FFPE kit (QIAGEN) according to manufacturer's protocol (Control: *N*=17 litters, male, *n*=31 female, *n*=30; HIV-1 Tg: *N*=20 litters, male *n*=32, female *n*=30). The total RNA quality and quantity were assessed by a Nano drop spectrophotometer (Thermo Scientific, USA). One µg of total RNA from each sample was converted into cDNA by Cloned AMV first-strand cDNA synthesis kit (Invitrogen) for real-time PCR. The 20 µl first-strand cDNA synthesis reaction mixture contained 1 µl random-hexamer primer, 1 µg total sample RNA sample, 2 µl of 10 mM dNTP mix, 5x cDNA synthesis buffer, 1 µl of 0.1 M DTT, 1 µl RNaseOUT, 1 µl cloned AMV RT and 1 µl DEPC-treated water. The following conditions were used: 65 °C for 5 min, 25 °C for 10

min, 50 °C for 50 min and terminated at 85 °C for 5 min. The cDNA products were used immediately for further analysis.

Multiplex PCR (mPCR). Initially, hippocampal samples were probed for the expression of TNF-α, IL-1β, IL-6, NFκ-β and Iκ-β, and the internal control, GAPDH. Cytokine primers, a PCR reaction buffer containing dNTPs and a positive control were provided in a commercial mPCR kit from Maxibio Company (Rat Inflammatory Cytokines–Set 2, Cat. No. MP-70207, San Francisco, CA, as previously employed by Moran et al. (2014b). However, there was no significant expression of TNF-α, IL-1β, IL-6, NFκ-β or Iκ-β in samples from HIV-1 Tg or F344/N control animals. Accordingly, we pursued analysis via real-time PCR.

Real-time PCR. The neuroinflammation related cytokines (TNF-α, IL-1β, IL-6) were quantified using a real-time PCR detection system and SsoAdvanced Universal SYBR Green Supermix kit (BIO-RAD). In brief, the 20 μl reaction mixture contained 10 μl 2x SsoAdvanced universal SYBR Green supermix, 1 μl forward primer and reverse primers (250 nM each), 1 μl template (100 ng) and 7 μl of DEPC-treated water. Reactions were performed with the DNA Engine Opticon 2 system (M J Research, USA) using the following cycling conditions: 30 sec at 95 °C and 40 cycles of 15 sec at 95 °C and 30 sec at 58 °C. Animals failing to reach threshold after 40 cycles were considered to have undetectable gene expression and accordingly these censored data were not included in the figures or statistical analysis, yielding Control, N=8-15 litters, male, n=7-18, female, n=8-12, and HIV-1 Tg N=11-13 litters, male, n=6-14, female, n=9-15, dependent upon gene. The data were analyzed using Intuitive Opticon Monitor TM software. Each primer, including the corresponding GenBank numbers, are listed in Table B.1, and β-Actin was

used as an internal control. The relative gene expression of each neuroinflammatory marker (i.e., TNF-α, IL-1β, IL-6) was analyzed using the $2^{-\Delta\Delta Ct}$ method to examine relative changes in expression dependent upon genotype and biological sex (Livak & Schmittgen, 2001).

Statistical Analysis

Given the nested experimental design (i.e., pups within litter), figures, created using GraphPad Prism 5 (GraphPad Software, Inc., La Jolla, CA), represent litter means and standard errors, dependent upon biological sex (Denenberg, 1984; Wears, 2002).

ANOVA and regression techniques were used for the analysis of all data (SAS/STAT Software 9.4, SAS Institute, Inc., Cary, NC; SPSS Statistics 24, IBM Corp., Somer, NY; GraphPad Software, Inc., La Jolla, CA). For all statistical analyses, litter was used as the unit of analysis to preclude the violation of the assumption of independence, leading to an inflation of Type 1 error rate (Holson & Pearce, 1992). Orthogonal decomposition of the repeated-measures factors or the conservative Greenhouse-Geisser *df* correction factor (p_{GG}; Greenhouse & Geisser, 1959) were used to preclude potential violations of sphericity. Effect size was assessed using η_p^2. An alpha value of $p \leq 0.05$ was considered significant for all statistical tests. Additional details on the statistical analyses are available in the Appendix B.

Data Availability Statement

All relevant data are within the paper.

RESULTS

Phase 1: Original Acquisition

The factor of biological sex was the driving factor for observed differences in the temporal process of acquisition and sustained attention during the initial acquisition of signal detection.

Temporal Process of Acquisition. All HIV-1 Tg and control animals were able to successfully acquire the task, achieving 70% accuracy for 5 consecutive or 7 non-consecutive days in each of the three vigilance programs. Profound sex differences were observed in the temporal process of task acquisition, best fit using a sigmoidal dose-response curve (Figure 4.2; R^2s$\geq$0.98). Female animals, independent of genotype, acquired the task significantly slower than male animals (Main Effect: Sex [$F(1,61)=101.1$, $p\leq0.001$]). Presence of the HIV-1 transgene failed to significantly alter the temporal process of initial acquisition of signal detection (Figure 4.2; $p>0.05$).

Signal Detection. The factor of biological sex (Figure 4.2) was the driving factor for observed differences in sustained attention during the initial acquisition of signal detection. Female animals, collapsed across genotype, displayed a decreased response rate, as well as a prominent rightward shift in the loss of signal detection (i.e., where the number of hits and misses intersect), relative to male animals (approximately 535 msec vs. 436 msec, respectively; Sex x Response Type x Duration Interaction [$F(2,122)=74.0$, $p_{GG}\leq0.0001$, $\eta_p^2=0.548$, Power=1.0]) with a prominent linear-linear component [$F(1,61)=87.2$, $p\leq0.0001$, $\eta_p^2=0.588$, Power=1.0]. In sharp contrast, presence of the HIV-1 transgene failed to alter signal detection during initial acquisition (Figure 4.2; Genotype x Response Type x Duration Interaction [$p>0.05$]).

Phase 2: Retest Assessments

HIV-1 Tg animals, independent of biological sex, exhibited a progressive impairment in task acquisition across retest assessment.

Days to Criteria. HIV-1 Tg and control animals were retested every 60 days in the final vigilance program, which manipulated signal duration length (1000, 500, 100 msec). Completion of the retest assessment required animals to meet criteria of 70% accuracy for 5 consecutive or 7 non-consecutive days. To assess the progression of task acquisition across retest assessments, the number of days required for 80% of the population sampled to meet criteria was quantified (Figure 4.3). Control animals displayed a continuous improvement in task acquisition across retest assessments, reaching asymptotic performance at approximately 7 days. In sharp contrast, HIV-1 Tg animals exhibited an improvement in task acquisition through retest session 2, followed by a progressive decline. Assessment of the temporal process of acquisition at each individual retest assessment (Figure B.1) revealed a significant main effect of genotype ($p \leq 0.05$) at all retest assessments.

Despite the "savings" afforded by repeated testing, HIV-1 Tg animals displayed a progressive, relative impairment in the detection of shorter signal durations.

Signal Detection. Across retest assessments, genotype became the driving factor for observed differences in sustained attention. Independent of genotype, HIV-1 Tg and control animals exhibited a significant improvement in the detection of shorter signal durations across retest assessments (Figure 4.4). However, HIV-1 Tg animals displayed a progressive, relative impairment in the detection of shorter signal durations relative to

control animals (Genotype x Response Type x Duration x Retest Assessment Interaction [$F(8,488)=2.2$, $p_{GG}\leq 0.05$, $\eta_p^2=0.034$, Power=0.763] with a prominent quadratic-quadratic component [$F(1,61)=7.3$, $p\leq 0.009$, $\eta_p^2=0.106$, Power=0.756]). Specifically, HIV-1 Tg animals took significantly longer to reach the same level of performance (e.g., Loss of Signal Detection at 10 msec: Control animals (Retest 1); HIV-1 Tg animals (Retest 5)) and failed to improve to the level of control animals at any retest assessment.

Relative to genotype, the factor of biological sex played a less prominent role in the progression of sustained attention (Sex x Response Type x Duration x Retest Assessment Interaction with a prominent linear-linear component [$F(1,61)=5.3$, $p\leq 0.025$, $\eta_p^2=0.080$, Power=0.622]). Female animals, independent of genotype, failed to improve to the same level of performance as male animals.

Phase 3: 18 Month Assessment

A more challenging signal detection task at 18 months of age, in combination with a reversal task, tapping flexibility and inhibition, revealed marked impairment, dependent upon task and biological sex, in HIV-1 Tg rats relative to control animals.

Temporal Process of Acquisition. At 18 months of age, HIV-1 Tg and control animals were challenged for 5 consecutive days with shorter signal durations (i.e., 1000, 100, 10 msec). The number of days HIV-1 Tg and control animals met criterion was analyzed using a curve-fitting analysis. For male animals, independent of genotype, an exponential growth equation provided a well-described fit (Figure 4.5; $R^2s\geq 0.98$). However, significant differences in the parameters of the function were observed ($F(2,15)=57.4$, $p\geq 0.001$), indicating a shift in the distribution, with male HIV-1 Tg animals

meeting criterion on fewer days relative to male control animals. In sharp contrast, a global, exponential growth equation ($R^2 \geq 0.96$) provided a well-described fit for female HIV-1 Tg and control animals (Figure 4.5), indicating no significant genotype differences in the number of days meeting criterion during the 18 month acquisition.

Subsequently, animals were assessed in a reversal task, tapping flexibility and inhibition. Presence of the HIV-1 transgene had a profound effect on the temporal process of acquisition in reversal, dependent upon the factor of biological sex (Figure 4.5; Genotype x Sex Interaction: [$F(1,51)=4.8$, $p \leq 0.033$]).

Complementary analyses were conducted for each sex to determine the locus of the interaction. In male animals (Figure 4.5), presence of the HIV-1 transgene significantly altered the temporal process of acquisition with male HIV-1 Tg animals acquiring the task significantly slower than male control animals (Main Effect, Genotype: [$F(1,26)=9.5$, $p \leq 0.005$]). In sharp contrast, presence of the HIV-1 transgene failed to significantly alter the temporal process of acquisition in female animals (Figure 4.5; $p>0.05$).

Signal Detection. Assessment of signal detection data revealed a significant Task x Response Type x Duration x Genotype x Sex interaction [$F(2,108)=7.2$, $p_{GG} \leq 0.002$, $\eta_p^2=0.117$, Power=0.886] with a prominent linear-quadratic component [$F(1,54)=10.0$, $p \leq 0.003$, $\eta_p^2=0.156$, Power=0.874].

Male HIV-1 Tg animals revealed marked impairment in signal detection relative to male control animals evidenced by a significant rightward shift in the loss of signal detection during the 18 month acquisition (Figure 4.6). During the reversal assessment, male control animals displayed a significant increase in both the number of hits and misses, suggesting an overtraining reversal effect. No significant alterations in the number of hits

and/or misses was observed in the male HIV-1 Tg animals, suggesting that, despite extensive training, there was no improvement in their performance during the reversal task.

In sharp contrast, at 18 months of age, female HIV-1 Tg animals displayed no impairment in the detection of shorter signal durations relative to female control animals (Figure 4.6). However, female HIV-1 Tg animals, relative to female control animals, exhibited marked impairment in the reversal task evidenced by an inability to reliably detect the signal at any duration assessed.

Phase 4: Neuroanatomical Assessments

Selective alterations in neuronal morphology were observed in pyramidal neurons from layers II-III of the medial prefrontal cortex in HIV-1 Tg animals, suggesting an alteration in dendritic branching complexity, but not neuronal arbor complexity or dendrite length.

Branch Order. A centrifugal branch ordering method was utilized in Neurolucida 360 to automatically assign each dendrite with a branch order by counting the number of segments traversed. Presence of the HIV-1 transgene had a profound effect on the number of dendritic branches at each branch order (Figure 4.7; Genotype x Branch Order Interaction [$F(1,952)=10.1$, $p\leq 0.002$]). Specifically, HIV-1 Tg animals exhibited an increased relative frequency of dendritic branches at lower branch orders relative to controls, suggesting an alteration in dendritic branching complexity.

Sholl Analyses. Subsequently, *a* Sholl analysis was conducted as a complementary measure of neuronal arbor complexity, whereby the number of dendritic intersections occurring every 10 µm from the soma were quantified in HIV-1 Tg and control animals. Neither presence of the HIV-1 transgene nor the factor of biological sex influenced the

number of intersections at successive radii (Figure 4.7; $p>0.05$) or the total dendrite length ($p>0.05$; Control Male: 729.3 ± 83.1 µm, Control Female: 740.6 ± 49.7 µm; HIV-1 Tg Male: 679.1 ± 81.0 µm; HIV-1 Tg Female: 758.4 ± 42.5 µm). Thus, HIV-1 Tg animals exhibited selective alterations in the morphology of pyramidal neurons from layers II-III of the mPFC, characterized by decreased dendritic branching complexity.

HIV-1 Tg animals displayed a profound shift in the distribution of dendritic spines in pyramidal neurons from layers II-III of the medial prefrontal cortex, supporting an alteration in synaptic connectivity.

Sholl analyses were subsequently utilized to determine where dendritic spines were located on the neuron, assessed using spine type (i.e., Thin Spines, Stubby Spines, Mushroom Spines), determined using an observer-assisted automatic classification system in Neurolucida 360, genotype (i.e., HIV-1 Tg, Control), biological sex (i.e., Male, Female) and radii as factors (Figure 4.8). HIV-1 Tg animals exhibited a prominent shift in the distribution of dendritic spines dependent upon the factor of biological sex and spine type (Genotype x Sex x Spine Type x Radii Interaction [$F(2, 6265)=21.5$, $p\leq0.001$]). The effect or lack of effect of biological sex on spine type is illustrated in Figure B.2.

Complementary analyses were conducted on each spine type to determine the locus of these interactions. HIV-1 Tg animals displayed a prominent shift, with an increased relative frequency of thin dendritic spines on more distal branches relative to control animals (Genotype x Radii Interaction [$F(1,2057)=83.1$, $p\leq0.001$]); the magnitude of which was influenced by the factor of biological sex (Genotype x Sex x Radii Interaction [$F(1,2057)=19.1$, $p\leq0.001$]). In sharp contrast, an assessment of stubby dendritic spines revealed a population shift with an increased relative frequency on more proximal branches

in HIV-1 Tg animals relative to controls (Genotype x Radii Interaction [$F(1,2057)=14.1$, $p\leq0.001$]); an effect influenced by the factor of biological sex (Genotype x Sex x Radii Interaction [$F(1,2057)=27.3$, $p\leq0.001$]), whereby the effect was observed in female HIV-1 Tg animals (Genotype x Radii Interaction [$F(1,957)=50.9$, $p\leq0.001$]), but not male HIV-1 Tg animals (Genotype x Radii Interaction: $p>0.05$). No significant differences in the distribution of mushroom dendritic spines were observed ($p>0.05$).

A selective population shift in dendritic spine morphology was observed in layers II-III pyramidal neurons of the medial prefrontal cortex dependent upon presence of the HIV-1 transgene and biological sex.

Measurement of dendritic spine parameters, including backbone length, head diameter, and volume (Figure B.3) revealed a selective population shift in dendritic spine morphology in layers II-III pyramidal neurons of the mPFC dependent upon presence of the HIV-1 transgene and biological sex. Male HIV-1 Tg animals exhibited a population shift towards shorter dendritic spines with no observed alterations in head diameter or volume. In sharp contrast, female HIV-1 Tg animals displayed a population shift towards longer dendritic spines with decreased head diameter relative to female control animals; no significant alterations in dendritic spine volume were revealed in female HIV-1 Tg animals relative to female control animals. A generalized linear mixed effects model with a Poisson distribution confirmed these observations, revealing a significant Genotype x Sex x Bin interaction for both backbone length [$F(1,1659)=37.2$, $p\leq0.001$] and head diameter [$F(1,1154)=68.2$, $p\leq0.001$]; an effect not observed for dendritic spine volume ($p>0.05$).

There was no significant difference in neuroinflammation in the hippocampus between HIV-1 Tg and control animals.

Three putative neuroinflammatory markers, including IL-1β, IL-6, and TNF-α, were assessed in the hippocampus of HIV-1 Tg and control animals (Figure 4.9). Overall, HIV-1 Tg and control animals, independent of biological sex, reaching threshold after 40 cycles, displayed low levels of gene expression. No significant genotype ($p>0.05$) or sex ($p>0.05$) differences in gene expression, examined using the $2^{-\Delta\Delta Ct}$ method, were observed.

Phase 5: Mechanistic Basis of Neurocognitive Impairment

Neurocognitive impairments across the functional lifespan explain significant genotypic variance.

A DFA was utilized to determine whether neurocognitive assessments conducted across the functional lifespan could classify animals based on genotype (Figure 4.10). Variables included in the stepwise DFA represented alterations in sustained attention (Hits and Misses at 1000, 500, and 100 msec during Original Acquisition and Retest 1-5; Hits and Misses at 1000, 100, and 10 msec during the 18 Month Assessment), learning (Days to Criteria during Original Acquisition, Days to Criteria at Retest 1-5, Number of Days Meeting Criteria during the 18 Month Assessment), and flexibility and inhibition (Hits and Misses at 1000, 100, and 10 msec during the Reversal Assessment).

HIV-1 Tg and control animals were maximally separated (canonical correlation of 0.70) by selecting seven variables corresponding to sustained attention (i.e.,Hits at 1000 msec during Original Acquisition, Hits at 500 msec during Retest 1, Misses at 1000 msec during Retest 2, Misses at 100 msec during Retest 4, Hits at 1000 msec during Retest 5, and Misses at 10 msec during the 18 Month Assessment) and learning (i.e., Days to Criteria

during Retest 5). Animals were correctly classified for presence of the HIV-1 transgene (jack-knifed classification) with 78.5% accuracy (Approximately of Wilks' λ of 0.516, $\chi^2(7)=39.4$, $p\leq0.001$), accounting for approximately 61.6% of the genotypic variance.

Synaptic dysfunction, assessed in pyramidal neurons from layers II-III of the medial prefrontal cortex, explains significant genotypic variance.

A DFA was utilized to determine whether synaptic dysfunction in pyramidal neurons from layers II-III of the mPFC could classify animals based on genotype (Figure 4.10). Variables included in the stepwise DFA represented alterations in dendritic branching complexity, dendritic spine connectivity, and dendritic spine morphology.

HIV-1 Tg and control animals were maximally separated (canonical correlation of 0.72) by selecting seven variables corresponding to dendritic spine connectivity (i.e., Relative Frequency of Thin Dendritic Spines at 150 µm; Relative Frequency of Stubby Dendritic Spines at 40 µm, 110 µm, and 170 µm) and dendritic spine head diameter (i.e., Relative Frequency of Dendritic Spines within the 0.075 µm, 0.225 µm and 0.375 µm bin). Animals were correctly classified for presence of the HIV-1 transgene (jack-knifed classification) with 80.4% accuracy (Approximately of Wilks' λ of 0.489, $\chi^2(7)=32.5$, $p\leq0.001$), accounting for approximately 64.6% of the genotypic variance.

DISCUSSION

Progressive NCI, including alterations in learning, sustained attention, flexibility, and inhibition, were observed in the population of HIV-1 Tg rats sampled. During initial acquisition, biological sex was the driving factor for observed differences in learning and sustained attention. Across retest assessments, presence of the HIV-1 transgene became the prominent factor underlying alterations in the temporal process of task acquisition, as well

as sustained attention. Nevertheless, at 18 months of age, sex-dependent expression of NCI were observed in HIV-1 Tg animals, relative to controls. Pyramidal neurons from layers II-III of the mPFC revealed profound synaptic dysfunction in HIV-1 Tg animals relative to controls; dysfunction that was characterized by alterations in dendritic branching complexity, synaptic connectivity, and dendritic spine morphology. NCI across multiple domains (i.e., learning, sustained attention) and synaptic dysfunction in the mPFC independently identified the presence of the HIV-1 transgene with at least 78.5% accuracy, accounting for at least 61.6% of the genotypic variance. Thus, even in the absence of sensory or motor system deficits (McLaurin et al., 2018b) and comorbidities, HAND is a neurodegenerative disease characterized by age-related disease progression; impairments which may be due, at least partly, to synaptic dysfunction in the mPFC.

Located at the anterior pole of the mammalian brain, the PFC, recognized as an anatomically complex brain region (Siddiqui et al., 2008), is organized in a laminar fashion and comprised of three major subdivisions (i.e., mPFC, orbital PFC (oPFC) and lateral PFC). Executive functions, including attention, flexibility, and inhibition, are the primary, most basic function of the PFC (Fuster, 2008). Although executive functions cannot be localized to any single subdivision of the PFC, the mPFC, oPFC, and lateral PFC each exhibit some degree of functional specialization (Siddiqui et al., 2008; Fuster et al., 2008). Specifically, the mPFC has been implicated as having a primary role in attention, including pre-attentive processes (e.g., Ellenbroek et al., 1996) and sustained attention (e.g., Kim et al., 2016), whereas the oPFC is involved in stimulus-reinforcement learning (e.g.,Rolls, 2004) and reversal (i.e., flexibility and inhibition; McAlonan & Brown, 2003).

The utilization of a series of neurocognitive tasks across the functional lifespan tapped multiple subdivisions of the PFC, revealing progressive NCI in the HIV-1 Tg rat. At the genotypic level, HIV-1 Tg animals displayed a progressive, relative impairment in tasks tapping both the mPFC (i.e., sustained attention) and the oPFC (i.e., stimulus-reinforcement learning). Most notably, HIV-1 Tg animals also exhibited alterations in the progression of PPI, a pre-attentive process tapping the mPFC (McLaurin et al., 2018b). However, sex differences in the presentation of NCI at 18 months of age were dependent upon the brain region tapped via neurocognitive assessments (i.e., mPFC vs. oPFC). Specifically, male HIV-1 Tg animals exhibited significantly greater impairment, relative to male control animals, in sustained attention and stimulus-reinforcement learning in the reversal assessment, tasks tapping both the mPFC and oPFC. Female HIV-1 Tg animals, however, displayed profound impairment, relative to female control animals, in flexibility and inhibition, tasks predominantly associated with the oPFC. Elucidating the mechanisms underlying sex-dependent expression of NCI is vital for the development of therapeutic treatments and cure strategies.

The rich cortical and subcortical connections make the PFC ideally positioned to serve as a central hub, integrating and relaying information from multiple afferent sources (Miller & Cohen, 2001). Broadly, the PFC receives afferents from thalamic nuclei, the limbic system, the frontal cortex, and other brain regions (e.g., hypothalamus, cerebellum, mesencephalon; Fuster, 2008). Dense innervation from multiple neurotransmitter systems to the PFC has also been well-established (Fuster, 2008); afferents which play a prominent regulatory role across the PFC (Fuster, 2008) and are functionally involved in the control of executive functions (for review, Robbins & Arnsten, 2009). Specifically, noradrenergic

projections from the locus coeruleus (LC), DAergic afferents from the VTA, and serotonergic projections from the raphe nuclei innervate the PFC.

Excitatory pyramidal neurons, characterized by a single apical dendrite, multiple shorter dendrites, and thousands of dendritic spines are abundant throughout the PFC (Spruston, 2008). A synaptic relationship between pyramidal neurons and the major afferent systems is established via postsynaptic sites on dendritic shafts and spines; the vast majority of which occur on dendritic spines (e.g., Hersch & White, 1981). Morphologically, dendritic spines are classically characterized into three primary categories (i.e., thin, stubby, mushroom; Peters & Kaiserman-Abramof, 1970). Thin spines, the predominant spine type in both HIV-1 Tg and control animals, are characterized by a long, thin neck and a small bulbous head, whereas the head volume to neck volume ratio is higher in mushroom spines. In sharp contrast, stubby spines are devoid of a spine neck, exhibiting an approximately equal head and neck volume ratio (Peters & Kaiserman-Abramof, 1970). Most notably, asymmetric excitatory synapses are primarily formed between dendritic spine heads and presynaptic axons (e.g., Gray, 1959), however, some dendritic spines receive additional input on their neck (Yuste, 2010). Thus, morphological characteristics of dendritic spines, which are reflective of functionality and capacity for structural change (Lai & Ip, 2013), and their distribution along the dendrite, may be associated with synaptic dysfunction in the HIV-1 Tg rat.

Neuronal morphology, assessed using a branch order analysis, tapping dendritic branching complexity, as well as the classical Sholl analysis, tapping neuronal arbor complexity, revealed prominent alterations in HIV-1 Tg animals relative to controls (Figure 4.11). In pyramidal neurons from layers II-III of the mPFC, assessed in the present

study, HIV-1 Tg animals exhibited decreased dendritic branching complexity; an effect independent of biological sex. No statistically significant genotypic differences were observed in dendritic length, consistent with previous reports in younger HIV-1 Tg animals (Festa et al., 2015) or neuronal arbor complexity. In sharp contrast, in medium spiny neurons (MSNs) from the nucleus accumbens core subregion (NAcc), published results suggest sex-dependent alterations in neuronal morphology (McLaurin et al., 2018c). Specifically, female HIV-1 Tg animals, but not male HIV-1 Tg animals, displayed profound alterations in dendritic branching complexity and neuronal arbor complexity (McLaurin et al., 2018c). Morphological differences between pyramidal neurons, characterized as polar neurons, and MSNs, characterized by a centrifugal morphology, may underlie differences in branch order and Sholl analyses. Overall, results support alterations in neuronal morphology in HIV-1 Tg rats independent of brain region assessed. However, the comparison of results from branch order analyses with those from Sholl analyses suggests that the two analytic measures may reflect different measures of neuronal morphology.

HIV-1 Tg animals, independent of biological sex, exhibited a profound shift in the distribution of dendritic spines along the apical dendrite, supporting a prominent alteration in synaptic connectivity. Specifically, a preponderance of thin spines were observed on more distal dendrites, extending into layer I of the mPFC, in HIV-1 Tg animals, relative to controls. However, HIV-1 Tg animals, relative to controls, displayed an increased relative frequency of stubby spines on more proximal dendrites; an effect which was most prominent in female HIV-1 Tg rats. Notably, pyramidal neurons within layers II-III of the mPFC express multiple monoamine receptors, including noradrenergic receptors (i.e.,

primarily α_{1A}, α_{1D}), DAergic receptors (i.e., primarily D_1) and serotonergic receptors (i.e., primarily 5-HT_{1A}, 5-HT_{2A}); receptor expression not observed within layer I of the mPFC (Santana & Artigas, 2017). The preponderance of stubby spines, morphologically characterized by the absence of a dendritic spine neck (Peters & Kaiserman-Abramof, 1970) and a smaller postsynaptic density (Schmidt & Eilers, 2009), on more proximal dendrites suggests that HIV-1 Tg animals fail to receive afferent projections, and thus neurotransmitter innervation, from the VTA, LC, and raphe nuclei (Figure 4.11); consistent with neurotransmitter system alterations, specifically DAergic system dysfunction, commonly reported in HIV-1 (e.g., Kumar et al., 2011; Gelman et al., 2012; Javadi-Paydar et al., 2017; Bertrand et al., 2018). One previous study (Festa et al., 2015) and one conference abstract (Festa et al., 2017) have also suggested alterations in dendritic spine density in the mPFC in younger HIV-1 Tg animals; an effect which may also influence synaptic connectivity. Thus, profound synaptic dysfunction was observed in HIV-1 Tg animals, characterized by alterations in dendritic branching complexity, synaptic connectivity (i.e., VTA-PFC-LC), and dendritic spine morphology, supporting a key neural mechanism for expression of NCI in HAND.

Multiple animal systems are available to model components of neuroHIV, each with their own advantages and constraints. Several major considerations of the prominent animal species and their applicability to provide a biological system to model neuroHIV in the post-cART era are highlighted in Figure 4.12. CNS infection occurs within two weeks of HIV-1 infectivity in humans (Price et al., 1988; Valcour et al., 2012), leading to NCI (e.g., Heaton et al., 2011; Cysique et al., 2004) and behavioral alterations (e.g., Apathy: Kamat et al., 2012; Depression: Ciesla & Roberts, 2001). Selective NCI (e.g., selective

attention appears relatively spared, Moran et al., 2014a) have been observed across multiple domains in multiple prominent animals systems (e.g., HIV-1 Tg rat, pre-attentive processes: Moran et al., 2013a; learning and memory: Vigorito et al., 2007, Repunte-Canonigo et al., 2014; executive function: Moran et al., 2014a; SIV, spatial working memory: Weed et al., 2004; Humanized Mice, memory: Boska et al., 2014; Tat Transgenic Mice, spatial learning: Carey et al., 2012, Marks et al., 2016, reversal learning: Carey et al., 2012). Examples of behavioral alterations, similar to those observed in HIV-1 seropositive individuals, include depressive-like behaviors (e.g., HIV-1 Tg rat: Nemeth et al., 2014; Tat transgenic mice: Lawson et al., 2011, McLaughlin et al., 2017) and motivational alterations (e.g., HIV-1 Tg rat: Bertrand et al., 2018). Furthermore, although generally understudied, prominent sex differences in the expression of NCI have been observed in HIV-1 seropositive individuals, with HIV-1 seropositive females displaying more severe deficits relative to HIV-1 seropositive males (Royal et al., 2016; Maki et al., 2018). Sex differences in the expression of NCI have been translationally modeled in the HIV-1 Tg rat (McLaurin et al., 2016b; Rowson et al., 2016; McLaurin et al., 2017d), but inconsistent results have been reported in other animal systems (e.g., Tat transgenic mice: Hanh et al., 2015). Given the increased life expectancy of HIV-1 seropositive individuals in the post-cART era, as well as the persistence of NCI, an *in vivo* biological system able to provide a longitudinal study of HIV-1 is critical. HIV-1 seropositive individuals display progressive NCI, with individuals exhibiting asymptomatic NCI at baseline having an increased risk (i.e., two to six times) of developing symptomatic HAND (Grant et al., 2014). The HIV-1 Tg rat, as demonstrated in the present study, displays age-related disease progression in multiple neurocognitive domains across the functional lifespan. Thus, the

present study further elucidates the advantages and constraints of the HIV-1 Tg rat biological system to model neuroHIV in the post-cART era.

Despite the aforementioned strengths of the present study, a few caveats are acknowledged. First, the neuronal analysis focused exclusively on pyramidal neurons from layers II-III of the mPFC. Although the generalizability of synaptic dysfunction cannot be directly assessed within the present study, observations across multiple brain regions (i.e., nucleus accumbens, mPFC; Roscoe et al., 2014; Festa et al., 2015; McLaurin et al., 2018a; McLaurin et al., 2018c), ages (i.e., 4 months; 14-17 months; 20 months; Roscoe et al., 2014; McLaurin et al., 2018a; McLaurin et al., 2018c) and in HIV-1 Tg rats following psychostimulant exposure (i.e., methylphenidate; McLaurin et al., 2018a) suggests the importance of further studies investigating synaptic dysfunction as a neural mechanism underlying NCI in HAND. Second, neuroinflammatory markers were assessed exclusively in the hippocampus and using only three cytokines (i.e., IL-1β, IL-6, and TNF-α). Despite the utilization of two experimental methodologies and sufficient statistical power, no significant differences in neuroinflammation in the hippocampus were suggested between HIV-1 Tg and control animals; results consistent with those observed using [(18)F]-DPA714 PET imaging and a profile of 24 neuroinflammatory markers in (3 and 9 month) adult HIV-1 Tg animals (Lee et al., 2015) and following PD 1 stereotaxic injections of HIV-1 viral proteins (i.e., Tat_{1-86}, gp120; Moran et al., 2014b). However, this does not preclude neuroinflammation in the adolescent brain, in other brain regions, or using other methodology (e.g., ELISA, Royal et al., 2012). For example, results of the present study are in contrast to those reported by Royal et al. (2012), which observed significant increases

in the expression of INF-γ, TNF-α, and IL-β, assessed using ELISA, in brain lysates prepared from the frontal cortex and subcortical white matter of the HIV-1 Tg rat.

Even in the absence of sensory or motor system deficits (McLaurin et al., 2018b) and comorbidities, HAND is a neurodegenerative disease. NCI are characterized by age-related disease progression across multiple neurocognitive domains, tapping two primary subdivisions of the PFC. Most notably, alterations in sustained attention and learning across the functional lifespan, account for approximately 61.6% of the genotypic variance in NCI, independent of biological sex. Synaptic dysfunction in pyramidal neurons from layers II-III of the mPFC, characterized by alterations in dendritic branching complexity, synaptic connectivity, and dendritic spine morphology, supports a key, albeit not exclusive, neural mechanism underlying HAND, accounting for approximately 64.6% of the genotypic variance. Thus, the progression of HAND with age in the HIV-1 Tg rat and the associated synaptic dysfunction affords an instrumental model system for the development of therapeutics and functional cure strategies.

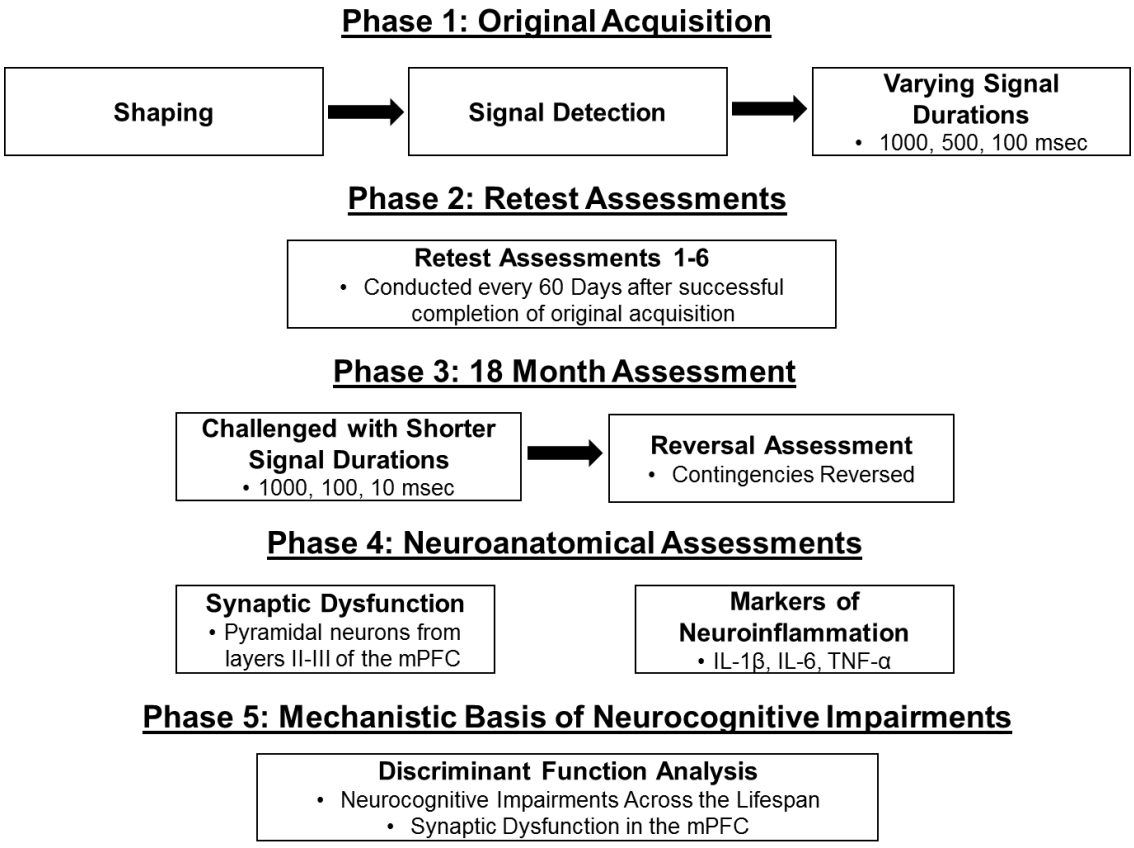

Figure 4.1 Experimental Design. Schematic of the experimental design.

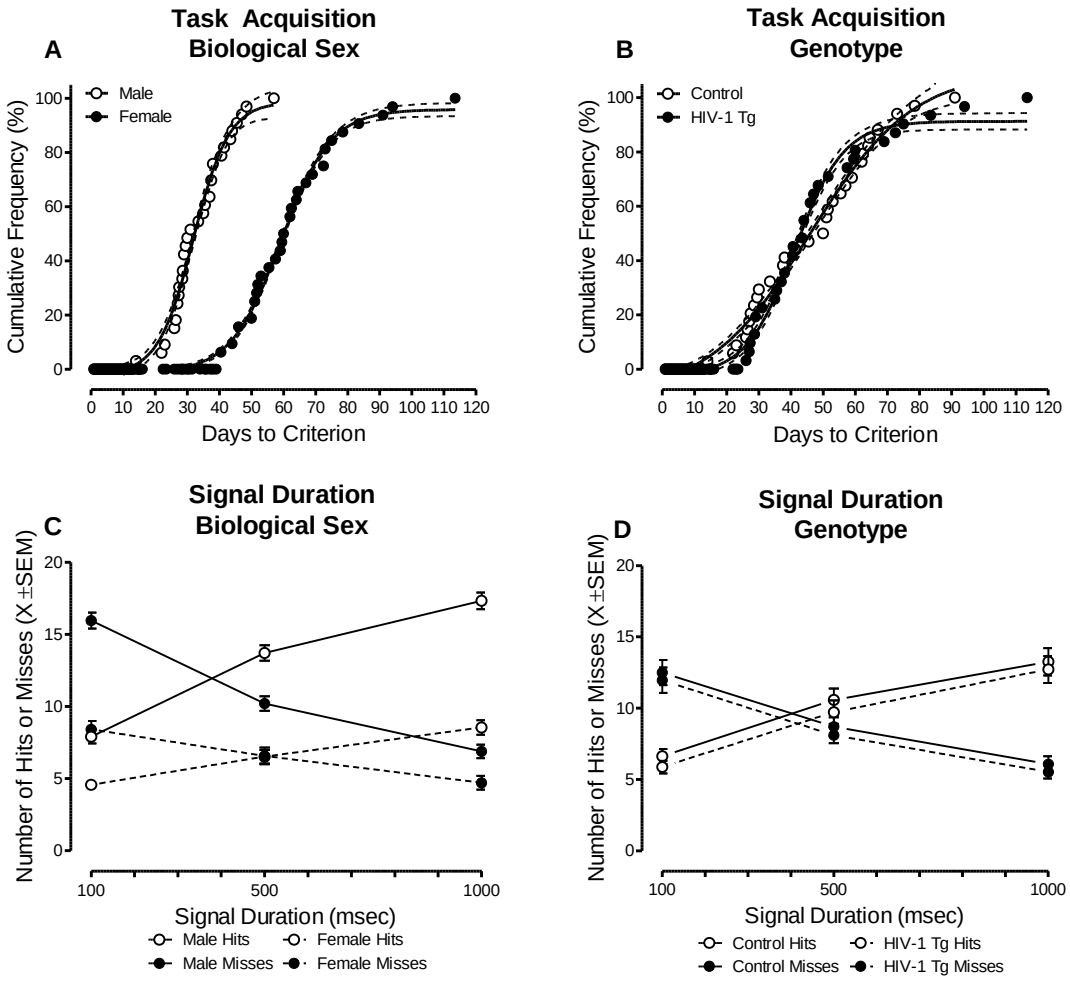

Figure 4.2 Signal Detection: Original Acquisition. Initial acquisition of signal detection. (**A**) Assessment of the temporal process of acquisition revealed a main effect of sex ($p \leq 0.001$), with female animals, independent of genotype, acquiring the signal detection operant task significantly slower than male animals. (**B**) Genotype failed to alter the temporal process of acquisition during the original acquisition phase ($p > 0.05$). (**C**) Assessment of sustained attention during the initial acquisition of signal detection revealed that female animals displayed a decreased response rate, as well as a prominent rightward shift in the loss of signal detection (i.e., the intersection of hits and misses; $p \leq 0.001$) relative to male animals. (**D**) Presence of the HIV-1 transgene failed to alter sustained attention during initial acquisition ($p > 0.05$). Data are presented as cumulative frequencies with 95% confidence intervals fit to the curve (**A**,**B**) or mean (X) ± SEM (**C**,**D**).

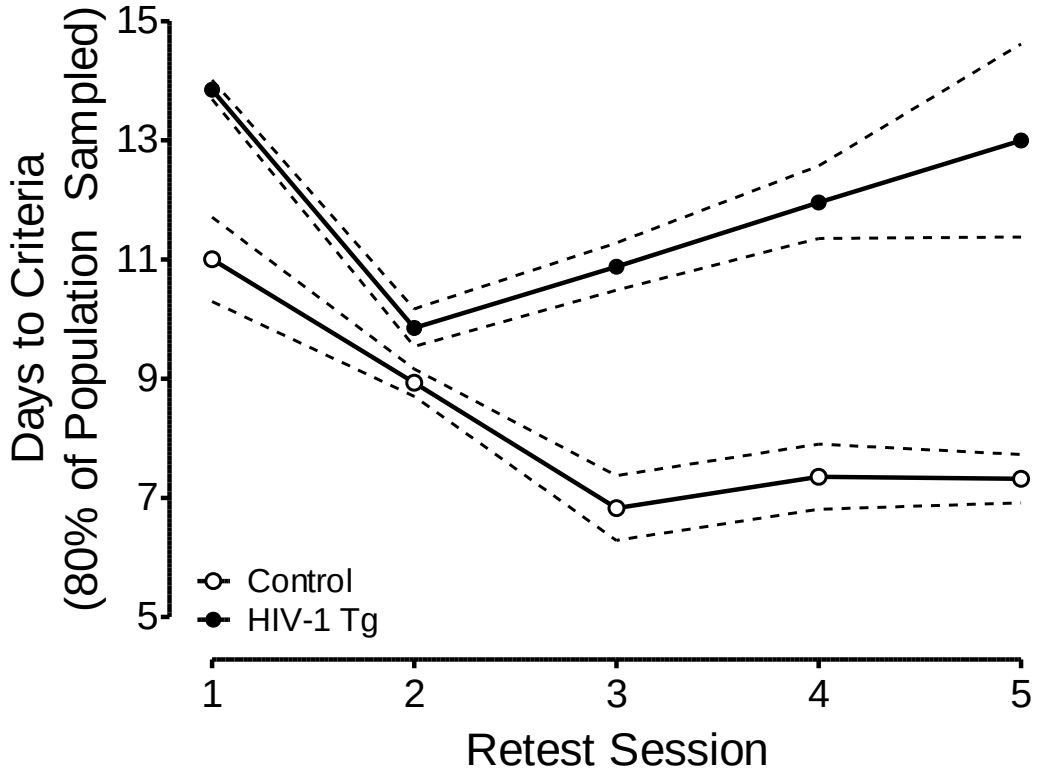

Figure 4.3 Days to Criteria: Retest Assessments. The number of days at which 80% of the population sampled met criteria (±95% Confidence Intervals (CI)) is illustrated as a function of genotype (HIV-1 Tg vs. control) and retest session. Points and 95% CI were derived from the cumulative frequency curves presented in Figure B.1. Control animals exhibited an improvement in performance as a function of retest assessment, reaching asymptotic performance at approximately 7 days. In sharp contrast, HIV-1 Tg animals exhibited an initial improvement through retest assessment 2, followed by a progressive decline.

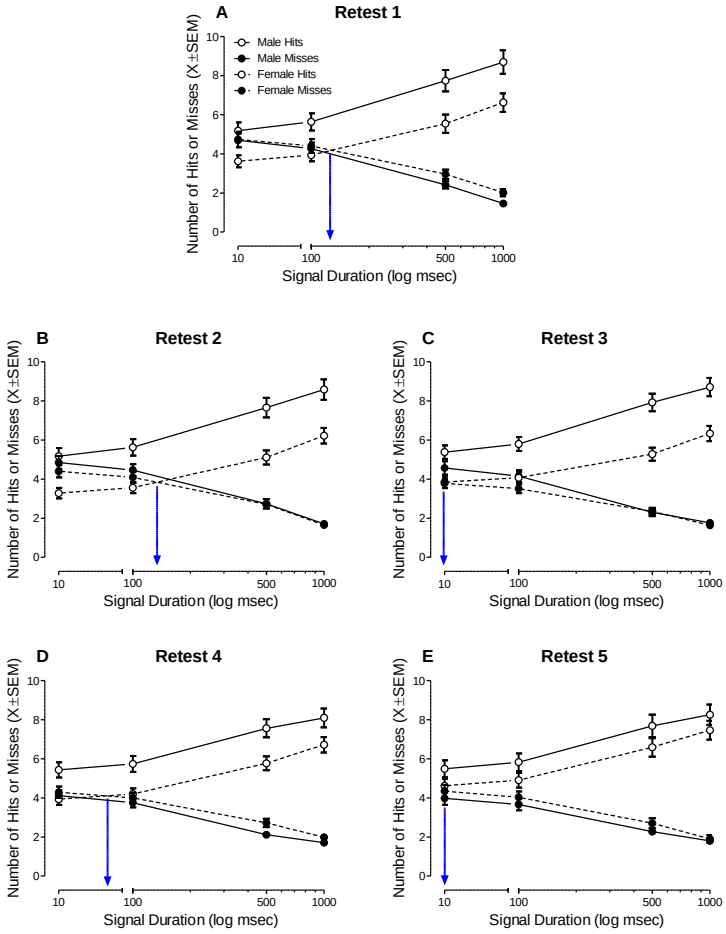

Figure 4.4 Signal Detection: Retest Assessments. Sustained attention as a function of retest assessment. At each individual retest session (i.e, Retest 1: **A**, Retest 2: **B**, Retest 3: **C**, Retest 4: **D**, Retest 5: **E**) HIV-1 Tg animals, independent of biological sex, displayed an impairment in the detection of shorter signal durations (1000, 500, 100 msec). Across retest sessions, HIV-1 Tg animals displayed a progressive, relative impairment in sustained attention ($p \leq 0.05$). Despite an improvement in the detection of shorter signal durations as a function of retest session, HIV-1 Tg animals failed to improve as quickly or to the same magnitude as control animals. Data were extrapolated to 10 msec using linear regression calculations to demonstrate the point at which animals experiences a loss of signal detection (i.e., the intersection of hits and misses). A blue line indicates the point at which HIV-1 Tg animals experienced a loss of signal detection. Data are presented as mean ± SEM.

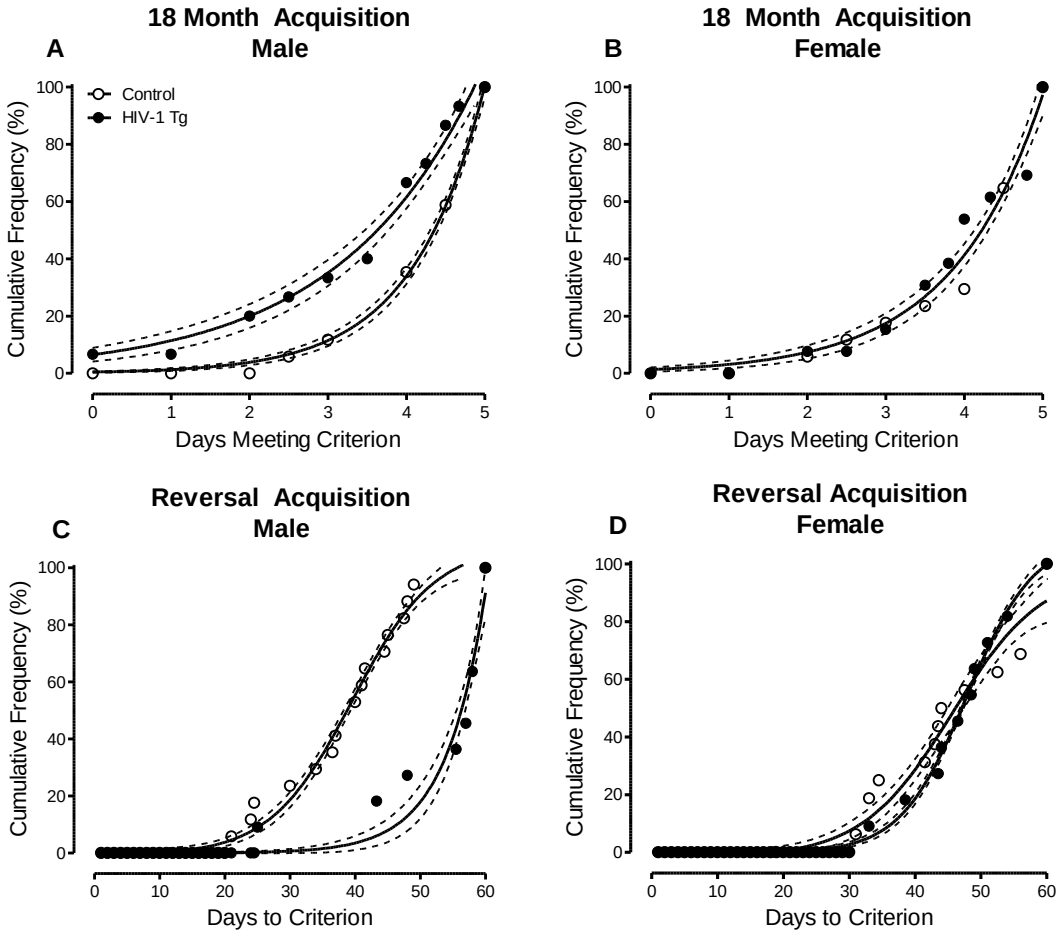

Figure 4.5 Days to Criteria: 18 Month Acquisition and Reversal. Temporal process of acquisition during the 18 month acquisition (**A,B**) and reversal (**C,D**) task. During the 18 month acquisition task, HIV-1 Tg and control animals were challenged for 5 consecutive days with shorter signal durations (i.e., 1000, 100, 10 msec). Male HIV-1 Tg animals (**A**) displayed a shift towards a decreased number of days meeting criteria (i.e., 70% accuracy) relative to male control animals ($p \leq 0.001$); a distribution shift not observed in female HIV-1 Tg animals (**B**; $p > 0.05$). The temporal process of acquisition in the reversal task was assessed for HIV-1 Tg animals that had two months (i.e., 60 days) to acquire the task. Male HIV-1 Tg animals took significantly longer to acquire the reversal task relative to male control animals (**C**; $p \leq 0.005$); an impairment not observed in female HIV-1 Tg animals (**D**; $p > 0.05$). Data are presented as cumulative frequencies with 95% confidence intervals fit to the curve.

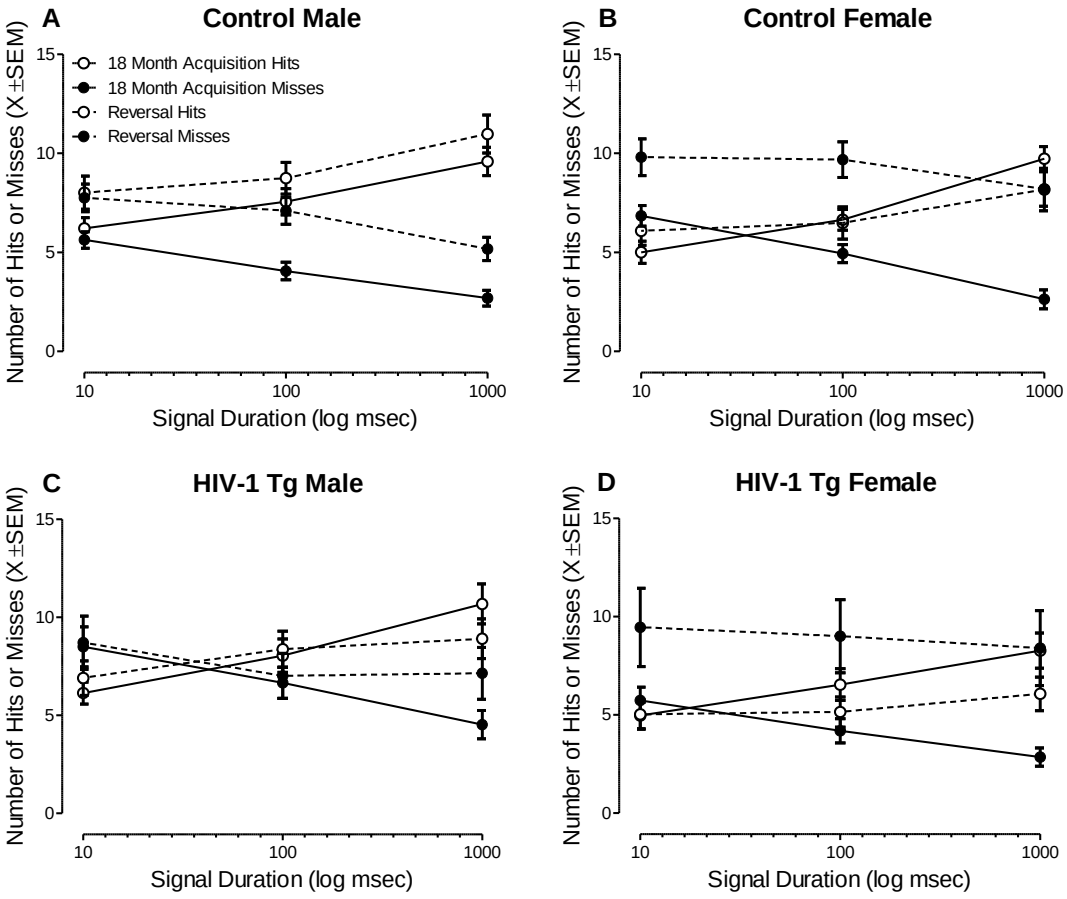

Figure 4.6 Signal Detection: 18 Month Acquisition and Reversal. Signal detection data, presented as mean ± SEM, during the 18 month acquisition and reversal task are illustrated as a function of genotype and sex. A significant Task x Response Type x Genotype x Sex interaction [$F(2,108)=7.2$, $p_{GG}\leq 0.002$, $\eta_p^2=0.117$] was observed. Male HIV-1 Tg (**C**) animals displayed a profound impairment in the detection of shorter signals during 18 month acquisition task and reversal task relative to male control (**A**) animals. Female HIV-1 Tg animals (**D**) failed to exhibit a deficit in the detection of shorter signals during the 18 month acquisition task relative to female control (**B**) animals. However, female HIV-1 Tg animals exhibited prominent impairments in flexibility and inhibition, evidenced by an inability to reliably detect the signal at any duration assessed during the reversal task.

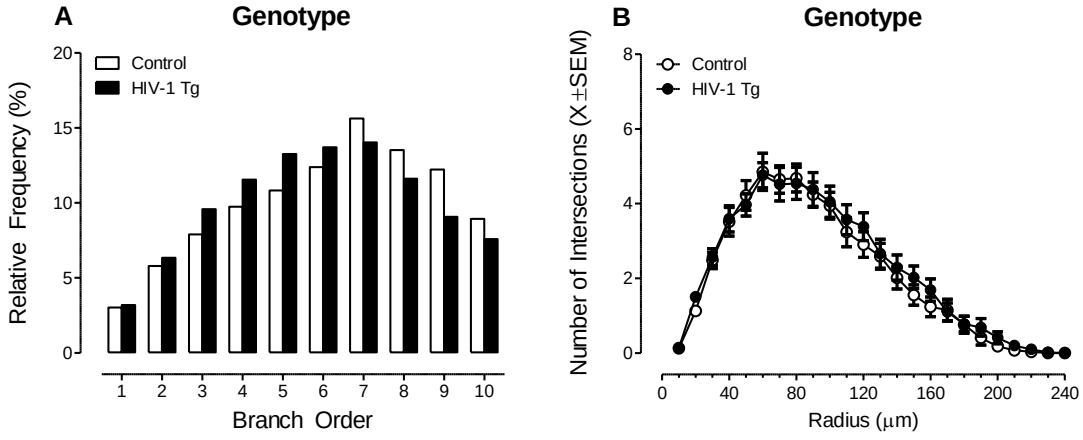

Figure 4.7 Neuronal Morphology. Two assessments of neuronal morphology, including a branch order analysis (**A**) and Sholl analysis (**B**) were conducted in pyramidal neurons from the medial prefrontal cortex. Branch order analyses (**A**) revealed an increased relative frequency of dendritic branches at lower branch orders in HIV-1 Tg animals relative to controls. In sharp contrast, neither presence of the HIV-1 transgene nor the factor of biological sex influenced the number of dendritic intersections occurring every 10 μm from the soma, assessed using a Sholl analysis (**B**). Thus, HIV-1 Tg animals exhibited selective alterations in the morphology of pyramidal neurons from layers II-III of the mPFC, characterized by decreased dendritic branching complexity. Data are illustrated as relative frequencies of the entire dataset (**A**) or mean ± SEM (**B**).

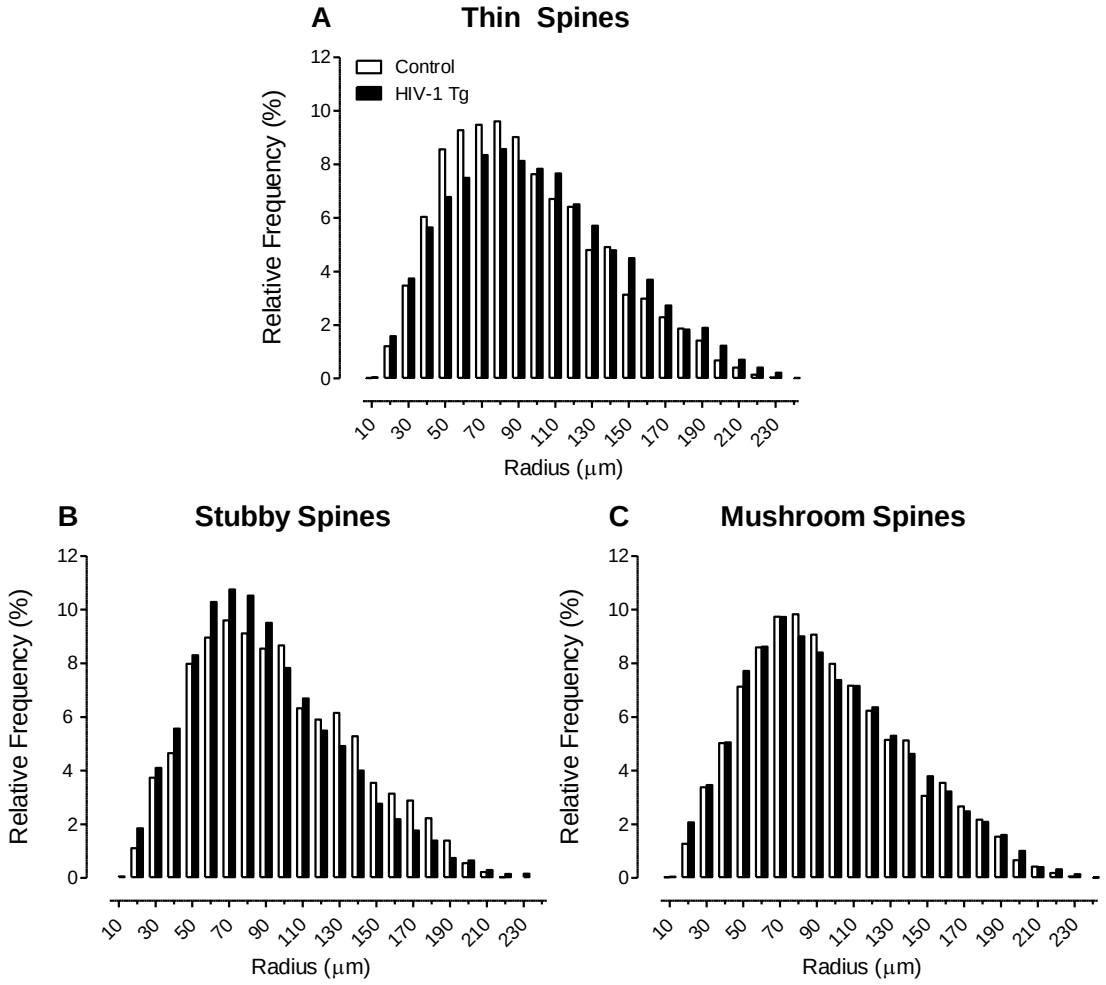

Figure 4.8 Synaptic Connectivity. The distribution of dendritic spines on pyramidal neurons from the medial prefrontal cortex are illustrated as a function of spine type (i.e., Thin: **A**, Stubby: **B**, Mushroom: **C**), genotype (HIV-1 Tg vs. control) and radii. HIV-1 Tg animals exhibited a prominent distributional shift in the relative frequency of thin spines (**A**), with an increased relative frequency on more distal branches, relative to controls. In sharp contrast, HIV-1 Tg animals displayed an increased relative frequency of stubby spines (**B**) on more proximal branches, relative to controls. No genotypic alterations were observed in the distribution of mushroom spines (**C**). Data are illustrated as relative frequencies of the entire dataset.

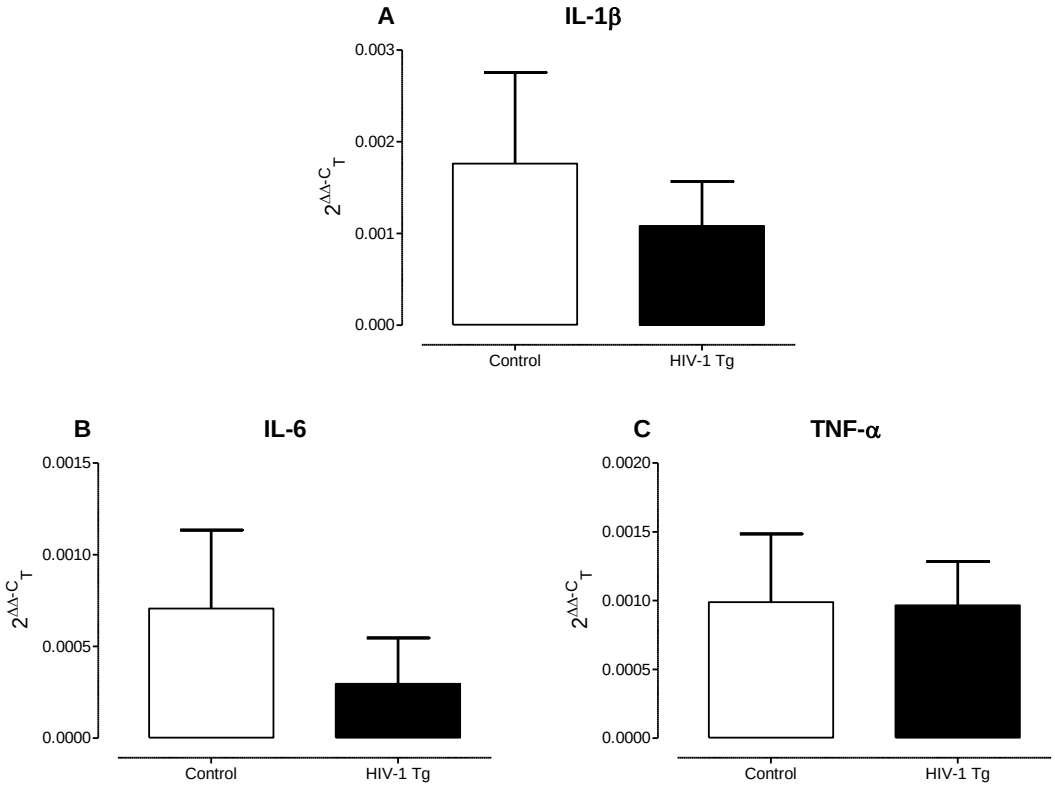

Figure 4.9 Neuroinflammatory Markers. Three neuroinflammatory markers, including IL-1β (**A**), IL-6 (**B**), and TNF-α (**C**), were assessed in the hippocampus of HIV-1 Tg and control animals. Overall, HIV-1 Tg and control animals, independent of biological sex, reaching threshold after 40 cycles, displayed low levels of gene expression; levels which were dependent upon genotype or sex (p>0.05). Data are presented as mean ± SEM.

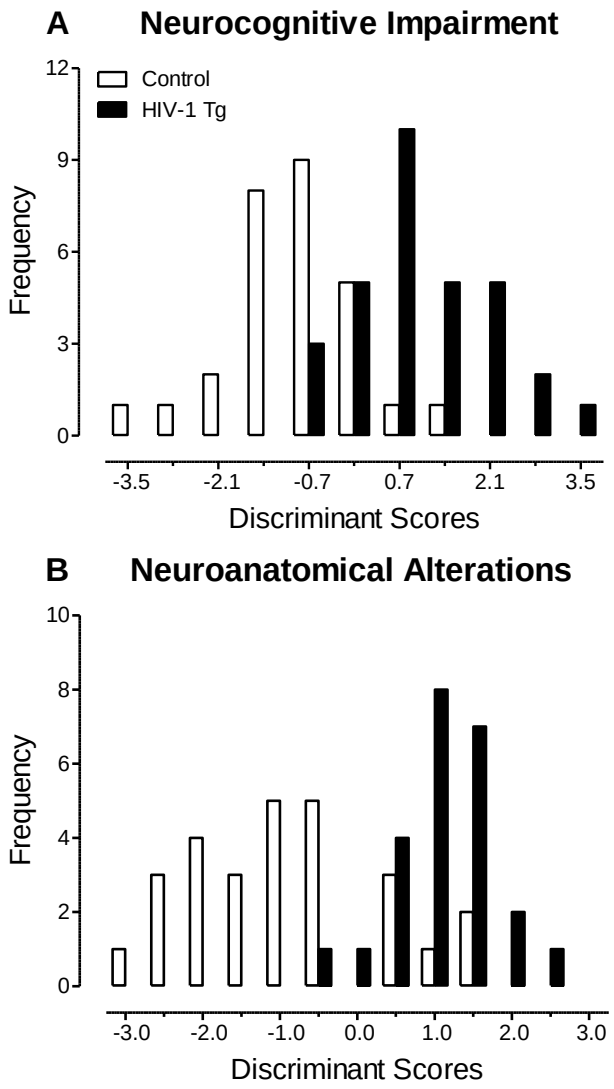

Figure 4.10 Discriminant Function Analysis. A DFA was utilized to determine whether neurocognitive impairments (**A**) and synaptic dysfunction in the medial prefrontal cortex (mPFC; **B**) could classify animals based on genotype. Seven variables, corresponding to alterations in learning and sustained attention, correctly classified the presence of the HIV-1 transgene with 78.5% accuracy, accounting for 61.6% of the genotypic variance in neurocognitive function (**A**). Seven variables, corresponding to alterations in dendritic spine connectivity and dendritic spine head diameter, correctly classified the presence of the HIV-1 transgene with 80.4% accuracy, accounting for 64.6% of the genotypic variance in synaptic dysfunction in the mPFC (**B**).

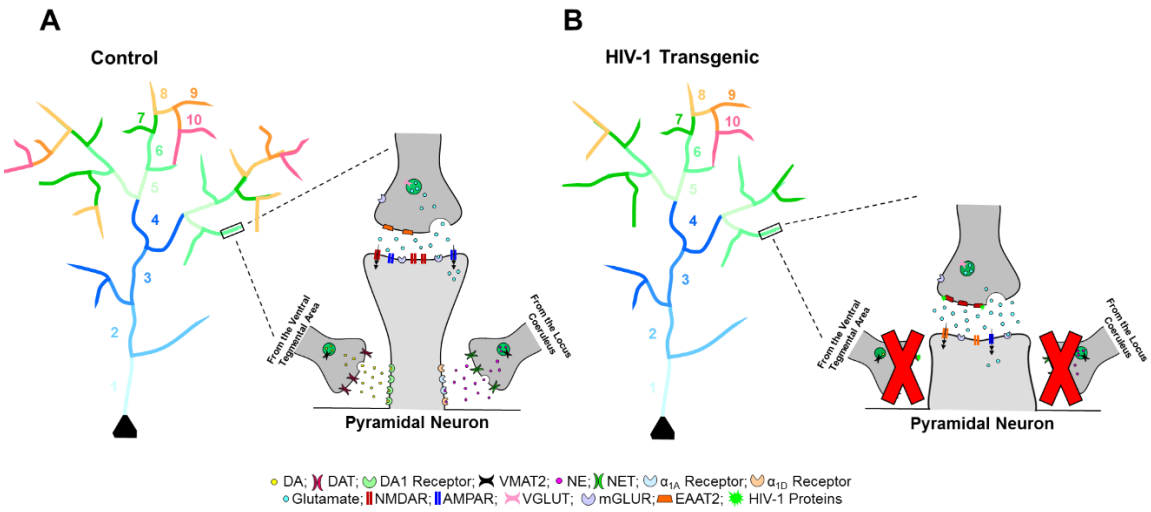

Figure 4.11 Pyramidal Neuron Schematic. Dendritic spine connectivity in pyramidal neurons of the medial prefrontal cortex is illustrated as a function of genotype (HIV-1 Tg vs. control). Pyramidal neurons in HIV-1 Tg animals (**B**) displayed decreased dendritic branching complexity, with a decreased relative frequency of higher order branches relative to control animals (**A**) with no observed alterations in total dendrite length. Control animals exhibited a preponderance of thin spines on more proximal branches, receiving DAergic afferents from the VTA and noradrenergic innervation from the LC. In sharp contrast, HIV-1 Tg animals displayed a preponderance of stubby spines on more proximal branches. Morphological characteristics of stubby spines, including the absence of a spine neck (Peters & Kaiserman-Abramof, 1970) and decreased PSD on the dendritic spine head (Schmidt & Eilers, 2009) suggest that HIV-1 Tg animals failed to receive appropriate DAergic afferents from the VTA or noradrenergic innervation from the LC. Illustrated here is the reception of DAergic and noradrenergic afferents on the dendritic spine neck, although other mechanisms are possible. Abbreviations: DA: Dopamine, DAT: Dopamine Transporter, DA1 Receptor: Dopamine Receptor D1, VMAT2: Vesicular Monoamine Transporter 2, NE: Norepinephrine, NET: Norepinephrine Transporter, α_{1A} Receptor: Alpha-1A Adrenergic Receptor, α_{1D} Receptor: Alpha-1D Adrenergic Receptor, NMDAR: NMDA Receptor, AMPAR: AMPA Receptor, VGLUT: Vesicular Glutamate Transporter, mGLUR: Metabotropic Glutamate Receptor, EAAT2: Excitatory Amino Acid Transporter 2.

Species	Virus	Advantage & Utility	Disadvantage & Constraints	GOAL: Longitudinal NeuroCognitive Research
Non-Human Primate	HIV-1, HIV-2, SIV, SHIV	Genetic relatedness of lentiviruses; Genetic similarity to humans; similar neuropathology	Differences in time course, cellular and molecular markers; SIV/SHIV– surrogate models; Significant financial and ethical concerns	Great for cognitive testing; brain imaging, but lifespan and sample size are practical constraints for rapid research progress
Feline	FIV	Genetic relatedness of lentiviruses; similar neuropathology; Pharmacology/vaccines	Strictly surrogate model; species concerns with institutional IACUC	Limited normative species data on cognitive testing
SCID mice	HIV-1	Cost, availability & accessibility; Genome manipulation; platform for cART evaluations	Engrafted human cells confined to developed organoid	Severe immunodeficiency practical constraint to longitudinal/repeated cognitive testing.
Tg Mice	HIV-1	Cost, availability & accessibility; Genome manipulation; effect of virus on different tissues	Expression in atypical tissues; mouse cyclin T does not interact functionally with Tat	Normative species cognitive and brain tests available; no relevant clinical neuropathologies
Tg Rats	HIV-1		No viral replication, but develops immune abnormalities, clinical manifestations and pathologies	Normative species cognitive and brain tests available; Longitudinal assessment of neurocognitive deficits

Figure 4.12 Prominent Animal Species to Study HIV-1. Several major considerations of the prominent animal species and their applicability to provide a biological system to model neuroHIV in the post-cART era are highlighted.

CHAPTER 5

REMODELING NEURONAL CIRCUITRY VIA S-EQUOL AMELIORATES NEUROCOGNITIVE IMPAIRMENTS CHARACTERISTIC OF HIV-1 ASSOCIATED NEUROCOGNITIVE DISORDERS

INTRODUCTION

Neurodegenerative diseases, including AD and other dementias (43.8 million individuals; GBD 2016 Dementia Collaborators, 2019), HAND (40-70% of the 37.9 million individuals with HIV-1; UNAIDS, 2019), and Parkinson's disease (6.1 million individuals; GBD 2016 Parkinson's Disease Collaborators, 2018), afflict millions of individuals worldwide. Despite differences in clinical symptomology, neurodegenerative diseases share many histopathological features, including neuronal damage and glial activation (Katsuno et al., 2018). Current therapeutics for neurodegenerative diseases, however, remain inadequate due to their inability to modify disease progression (Barchet & Amiji, 2009). The development of a neuroprotective and/or neurorestorative therapeutic that penetrates the central nervous system and targets the salient histopathological features of neurodegenerative diseases has the potential for great clinical significance.

Frontal-subcortical circuit dysfunction may underlie the NCI commonly observed in neurodegenerative diseases, including AD (e.g., Zhao et al., 2015), HAND (e.g., Cole et al., 2007), and Parkinson's disease (e.g., Zgalijardi et al., 2006). Proposed by Alexander et al. (1986), the frontal-subcortical circuits, which are modulated by neurotransmitter system interactions, include five parallel segregated circuits linking regions of the prefrontal cortex to the striatum, basal ganglia and thalamus (Alexander & Crutcher, 1990; Alexander, 1994). Executive dysfunction, which encompasses neurocognitive impairments in higher-order cognitive processes, is associated with alterations in the dorsolateral prefrontal circuit (dlPFC; for review, Bonelli & Cummings, 2007). Excitatory glutamateric neurons, originating in the dorsolateral prefrontal cortex, send projections to the dorsolateral head of the caudate nucleus, which subsequently innervate the basal ganglia via the lateral dorsomedial globus pallidus and rostrolateral substantia nigra pars reticulata. Inhibitory γ-

aminobutyric acid (GABA) fibers project from the basal ganglia to the ventral anterior and mediodorsal thalamus; a brain region that then closes the circuit by sending glutamatergic and excitatory fibers back to the dorsolateral prefrontal cortex.

Dendritic spines, serving as the primary site for excitatory synaptic transmission (Uchizono, 1965), are dynamic structures that facilitate contact between two neurons. Emerging from dendritic shafts, dendritic spines can be broadly divided into two components: a spine head and spine neck. The dendritic spine head typically contains a single type 1 asymmetric synapse, which is characterized by the presence of a protein rich postsynaptic density (PSD; Gray, 1959). The dendritic spine neck, a thin membrane tube, connects the head of the spine to the dendritic shaft. Morphological parameters of dendritic spines fall along a continuum and may reflect functionality and capacity for structural change (Lai and Ip, 2013). Indeed, strong linear relationships between dendritic spine morphological parameters (i.e., total spine volume, head volume, neck length, neck diameter) and PSD area (Harris and Stevens, 1988; Harris and Stevens, 1989; Arellano et al., 2007), presynaptic vesicles (Harris and Stevens, 1989), as well as synaptic strength (Araya et al., 2014) have been observed. Given the dynamic nature of dendritic spines (for review, Yuste, 2010), and their functional significance, therapeutics targeted at restoring synaptic efficacy may be key to ameliorating neurocognitive impairments resulting, at least partly, from synaptic dysfunction (e.g., Lambert et al., 1998; Gelman et al., 2012; Phan et al., 2017; McLaurin et al., 2019b).

Strong evidence supports the utility of the ovarian steroid estrogen (17β-estradiol) to remodel neuronal circuitry at the synaptic level. Specifically, in healthy, control animals 17β-estradiol increases dendritic spine density (e.g., Khan et al., 2013; Hao et al., 2006;

Tuscher et al., 2016; Wang et al., 2018), induces a morphological shift towards smaller, thin dendritic spines (Hao et al., 2006), and enhances cholinergic and monoaminergic neurotransmission (Kritzer & Kohama, 1998). Mechanistically, 17β-estradiol promotes the growth and stability of new dendritic spines via the ERβ pathway (Wang et al., 2018) supporting a key target for the development of novel therapeutics.

Phytoestrogens are plant-derived compounds that are structurally similar to 17β-estradiol (Glazier & Bowman, 2001) and exhibit a selective affinity for ERβ (e.g., Kuiper et al., 1998; Mueller et al., 2004). SE, the only enantiomer produced by humans (Setchell et al., 2005), is the major metabolite produced by the gut microbiota following ingestion of the soy derived phytoestrogen DAI (Setchell et al., 1984). Within the brain, SE penetrates the CNS via the blood-brain barrier, distributing most significantly to the prefrontal cortex in rats (Lund et al., 2001). Preclinical studies in the HIV-1 Tg rat, a biological system promoted for the assessment of HAND, support the therapeutic efficacy of SE for neurocognitive impairments (Moran et al., 2019; McLaurin et al., 2019a). Furthermore, the translational relevance of SE for the treatment of neurocognitive impairments is evidenced by its utilization in an ongoing clinical trial for AD (Ausio Pharmaceuticls; NCT03101085). Despite the potential utility of SE for the treatment of neurodegenerative diseases, the mechanism of SE action has not yet been fully elucidated.

Thus, the present study utilized the HIV-1 Tg rat as a biological system to model key aspects of HAND, a neurodegenerative disease (Cohen et al., 2015; McLaurin et al., 2019b), to critically test SE and the mechanism of SE action. The HIV-1 Tg rat, originally reported by Reid et al. (2001), exhibits age-related, progressive neurocognitive impairments (McLaurin et al., 2019b), in the absence of sensory or motor system deficits

and comorbidities (McLaurin et al., 2018b). Prominent alterations in synaptic dysfunction (Roscoe et al., 2014; McLaurin et al., 2018c; McLaurin et al., 2019b) have been repeatedly observed in the HIV-1 Tg rat. Elucidating the neural mechanism underlying the therapeutic effects of SE in HAND affords an opportunity to evaluate its therapeutic potential for other neurodegenerative diseases characterized by synaptic dysfunction.

METHODS

Study Design

Research Objectives

The primary objective of the present study was to critically test the therapeutic efficacy of SE for the treatment of neurocognitive impairments and to assess the mechanism by which SE exerts its therapeutic effects. The guiding hypothesis of the present study was that treatment with SE during the formative period would enhance neurocognitive function in HIV-1 Tg animals to approximate controls by targeting synaptic dysfunction.

The HIV-1 Tg rat, which has been promoted as an advantageous biological system to model key aspects of HAND (for review, Vigorito et al., 2015) was utilized in the present study. Developed by Reid et al. (2001), the non-infectious HIV-1 Tg rat contains a *gag-pol* deleted provirus regulated by the natural HIV-1 promotor, LTR. F344/N controls, rather than littermates, were used to assure the most developmentally appropriate and genetically stable baseline. Given the recommendations from the National Institutes of Health, the factor of biological sex was an integral component of the experimental design. HIV-1 Tg and F344/N control animals were randomly assigned to treatment group (i.e., SE or

placebo). Thus, the present study utilized a 2 (Genotype) x 2 (Biological Sex) x 2 (Treatment) experimental design.

Neurocognitive assessments were conducted to tap multiple neurocognitive domains, including stimulus-response learning, sustained attention, selective attention, and flexibility and inhibition. Given observations of synaptic dysfunction across multiple neurodegenerative diseases (e.g. Lambert et al., 1998; Phan et al., 2017; McLaurin et al., 2019b), a ballistic labeling technique was used to assess whether SE enhances synaptic efficacy in pyramidal neurons from the mPFC; a brain region that partially resembles some of the features associated with the primate anterior cingulate cortex and dlPFC (for review, Ulyings et al., 2003; for review, Seamans et al., 2008). The sensitivity of the signal detection operant task to DAergic and noradrenergic system function was assessed using an *in situ* hybridization technique. Neuroanatomical assessments were conducted blind to genotype, biological sex and/or treatment.

A statistical power analysis and an estimate of variance were calculated to determine the number of animals needed for the proposed studies. A power analysis suggested sample sizes of n=16 per group to detect sex (i.e., male, female) differences at the 10-15% level. Based on our recent data variance with the proposed methods for the assessment of the core components of executive function (Moran et al., 2014a; McLaurin et al., 2019b), this sample size estimate should be adequate for detecting significant differences with a power of 0.8 at $p \leq 0.05$ (Cohen et al., 2003).

Animals

Between PD 7 and PD 9, Fischer (F344/N; Harlan Laboratories Inc., Indianapolis, IN) HIV-1 Tg (N=24 litters) and control (N=19 litters) animals, housed with their biological

dam, were received at the animal vivarium. At approximately PD 24, animals were randomly sampled from each litter (HIV-1 Tg: male, *n*=33, female, *n*=34; Control: male *n*=38; female, *n*=34), weaned and pair- or group-housed with animals of the same sex for the duration of experimentation. To control for independence of observations, the goal was to select one rat for each treatment group from each litter (i.e., two male rats per litter and two female rats per litter).

Beginning at approximately PD 28, HIV-1 Tg and control animals began daily treatment with either SE or placebo (i.e., sucrose pellets (Bio-Serv, Inc., Flemington, NJ)). SE, obtained from Cayman Chemical Company (Ann Arbor, MI), was incorporated into sucrose pellets by Bio-Serv, with each pellet containing 0.2 mg SE.

Animals were randomly assigned to either the SE or placebo group (Control: SE, *n*=35 (male, *n*=18, female, *n*=17), Placebo, *n*=37 (male, *n*=20, female, *n*=17); HIV-1 Tg: SE, *n*=35 (male, *n*=17, female, *n*=18), Placebo, *n*=32 (male, *n*=16, female, *n*=16)). HIV-1 Tg and control animals treated with SE received a daily oral dose of 0.2 mg of SE; a dose which was previously established as the most effective dose using a dose-response experimental design (Moran et al., 2019). Furthermore, the dose selected yielded a daily amount of 0.25-1.0 mg/kg SE; an amount equivalent to a 2.5-10 mg dose in a 60 kg human (Cf., most elderly Japanese have a daily isoflavone intake of 30-50 mg, Akaza, 2012).The placebo group received a sucrose pellet. Treatment was administered daily after the completion of neurocognitive testing to promote the long-term remodeling of neuronal circuitry (e.g., Bertrand et al., 2014, Bertrand et al., 2015). HIV-1 Tg and control animals were treated through PD 90.

HIV-1 Tg and control animals were sacrificed following the successful completion of either the assessment of selective attention (i.e., 5 days in the task) or the assessment of flexibility and inhibition (i.e., 70% accuracy for 5 consecutive or 7 non-consecutive days or 60 days in the task). Brains from animals sacrificed following the assessment of selective attention were processed for RNA *in situ* hybridization to assess dopamine D1 and norepinephrine α2 receptor expression in the PFC. Animals were selected for RNA *in situ* hybridization based on the number of days to criterion in the signal detection operant task with the goal of reflecting the spectrum (i.e., animals completing the task early, middle, and late) of cognitive function observed in HIV-1 Tg and control animals. Brains from animals sacrificed following the assessment of flexibility and inhibition were utilized to examine synaptic dysfunction in pyramidal neurons from layers II-III of the mPFC.

Recommendations in the Guide for the Care and Use of Laboratory Animals of the NIH were used for the maintenance of HIV-1 Tg and control animals in AAALAC-accredited facilities. The targeted environmental conditions for the animal vivarium were 21°± 2°C, 50% ± 10% relative humidity and a 12-h light:12-h dark cycle with lights on at 0700 h (EST). The IACUC at the University of South Carolina approved the project protocol (Federal Assurance # D16-00028).

Neurocognitive Assessments

Apparatus

Thirty-two operant chambers, located inside sound-attenuating chambers (Med Associates, Inc., VT) were used to assess animals in a series of tasks tapping multiple neurocognitive domains, including stimulus-response learning, sustained attention, selective attention, and flexibility and inhibition. The front wall of the operant chamber included a pellet dispenser (45 mg), located between two retractable levers, and three panel

lights. The present experiment utilized only the panel light (LED, 11 lux) located above the pellet dispenser for signal presentation. The top of the rear wall of the operant chamber included a house light (incandescent, 5.5 lux), which was utilized for shaping. Signal presentation, lever operation, reinforcement delivery, and data collection were controlled using PC and Med-PC for Windows software (V 4.1.3; Med Associates, Inc., Fairfax, VT).

Shaping

A standard shaping response protocol was used to train animals to lever-press at approximately 2 months of age, described in detail by McLaurin et al. (2017d) with minor modifications. All animals were assessed in the shaping response protocol for 45 days prior to beginning the signal detection operant task.

Sustained Attention: Signal Detection Operant Task

After 45 days in shaping, all HIV-1 Tg (SE, *n*=35 (male, *n*=17, female, *n*=18), Placebo, *n*=32 (male, *n*=16, female, *n*=16) and control (SE, *n*=35 (male, *n*=18, female, *n*=17), Placebo, *n*=37 (male, *n*=20, female, *n*=17)) animals were trained in a signal detection operant task, tapping sustained attention.

The signal detection operant task, initially described by McGaughy and Sarter (1995), included a series of four tasks. In brief, animals were trained to discriminate between signal (i.e., central panel light illumination) and non-signal (i.e., no illumination) trials. In the first program, consisting of 160 trials per session, the stimulus light was terminated after an animal made a response. In the second program, consisting of 160 trials per session, the length of the stimulus light was 1 sec. Integral to the first two programs were correction trials, which included up to three repetitions of the trial, and forced-choice trials; trials which occurred when an animal responded incorrectly. In the third and fourth

programs, each consisting of 162 trials per session, the length of the stimulus was manipulated (i.e., 1000, 500, 100 msec and 1000, 100, 10 msec, respectively) across trials using a block randomized experimental design. Correction trials and forced-choice trials were removed from the third and fourth programs.

HIV-1 Tg and control animals were trained on each program until achieving at least 70% accuracy on five consecutive, or seven non-consecutive, test sessions. Accuracy was calculated using the following equation:

$$\frac{Hits + Correct\ Rejections}{Hits + Correct\ Rejection + Misses + False\ Alarms}$$

Selective Attention: Visual Distractor Task

After the successful completion of the signal detection operant task, HIV-1 Tg (SE, *n*=35 (male, *n*=17, female, *n*=18), Placebo, *n*=32 (male, *n*=16, female, *n*=16) and control (SE, *n*=35 (male, *n*=18, female, *n*=17), Placebo, *n*=37 (male, *n*=20, female, *n*=17)) animals were challenged for five consecutive days in a visual distractor task, tapping selective attention. During the visual distractor task, the signal detection operant task with varying signal durations (1000, 100, 10 msec) was divided into three trial blocks, each containing 54 trials. During the second trial block, a 1.5 sec visual distractor stimulus was presented at the beginning of each trial. The visual distractor stimulus onset and offset was 1 sec prior to and 0.5 sec after the signal onset (center panel light), for a 1.5 sec total duration. The house light was used as the visual distractor, with an intensity of 5.5 lux measured from the center of the chamber at the level of the animal's height.

Flexibility and Inhibition: Reversal Task

Subsequently, HIV-1 Tg (SE, *n*=25 (male, *n*=11, female, *n*=14), Placebo, *n*=23 (male, *n*=12, female, *n*=11) and control (SE, *n*=24 (male, *n*=11, female, *n*=13), Placebo,

n=24 (male, *n*=13, female, *n*=12)) animals were challenging in a reversal task, tapping flexibility and inhibition. During the reversal task, response contingencies learned during the signal detection operant task were reversed. Animals were given at least 60 days to successfully complete the reversal assessment.

Neuroanatomical Assessments

RNA in situ hybridization

A novel RNA *in situ* hybridization technique was used to evaluate dopamine (DA) receptor and norepinephrine (NE) receptor expression in the mPFC (Control: SE, *n*=6 (male, *n*=3, female, *n*=3), Placebo, *n*=6 (male, *n*=3, female, *n*=3); HIV-1 Tg: SE, *n*=6 (male, *n*=3, female, *n*=3), Placebo, *n*=6 (male, *n*=3, female, *n*=3). Specifically, DA receptor expression was assessed using D1-alpha subtype receptor probe (Rn-Drd1α) and NE receptor expression was examined using the alpha-2 NE receptor probe (Rn-Adra2a).

Methodology for RNA *in situ* hybridization was described in detail by Li et al. (2018), with minor modifications for the present study. In brief, fresh frozen brain sections were obtained and 30 µm sections were cut from the mPFC (approximately 3.7 mm to 2.2 mm anterior to Bregma (Paxinos & Watson, 2014). Sections were mounted onto slides and allowed to dry. Brain sections were pretreated and incubated for 30 minutes. Subsequently, 3 drops (90 µL) of the Rn-Drd1α probe and Rn-Adra2a probe were added to the brain sections. Next, amplification steps were performed using the Amp 1-FL, Amp 2-FL, Amp 3-FL, and Amp 4-FL reagents. Slides were cover-slipped and stored in the dark until Z-stack images were obtained using confocal microscopy.

RNA Analysis and Quantification. A Nikon TE-2000E confocal microscope, utilizing Nikon's EZ-C1 software (version 3.81b), was used to acquire z-stack images at the 60x objection (n.a.=1.4) from the mPFC. Two images were obtained for each animal.

Both the Rn-Drd1α probe and Rn-Adra2a probe exhibited a "discrete dots" staining pattern (Li et al., 2018). Given the observed staining pattern, a cell region was defined and fluorescent signals were quantified by counting the number of dots per cell which were used for the assignment of a cell score ranging from 1 to 9, whereby higher categories reflect a greater number of mRNA molecules within the cell.

Synaptic Dysfunction

Preparation of Tissue. Sevoflurane (Abbot Laboratories, North Chicago, IL) was used to deeply anesthetize animals for transcardial perfusion. Methodology for transcardial perfusion is reported in Roscoe et al. (2014).

DiOlistic Labeling. Pyramidal neurons from layers II-III of the mPFC were visualized using a DiOlisitc labeling technique, originally described by Seabold et al. (2010). Methodology for the preparation of DiOlistic cartridges, preparation of Tefzel tubing, and DiOlistic labeling is described in detail by McLaurin et al. (2018a).

Pyramidal Neuron Dendritic Analysis and Spine Quantification. Analyses were conducted on pyramidal neurons from layers II-III of the mPFC, including both the anterior cingulate cortex and infralimbic cortex. Specifically, neurons were located approximately 3.7 mm to 2.2 mm anterior to Bregma (Paxinos & Watson, 2014). Z-stack images were obtained using methodology previously reported (Roscoe et al., 2014) on three to four pyramidal neurons from each animal [Control: SE, *n*=28 (male, *n*=15, female, *n*=13), Placebo, *n*=30 (male, *n*=16, female, *n*=14); HIV-1 Tg: SE, *n*=28 (male, *n*=13, female, *n*=15), Placebo, *n*=24 (male, *n*=11, female, *n*=13)].

Spine analyses, conducted using the AutoNeuron and AutoSpine extension models in Neurolucida 360 (MicroBrightfield, Williston, VT), were completed on neurons meeting selection criteria (e.g., continuous dendritic staining, low background/dye clusters, and

minimal diffusion of the DiI dye into the extracellular space; Li et al., 2020). Based on the selection criteria, one neuron from each animal was chosen for the analysis of spine parameters. Neurons not meeting the selection criteria were not included in the analysis, yielding Control: SE, *n*=25 (male, *n*=14, female, *n*=11), Placebo, *n*=27 (male, *n*=15, female, *n*=12); HIV-1 Tg: SE, *n*=25 (male, *n*=12, female, *n*=13), Placebo, *n*=22 (male, *n*=10, female, *n*=12).

Neuronal and Spine Parameters. Analyses were conducted to assess neuronal morphology (i.e., Sholl analysis) and dendritic spine morphology. The classical Sholl analysis (Sholl, 1953) was utilized to count the number of intersections at each successive radii (10 μm) as a method to evaluate neuronal complexity. Dendritic spine morphology was assessed using three parameters, including the backbone length (μm), head diameter (μm), and neck diameter (μm). Spine parameters were defined using well-accepted previously published results [i.e., volume, 0.05 to 0.85 μm: Hering & Sheng, 2001; backbone length, 0.4 to 4.0 μm: Ruszcycki et al., 2012; head diameter, 0 to 1.2 μm: Konur et al., 2003; neck diameter, 0 to 1.0 μm].

Statistical Analysis

Data were analyzed using ANOVA and regression techniques (SAS/STAT Software 9.4, SAS Institute, Inc., Cary, NC; SPSS Statistics 26, IBM Corp., Somer, NY; GraphPad Software, Inc., La Jolla, CA). Statistical significance was established at an alpha criterion of $p \leq 0.05$. *A priori* planned comparisons were conducted to establish the presence of neurocognitive impairment (i.e., Control Placebo vs. HIV-1 Tg Placebo) and the magnitude of the SE effect (i.e., HIV-1 Tg Placebo vs. HIV-1 Tg SE and/or Control Placebo vs. HIV-1 Tg SE).

The temporal process of acquisition (i.e., the number of days to meet criterion) during the acquisition of the signal detection operant task, under additional attentional demands, and during reversal acquisition was analyzed using a curve-fitting analysis, fit with a 95% CI, to directly assess functional form (GraphPad Software, Inc., La Jolla, CA, USA). Additionally, the number of days meeting criterion during the visual distractor task was analyzed using a curve-fitting analysis, fit with a 95% CI (GraphPad Software, Inc., La Jolla, CA, USA).

The response profile and signal duration data during the acquisition of the signal detection operant task and under additional attentional demands were analyzed using a mixed-factor ANOVA (SPSS Statistics 26, IBM Corp., Somer, NY). Additionally, the response profile and signal duration data from the reversal task were assessed by conducting a mixed-factor ANOVA with a compound symmetry covariance structure (SAS/STAT Software 9.4, SAS Institute, Inc., Cary, NC). with genotype (HIV-1 Tg vs. control), sex (male vs. female), and treatment (SE vs. placebo) serving as between-subject's factors, as appropriate. Response type (correct rejections, hits, misses and false alarms) and signal duration (e.g., 1000, 500, 100 msec) served as the within subject's factors, as appropriate. During the acquisition of the signal detection operant task and under additional attentional demands, signal detection data was analyzed for the first five days in the task. For the reversal task, when an animal met criteria, the first five consecutive or seven non-consecutive days that an animal achieved 70% accuracy were included. In the reversal assessment, if an animal failed to meet criteria, but had completed 60 days in the task, the seven days with the highest percent accuracy were included in the analysis.

The number of false alarms during each trial block were analyzed using a repeated-measures ANOVA (SPSS Statistics 26, IBM Corp., Somer, NY) to validate the assessment of selective attention in the visual distractor task. For task validation, all animals independent of genotype, sex and/or treatment, were included in the analysis. The response profile for non-signal trials (i.e., false alarms and correct rejections) was also examined using a repeated-measures ANOVA (SPSS Statistics 26, IBM Corp., Somer, NY), with the number of responses during the first and second trial block serving as the dependent variable. Signal duration data from the visual distractor task were analyzed for only trial block two (i.e., when the distractor was present) using a mixed-modal ANOVA (SPSS Statistics 26, IBM Corp., Somer, NY).

Simple linear regression analyses were conducted to examine the relationship between the mean cell score, reflecting DA (Drd1α) and NE (Adra2a) receptor expression in the mPFC, and the number of days to meet criterion in the signal detection operant task. The number of days to acquisition included performance across all four vigilance programs.

Dendritic branching complexity was assessed to evaluate neuronal morphology by examining branch orders one through fifteen. A curve-fitting analysis, fit with a 95% CI, to directly assess functional form (GraphPad Software, Inc., La Jolla, CA, USA), was conducted on the cumulative frequency of branch order. The number of dendritic spines at each radii and dendritic spine morphology were analyzed using a generalized linear mixed effects model with a Poisson distribution and an unstructured covariance pattern (SAS/STAT Software 9.4, SAS Institute, Inc., Cary, NC). Between subject's factors included genotype, sex, and treatment, as appropriate. Within subjects' factors included

radii and bin, as appropriate. Analyses were conducted on the number of dendritic spines in each bin.

RESULTS

Neurocognitive Assessments

Neurocognitive impairments, including alterations in temporal processing, attention, memory, and executive function (e.g., Cysique et al., 2004; Garvey et al., 2009; Heaton et al., 2011), are a hallmark of HIV-1 in the post-cART era; deficits which have been translationally modeled in the HIV-1 Tg rat (e.g., Vigorito et al., 2007; Moran et al., 2013a; Moran et al., 2014a; Repunte-Canonigo et al., 2014; McLaurin et al., 2019b). Therefore, in the present study, it was hypothesized that HIV-1 Tg animals would exhibit selective neurocognitive impairments across multiple neurocognitive domains, including stimulus-reinforcement learning, sustained attention, selective attention, and flexibility and inhibition. To critically test the hypothesis, *a priori* planned comparisons between HIV-1 Tg animals treated with placebo and control animals treated with placebo were conducted.

Presence of the HIV-1 Transgene

Signal Detection Operant Task: 1000, 500, 100 msec. Beginning at approximately two months of age, HIV-1 Tg and control animals were trained in a signal detection operant task, containing three vigilance programs, originally described by McGaughy and Sarter (1995). The task, tapping sustained attention, required HIV-1 Tg and control animals to attend to a randomly presented stimulus (i.e., illumination of the central panel) across 160-162 testing trials. The presence or absence of the stimulus indicated which response to make (i.e., which lever to press) to receive a reinforcer (i.e., sucrose pellet). On each trial, the animal may emit one of four response choices (i.e., hits, misses, correct rejections, false

alarms). Hits and correct rejections, indicative of the ability to attend to the stimulus, were rewarded with a reinforcer. Misses, reflecting a lapse of attention, and false alarms, indicative of failure of response inhibition, were not rewarded. Furthermore, the third vigilance program systematically manipulated the signal duration (i.e., 1000, 500, 100 msec), which afforded an opportunity to assess the temporal components of sustained attention.

All HIV-1 Tg and control animals treated with placebo, independent of biological sex, were able to successfully acquire the task, achieving 70% accuracy for five consecutive or seven non-consecutive test sessions. Presence of the HIV-1 transgene failed to significantly alter the temporal process of acquisition ($p>0.05$), best fit using a sigmoidal dose response curve (Figure 5.1; $R^2 s \geq 0.99$). Results support, therefore, no prominent genotypic deficits in stimulus-reinforcement learning during the initial task acquisition.

Sustained attention was assessed by averaging the performance of each animal across their first five days in the third vigilance program. Presence of the HIV-1 transgene failed to significantly alter the response profile (i.e., number of correct rejections, hits, misses, and false alarms; Figure 5.1; $p>0.05$). Investigating the temporal components of sustained attention, however, revealed profound impairments in HIV-1 Tg animals treated with placebo relative to their control counterparts (Figure 5.1; Genotype x Response Type x Duration with a prominent linear-quadratic component, [$F(1,65)=5.3$, $p \leq 0.03$, $\eta_p^2=0.075$]). A pronounced rightward shift in the loss of signal detection (i.e., where the number of hits and misses intersect), was observed in HIV-1 Tg animals treated with placebo relative to control animals treated with placebo (approximately 720 msec vs. 420 msec, respectively). Thus, HIV-1 Tg animals displayed a prominent deficit in the

perception of time, a potential elemental dimension of HAND (e.g., Chao et al., 2004; Matas et al., 2010; Moran et al., 2013a), in sustained attention.

Signal Detection Operant Task: 1000, 100, 10 msec. After successfully acquiring the first three vigilance programs, HIV-1 Tg and control animals were challenged with a fourth vigilance program that included shorter signal durations (1000, 100, 10 msec) to increase attentional load.

All HIV-1 Tg and control animals treated with placebo, independent of biological sex, were able to successfully acquire the fourth vigilance program, achieving 70% accuracy for five consecutive or seven non-consecutive test sessions. A one-phase association provided a well-described fit for both control and HIV-1 Tg animals treated with placebo (Figure 5.1; R^2s$\geq$0.97). Under increased attentional demands, however, HIV-1 Tg animals treated with placebo exhibited profound deficits in stimulus-reinforcement learning, evidenced by a significantly slower rate (i.e., K) of learning [$F(1,38)=17.5$, $p\leq0.001$].

The effects of an increased attentional load on sustained attention were assessed by averaging the performance of each animal across their first five days in the fourth vigilance program. Presence of the HIV-1 transgene failed to significantly alter the response profile (Figure 5.1; $p>0.05$) or temporal components of sustained attention (Figure 5.1; $p>0.05$) under increased attentional demands. Thus, HIV-1 Tg animals treated with placebo displayed a prominent deficit in stimulus-reinforcement learning, but not sustained attention, when challenged with an increased attentional load.

Visual Distractor Task: 1000, 100, 10 msec. After successfully acquiring all four vigilance programs, HIV-1 Tg and control animals completed five test sessions in a visual

distractor task to assess selective attention. During the second trial block (i.e., Trials 54-108), a 1.5 second visual distractor was presented at the beginning of each trial.

A curve-fitting analysis was utilized to examine the number of days HIV-1 Tg and control animals treated with placebo met criterion. A global first-order polynomial provided a well-described fit for HIV-1 Tg and control animals treated with placebo (Figure 5.1; R^2s$\geq$0.98), supporting no prominent genotypic deficits in stimulus-reinforcement learning during the visual distractor task.

To validate the assessment of selective attention in all animals, independent of genotype, biological sex and/or treatment, the relative frequency of false alarms during each trial block were examined (Figure 5.1). During the second trial block (i.e., when the distractor was present), a dramatic increase in the relative frequency of false alarms was observed relative to either the first or third trial blocks (Main Effect, Trial Block [$F(2,262)=171.0$, $p_{GG}\leq0.001$]); results which support the assessment of selective attention. Examination of the relative frequency of false alarms and correct rejections in HIV-1 Tg and control animals treated with placebo during the first and second trial blocks (Figure 5.1) provided additional support for the assessment of selective attention (Trial Block x Response Type, [$F(1,65)=120.7$, $p_{GG}\leq0.001$]) and absence of any genotypic effect ($p>0.05$). Furthermore, no significant genotypic differences in the temporal components of selective attention ($p>0.05$) were observed during the second trial block of the visual distractor task. Thus, there was no evidence for any prominent deficits in selective attention in the HIV-1 Tg rat.

Reversal Task: 1000, 100, 10 msec. After completing the visual distractor task, a subset of HIV-1 Tg and control animals were challenged with a reversal task, tapping

flexibility and inhibition. Response contingencies were reversed from those originally learned in the signal detection operant task. Animals completed the reversal task by either meeting criteria (i.e., 70% accuracy for five consecutive or seven non-consecutive test sessions) or completing at least 60 test sessions.

Presence of the HIV-1 transgene significantly altered the temporal process of acquisition in the reversal task supporting a prominent deficit in stimulus-reinforcement learning (Figure 5.2). Independent of genotype, a first-order polynomial provided a well-described fit for the cumulative proportion of placebo-treated animals successfully acquiring the task (R^2s$\geq$0.97). Significant differences, however, were observed in the fit of the first-order polynomial [$F(2,33)=6.7$, $p\leq 0.01$] reflecting the decreased proportion of HIV-1 Tg animals treated with placebo successfully acquiring the task (i.e., 47.8%) relative to their control counterparts (i.e., 64%) .

Flexibility and inhibition were assessed by averaging an animal's best performances, based on percent accuracy, during the first 60 days in the reversal task. Presence of the HIV-1 transgene significantly altered the response profile (Figure 5.2) dependent upon the factor of biological sex (Genotype x Sex x Response Type, [$F(3,129)=2.9$, $p\leq 0.04$]). Specifically, male HIV-1 Tg animals treated with placebo exhibited an increased number of correct rejections and misses relative to male control animals treated with placebo. In sharp contrast, female HIV-1 Tg animals treated with placebo displayed no deficits in flexibility and inhibition.

Consistent with alterations in the observed response profile, HIV-1 Tg animals treated with placebo exhibited prominent deficits in the temporal components of flexibility and inhibition (Figure 5.2), dependent upon the factor of biological sex (Genotype x Sex x

Response Type, [$F(1, 43)=15.5$, $p\leq 0.001$]). Independent of signal duration, male HIV-1 Tg animals treated with placebo exhibited an increased number of misses relative to male control animals treated with placebo; an effect that led to HIV-1 Tg animals treated with placebo to be unable to reliably detect the signal at any duration assessed. Male control animals, however, displayed a loss of signal detection at approximately 520 msec. Thus, although deficits in stimulus-reinforcement learning in the reversal task were independent of biological sex, only male HIV-1 Tg animals displayed alterations in flexibility and inhibition.

Therapeutic Efficacy of S-Equol

Given the marked neurocognitive impairments in HAND, a neuroprotective and/or neurorestorative therapeutic may be advantageous in the post-cART era. To evaluate the magnitude of the SE effect, two *a priori* planned comparisons were conducted, 1) By comparing HIV-1 Tg animals treated with placebo and HIV-1 Tg animals treated with SE and 2) By comparing control animals treated with placebo and HIV-1 Tg animals treated with SE.

Signal Detection Operant Task: 1000, 500, 100 msec. Independent of biological sex, treatment with SE enhanced the temporal components of sustained attention in HIV-1 Tg animals (Figure 5.3; Genotype x Treatment x Response Type x Duration interaction with a prominent linear-quadratic component [$F(1,131)=5.7$, $p\leq 0.02$, $\eta_p^2=0.042$]). A loss of signal detection was observed at approximately 720 msec in HIV-1 Tg animals treated with placebo, approximately 570 msec in HIV-1 Tg animals treated with SE, and approximately 420 msec in control animals treated with placebo.

Subsequently, *a priori* comparisons were conducted to evaluate the magnitude of the SE effect. Sustained attention in HIV-1 Tg animals treated with SE was statistically indistinguishable from either HIV-1 Tg animals treated with placebo (Treatment x Response Type x Duration, $p>0.05$) or control animals treated with placebo (Genotype x Response Type x Duration, $p>0.05$). Treatment with SE, therefore, precluded the development of a statistically significant deficit in the temporal components of sustained attention in the HIV-1 Tg rat.

Signal Detection Operant Task: 1000, 100, 10 msec. Treatment with SE failed to preclude the development of profound deficits in the temporal process of acquisition of the fourth vigilance program, requiring an increased attentional load.

All HIV-1 Tg and control animals, independent of treatment and/or biological sex, were able to successfully acquire the fourth vigilance program, achieving 70% accuracy for five consecutive or seven non-consecutive test sessions. A one-phase association provided a well-described fit for HIV-1 Tg animals treated with SE, HIV-1 Tg animals treated with placebo, and control animals treated with placebo (Figure 5.3; R^2s$\geq$0.97). Under increased attentional demands, however, HIV-1 Tg animals treated with SE exhibited no statistically significant improvement in the rate (i.e., K) of learning relative to HIV-1 Tg animals treated with placebo ($p>0.05$) and a significantly slower rate of learning relative to control animals treated with placebo [$F(1,40)=16.7$, $p\leq0.001$]. Thus, treatment with SE during the formidable period (i.e., PD 28-90) failed to prevent the development of deficits in the temporal process of acquisition under increased attentional demands.

Reversal Task: 1000, 100, 10 msec. Treatment with SE failed to preclude the development of profound deficits in the temporal process of acquisition in the reversal task.

Despite SE treatment, only 40% of the HIV-1 Tg animals were able to successfully acquire the reversal task, well-described by a segmental linear regression ($R^2 \geq 0.98$; Figure 5.3). Thus, treatment with SE during the formidable period (i.e., PD 28-90) failed to prevent deficits in the temporal process of acquisition in the reversal task.

In sharp contrast, treatment with SE enhanced the temporal components of flexibility and inhibition in male HIV-1 Tg animals (Figure 5.3; Genotype x Treatment x Response Type, [$F(1, 43)=5.9$, $p \leq 0.02$]). Independent of signal duration, male HIV-1 Tg animals treated with SE exhibited an increased number of hits relative to either male HIV-1 Tg or male control animals treated with placebo; an effect that led to a robust leftward shift in the loss of signal detection. Specifically, a loss of signal detection was observed at approximately 190 msec in male HIV-1 Tg animals treated with SE, and approximately 520 msec in male control animals treated with placebo. Male HIV-1 Tg animals treated with placebo failed to reliably detect the signal at any duration assessed.

Subsequently, *a priori* comparisons were conducted to evaluate the magnitude of the SE effect. Comparison of HIV-1 Tg animals treated with SE and HIV-1 Tg animals treated with placebo revealed a statistically significant treatment x response type interaction [$F(1,21)=7.4$, $p \leq 0.01$]; a result reflecting the increased number of hits observed in HIV-1 Tg animals treated with SE. Furthermore, comparison of HIV-1 Tg animals treated with SE and control animals treated with placebo revealed a main effect of genotype [$F(1,22)=8.4$, $p \leq 0.01$], but no statistically significant interactions ($p>0.05$); a main effect reflecting, again, the increased responding exhibited by HIV-1 Tg animals treated with SE. Thus, treatment with SE, increased responding in HIV-1 Tg animals, producing a robust shift in the temporal components of flexibility and inhibition.

Neuroanatomical Assessments

In Situ Hybridization: Dopamine and Norepinephrine Receptor Expression

A subset of HIV-1 Tg and control animals were sacrificed after the completion of the visual distractor task to evaluate DA (Drd1α) and NE (Adra2a) receptor expression in the mPFC. Animals were selected based on the number of days to criterion in the four vigilance programs comprising the signal detection operant task to reflect the spectrum of cognitive function observed in HIV-1 Tg and control animals.

The signal detection operant task is sensitive to both DA (Figure 5.4) and NE (Figure 5.4) receptor expression. For DA, a segmental linear regression provided a well-described fit for the relationship between the number of days to criterion and mean cell score, revealing a regression coefficient (r) of 0.679. The relationship between the number of days to criterion and mean cell score for NE was also described by a segmental linear regression, revealing a regression coefficient (r) of 0.845. The number of days to criterion, therefore, explained 46.1% of the variance in the mean cell score for Drd1α and 71.4% of the variance in the mean cell score for Adra2a. A linear increase in mean cell score was observed for both DA and NE when animals needed more than 121 days to acquire the signal detection operant task, supporting suboptimal neurotransmitter system function.

Presence of the HIV-1 Transgene: Synaptic Dysfunction

Additional HIV-1 Tg and control animals were sacrificed after the completion of the reversal task to evaluate synaptic dysfunction in pyramidal neurons from layers II-III of the mPFC. A ballistic labeling technique was utilized to visualize pyramidal neurons, which were subsequently analyzed using sophisticated neuronal reconstruction software.

Neuronal Morphology. Dendritic branching complexity was examined using a centrifugal branch ordering method, which assigned each dendrite with a branch order by counting the number of segments traversed. Branch orders one through fifteen were analyzed using regression analyses.

Presence of the HIV-1 transgene significantly altered the branch order distribution in pyramidal neurons (Figure 5.5). Independent of genotype, a sigmoidal dose-response curve provided a well-described fit for the cumulative frequency of the number of dendrites at each branch order in placebo-treated animals (R^2s$\geq$0.99). However, significant differences were observed in the fit of the sigmoidal dose-response curve [F(4,22)=33.6, $p\leq$0.01], supporting a prominent alteration in dendritic branching complexity. Notably, deficits in dendritic branching complexity occurred in the absence of any statistically significant differences in total dendrite length (p>0.05).

Excitatory Synapses. HIV-1 Tg animals treated with placebo, independent of biological sex, had a decreased number of dendritic spines dependent upon distance from the soma (Figure 5.5; Radii x Genotype, [F(1,3606)=55.7, $p\leq$0.001]), relative to control animals treated with placebo. A cubic-polynomial provided a well-described fit for the number of dendritic spines, independent of genotype (R^2s$\geq$0.96); albeit statistically significant differences in the fit of the function were observed [F(4,36)=5.1, $p\leq$0.002]. Furthermore, HIV-1 Tg animals treated with placebo exhibited a population shift towards decreased dendritic spine volume relative to control animals treated with placebo (Figure 5.5; Genotype x Bin, [F(15, 675)=2.9, $p\leq$0.001]). HIV-1 Tg animals treated with placebo, therefore, may have fewer and weaker synapses, relative to their control counterparts.

Dendritic Spine Morphology. Presence of the HIV-1 transgene produced a selective, sex-dependent population shift in dendritic spine morphology. Four parameters, including dendritic spine backbone length, dendritic spine head diameter, and dendritic spine neck diameter, were examined. Measurements of dendritic spine backbone length [$F(18, 810)=29.4$, $p\leq0.001$], head diameter [$F(12, 540)=8.1$, $p\leq0.001$], and neck diameter [$F(10, 450)=11.2$, $p\leq0.001$], however, were dependent upon presence of the HIV-1 transgene and the factor of biological sex (i.e., Genotype x Sex x Bin interaction). Complementary analyses were conducted independently for each sex.

Male HIV-1 Tg animals treated with placebo exhibited a population shift towards decreased dendritic spine backbone length (Figure 5.5) and increased neck diameter (Figure 5.5) relative to their control counterparts (Genotype x Bin: Backbone Length, [$F(18, 414)=12.2$, $p\leq0.001$]; Neck Diameter: [$F(10,230)=2.1$, $p\leq0.03$]). No statistically significant alterations in dendritic spine head diameter were observed in male animals ($p>0.05$). Morphological characteristics of dendritic spines in male HIV-1 Tg animals treated with placebo, therefore, suggest a population shift towards 'stubby' spines.

In sharp contrast, female HIV-1 Tg animals treated with placebo displayed a population shift towards increased dendritic spine backbone length (Figure 5.5) with decreased neck (Figure 5.5) and head diameter (Figure 5.5) relative to female control animals treated with placebo (Genotype x Bin: Backbone Length, [$F(18, 396)=19.4$, $p\leq0.001$]; Head Diameter, [$F(12,264)=10.9$, $p\leq0.001$]; Neck Diameter, [$F(10,220)=13.4$, $p\leq0.001$]). Morphological characteristics of dendritic spines in female HIV-1 Tg animals treated with placebo, therefore, suggest a population shift towards 'thin' spines.

Independent of biological sex, however, dendritic spines in HIV-1 Tg animals were indicative of a more immature phenotype relative to their control counterparts.

Therapeutic Efficacy of S-Equol: Synaptic Dysfunction

Profound synaptic dysfunction, characterized by alterations in dendritic branching complexity, synaptic connectivity and dendritic spine morphology, was observed in HIV-1 Tg animals treated with placebo supporting a key neural mechanism underlying HAND in the post-cART era. Given the therapeutic effects of SE on HIV-1 Tg animals, SE may exert its effects by remodeling neuronal circuitry at the synaptic level. To evaluate the magnitude of the SE effect on synaptic dysfunction, two a priori planned comparisons were conducted, 1) By comparing HIV-1 Tg animals treated with placebo and HIV-1 Tg animals treated with SE and 2) By comparing control animals treated with placebo and HIV-1 Tg animals treated with SE.

Neuronal Morphology. Alterations in the branch order distribution in pyramidal neurons was mitigated in HIV-1 Tg animals by treatment with SE during the formative period (Figure 5.6). Dendritic branching complexity, examined by evaluating the cumulative frequency of the number of dendrites at each branch order, in HIV-1 Tg animals treated with placebo was well-described by a sigmoidal dose-response curve ($R^2 \geq 0.99$). More notably, however, dendritic branching complexity in control animals treated with placebo and HIV-1 Tg animals treated with SE was best fit using a global sigmoidal dose-response curve ($R^2 \geq 0.99$). HIV-1 Tg animals treated with SE during the formative period, therefore, exhibited a shift in dendritic branching complexity that was statistically indistinguishable from control animals treated with placebo.

Synaptic Contacts. HIV-1 Tg animals treated with SE exhibited long-term alterations in the number of dendritic spines dependent upon distance from the soma (Figure 5.6; Genotype x Treatment x Radii, [$F(1,7286)=11.8$, $p\leq0.001$]). Independent of genotype and/or treatment, a cubic-polynomial provided a well-described fit for the number of dendritic spines (R^2s≥0.96).

Subsequently, a priori comparisons were conducted to evaluate the magnitude of the SE effect. Comparison of HIV-1 Tg animals treated with SE and HIV-1 Tg animals treated with placebo revealed a statistically significant treatment x radii interaction [$F(1,3458)=405.3$, $p\leq0.001$]. Additionally, comparison of HIV-1 Tg animals treated with SE and control animals treated with placebo also revealed a statistically significant genotype x radii interaction [$F(1,3828)=208.8$, $p\leq0.001$]. Specifically, HIV-1 Tg animals treated with SE exhibited an increased number of dendritic spines on more distal radii relative to either HIV-1 Tg animals treated with placebo or control animals treated with placebo.

Furthermore, treatment with SE significantly altered the distribution of dendritic spine volume in HIV-1 Tg animals (Figure 5.6; Genotype x Treatment x Bin, [$F(15, 1365)=2.3$, $p\leq0.004$]). Despite a shift towards increased dendritic spine volume in HIV-1 Tg animals treated with SE, the distribution of dendritic spine volume was statistically indistinguishable from HIV-1 Tg animals treated with placebo (Treatment x Bin, $p>0.05$). Most critically, however, the distribution of dendritic spine volume was also statistically indistinguishable from control animals treated with placebo (Genotype x Bin, $p>0.05$); results which support a shift towards increased dendritic spine volume in HIV-1 Tg animals

treated with SE. Thus, HIV-1 Tg animals treated with SE may have stronger synapses relative to HIV-1 Tg animals treated with placebo.

Dendritic Spine Morphology. Treatment with SE during the formative period led to long-term modifications in dendritic spine morphology in HIV-1 Tg animals; morphological changes that are consistent with population shifts towards more mature spines. The overall linear mixed effects model with a Poisson distribution revealed a statistically significant genotype x sex x treatment x bin interaction for backbone length [$F(18, 1638)=13.2$, $p\leq0.001$], head diameter [$F(12, 1092)=20.1$, $p\leq0.001$] and neck diameter [$F(10, 910)=17.9$, $p\leq0.001$]. Subsequently, an a priori contrast between HIV-1 Tg animals treated with placebo and HIV-1 Tg animals treated with SE was conducted, revealing that SE produced a statistically significant population shift in the morphological parameters of dendritic spines (Treatment x Sex x Bin interaction: Backbone Length [$F(18, 774)=26.0$, $p\leq0.001$]; Head Diameter [$F(12,516)=35.6$, $p\leq0.001$]; Neck Diameter [$F(10,430)=40.3$, $p\leq0.001$]).

Male HIV-1 Tg animals treated with SE exhibited a population shift towards increased dendritic spine backbone length (Figure 5.6) and decreased neck diameter (Figure 5.6) relative to HIV-1 Tg animals treated with placebo (Treatment x Bin: Backbone Length, [$F(18, 360)=5.0$, $p\leq0.001$]; Neck Diameter: [$F(10,200)=3.2$, $p\leq0.001$]). Treatment with SE during the formative period, therefore, shifted the morphological characteristics of dendritic spines in male HIV-1 Tg animals, suggesting a population shift from 'stubby' spines to 'thin' spines.

SE treatment during the formative period also led to long-term changes in dendritic spine morphology in female HIV-1 Tg animals, evidenced by decreased dendritic spine

backbone length (Figure 5.6) and increased head (Figure 5.6) and neck (Figure 5.6) diameter relative to female HIV-1 Tg animals treated with placebo (Treatment x Bin: Backbone Length, [$F(18, 414)=30.4$, $p\leq0.001$]; Head Diameter [$F(12,276)=48.9$, $p\leq0.001$]; Neck Diameter: [$F(10,230)=56.9$, $p\leq0.001$]). Morphological characteristics of dendritic spines in female HIV-1 Tg animals treated with SE, therefore, suggest a population shift towards 'mushroom' spines. Thus, independent of biological sex, dendritic spines in HIV-1 Tg animals treated with SE were shifted towards a more mature phenotype relative to HIV-1 Tg animals treated with placebo; results which support the utility of SE to remodel neuronal circuitry at the synaptic level in HIV-1 Tg animals.

DISCUSSION

Treatment with SE during the formative period (i.e., PD 28 to PD 90) precluded the development of neurocognitive impairments in the HIV-1 Tg rat by remodeling neuronal circuitry at the synaptic level. HIV-1 Tg animals treated with placebo exhibited prominent neurocognitive deficits, dependent upon the factor of biological sex, in sustained attention, stimulus-response learning, and flexibility and inhibition. Treatment with SE during the formative period served as a neuroprotective therapeutic, selectively precluding the development of neurocognitive impairments in the HIV-1 Tg rat, independent of biological sex; effects which persisted despite the cessation of treatment. Neuronal circuitry in the HIV-1 Tg rat was remodeled by treatment with SE, evidenced by profound long-term modifications in dendritic branching complexity, synaptic efficacy, and dendritic spine morphology in pyramidal neurons from layers II-III of the mPFC. Results support SE as an efficacious neuroprotective therapeutic for HAND; a therapeutic approach that exerts its effects by targeting synaptic dysfunction. Understanding the mechanism of SE action in

HAND affords an opportunity to evaluate its therapeutic potential for other diseases characterized by synaptic dysfunction.

Tapping multiple neurocognitive domains afforded an opportunity to assess the effect of HIV-1 viral proteins, biological sex, and/or SE treatment on the three major subdivisions (i.e., mPFC, oPFC and lateral PFC) of the PFC. Additionally, as evidenced by *in situ* hybridization, stimulus-reinforcement learning, one neurocognitive domain tapped in the present study, in the signal detection operant task is also sensitive to DA and NE receptor expression; an effect that was independent of genotype, sex and/or treatment. HIV-1 Tg animals treated with placebo exhibited prominent deficits, characterized by sex-dependent expression of neurocognitive impairments, in tasks tapping both the mPFC (i.e., sustained attention, Kim et al., 2016) and oPFC (i.e., stimulus-response learning, Rolls, 2004; flexibility and inhibition, McAlonan & Brown, 2003); results which replicate and extend those previously reported (e.g., Moran et al., 2014a; McLaurin et al., 2019b). However, the lateral PFC, which plays a primary role in selective attention (Kam et al., 2018), appears relatively spared. Most notably, treatment with SE prevented the development of neurocognitive impairments in the temporal components of both sustained attention (mPFC) and flexibility and inhibition (oPFC). Treatment with SE, however, was unable to preclude deficits in stimulus-response learning under increased attentional demands or in the acquisition of the reversal task.

A series of cross-sectional studies in the HIV-1 Tg rat (Moran et al., 2019; McLaurin et al., 2019a) have assessed multiple factors (i.e., dose, age, neurocognitive domains, biological sex) to optimize treatment conditions and improve the therapeutic efficacy of SE for HAND. First, a dose-response experimental design in ovariectomized

female HIV-1 Tg animals revealed a linear relationship between SE dose (0, 0.05 mg, 0.1 mg, 0.2 mg) and sustained attention, with the most efficacious dose at 0.2 mg SE, approximating controls (Moran et al., 2019). Second, investigating the efficacy of SE at multiple ages (i.e., 6-8 months of age, Moran et al., 2019; 2-3 months of age, McLaurin et al., 2019a; PD 28, present study) afforded an opportunity to evaluate whether SE served as a neuroprotective and/or neurorestorative therapeutic. SE is most efficacious when utilized as a neuroprotective therapeutic, evidenced by the preclusion of NCI in all HIV-1 Tg animals, independent of biological sex, in the present study. However, SE may also serve as a neurorestorative therapeutic, albeit with decreased efficacy (i.e., 40%; Moran et al., 2019). Third, the therapeutic efficacy of SE generalizes across multiple neurocognitive domains, including preattentive processes, stimulus-response learning (albeit under select conditions, Moran et al., 2019; McLaurin et al., 2019a), sustained attention, selective attention, and flexibility and inhibition; a generalizability which supports the utility of SE to more broadly target frontal-subcortical circuits and neurotransmitter systems. Finally, as demonstrated in the present study, SE serves as a neuroprotective therapeutic for both male and female HIV-1 Tg animals, despite the presence of endogenous hormones.

Glutamatergic pyramidal neurons are characterized by a pyramidal shaped soma, one large apical dendrite, several shorter basal dendrites, and thousands of dendritic spines (for review, Spruston, 2008). The function of glutamatergic pyramidal neurons is modulated by multiple neurotransmitter systems, whereby the soma and axon receive inhibitory GABA inputs, whereas dendrites and dendritic spines receive excitatory (e.g., glutamatergic, dopaminergic, noradrenergic) inputs (Spruston, 2008). Specifically, glutamatergic afferents establish synaptic contact on the dendritic spine head, while

DAergic and noradrenergic afferents are targeted at the dendritic spine neck (Freund et al., 1984). Morphological changes in dendritic spines, therefore, may be indicative of alterations in synaptic neurotransmission, and ultimately neuronal circuits.

Synaptic dysfunction, characterized by alterations in neuronal and dendritic spine morphology, may be a key histopathological feature underlying neurocognitive impairments observed in neurodegenerative diseases (e.g., Lambert et al., 1998; Phan et al., 2017; McLaurin et al., 2019b). In the present study, HIV-1 Tg animals treated with placebo, independent of biological sex, exhibited altered dendritic branching complexity and weaker synapses, evidenced by decreased dendritic spine volume (Kasai et al., 2003; Hayashi & Majewska, 2005), relative to control animals treated with placebo; alterations which likely reflect deficits in glutamatergic synaptic transmission. First, the blockade of glutamate receptors (i.e., AMPA- or NMDA-type) leads to profound decreases in dendritic arbor growth (Rajan & Cline, 1998; Sin et al., 2002; Haas et al., 2006). Second, the PSD, which is strongly correlated with dendritic spine volume (Freire, 1978; Arellano et al., 2007), is comprised of glutamate receptors, signaling proteins, and cytoskeletal elements (for review, Sheng & Hoogenraad, 2007). Dendritic spines with large PSDs express a greater number of glutamate receptors (for review, Kasai et al., 2003). Most critically, strong evidence suggests that HIV-1 viral proteins induce alterations in glutamatergic synaptic transmission both *in vitro* (e.g., Patton et al., 2000; Wang et al., 2003; Askenova et al., 2009; Gupta et al., 2010; Aksenov et al., 2012; Melendez et al., 2016) and *in vivo* (Melendez et al., 2016).

Sex-dependent morphological changes in dendritic spines from pyramidal neurons of layers II-III of the mPFC provide additional evidence for synaptic dysfunction in HIV-

1 Tg rats treated with placebo. Male HIV-1 Tg animals treated with placebo exhibited a population shift towards shorter dendritic spines with increased neck diameter relative to male control animals treated with placebo. The absence of a dendritic spine neck in male HIV-1 Tg animals supports the failure to receive either DAergic afferents from the VTA or noradrenergic projections from the LC. In female HIV-1 Tg animals treated with placebo, a population shift towards longer dendritic spines with decreased head diameter and decreased neck diameter was observed relative to female control animals treated with placebo. The decreased head diameter in female HIV-1 Tg animals may reflect a smaller PSD, supporting alterations in neurotransmitter release. Notably, neurotransmitter system dysfunction is well recognized consequence of HIV-1 infection; a finding that has been reported in clinical (e.g., Kumar et al., 2011; Gelman et al., 2012) and preclinical (Sinharay et al., 2017; Denton et al., 2019) studies.

Treatment with SE, however, remodeled neuronal circuitry by ameliorating synaptic dysfunction in the HIV-1 Tg rat. Independent of biological sex, SE mitigated deficits in dendritic branching complexity and strengthened synapses, evidenced by a shift towards increased dendritic spine volume, in HIV-1 Tg animals. Furthermore, sex-dependent long-term modifications in dendritic spine morphology were observed in HIV-1 Tg animals after SE treatment during the formative period. Specifically, male HIV-1 Tg animals treated with SE displayed a population shift towards longer dendritic spines with decreased neck diameter relative to male HIV-1 Tg animals treated with placebo; a population shift towards parameters consistent with ‘thin’ spines (Peters & Kaiserman-Abramof, 1970). Additionally, enhanced DAergic and noradrenergic neurotransmission may also underlie the prevention of neurocognitive deficits in male HIV-1 Tg animals

treated with SE; a plausible hypothesis given evidence for increased noradrenergic and DAergic activity in the PFC following estrogen treatment (Kritzer, 2000; Jacome et al., 2010). In female HIV-1 Tg animals, SE induced a population shift towards shorter dendritic spines with increased head diameter and increased neck diameter relative to female HIV-1 Tg animals treated with placebo; a shift towards parameters consistent with 'mushroom' spines (Peters & Kaiserman-Abramof, 1970). Thus, treatment with SE during the formative period produced long-term remodeling in the neuronal circuit, evidenced by modifications to neuronal morphology and dendritic spine morphology; modifications which support enhanced synaptic transmission.

The rigor and reproducibility crisis in the behavioral and biomedical sciences stems, at least in part, from concern regarding the failure to effectively translate preclinical studies into the clinic. A multitude of factors, including poor experimental design (Collins & Tabak, 2014), low statistical power (Button et al., 2013), and inappropriate statistical analyses (Collins & Tabak, 2014) contribute to the reproducibility challenges in preclinical research. In light of these concerns, the present study was designed to target the key aspects of translational relevance. First, the biological system utilized to model key aspects of HAND, which resembles HIV-1 seropositive individuals on cART, the dose of SE, which yields a daily amount less than the daily isoflavone intake of most elderly Japanese individuals (i.e., 30-50 mg; Akaza, 2012), and the inclusion of biological sex, reflect the clinical population of interest. Second, animals were sampled using methods that provide an opportunity to control for independence of observations; an assumption that underlies many common statistical techniques (e.g., *t*-tests, ANOVA). Violating the independence of observation assumption results in spuriously significant effects, evidenced by inflated

type I error rates (e.g., Haseman & Hogan, 1975; Holson & Pearce, 1992; Aarts et al., 2014). Finally, as discussed above, the present study replicates and extends a series of cross-sectional *in vivo* studies (Moran et al., 2019; McLaurin et al., 2019a). Each study has uniquely demonstrated the therapeutic efficacy of SE, and now the mechanism of SE action, for the treatment of neurocognitive impairments in HAND.

Despite the aforementioned strengths of the present study, a few caveats are acknowledged. First, although the long-term modifications in both neurocognitive function and synaptic efficacy support a disease modifying therapeutic, there remains a critical need to test this hypothesis using a longitudinal experimental design. Second, the present study utilized a biological system modeling key aspects of HAND to assess the therapeutic efficacy of SE, and its mechanism of action. Although SE targets one of the histopathological features (i.e., synaptic dysfunction), characteristic of multiple neurodegenerative diseases, and is being assessed in ongoing clinical trial for AD (Ausio Pharmaceuticls; NCT03101085), additional studies are required to test its therapeutic potential for other neurodegenerative diseases. Finally, to date, the duration of SE treatment has not been systematically manipulated. Treatment of 0.2 mg SE for 62 days, as in the present study, selectively precluded the development of neurocognitive impairments and led to long-term modifications in synaptic efficacy. However, given the increased lifespan of HIV-1 seropositive individuals (Romley et al., 2014; Teeraananchai et al., 2017), longer treatment durations may be more efficacious.

In conclusion, treatment with SE during the formative period (i.e., PD 28 to PD 90) prevented the development of neurocognitive impairments in the HIV-1 Tg rat by remodeling neuronal circuitry at the synaptic level. SE, which crosses the blood-brain

barrier, distributes most significantly to the PFC, and ameliorates synaptic dysfunction in the HIV-1 Tg rat, may serve as a neuroprotective or neurorestorative therapeutic to modify the progression of HAND; a hypothesis which needs to be critically tested via a longitudinal experimental design. Most critically, however, elucidating the neural mechanism underlying the therapeutic effects of SE in HAND affords an opportunity to evaluate its therapeutic potential for other neurodegenerative diseases characterized by synaptic dysfunction.

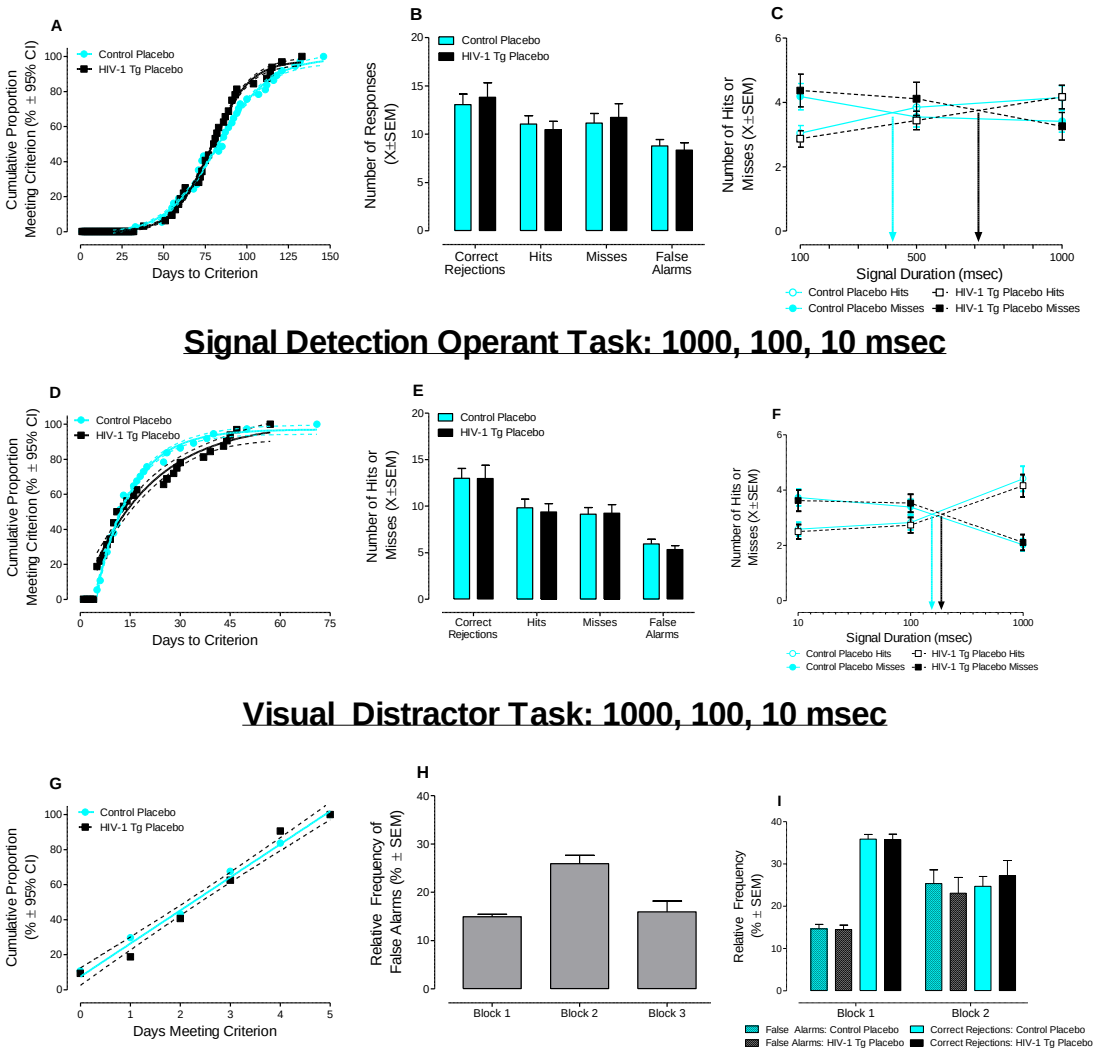

Figure 5.1 Genotypic Neurocognitive Impairments. Presence of the HIV-1 transgene on neurocognitive function was assessed by comparing HIV-1 Tg animals treated with placebo and control animals treated with placebo. In the signal detection operant task, tapping sustained attention, HIV-1 Tg animals did not display any statistically significant alterations in the number of days to meet criterion (**A**) or the response profile (**B**). However, HIV-1 Tg animals exhibited a prominent rightward shift in the loss of signal detection relative to their control counterparts, supporting a deficit in the temporal components of sustained attention (**C**). Under increased attentional demands (i.e., shorter signal durations), HIV-1 Tg animals exhibited a profound deficit in the temporal process of acquisition (**D**), but no alterations in response profile (**E**) or the temporal components of sustained attention (**F**). In the visual distractor task, tapping selective attention, HIV-1 Tg animals displayed no alterations in the number of days at criterion (**G**) or selective attention (**I**), despite strong evidence for validation of the task (**H**).

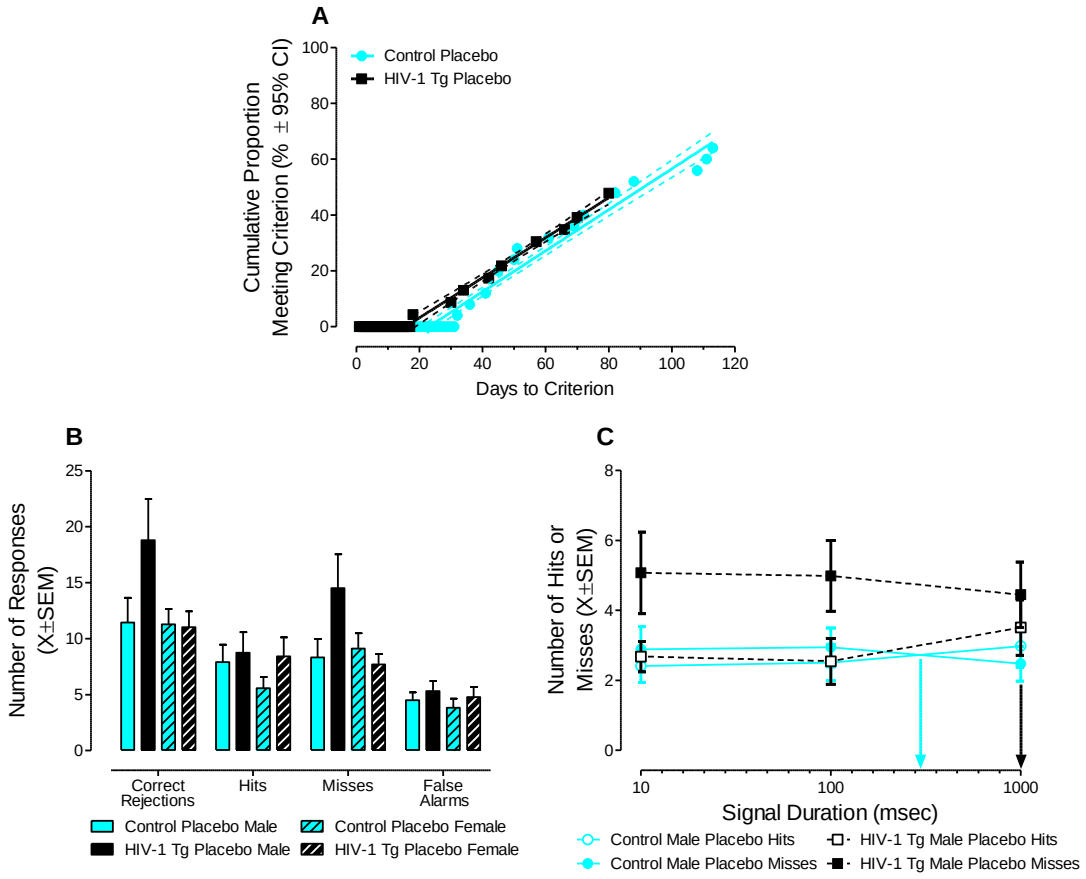

Figure 5.2 Flexibility and Inhibition. Presence of the HIV-1 transgene on flexibility and inhibition was assessed by comparing HIV-1 Tg animals treated with placebo and control animals treated with placebo. HIV-1 Tg animals displayed prominent deficits in stimulus-reinforcement learning during the acquisition of reversal (**A**), with a decreased proportion of HIV-1 Tg animals treated with placebo successfully acquiring the task (i.e., 47.8%) relative to their control counterparts (i.e., 64%). Male HIV-1 Tg animals treated with placebo, but not female HIV-1 Tg animals treated with placebo, exhibited alterations in the response profile (**B**) and temporal components of flexibility and inhibition (**C**).

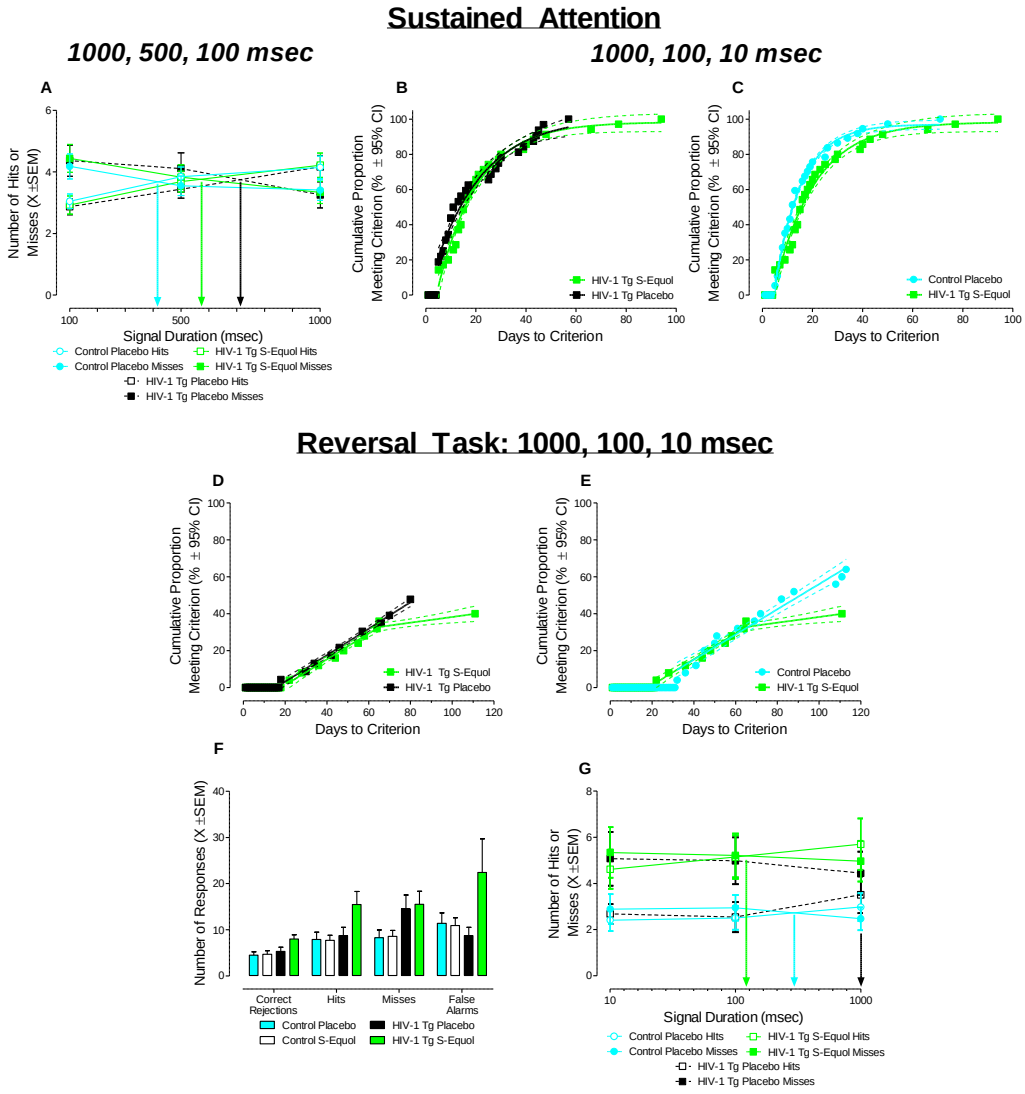

Figure 5.3 Therapeutic Efficacy of S-Equol. Therapeutic efficacy of SE for the marked impairments in neurocognitive function. Treatment with SE enhanced the temporal components of sustained attention in HIV-1 Tg animals (**A**); an enhancement which made them statistically indistinguishable from either HIV-1 Tg animals treated with placebo or control animals treated with placebo. However, SE failed to ameliorate deficits in stimulus-reinforcement learning under increased attentional demands (**B**,**C**) or in the acquisition of the reversal task (**D**, **E**). In male HIV-1 Tg animals, SE enhanced the temporal components of flexibility and inhibition (**G**); an effect which resulted from a dramatic increase in the number of hits relative to other groups (**F**).

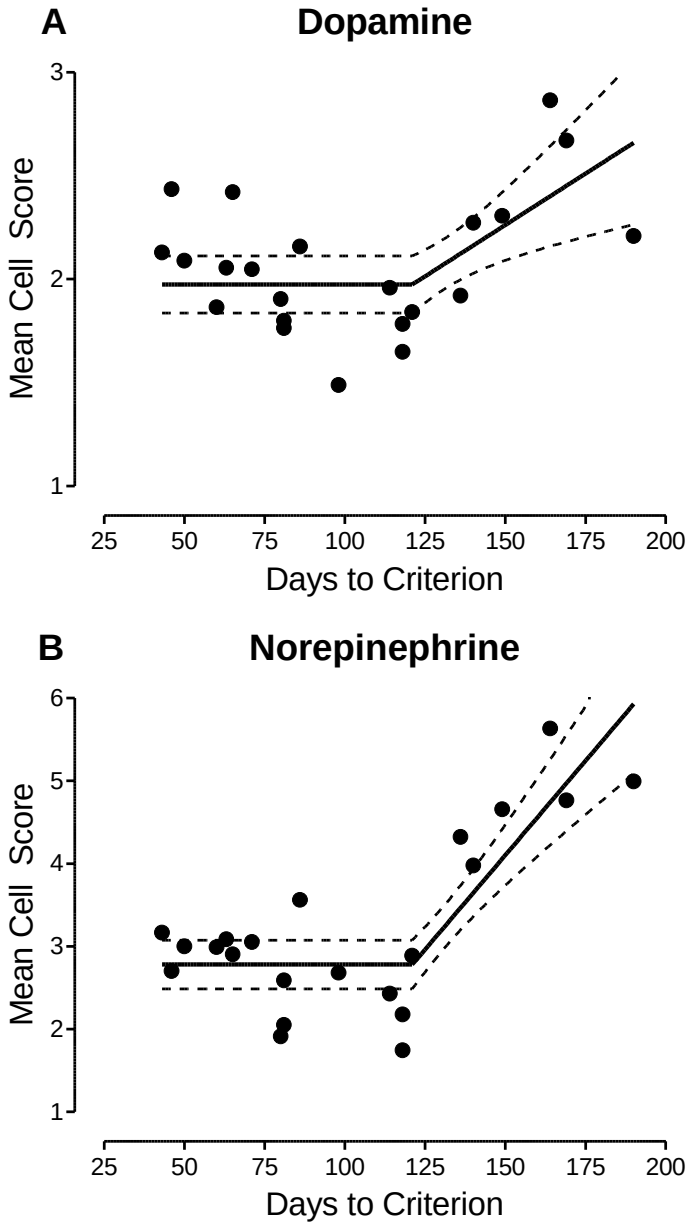

Figure 5.4 *In situ* Hybridization. *In situ* hybridization assessing dopamine (Drd1α) and norepinephrine (Adra2a) receptor expression in the medial prefrontal cortex. A segmental linear regression provided a well-described fit for the relationship between the number of days to criterion and mean cell score for both DA (correlation coefficient, *r*, 0.679) and NE (*r*, 0.845). Results support, therefore, the sensitivity of the signal detection operant task to alterations in Drd1α and Adra2a receptor expression.

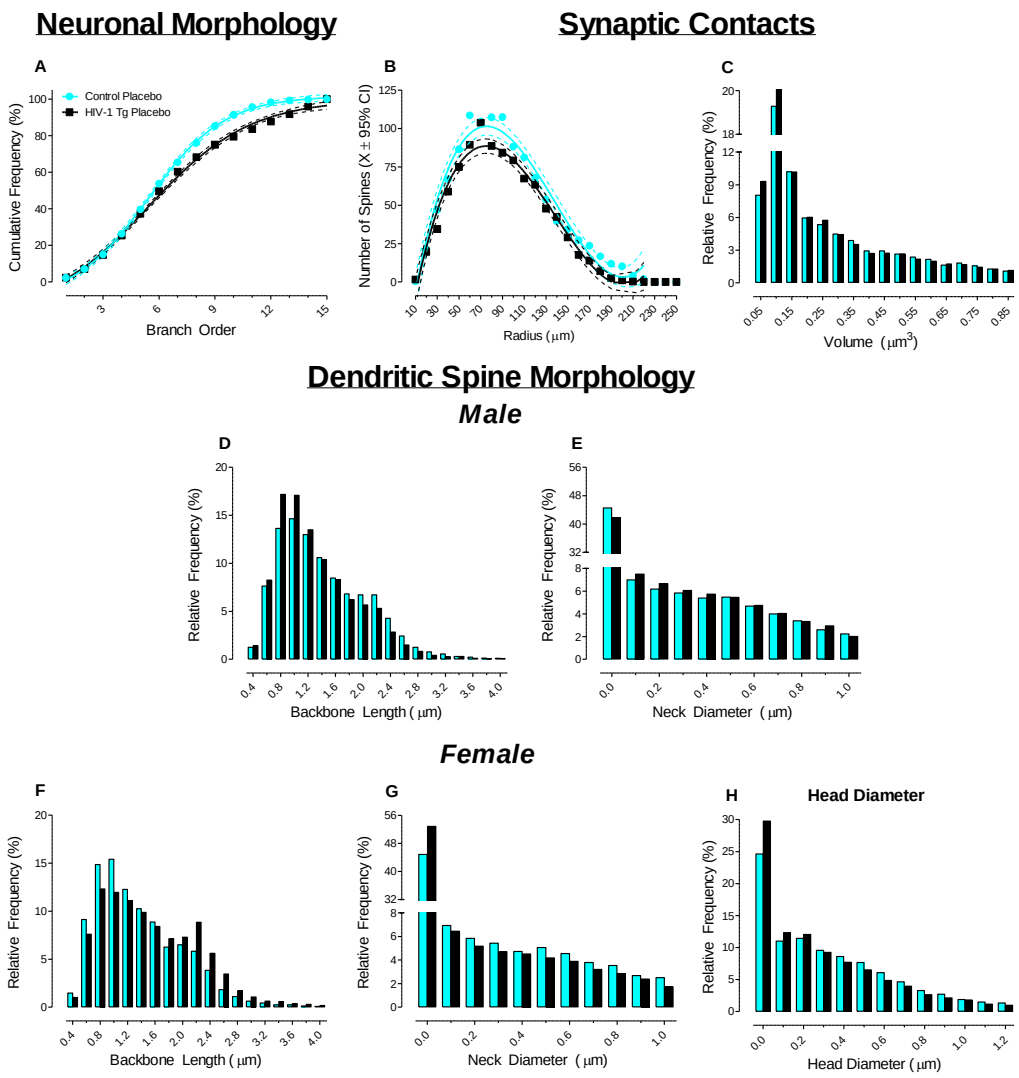

Figure 5.5 Genotypic Synaptic Dysfunction. Presence of the HIV-1 transgene on synaptic dysfunction was assessed by comparing pyramidal neurons from layers II-III of the mPFC in HIV-1 Tg animals treated with placebo and control animals treated with placebo. Independent of biological sex, HIV-1 Tg animals treated with placebo exhibited significant alterations in dendritic branching complexity (**A**), a decreased number of dendritic spines dependent upon distance from the soma (**B**), and a prominent population shift towards decreased dendritic spine volume (**C**) relative to control animals treated with placebo. Male HIV-1 Tg animals, relative to male control animals, displayed a population shift towards decreased dendritic spine backbone length (**D**) and increased neck diameter (**E**). In sharp contrast, female HIV-1 Tg animals exhibited a population shift towards increased dendritic spine backbone length (**F**) with decreased neck diameter (**G**) and head diameter (**H**).

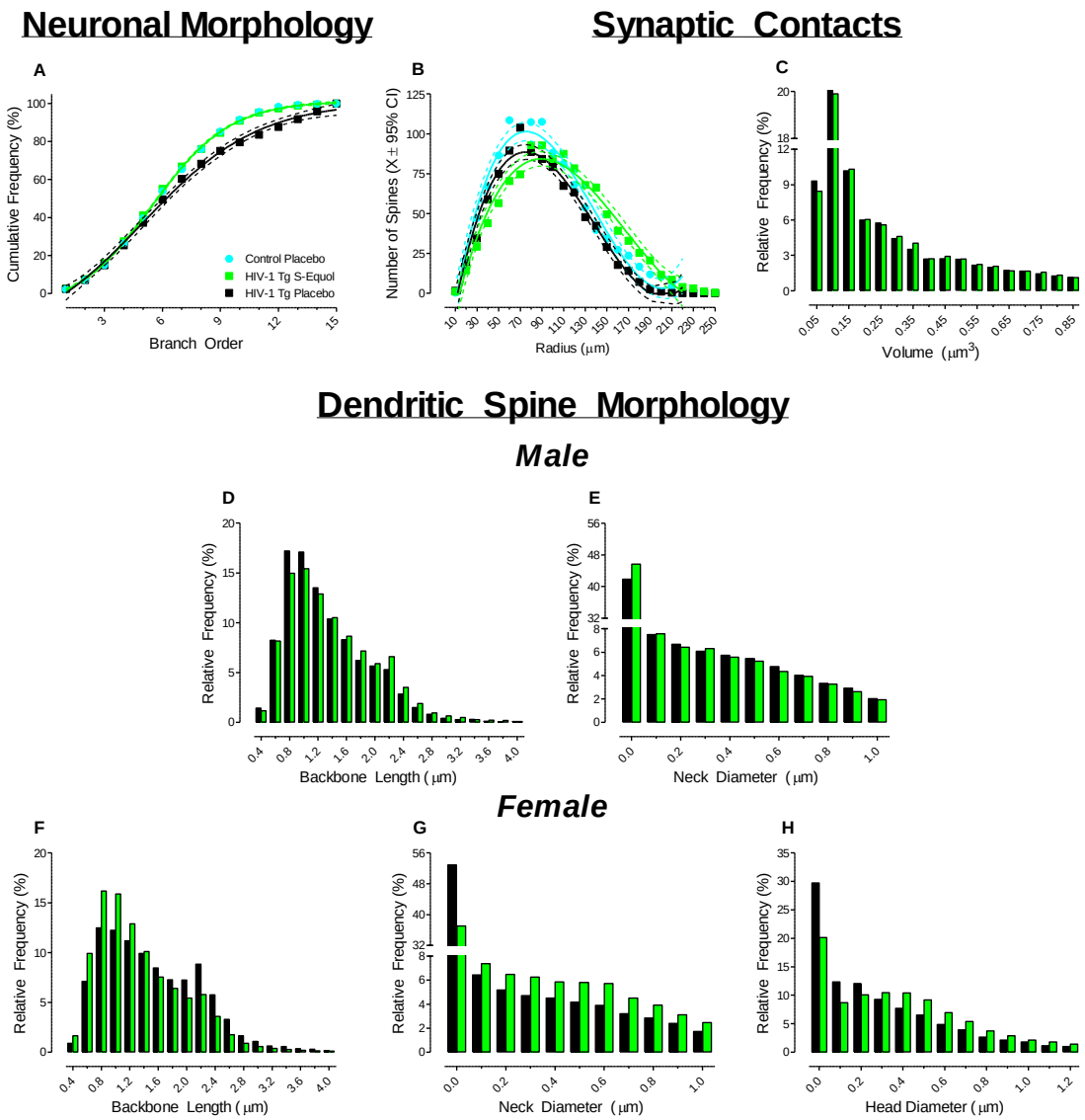

Figure 5.6 Remodeled Neuronal Circuitry. Therapeutic efficacy of S-Equol (SE) for the prominent alterations in synaptic function in pyramidal neurons from layers II-III of the mPFC. Independent of biological sex, treatment with SE mitigated the alterations in dendritic branching complexity (**A**), increased the number of dendritic spines on more distal radii (**B**), and produced a prominent shift towards increased dendritic spine volume (**C**) in HIV-1 Tg animals. In male HIV-1 Tg animals, treatment with SE produced a population shift towards increased dendritic spine backbone length (**D**) and decreased neck diameter (**E**) relative to male HIV-1 Tg animals treated with placebo. Female HIV-1 Tg animals treated with SE, relative to female HIV-1 Tg animals treated with placebo, displayed a population shift towards decreased dendritic spine backbone length (**F**) and increased neck diameter (**G**) and increased head diameter (**H**).

CHAPTER 6

S-EQUOL PARTIALLY RESTORES THE DEVELOPMENTAL TRAJECTORY OF NEUROCOGNITIVE FUNCTION IN THE HIV-1 TRANSGENIC RAT

INTRODUCTION

PHIV, which afflicts approximately 1.7 million children (<15 years of age) worldwide (UNAIDS, 2019), continues to be a public health concern. cART, the primary treatment regimen for HIV-1, suppresses viral replication in the periphery (Markowitz et al., 1995), but poorly penetrate the blood-brain barrier (Gimenez et al., 2004; Letendre et al., 2008). Due to the ineffective treatment of HIV-1 in the CNS, chronic neurologic impairments are a commonly reported consequence of PHIV (Franklin et al., 2005; Paramesparan et al., 2010). Although early initiation of cART has a beneficial effect on neurocognitive development (e.g., Laughton et al., 2012; Crowell et al., 2015), HIV-1 seropositive children continue to perform below their HIV-uninfected peers (Lowick et al., 2012). There remains, therefore, a critical need to develop neuroprotective therapeutics that penetrate the CNS and alter the developmental trajectory of chronic neurological impairments.

Isoflavones, including DAI and genistein, are a subclass of flavonoids that act as phytoestrogens by selectively binding to ERβ (Casanova et al., 1999; Mersereau et al., 2008). Equol, which can exist in either the R- or S- conformation, is a metabolite produced by the gut microbiota following the ingestion of DAI (Setchell et al., 1984). Relative to its precursor (i.e., DAI), SE, the only enantiomer produced by humans (Setchell et al., 2005), has a slower clearance rate, higher bioavailability, and stronger, selective affinity for ERβ (Setchell & Clerici, 2010). Notably, cells containing ERβ mRNA or immunoactivity are widely dispersed throughout the brain (e.g., Li et al. 1997; Shughrue et al. 1997; Zhang et al. 2002; Gonzalez et al. 2007) and have been observed in brain regions (e.g., PFC, hippocampus) commonly associated with higher-order cognitive functioning (Sweatt, 2004; Fuster, 2008). Furthermore, activation of ERβ, via either phytoestrogens or soy

isoflavones, has been associated with enhancements in a variety of cognitive functions, including memory (e.g., File et al., 2001; Henderson et al., 2012), sustained attention (e.g., Duffy et al., 2003), and flexibility and planning (e.g., File et al., 2001; File et al., 2005); although inconsistencies in the literature may reflect the inability of most (i.e., 70-75%) of the Western population to convert DAI to SE (Rowland et al., 2000; Setchell & Cole, 2006). Therefore, utilization of the metabolite SE, rather than the parent compound, may afford the most direct and efficacious target for the development of novel therapeutics for neurocognitive dysfunction.

A series of three independent cross-sectional studies in the HIV-1 Tg rat support SE as a neuroprotective and/or neurorestorative therapeutic for NCIassociated with HIV-1 (Moran et al., 2019; McLaurin et al., 2019a; Chapter 5). The systematic manipulation of SE dose (i.e., 0, 0.05, 0.1, 0.2 mg) revealed a linear dose response, with 0.2 mg SE serving as the most efficacious dose for the mitigation of sustained attention deficits (Moran et al., 2019). Furthermore, the efficacy of SE generalizes across neurocognitive domains (i.e., preattentive processes, stimulus-reinforcement learning, sustained attention, selective attention, and flexibility and inhibition), and the factor of biological sex. Soy isoflavones and their derivatives (i.e., SE) have also been implemented as effective therapeutics for cognitive dysfunction associated with other neurodegenerative diseases, including AD (e.g., Bagheri et al., 2011) and Sanfilippo syndrome (Piotrowska et al., 2008). However, extrapolating cross-sectional findings to disease progression is inferentially fraught (Kraemer et al., 2000), necessitating the use of a longitudinal experimental design to critically test if and/or how SE modifies the progression of chronic neurological impairment.

Chronic neurological impairments associated with PHIV are characterized by alterations in executive function, preattentive processing, and long-term episodic memory (e.g., Koekkoek et al., 2008; Ruel et al., 2012; Moran et al., 2014b; McLaurin et al., 2017c). Specifically, deficits in preattentive processing are recognized as one of the most sensitive neurocognitive measures for HIV-1 disease (Koekkoek et al., 2008). Alterations in preattentive processes generalize across species (e.g., HIV-1 seropositive humans, Minassian et al., 2013; HIV-1 transgenic (Tg) rat, Moran et al., 2013a; gp120 and Tat transgenic mice, Henry et al., 2014; Paris et al., 2015), age (e.g., McLaurin et al., 2017a; McLaurin et al., 2017b), the factor of biological sex (e.g., McLaurin et al., 2016b; McLaurin et al., 2018b) and are sensitive to treatment with SE (McLaurin et al., 2019a). Alterations in preattentive processing mediate, at least partially, deficits in higher-order cognitive processes (i.e., stimulus-reinforcement learning, sustained attention, long-term episodic memory; McLaurin et al., 2019e) across the functional lifespan; results which demonstrate the componential relationship between neurocognitive functions impaired by HIV-1 viral proteins. Furthermore, PPI, an assessment of preattentive processing, has been heralded as a diagnostic and prognostic biomarker for HAND (for review, McLaurin et al., 2019c). Therefore, critically testing the effect of SE on the progression of preattentive processes may reflect its potential for modifying progressive neurological impairments in PHIV.

Introduced and popularized by Hoffman and Ison (e.g., Hoffman & Searle, 1965; Ison & Hammond, 1971), PPI of the ASR is a translational experimental paradigm commonly used to assess preattentive processing. The brief PPI experimental paradigm relies upon the addition or removal of a salient prestimulus (i.e., tone, light, gap in

background noise) and a startling stimulus; a prestimulus that, when presented 30 to 500 msec before the starting stimulus, produces a dramatic reduction in ASR (Hoffman & Ison, 1980). Utilization of the classical ISI approach, which systematically manipulates the time interval between the salient prestimulus and startling stimulus, establishes the shape of the ISI function, affording an opportunity to infer preattentive processing (McLaurin et al., 2019d). Notably, when the classical ISI approach is employed PPI has high test-retest reliability (Braff et al., 1978); an important consideration when conducting a longitudinal experimental design.

Thus, the aims of the present study were twofold. First, to assess whether SE alters somatic growth, the integrity of sensory system function and/or the integrity of gross-motoric function. Evaluating the functional health of HIV-1 Tg and control animals six months after the cessation of SE treatment provides an opportunity to establish the long-term safety of SE treatment. Second, to evaluate if and/or how SE modifies the progression of preattentive processing in the HIV-1 Tg rat. The HIV-1 Tg rat, which expresses 7 of the 9 HIV-1 genes constitutively throughout development, affords a biological system to model key aspects of chronic neurological impairments in PHIV (for review, Vigorito et al., 2015). Three experimental paradigms, including auditory PPI, visual PPI, and auditory gap-PPI, were conducted every 30 days from PD 60 to PD 210 to assess preattentive processing. Development of an efficacious therapeutic that modifies the progression of chronic neurological impairment resulting from PHIV has the potential for great clinical significance.

METHODS

Animals

Fischer (F344/N; Envigo, Indianapolis, IN) HIV-1 Tg (*N*=24 litters) and control animals (*N*=19 litters) were procured at the animal vivarium, housed with their biological dam, between PD 7 and PD 9. HIV-1 Tg (male, *n*=33, female, *n*=34) and F344/N control (male *n*=38; female, *n*=34) animals were randomly sampled from each litter. The goal was to select only one rat of each sex was selected for each treatment to control for independence of observation, an assumption underlying many traditional statistical techniques (i.e., ANOVA). After weaning, which occurred at approximately PD 24, animals were pair- or group-housed with animals of the same sex for the duration of experimentation.

AAALAC-accredited facilities were utilized to maintain HIV-1 Tg and control animals throughout the duration of experimentation using guidelines provided by the Guide for the Care and Use of Laboratory Animals of the NIH. The targeted environmental conditions for the animal vivarium were 21°± 2°C, 50% ± 10% relative humidity and a 12-h light:12-h dark cycle with lights on at 0700 h (EST). The project protocol was approved by the IACUC at the University of South Carolina under federal assurance (# D16-00028).

S-Equol

HIV-1 Tg and control animals were treated daily with either SE or placebo (i.e., sucrose pellets (Bio-Serv, Inc., Flemington, NC) during the formative period (i.e., approximately PD 28 to PD 90). SE (Cayman Chemical Company, Ann Arbo, MI), was incorporated into sucrose pellets by Bio-Serve, with each pellet containing 0.2 mg SE.

Animals were randomly assigned to receive either SE or placebo (Control: SE, *n*=35 (male, *n*=18, female, *n*=17), Placebo, *n*=37 (male, *n*=20, female, *n*=17); HIV-1 Tg:

SE, *n*=35 (male, *n*=17, female, *n*=18), Placebo, *n*=32 (male, *n*=16, female, *n*=16)). A dose-response experimental design (Moran et al., 2019) previously established 0.2 mg of SE as the most efficacious dose for the treatment of sustained attention in the HIV-1 Tg rat. Translationally, the dose utilized yielded a daily amount of 0.25-1.0 mg/kg SE; an amount equivalent to a 2.5-10 mg dose in a 60 kg human (Cf., most elderly Japanese have a daily isoflavone intake of 30-50 mg, Akaza, 2012).Therefore, HIV-1 Tg and control animals assigned to the SE treatment group received a daily oral dose of 0.2 mg of SE. The placebo group received a sucrose pellet. Treatment was administered daily after the completion of neurocognitive testing to promote the long-term remodeling of neuronal circuitry (e.g., Bertrand et al., 2014, Bertrand et al., 2015).

Cross-Modal Prepulse Inhibition

Apparatus

The startle chambers utilized to conduct cross-modal PPI has been previously reported (McLaurin et al., 2018b). In brief, a startle platform (SR-Lab Startle Reflex System, San Diego Instruments, Inc., San Diego, CA) was enclosed within an isolation cabinet (external dimensions: 10 cm-thick, double-walled, 81 x 81 x 116-cm) (Industrial Acoustic Company, INC., Bronx, NY), to provide sound attenuation (30 db(A)) relative to the external environment. A SR-Lab system high-frequency loudspeaker (model#40-1278B, Radio Shack, Fort Worth, TX), mounted 30 cm aboe the Plexiglas animal test cylinder, was used to present continuous background noise (22dB(A)), auditory prepulse stimuli (85 db(A), duration: 20 msec) and the startle stimulus (100 db(A), duration: 20 msec). A 22 lux white LED light, affixed on the wall in front of the test cylinder, was utilized to present visual prepulse stimuli (duration: 20 msec). A piezoelectric

accelerometer, attached to the bottom of the Plexiglas animal test cylinder, converted the deflection of the test cylinder, resulting from animal's response to the startle stimulus, into analog signals. Response signals were digitized (12 bit A to D, recorded at a rate of 2000 samples/sec) and saved to a hard disk. Two individual startle apparatuses were used throughout the duration of experimentation.

Procedure

Cross-modal PPI was conducted on PD 20, prior to weaning, as a baseline measurement. Subsequently, the developmental trajectory of temporal processing was assessed by utilizing repeated measurements of cross-modal PPI every 30 days from PD 60 to PD 210 (Control: SE, *n*=35 (male, *n*=18, female, *n*=17), Placebo, *n*=37 (male, *n*=20, female, *n*=17); HIV-1 Tg: SE, *n*=35 (male, *n*=17, female, *n*=18), Placebo, *n*=32 (male, *n*=16, female, *n*=16)). A final cross-modal PPI assessment was conducted at PD 270 (Control: SE, *n*=29 (male, *n*=13 female, *n*=16), Placebo, *n*=29 (male, *n*=15, female, *n*=14); HIV-1 Tg: SE, *n*=27 (male, *n*=11, female, *n*=16), Placebo, *n*=28 (male, *n*=14, female, *n*=14)) to examine the integrity of auditory and visual sensory system function. The protocol used to conduct cross-modal PPI is reported by McLaurin et al. (2018b).

In brief, cross-modal PPI was conducted using a 30-minute test session that began with a 5-min acclimation period (70 dB(A) background white noise). The session began with six pulse-only ASR trials with a fixed 10 sec intertrial interval. The 72 test trials, which included an equal number of visual and auditory prepulse trials, were presented in a counterbalanced order (i.e., ABBA) to control for order-effects. Six interstimulus intervals (i.e., 0, 30, 50, 100, 200, and 4000 msec), affording an opportunity to evaluate the shape of the function, were presented in 6-trial blocks according to a Latin-square design. Control

trials (i.e., 0, 4000 msec ISIs) were included to provide a reference ASR within cross-modal PPI. During the test trials, the ITI was variable from 15 sec to 25 sec. Mean peak ASR amplitude values were collected for analysis. All test sessions were conducted in the dark.

Auditory Gap Prepulse Inhibition

Apparatus

Auditory gap-PPI was conducted using the startle apparatus described above.

Procedure

A baseline assessment of auditory gap-PPI was conducted on PD 21, prior to weaning. Subsequently, a longitudinal experimental design was utilized to assess whether alterations, resulting from presence of HIV-1 viral proteins, biological sex, and/or treatment with SE, in the developmental trajectory of temporal processing generalize across experimental paradigms. Repeated measurements of auditory gap-PPI were conducted every 30 days from PD 60 to PD 210. At PD 270, a final auditory gap-PPI assessment was conducted to examine the integrity of auditory system function. Sample sizes reported for cross-modal PPI (above) reflect those utilized for auditory gap-PPI. Assessments of auditory gap-PPI were always conducted after cross-modal PPI. The protocol used to conduct auditory gap-PPI is reported by McLaurin et al. (2016b).

In brief, a 20-min test session, beginning with a 5-min acclimation period (70 dB(A) background white noise) was utilized to conduct auditory gap-PPI. After the acclimation period, six pulse-only ASR trials, with a fixed 10 sec ITI, were presented. Six trial blocks, interdigitated using a Latin-square experimental design, were utilized for the presentation of the 36 test trials. A 20-msec gap in background noise served as the prestimulus. The systematic manipulation of the time interval (i.e., ISIs 0, 30, 50, 100, 200, and 4000 msec)

between the prestimulus and auditory startle stimulus afforded a critical opportunity to evaluate the shape of the function. Control trials (i.e., 0, 4000 msec ISIs) were included to provide a reference ASR within auditory gap-PPI. During the test trials, the ITI was variable from 15 sec to 25 sec. Mean peak ASR amplitude values were collected for analysis. All test sessions were conducted in the dark.

Locomotor Activity

Apparatus

Perspex inserts were utilized to convert square (40 x 40 cm) activity monitors (Hamilton Kinder, San Diego Instruments, San Diego, CA) into round (~40 cm diameter) compartments. Free movement was detected throughout the test sessions by interruptions of infrared photocells (32 emitter/detector pairs). Notably, the sensitivity of the infrared photocells was tuned by the manufacturer to work with the additional layer of perspex. For the assessment of gross motoric movement, the total number of photocell interruptions within the 60-min test session were calculated. To assess habituation, as a measurement of long-term episodic memory, the total number of photocell interruptions were binned into five-min intervals.

Procedure

Locomotor activity was conducted at PD 270 to examine the integrity of gross-motoric system function (Control: SE, *n*=29 (male, *n*=13 female, *n*=16), Placebo, *n*=29 (male, *n*=15, female, *n*=14); HIV-1 Tg: SE, *n*=27 (male, *n*=11, female, *n*=16), Placebo, *n*=26 (male, *n*=13, female, *n*=13)). Locomotor activity consisted of a 60-min test session conducted between 700 and 1200h (EST) under dim light conditions (<10 lux) in an isolated room.

Statistical Analysis

ANOVA and regression techniques were used to statistically analyze all data (SPSS Statistics 26, IBM Corp., Somer, NY; GraphPad Software, Inc., La Jolla, CA). Given potential violations of sphericity inherent in repeated-measures experimental designs, planned orthogonal contrasts and/or the post-hoc Greenhouse-Geisser *df* correction factor (Greenhouse & Geisser, 1959) were applied. An alpha criterion of $p \leq 0.05$ was considered statistically significant for all analyses.

Early alterations in preattentive processing were analyzed using a mixed-factor ANOVA (SPSS Statistics 26, IBM Corp., Somer, NY) with the mean peak ASR amplitude serving as the dependent variable. Genotype (HIV-1 Tg vs. Control) and biological sex (Male vs. Female) served as between subjects factors. Furthermore, ISI (0, 30, 50, 100, 200, and 4000) and trial (1 to 6) were included in the analysis as within subjects factors.

Body weight and sensory function at PD 270 were also analyzed using a mixed-factor ANOVA (SPSS Statistics 26, IBM Corp., Somer, NY). A univariate ANOVA utilized to evaluate gross-motoric system function at PD 270, where the mean number of photocell interruptions served as the dependent variable. Genotype, biological sex, and treatment (SE vs. Placebo) served as between subjects factors. ISI, trial, and age served as within subjects factors, as appropriate.

The area of the inflection of the ASR amplitude response curve (McLaurin et al., 2016b), a measure of PPI, was calculated to assess the developmental trajectory of preattentive processes. Regression analyses (GraphPad Software, Inc., La Jolla, CA) and mixed-model ANOVA techniques (SPSS Statistics 26, IBM Corp., Somer, NY) were used to conduct *a priori* planned comparisons. Specifically, planned comparisons were

conducted to establish the absence of an SE effect on the progression of preattentive processes in control animals (i.e., Control Placebo vs. Control SE). When there was no statistically significant treatment effect in control animals, subsequent analyses were conducted on all control animals, collapsed across treatment. Additionally, planned comparisons were conducted 1) to establish the how the HIV-1 transgene altered the developmental trajectory of preattentive processes (i.e., Control Placebo vs. HIV-1 Tg Placebo) and 2) to evaluate if and to what extent SE enhanced the progression of preattentive processes (i.e., HIV-1 Tg Placebo vs. HIV-1 Tg SE and/or Control Placebo vs. HIV-1 Tg SE). Between subjects' factors included genotype, biological sex, and treatment. Age was included as a within subjects' factor.

RESULTS

Early Neurocognitive Impairments

HIV-1 Tg animals exhibited early neurocognitive impairments in preattentive processing; impairments which were dependent upon the factor of biological sex, sensory modality (i.e., auditory, visual) and experimental paradigm (i.e., cross-modal PPI, gap-PPI).

In auditory PPI (Figure 6.1), HIV-1 Tg animals, independent of biological sex, displayed a relative insensitivity to the manipulation of ISI relative to control animals. Maximal inhibition for both HIV-1 Tg and control animals was observed at the 100 msec ISI. However, HIV-1 Tg animals exhibited a relatively flatter ISI function relative to control animals. The overall mixed-model ANOVA, conducted on the mean peak ASR amplitude, confirmed these observations, revealing a statistically significant genotype x ISI interaction with a prominent cubic component [$F(1,135)=7.0$, $p\leq 0.009$, $\eta_p^2=0.05$].

Male HIV-1 Tg animals, but not female HIV-1 Tg animals, exhibited a relative insensitivity to the manipulation of ISI in visual PPI (Figure 6.1). Independent of biological sex, both HIV-1 Tg and control animals displayed maximal inhibition at the 50 msec ISI. However, male HIV-1 Tg animals exhibited a relatively flatter ISI function relative to male control animals. The overall mixed-model ANOVA, conducted on the mean peak ASR amplitude, confirmed these observations, revealing a statistically significant genotype x sex x ISI interaction with a prominent cubic component [$F(1,135)=4.2$, $p\leq0.05$, $\eta_p^2=0.030$].

No statistically significant impairments in preattentive processing were observed in auditory gap-PPI (Figure 6.1). Independent of biological sex, HIV-1 Tg and control animals displayed significant inhibition following the presentation of a 20 msec gap in background noise with maximal inhibition observed at the 30 msec ISI. A downward mean shift in the mean peak ASR amplitude curve was observed in HIV-1 Tg animals relative to control animals, evidenced by a statistically significant main effect of genotype [$F(1,137)=11.0$, $p\leq0.001$, $\eta_p^2=0.075$]. However, HIV-1 Tg animals failed to exhibit an impairment in preattentive processing, *per se*, in gap-PPI (Genotype x ISI interaction, $p>0.05$); results which are consistent with those previously reported at PD 18 (McLaurin et al., 2017c).

Body Weight: Somatic Growth

Body weight (Figure 6.2), an assessment of somatic growth, was measured weekly in HIV-1 Tg and control animals from 4 weeks of age (i.e., PD 28) through 40 weeks of age (i.e., PD 280). HIV-1 Tg animals, independent of biological sex, weighed significantly less than control animals throughout the duration of the experiment. A one-phase association provided a well-described fit for HIV-1 Tg and control animals, independent

of biological sex and/or treatment (R^2s≥0.99). Significant differences, however, were observed in the rate of growth, evidenced by a statistically significant genotype x age interaction (Male: [F(36, 2376)=78.0, p≤0.001, η_p^2=0.542] with a prominent linear component [F(1, 66)=271.9, p≤0.001, η_p^2=0.805]; Female: [F(36, 2268)=18.5, p≤0.001, η_p^2=0.227] with a prominent linear component [F(1, 63)=53.8, p≤0.001, η_p^2=0.461]). Most critically, however, treatment with SE did not alter the growth trajectory of either HIV-1 Tg or control animals, independent of biological sex, evidenced by the failure to observe a statistically significant main effect of treatment (p>0.05) or any statistically significant higher-order interactions with treatment (p>0.05).

Integrity of Sensory and Motor System Function: Postnatal Day 270

Sensory System Function

Cross-modal PPI and auditory gap-PPI assessed at PD 270 to evaluate the integrity of sensory auditory and visual system function in HIV-1 Tg and control animals following treatment with SE during the formative period.

Robust inhibition to the presentation of either an auditory prepulse (Figure 6.3) or a gap in background noise (Figure 6.3) was observed, independent of genotype, biological sex, and/or treatment, at PD 270, supporting the integrity of auditory system function. In auditory PPI (Figure 6.3), control animals, independent of treatment, and HIV-1 Tg animals treated with SE exhibited maximal inhibition at the 200 msec ISI. In contrast, HIV-1 Tg animals treated with placebo displayed a prominent leftward shift in the point of maximal inhibition (i.e., 50 msec ISI). In auditory gap PPI (Figure 6.3), both HIV-1 Tg and control animals displayed maximal inhibition at the 50 msec ISI.

The integrity of visual system function was evidenced by robust inhibition to the presentation of a 20 msec visual prepulse, independent of genotype, biological sex, and/or treatment, at PD 270 (Figure 6.3). Both HIV-1 Tg and control animals, independent of treatment, displayed robust inhibition to the visual prepulse at the 50 msec ISI, supporting the integrity of visual system function.

However, across all three experimental paradigms (i.e., auditory PPI, auditory gap PPI, visual PPI), profound deficits in temporal processing were observed at PD 270 in HIV-1 Tg animals; deficits that were not precluded by treatment with SE during the formative period. Specifically, HIV-1 Tg animals, independent of experimental paradigm, exhibited a relative insensitivity to the manipulation of ISI, evidenced by a relatively flatter ISI function compared to control animals. The overall mixed-model ANOVA, conducted on the mean peak ASR amplitude, confirmed these observations, revealing a statistically significant genotype x ISI interaction (Auditory PPI: [$F(5,525)=78.2$, $p_{GG}\leq 0.001$, $\eta_p^2=0.427$] with a prominent quadratic component [$F(1, 105)=99.0$, $p\leq 0.001$, $\eta_p^2=0.485$]; Auditory Gap PPI: [$F(5,525)=51.5$, $p_{GG}\leq 0.001$, $\eta_p^2=0.329$] with a prominent quadratic component [$F(1, 105)=93.0$, $p\leq 0.001$, $\eta_p^2=0.470$] ;Visual PPI: [$F(5,525)=52.8$, $p_{GG}\leq 0.001$, $\eta_p^2=0.335$] with a prominent quadratic component [$F(1, 105)=71.4$, $p\leq 0.001$, $\eta_p^2=0.405$]. A statistically significant sex x ISI interaction (Auditory PPI: [$F(10,525)=19.6$, $p_{GG}\leq 0.001$, $\eta_p^2=0.158$] with a prominent quadratic component [$F(1,105)=25.2$, $p\leq 0.001$, $\eta_p^2=0.193$]; Auditory Gap PPI: [$F(5,525)=18.3$, $p_{GG}\leq 0.001$, $\eta_p^2=0.148$] with a prominent quadratic component [$F(1, 105)=33.7$, $p\leq 0.001$, $\eta_p^2=0.243$] ;Visual PPI: [$F(5,525)=13.8$, $p_{GG}\leq 0.001$, $\eta_p^2=0.116$] with a prominent quadratic component [$F(1,105)=24.5$, $p\leq 0.001$, $\eta_p^2=0.189$]) was also observed. There was not a statistically significant main effect of treatment and/or

any higher-order interactions between genotype and treatment (p>0.05) for any of the experimental paradigms.

Notably, in auditory gap-PPI, a statistically significant genotype x sex x ISI interaction was also observed [$F(5,525)=4.9$, $p_{GG}\leq 0.003$, $\eta_p^2=0.044$]. The statistically significant three-way interaction reflects sex differences in temporal processing, but not the integrity of auditory system functioning. Treatment with SE during the formative period, therefore, has no adverse effects on sensory system function. Furthermore, despite the strong evidence for intact sensory system function, prominent alterations in temporal processing persist.

Motor System Function

Gross motoric system function was examined using the mean number of photocell interruptions in a 60 minute locomotor activity test session at PD 270. All animals, independent of genotype, biological sex, and/or treatment exhibited significant motor movement during the test session (Figure 6.3). HIV-1 Tg animals, collapsed across biological sex and treatment, displayed a statistically significantly greater number of photocell interruptions relative to control animals (Main Effect, Genotype [$F(1,103)=6.8$, $p\leq 0.01$, $\eta_p^2=0.062$]). There was not a statistically significant main effect of treatment and/or any higher-order interactions between genotype and treatment (p>0.05). Thus, treatment with SE during the formative period had no adverse effect on gross motoric system function.

Preattentive Processing

The progression of preattentive processing was established by evaluating the area of the inflection of the ASR response curve (McLaurin et al., 2016b). Planned comparisons were utilized to statistically test *a priori* hypotheses (detailed above).

Auditory Prepulse Inhibition

In auditory PPI, treatment with SE during the formative period had neither beneficial nor adverse effects on the progression of preattentive processing in control animals (Figure 6.4). Independent of treatment, a global one-phase association afforded a well-described fit ($R^2 \geq 0.98$) for control animals. The planned comparison was examined using a mixed-modal ANOVA, which failed to reveal a statistically significant main effect of treatment or any higher-order interactions with treatment ($p > 0.05$) in control animals.

HIV-1 Tg animals treated with placebo exhibited prominent alterations in the progression of preattentive processing in auditory PPI relative to control animals (Figure 6.4). A segmental linear regression, with maximal PPI at PD 120, afforded a well-described fit for HIV-1 Tg animals treated with placebo ($R^2 \geq 0.90$) whereas a one-phase association provided the best fit for control animals ($R^2 \geq 0.99$); observations which were confirmed by conducting a planned comparison revealing a statistically significant genotype x age interaction [$F(5, 325)=3.6$, $p_{GG} \leq 0.01$, $\eta_p^2=0.052$] with a prominent linear component [$F(1, 65)=17.9$, $p \leq 0.001$, $\eta_p^2=0.216$].

Despite the prominent genotype effect, treatment with SE during the formative period failed to mitigate deficits in the progression of preattentive processing in HIV-1 Tg animals (Figure 6.4). Specifically, independent of treatment, a global segmental linear regression ($R^2 \geq 0.82$), with maximal PPI observed at PD 120, provided the best fit for the

progression of preattentive processing in HIV-1 Tg animals. Neither a statistically significant main effect of treatment nor any higher-order interactions with treatment (p>0.05) were observed in HIV-1 Tg animals. Therefore, SE was unable to mitigate the profound effect of the HIV-1 transgene on the developmental trajectory of preattentive processing in auditory PPI.

Visual Prepulse Inhibition

In visual PPI, treatment with SE during the formative period had neither beneficial nor adverse effects on the progression of preattentive processing in control animals (Figure 6.5); results which were consistent with observations in auditory PPI. Specifically, a global segmental linear regression (R^2≥0.70), with maximal PPI at PD 120, provided a well-described fit for the preattentive processing in control animals.

Presence of the HIV-1 transgene significantly altered the developmental trajectory of preattentive processing in visual PPI (Figure 6.5). A segmental linear regression provided the best fit for both HIV-1 Tg animals treated with placebo (R^2≥0.97) and control animals collapsed across treatment (R^2≥0.82). HIV-1 Tg animals treated with placebo, however exhibited a prominent rightward shift in the point of maximal PPI relative to control animals (PD 150 vs. PD 120, respectively); a shift which supports an alteration in the development of preattentive processing (Figure 6.5).

Treatment with SE during the formative period enhanced the progression of preattentive processes in HIV-1 Tg animals (Figure 6.5). Independent of treatment, a segmental linear regression provided the best fit in HIV-1 Tg animals (R^2s≥0.97). However, HIV-1 Tg animals treated with SE exhibited a prominent leftward shift in the point of maximal inhibition relative to HIV-1 Tg animals treated with placebo (PD 120 vs.

PD 150, respectively); a shift which supports a significant effect of SE in HIV-1 Tg animals. The magnitude of the SE effect was evaluated by comparing HIV-1 Tg animals treated with SE and control animals; an examination which revealed maximal inhibition at PD 120 independent of genotype. After PD 120, however, HIV-1 Tg animals treated with SE exhibited a significant decrease in PPI, whereas control animals displayed no significant change in PPI. Treatment with SE during the formative period, therefore, was able to alter the developmental trajectory of visual PPI; albeit only through PD 120.

Auditory Gap Prepulse Inhibition

In auditory gap-PPI, treatment with SE during the formative period had neither beneficial nor adverse effects on the development of preattentive processing in control animals (Figure 6.6); results which were consistent with observations in both auditory and visual PPI. A global segmental linear regression ($R^2 \geq 0.94$), with a change in the rate of preattentive processing development at PD 120, provided a well-described fit for the progression of preattentive processing in control animals. Neither a statistically significant main effect of treatment or any higher-order interactions with treatment ($p > 0.05$) were observed when the planned comparison was evaluated using a mixed-modal ANOVA.

HIV-1 Tg animals treated with placebo displayed profound alterations in the development of preattentive processes in auditory gap-PPI (Figure 6.6). A first-order polynomial provided the best fit for HIV-1 Tg animals treated with placebo ($R^2 \geq 0.97$), whereas a segmental linear regression afforded a well-described fit for control animals ($R^2 \geq 0.99$); results which were confirmed by planned comparisons, revealing a statistically significant genotype x age interaction with a prominent linear component [$F(1,100)=5.1$, $p \leq 0.03$, $\eta_p^2=0.049$].

Treatment with SE ameliorated, at least partially, alterations in the progression of preattentive processing in HIV-1 Tg animals (Figure 6.6). A segmental linear regression, with maximal PPI observed at approximately PD 135 was the best fit for HIV-1 Tg animals treated with SE ($R^2 \geq 0.99$). The progression of preattentive processing in HIV-1 Tg animals treated with placebo, however, was well-described using a first-order polynomial ($R^2 \geq 0.97$). Planned comparisons revealed a statistically significant treatment x age interaction with a prominent quadratic component [$F(1, 63)=5.5$, $p \leq 0.02$, $\eta_p^2=0.080$], supporting these observations. Evaluation of the magnitude of the SE effect (i.e., HIV-1 Tg animals treated with SE vs. Control animals) revealed that a segmental linear regression provided the best fit for both HIV-1 Tg animals treated with SE ($R^2 \geq 0.99$) and control animals ($R^2 \geq 0.99$). However, beginning at approximately PD 135, HIV-1 Tg animals treated with SE exhibited a decline in preattentive processing. In sharp contrast, control animals continued to display significant development of preattentive processing through PD 210. Although there was a statistically significant effect of SE in HIV-1 Tg animals, the progression of preattentive processing was still significantly different from controls (Genotype x Age interaction [$F(5,515)=2.3$, $p_{GG} \leq 0.05$, $\eta_p^2=0.022$] with a prominent linear component [$F(1,103)=9.8$, $p<0.002$, $\eta_p^2=0.087$]). Thus, treatment with SE enhances the developmental trajectory of preattentive processing in HIV-1 Tg animals; albeit not to the level of controls.

DISCUSSION

Treatment with SE during the formative period (i.e., PD 28 to PD 90) selectively restored, albeit only partially, the developmental trajectory of preattentive processes in the HIV-1 Tg rat. Selective early alterations in preattentive processes, characterized by a

relative insensitivity to the manipulation of ISI, were observed in HIV-1 Tg animals relative to control animals. Treatment with SE had no adverse long-term effects on somatic growth, sensory system function or gross-motoric system function in either HIV-1 Tg or control animals supporting the safety of 0.2 mg SE. Prominent alterations in the development of preattentive processes were observed in HIV-1 Tg animals, independent of experimental paradigm; results which are consistent with previous reports (e.g., Moran et al., 2013a; McLaurin et al., 2016b; McLaurin et al., 2018b). However, the developmental trajectory of preattentive processes in HIV-1 Tg animals was partially restored in visual PPI and auditory gap-PPI by treatment with SE. In auditory PPI, treatment with SE failed to alter the progression of preattentive processes. Utilization of a longitudinal experimental design afforded a critical test of SE as a novel therapeutic to modify the progressive chronic neurological impairments revealing its therapeutic benefits and opportunities for improvement.

Selective, early alterations in preattentive processes were revealed across a series of PPI experimental paradigms. A relative insensitivity to the manipulation of ISI was observed in HIV-1 Tg animals, independent of biological sex, in auditory PPI, but not auditory gap-PPI; results which replicate those previously reported (McLaurin et al., 2017c). Furthermore, male, but not female, HIV-1 Tg animals exhibited prominent alterations in visual PPI relative to their control counterparts reflecting early sex differences in neurocognitive impairments. Notably, in clinical studies of HIV-infected children, sex differences in HIV RNA levels and CD4 parameters have been observed in the presence (European Collaborative Study, 2002; Foca et al., 2006) and absence (Ruel et al., 2011) of cART. The effect of biological sex on chronic neurological impairments in

PHIV, however, remains understudied with the exception of a few recent manuscripts (McLaurin et al., 2016b; Bangirana et al., 2017). Presence of early deficits in preattentive processes, independent of biological sex, however, highlights the critical need for an adjunctive therapeutic to alter the progression of chronic neurological impairments.

Critically testing the long-term effects of a novel therapeutic on somatic growth, sensory system function and gross-motoric system function is integral to evaluating its potential utility. Although presence of the HIV-1 transgene slowed the rate of somatic growth, independent of biological sex, treatment with SE had no adverse effects. Six months after the cessation of SE (i.e., PD 270), there was no evidence for any long-term genotype and/or treatment effects on auditory system function, visual system function or gross-motoric system function in either HIV-1 Tg or control animals. Specifically, robust inhibition to the presentation of either an auditory or visual prepulse was observed in PPI; an experimental paradigm that has been promoted for the evaluation of sensory system function (Ison, 1984; Wecker et al., 1985; Crofton & Sheets, 1989). Locomotor activity was also conducted to index motor behavior (Pierce & Kalivas, 2007) revealing a significantly greater motor activity in HIV-1 Tg animals, independent of treatment, relative to controls. Additionally, previous studies report no evidence for adverse peripheral effects, assessed using uterine weight, following SE treatment in either HIV-1 Tg or control animals (Moran et al., 2019). Results of the present study, therefore, demonstrate both the functional health of the HIV-1 Tg rat, replicating previous reports (McLaurin et al., 2018b), and the safety of the SE as an innovative therapeutic.

Treatment with SE during the formative period (i.e., PD 28 to PD 90) restored, albeit only partially, the developmental trajectory of preattentive processes in the HIV-1

Tg rat in both visual PPI and auditory gap-PPI. Specifically, in visual PPI, HIV-1 Tg animals treated with placebo exhibited a significant rightward shift in the age at which the point of maximal PPI was observed relative to control animals (i.e., PD 150 vs. PD 120, respectively). HIV-1 Tg animals treated with SE, however, displayed a prominent leftward shift in the age at which the point of maximal PPI was observed (i.e., PD 120); a shift approximating the one observed in control animals. In auditory gap-PPI, the rate of preattentive processing development is significantly slower in HIV-1 Tg animals treated with placebo relative to control animals. Treatment with SE, however, significantly increased the rate of preattentive processing development in HIV-1 Tg animals; albeit not to the level of controls. The failure to observe restoration in the development of preattentive processes after PD 120 in either visual PPI or auditory PPI may be due to the cessation of SE treatment at PD 90. A longer treatment duration may be necessary for long-term modifications in disease progression, reflecting an opportunity for further therapeutic improvement.

Treatment with SE, however, was unable to alter the progression of preattentive processes in auditory PPI. Specifically, independent of treatment, control animals exhibited significant development of preattentive processes throughout the duration of experimentation. HIV-1 Tg animals, however, displayed an increased in preattentive processing through PD 120, but failed to exhibit any significant development at later assessments. Notably, the neural circuits mediating and/or regulating auditory PPI, visual PPI, and auditory gap-PPI have key differences which may explain the selective therapeutic efficacy of SE.

The serial neural circuit mediating PPI has been well-established by lesioning (e.g., Leitner & Cohen, 1985) and electrical stimulation (e.g., Li & Yeomans, 2000) studies. Initially, acoustic prepulse stimuli are relayed to the IC, whereas visual prepulse stimuli are relayed to the SC. Subsequently, sensory input projects to the PPTg, which triggers acetylcholine projections to the caudal pontine reticular nucleus activating motor neurons and eliciting a startle response (Fendt et al., 2001; Koch & Schnitzler, 1997).

Additional brain regions (e.g., mPFC, Nac, lateral globus pallidus (LGP)) and neurotransmitter systems (e.g., DA, GABA) are involved in the regulation of PPI, evidenced by pharmacological manipulations (e.g., Ellebroek et al., 1996; Japha & Koch, 1999; Pothuizen et al., 2005) and c-Fos induction (e.g., Takahasi et al., 2007; Moreno-Paublete et al., 2017). Specifically, c-Fos induction studies have revealed that auditory PPI and auditory gap-PPI are uniquely regulated by the LGP and auditory cortex, respectively (Moreno-Paublete et al., 2017). Within the LGP, which has significantly lower DA levels in HIV-1 seropositive individuals (Kumar et al., 2009), inhibitory GABAergic neurons project to the PPTg, playing a key regulatory role in PPI (Takahasi et al., 2007). In contrast, excitatory neurons project from the auditory cortex to the PPTg (Schofield & Motts, 2009). Auditory PPI, therefore, may be regulated by inhibitory neurons, whereas auditory gap-PPI is more likely regulated by excitatory neurons; regulatory differences that may underlie the selective therapeutic efficacy of SE.

Mechanistically, SE may remodel neuronal circuitry at the synaptic level by modifying neuronal morphology and dendritic spines, leading to subsequent enhancements in neurotransmission (Chapter 5). At the broadest level, strong evidence supports the utility of 17β-estradiol to increase dendritic spine density (e.g., Khan et al. 2013; Hao et al. 2006;

Tuscher et al. 2016; Wang et al., 2018), produce a robust shift in the morphological characteristics of dendritic spines (Hao et al., 2006) and enhance excitatory neurotransmission (Kritzer & Kohama, 1998); effects which occur via the ERβ pathway (Wang et al., 2018). In sharp contrast, 17β-estradiol reduces the efficacy of GABAergic inhibition (Mukherjee et al., 2017). In the context of HIV-1, estrogenic compounds block neurotoxic effects (Kendall et al., 2005), attenuate oxidative stress (Wallace et al., 2006) and prevent loss of DA transporter function (Wallace et al., 2006) induced by HIV-1 viral proteins (i.e., Tat, gp120). More specifically, SE prevents synapse loss (Bertrand et al., 2015) and enhances synaptic efficacy (Chapter 5) resulting from the presence of HIV-1 viral proteins.

Thus, in conclusion, the present study utilized a longitudinal experimental design to critically test SE as a novel therapeutic to modify the progressive chronic neurological impairments. Assessments of functional health, including somatic growth, sensory system function, and gross-motoric system function support the long-term safety of 0.2 mg SE. Furthermore, treatment with SE during the formative period selectively restored, albeit only partially, the developmental trajectory of preattentive processes in the HIV-1 Tg rat, supporting its potential as a therapeutic to modify progressive chronic neurological impairments commonly observed in PHIV. Long-term modifications in disease progression may require a longer duration of treatment, affording a key opportunity for improvement.

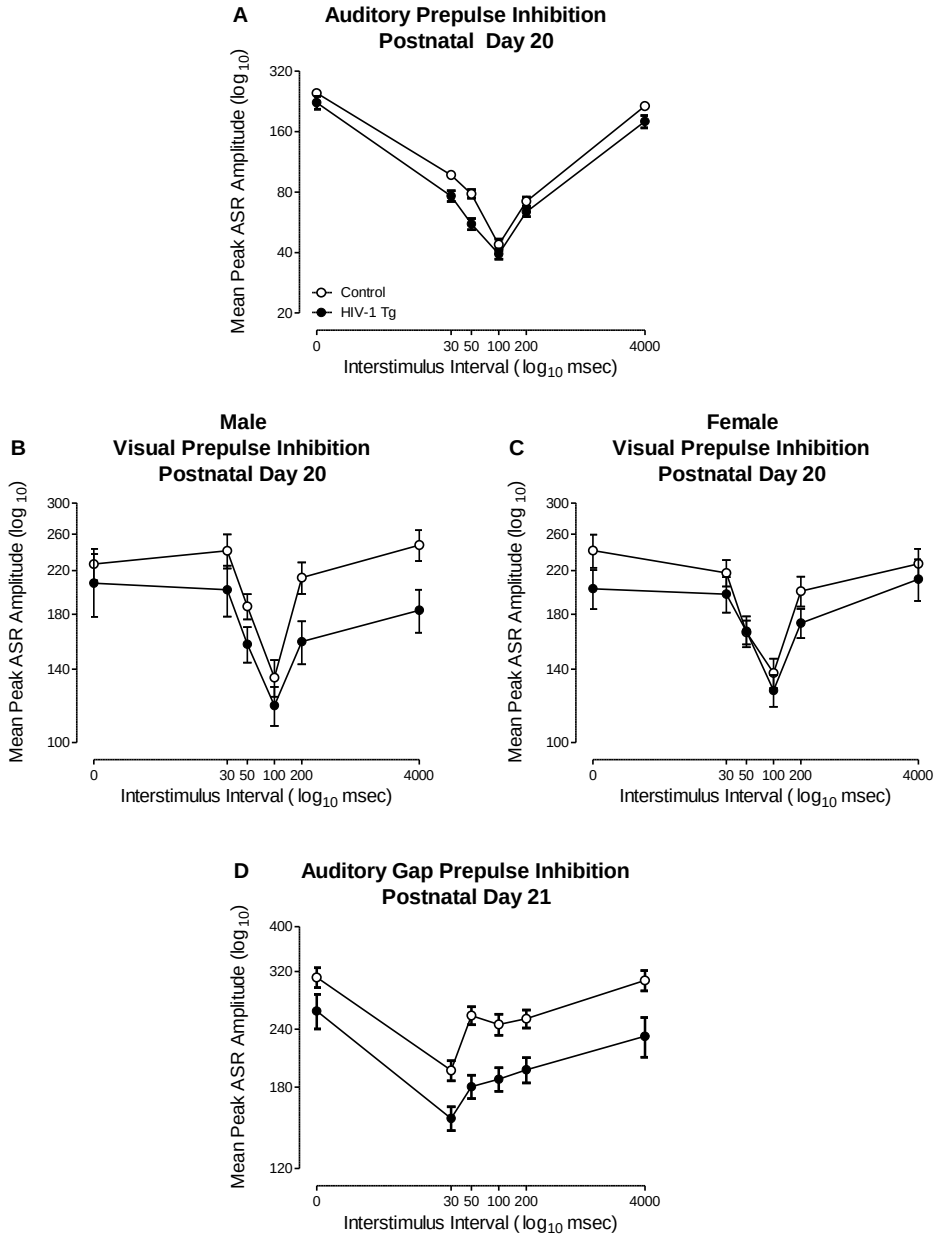

Figure 6.1 Early Neurocognitive Impairments. Mean peak ASR (± SEM) is illustrated as a function of genotype (HIV-1 Tg vs. Control). Early alterations in preattentive processes are evidenced by a relative insensitivity to the manipulation of ISI in auditory PPI (**A**), independent of biological sex. Male (**B**), but not female (**C**), HIV-1 Tg animals displayed prominent early alterations in visual PPI. There was no evidence for any early alterations in preattentive processes in auditory gap prepulse inhibition (**D**).

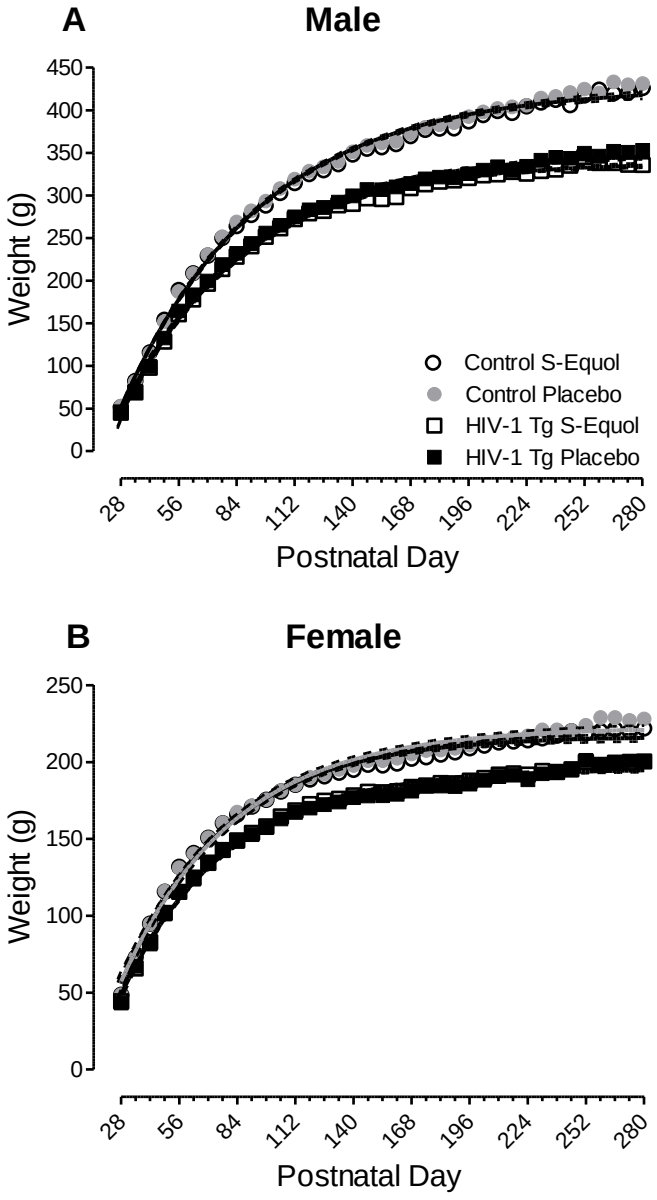

Figure 6.2 Somatic Growth. Mean body weight (±95% CI), a measure of somatic growth, is illustrated for males (**A**) and females (**B**) as a function of genotype (HIV-1 Tg vs. control), treatment (SE vs. placebo) and age. Independent of biological sex, HIV-1 Tg animals exhibited a slower rate of growth relative to control animals. Treatment with SE did not alter the growth trajectory of either HIV-1 Tg or control animals.

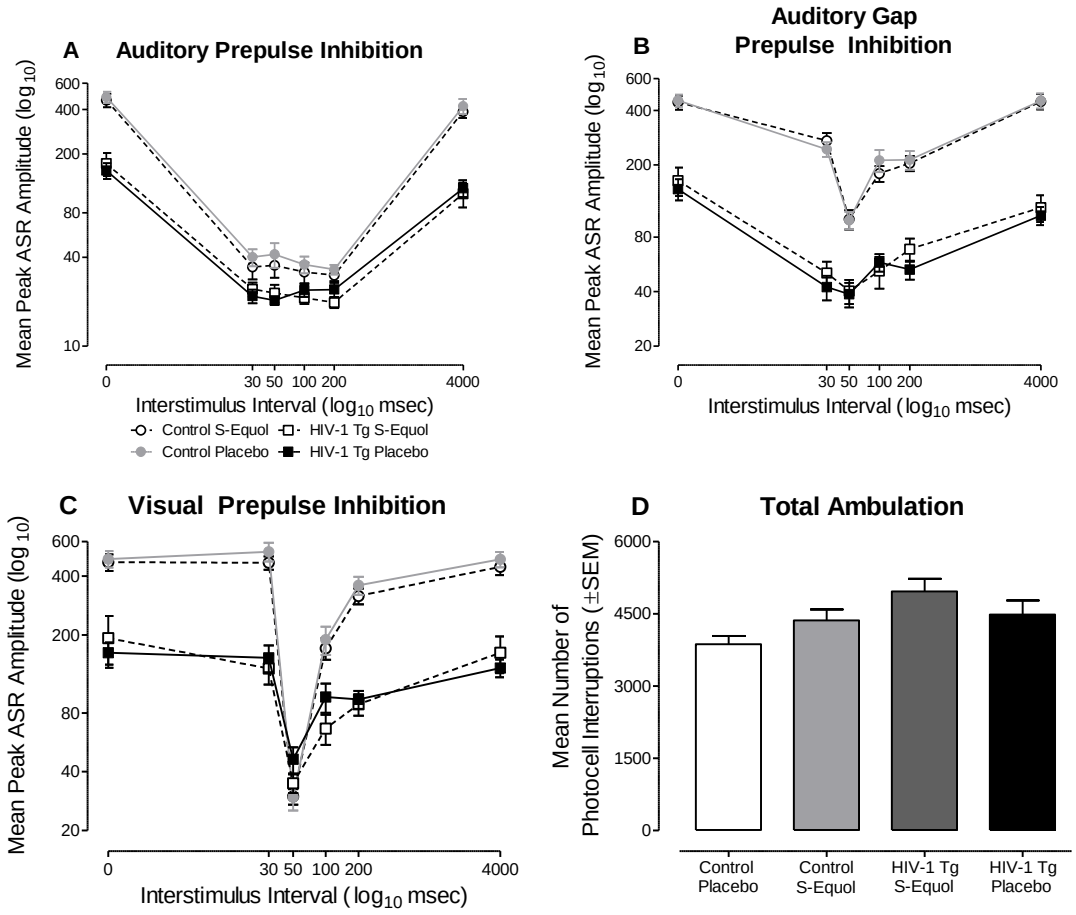

Figure 6.3 Sensory and Motor System Function. Integrity of sensory and gross-motoric system function was assessed at PD 270, six months after the cessation of SE treatment. Both HIV-1 Tg and control animals, independent of treatment, exhibited robust inhibition to the presentation of an auditory prepulse (**A**), a gap in background noise (**B**), and a visual prepulse (**C**) supporting the integrity of sensory system function. Locomotor activity (**D**) supported the integrity of gross-motoric system function, evidenced by significant motor movement, independent of genotype, biological sex, and/or treatment, during the test session.

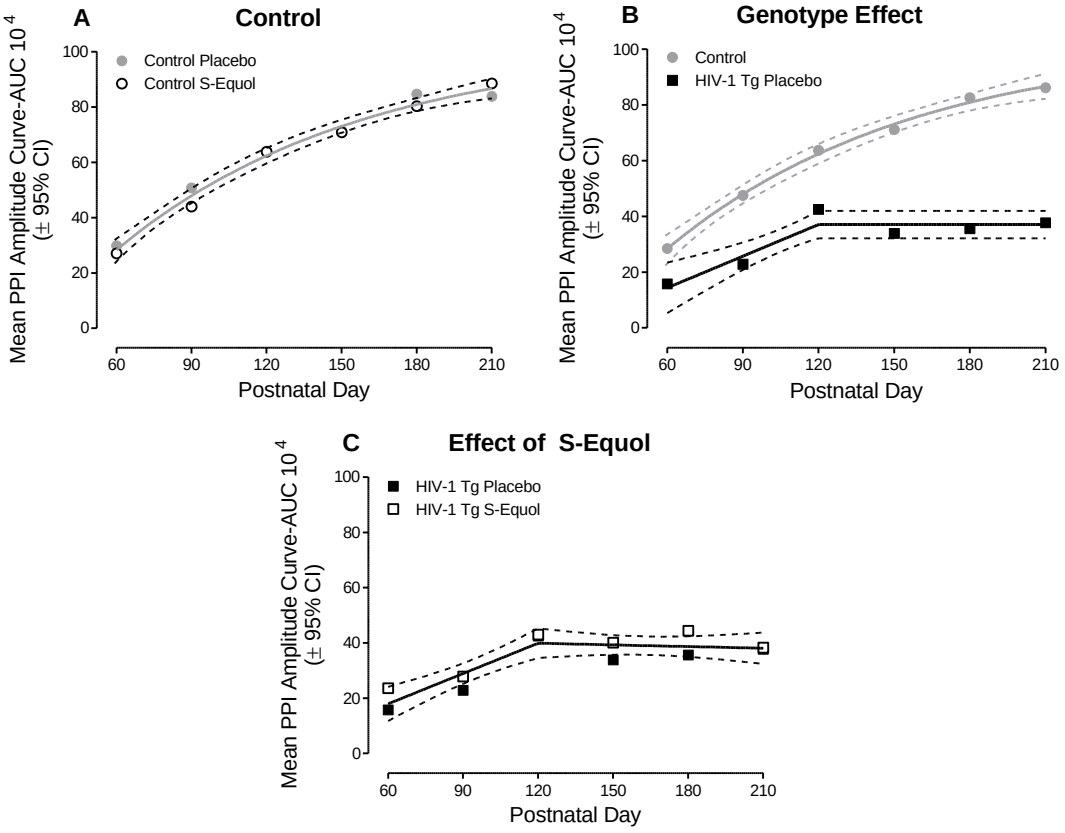

Figure 6.4 S-Equol: Auditory PPI. Auditory PPI, examined using mean area of the peak inflection curve (±95% CI), is illustrated as a function of genotype (HIV-1 Tg vs. control), treatment (SE vs. placebo) and age. (**A**) Treatment with SE had no beneficial or adverse effects on the progression of preattentive processes in control animals, evidenced by a global one-phase association ($R^2 \geq 0.98$). (**B**) Preattentive processes in control animals was well-described using a one-phase association($R^2 \geq 0.99$), whereas a segmental linear regression, with maximal PPI at PD 120, provided the best fit for HIV-1 Tg animals treated with placebo ($R^2 \geq 0.90$); results supporting a prominent alteration in the development of preattentive processes in HIV-1 Tg animals treated with placebo. (**C**) Treatment with SE failed to mitigate deficits in the developmental trajectory of preattentive processing in HIV-1 Tg animals, evidenced by a global segmental linear regression ($R^2 \geq 0.82$). Thus, SE was unable to mitigate the profound effect of the HIV-1 transgene on the developmental trajectory of preattentive processing in auditory PPI.

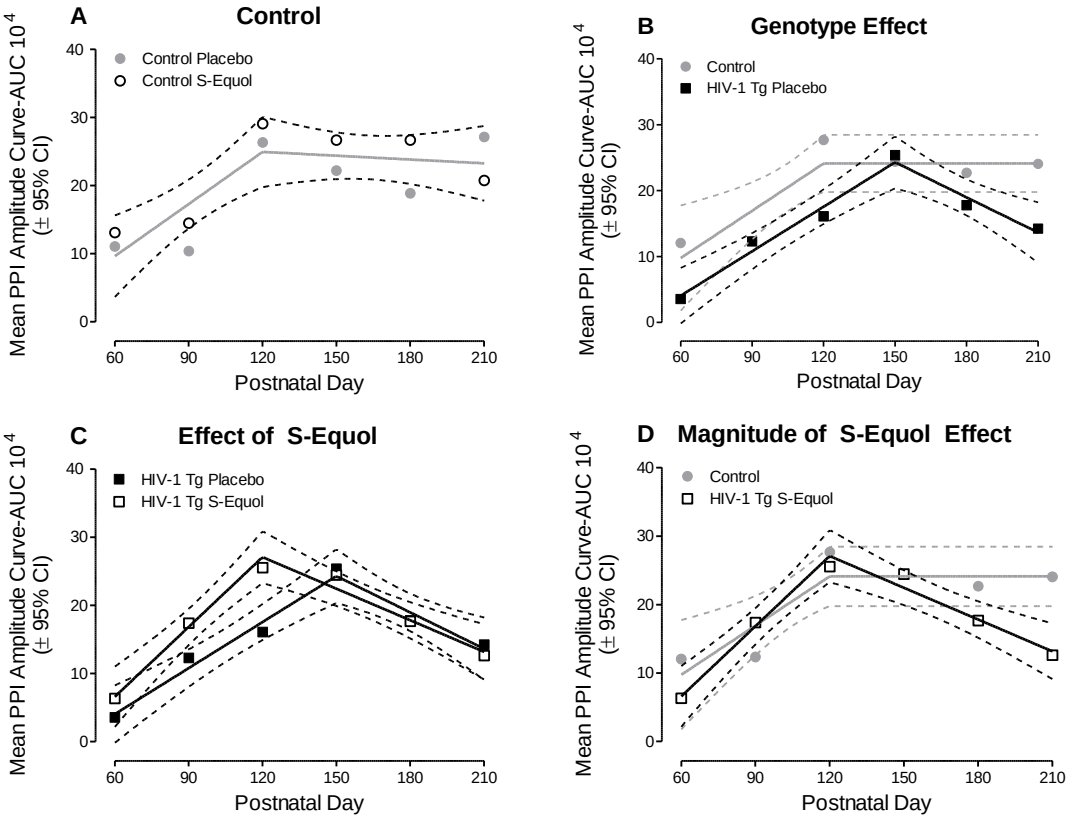

Figure 6.5 S-Equol: Visual PPI. Visual PPI, examined using mean area of the peak inflection curve (±95% CI), is illustrated as a function of genotype (HIV-1 Tg vs. control), treatment (SE vs. placebo) and age. (**A**) Treatment with SE had no beneficial or adverse effects on the progression of preattentive processes in control animals, evidenced by a global segmental linear regression ($R^2 \geq 0.70$), with maximal PPI at PD 120. (**B**) Although preattentive processes in both HIV-1 Tg and control animals were well-described by a segmental linear regression ($R^2 \geq 0.97$ and $R^2 \geq 0.82$, respectively), HIV-1 Tg animals displayed a prominent rightward shift in the point of maximal PPI relative to control animals (PD 150 vs. PD 120, respectively). (**C**) Treatment with SE enhanced the developmental trajectory of preattentive processes in HIV-1 Tg animals, evidenced by a prominent leftward shift in the point of maximal inhibition in HIV-1 Tg animals treated with SE relative to HIV-1 Tg animals treated with placebo (PD 120 vs. PD 150, respectively). (**D**) Both HIV-1 Tg animals treated with SE and control animals exhibited maximal inhibition at PD 120. However, after PD 120, HIV-1 Tg animals treated with SE displayed a significant decrease in PPI, whereas control animals displayed no significant change in PPI. Thus, treatment with SE during the formative period was able to partially restore the developmental trajectory of visual PPI in HIV-1 Tg animals.

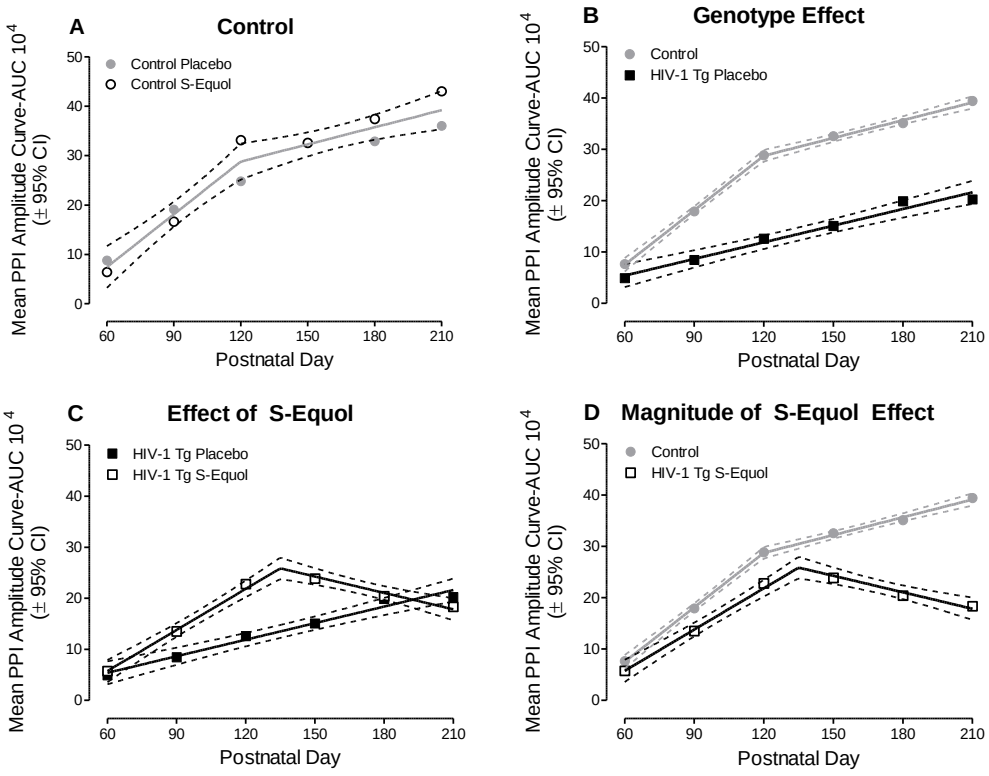

Figure 6.6 S-Equol: Auditory Gap-PPI. Auditory gap-PPI, assessed using mean area of the peak inflection curve (±95% CI), is illustrated as a function of genotype (HIV-1 Tg vs. control), treatment (SE vs. placebo) and age. (**A**) Treatment with SE had no beneficial or adverse effects on the progression of preattentive processes in control animals, evidenced by a global segmental linear regression ($R^2 \geq 0.94$), with a change in the rate of preattentive processing development at PD 120. (**B**) HIV-1 Tg animals treated with placebo displayed a prominent alteration in the developmental trajectory of preattentive processes. Specifically, a first-order polynomial provided a well-described fit for HIV-1 Tg animals treated with placebo ($R^2 \geq 0.97$), whereas a segmental linear regression afforded the best fit for control animals ($R^2 \geq 0.99$). (**C**) Treatment with SE mitigated alterations in the progression of preattentive processes in HIV-1 Tg animals. A segmental linear regression, with maximal PPI observed at approximately PD 135 was the best fit for HIV-1 Tg animals treated with SE ($R^2 \geq 0.99$). The progression of preattentive processing in HIV-1 Tg animals treated with placebo, however, was well-described by a first-order polynomial ($R^2 \geq 0.97$). (**D**) Treatment with SE partially restored the developmental trajectory of preattentive processes. Beginning at approximately PD 135, HIV-1 Tg animals exhibited a decline in preattentive processes. Control animals, however, continued to display significant preattentive processing development through PD 210.

CHAPTER 7

HIV-1 VIRAL PROTEINS ALTER THE MATURATIONAL PROCESSES OF PYRAMIDAL NEURONS IN THE MEDIAL PREFRONTAL CORTEX

INTRODUCTION

The PFC, located at the anterior pole of the mammalian brain, is well-recognized as an anatomically and functionally complex brain region (Siddiqui et al., 2008). In a seminal study, Rose and Woolsey (1948) defined the rodent PFC as areas connected with the mediodorsal nucleus of the thalamus. More recent research, however, has supported expanding the definition of the rodent PFC to also include functional considerations (e.g., Kesner, 2000) and additional cortico-cortical connections (e.g., Uylings & Van Eden, 1990). Utilization of these criteria has provided an opportunity to further subdivide the PFC into three distinct regions in the rat, including the mPFC, lateral PFC, and ventral PFC (for review, Dalley et al., 2004). Functionally, the PFC has two broad roles, including the temporal organization of behavior (Fuster, 2008) and executive functions (Fuster, 2008); neurocognitive functions which are fundamentally altered by HIV-1 viral proteins (e.g., Heaton et al., 2011; Chan & Brew, 2014; Moran et al., 2014a; Moran et al., 2019).

Longitudinal experimental designs have afforded a key opportunity to assess the progression of neurocognitive impairments associated with HAND, which afflict approximately 40-70% of HIV-1 seropositive individuals (Heaton et al., 2010; Letendre et al., 2010; McArthur et al., 2010). Clinical studies have reported progressive neurocognitive decline in a significant proportion (i.e., 13-30%) of HIV-1 seropositive individuals (e.g., Heaton et al., 2015; Sacktor et al., 2016; Rubin et al., 2017; Gott et al., 2017); results which were translationally modeled and extended in the HIV-1 Tg rat (McLaurin et al., 2018b; McLaurin et al., 2019b). Across the functional lifespan, the HIV-1 Tg rat displayed age-related disease progression across multiple neurocognitive domains commonly associated with the PFC (e.g., McLaurin et al., 2018b; McLaurin et al., 2019b; temporal processing: Ellenbroek et al., 1996, stimulus-reinforcement learning: Rolls, 2004, sustained attention:

Kim et al., 2016). Although recent research has enhanced our understanding of the progression of neurocognitive impairments in HAND, to date, longitudinal experimental designs remain underutilized for the investigation of the pathogenesis of HAND, with one notable exception (e.g., Casas et al., 2018). To address this knowledge gap, the present study examined the progression of synaptic dysfunction, a putative neural mechanism underlying HAND (e.g., Gelman & Nguyen, 2010; Desplats et al., 2013; Roscoe et al., 2014; McLaurin et al., 2019b), in the PFC.

Mature neuronal circuits are formed during a series of progressive (i.e., growth) and regressive (i.e., pruning) events throughout development (for review, Riccomagno & Kolodkin, 2015). Synaptogenesis, which involves the establishment, maintenance, refinement and elimination of synapses (Sachana et al., 2017), serves as one key example. In 1976, Changeau and Danchin proposed the selective-elimination hypothesis, whereby the development of mature neuronal circuits depends upon the selective stabilization of developing synapses (Changeau & Danchin, 1976). Observations of the initial overproduction and subsequent pruning of excitatory synapses, independent of brain region (e.g., Huttenlocher, 1979; Bourgeois et al., 1994; Huttenlocher & Dabholkar, 1997; Petanjek et al., 2011), provided strong evidence for the selective-elimination hypothesis. The PFC specifically exhibits the greatest overproduction of dendritic spines, a proxy for excitatory synapses (Berry & Nedivi, 2017), and the slowest rate of synaptic pruning (Elston et al., 2009). In regards to timing, synaptic pruning in the PFC typically begins at puberty and is completed during early adolescence (Huttenlocher et al., 1979; Drzewiecki et al., 2016). Notably, the timing of synaptic pruning coincides with the development of

higher-order cognitive processes supporting its potential functional significance (e.g., Selemon, 2013).

Evaluating the morphological parameters of dendritic spines, which are a key structural and functional element of neurons, may afford insight into the functionality and connectivity of synapses (Lai & Ip, 2013). Dendritic spine volume serves as a morphological parameter that encapsulates dendritic spine backbone length, head diameter, and neck diameter. Specifically, increased dendritic spine volume is associated with increased synaptic area (Freire, 1978; Arellano et al., 2007), which is correlated with the number of presynaptic vesicles (Harris & Stevens, 1988), the number of docked vesicles (Schikorski & Stevens, 1999), and the number of postsynaptic receptors (Yuste, 2010). Evaluation of dendritic spines across development, therefore, may not only provide information about synaptogenesis, but also the functional capacity of synapses.

Synaptic function has been examined in HIV-1 seropositive individuals (e.g., Gelman & Nguyen, 2010; Desplats et al., 2013), as well as biological systems used to model key aspects of HAND (e.g., Fitting et al., 2013; Roscoe et al., 2014; McLaurin et al., 2019b); results which illustrate profound functional deficits. In the mPFC, synaptic dysfunction, accounting for 64.6% of the genotypic variance, is characterized by prominent alterations in dendritic branching complexity, synaptic connectivity, and dendritic spine morphology (McLaurin et al., 2019b). Additional support for the importance of synaptic dysfunction is evidenced by the generalizability of observations across brain regions (i.e., mPFC (McLaurin et al., 2018a; McLaurin et al., 2019b), Nac (Roscoe et al., 2014; McLaurin et al., 2018c), hippocampus (Fitting et al., 2013)) and ages (i.e., 4 months (Roscoe et al., 2014); 14-17 months (McLaurin et al., 2018a); 20 months (McLaurin et al.,

2018c; McLaurin et al., 2019b). The cross-sectional nature of these studies, however, precludes evaluating key progressive (i.e., growth) and regressive (i.e., pruning) events and/or the progression of synaptic dysfunction across time; a critical consideration given the characterization of HAND as a progressive, age-related neurodegenerative disease (Cohen et al., 2015; McLaurin et al., 2019b).

In light of previous studies, the aim of the present study was to assess the progression of synaptic dysfunction in pyramidal neurons from layers II-III of the mPFC in the HIV-1 Tg rat in the absence of neurocognitive testing. A ballistic labeling technique was utilized to visualize neurons and distinguish dendritic spines (O'Brien & Lummis, 2007) at six ages across development (i.e., PD 30 to PD 180). Furthermore, use of sophisticated neuronal reconstruction software provided an opportunity to investigate neuronal structure (i.e., total dendrite length, Sholl analysis, dendritic branching) and morphological characteristics of dendritic spines (i.e., volume, backbone length, head diameter). Understanding how HIV-1 viral proteins alter progressive and/or regressive processes, as well as synaptic function, in the mPFC may afford a key target for the development of innovative therapeutics.

METHODS

Animals

Fischer (F344/N) control animals were procured from Envigo Laboratories Inc. (Indianapolis, IN) and delivered to the animal vivarium at least one week prior to sacrifice. All F344/N control animals were pair- or group-housed until sacrifice. HIV-1 Tg animals were bred at the University of South Carolina by pairing an F344/N female with an HIV-1 Tg male. At approximately PD 24, HIV-1 Tg animals were weaned and pair- or group-housed with animals of the same sex until sacrifice. To control for independence of

observations, the goal was to utilize no more than one rat pup per sex from each litter for each age.

HIV-1 Tg and control animals were sacrificed at six different ages (i.e., PD 30, PD 60, PD 90, PD 120, PD 150, and PD 180) to assess the progression of synaptic dysfunction in pyramidal neurons from layers II-III of the mPFC (Control: PD 30, *n*=20 (male, *n*=10, female, *n*=10), PD 60, *n*=20 (male, *n*=10, female, *n*=10), PD 90, *n*=20 (male, *n*=10, female, *n*=10), PD 120, *n*=20 (male, *n*=10, female, *n*=10), PD 150, *n*=20 (male, *n*=10, female, *n*=10), PD 180, *n*=18 (male, *n*=10, female, *n*=8); HIV-1 Tg: PD 30, *n*=15 (male, *n*=7, female, *n*=8), PD 60, *n*=18 (male, *n*=10, female, *n*=8), PD 90, *n*=17 (male, *n*=10, female, *n*=7), PD 120, *n*=20 (male, *n*=10, female, *n*=10), PD 150, *n*=20 (male, *n*=10, female, *n*=10), PD 180, *n*=20 (male, *n*=10, female, *n*=10). Ages for sacrifice were selected based on a longitudinal study of brain volumetric measurements in the HIV-1 Tg rat, suggesting the most prominent brain injury occurs earlier in life (Casas et al., 2018).

HIV-1 Tg and control animals were maintained in AAALAC-accredited facilities using recommendations in the Guide for the Care and Use of Laboratory Animals of the NIH. The targeted environmental conditions for the animal vivarium were 21°± 2°C, 50% ± 10% relative humidity and a 12-h light:12-h dark cycle with lights on at 0700 h (EST). The project protocol was approved under federal assurance (# D16-00028) by the IACUC at the University of South Carolina.

Estrous Cycle Tracking

Estrous cyclicity was examined prior to sacrifice by performing a vaginal lavage. Cellular cytology was examined in vaginal smears, as previously described (Booze et al., 1999), using a light microscope (10x). Stage of the estrous cycle was determined by the

predominant cell type (Waynforth & Flecknell, 1992; Westwood, 2008). The diestrus phase was characterized by the predominance of leukocytes (Marcondes et al., 2002).

Synaptic Dysfunction

Methodology for the ballistic labeling technique utilize to assess synaptic dysfunction was initially described by Seabold et al. (2010) and has been adapted for use in our laboratory (Li et al., 2020). For female animals, the goal was to sacrifice animals during the diestrus phase of the estrous cycle.

Preparation of Cartridges and Tefzel Tubing

In brief, dissolve polyvinylpyrrolidone (PVP; 100 mg) in double deionized H_2O (10 mL), vortex lightly and utilize the PVP solution to coat the Tefzel tubing (IDEX Health Sciences, Oak Harbor, WA). Cartridges were prepared by dissolving tungsten micro-carrier beads (170 mg; Bio-Rad, Hercules, CA) in methylene chorlide (250 µL). Separately, lipophilic DiIC18(3) dye (6 mg) was combined with methylene chloride (300 µL) and vortexed thoroughly. The tungsten bead suspension was pipetted onto a glass slide and allowed to air dry. Subsequently, the lipophili DiIC18(3) dye solution was pipetted on top of the tungsten bead suspension layer and mixed. The mixture was placed into centrifuge tubes filled with H_2O and sonicated. The dye mixture was drawn into the PVP-coated tubing, placed in the tubing prep station (Bio-Rad) and allowed to dry under nitrogen gas. Cartridges were cut into 13 mm segments.

Preparation of Brain Tissue

Animals were deeply anesthetized using sevoflurane (5%; Abbot Laboratories, North Chicago, IL) and transcardially perfused using 100 mM phosphate buffered saline (PBS; 50 mL) followed by 4% paraformaldehyde buffered in 100 mM PBS (100 mL). The brain was removed and postfixed for 10 minutes with 4% paraformaldehyde. Coronal

sections were cut (500 μm) using a rat brain matrix (Ted Pella Inc., Redding, CA) and placed in a well-plate with 100 mM PBS (1 mL).

Ballistic Labeling

Pyramidal neurons from layers II-III of the mPFC were visualized using a ballistic labeling technique. The previously prepared cartridges were loaded into the Helios gene gun (Bio-Rad) and delivered through pore filter paper (3 μm) using Helium gas (90 PSI). The Helios gene gun was targeted at the center of the well and placed approximately 2.5 cm away from the sample before firing the cartridges. After completing the ballistic labeling, brain sections were washed three times in 100 mM PBS (500 μL) and stored in the dark at 4°C for three hours. Subsequently, slides were transferred onto glass slides, mounted using Pro-Long Gold Antifade (Invitrogen, Carlsbad, CA) and coverslipped. Glass slides were stored in the dark for two days to allow for drying.

Confocal Imaging

Z-stack images were obtained on three to four pyramidal neurons (3.7 mm to 2.2 mm anterior to Bregma; Paxinos & Watson, 2014) from each animal using a Nikon TE-2000E confocal microscope and Nikon's EZ-C1 software (version 3.81b). Images were taken at 60x magnification (A/1.4, oil) using a Z-plane interval of 0.15 μm with a pinhole size of 30 μm and back-projected pinhole radius of 167 nm. A helium-neon laser with a 543 nm wavelength was used to acquire images.

Neuronal Analysis and Spine Quantification

Neuronal reconstruction software (Neurolucida 360 (MicroBrightfield, Williston, VT) was utilized to analyze morphological characterstics of pyramidal neurons and dendritic spines. To control for independence of observations, only one neuron was chosen

for analysis using selection criteria. Selection criteria, illustrated in Li et al. (2020), include continuous dendritic staining, low background/dye clusters, and minimal diffusion of the DiI dye into the extracellular space. Neurons not meeting the selection criteria were not included in the analysis, yielding (Control: PD 30, *n*=19 (male, *n*=9, female, *n*=10), PD 60, *n*=19 (male, *n*=10, female, *n*=9), PD 90, *n*=18 (male, *n*=10, female, *n*=8), PD 120, *n*=17 (male, *n*=9, female, *n*=8), PD 150, *n*=18 (male, *n*=8, female, *n*=10), PD 180, *n*=14 (male, *n*=9, female, *n*=5); HIV-1 Tg: PD 30, *n*=14 (male, *n*=7, female, *n*=7), PD 60, *n*=17 (male, *n*=10, female, *n*=7), PD 90, *n*=15 (male, *n*=8, female, *n*=7), PD 120, *n*=20 (male, *n*=10, female, *n*=10), PD 150, *n*=19 (male, *n*=9, female, *n*=10), PD 180, *n*=17 (male, *n*=9, female, *n*=8).

Neuronal morphology was examined using two approaches, including the classical Sholl analysis (Sholl, 1953) and branch order. Specifically, Sholl analysis affords an opportunity to infer alterations in neuronal complexity by counting the number of intersections at each successive radii (10 μm). A centrifugal branch ordering method was utilize to assign each dendrite with a branch order by counting the number of segments traversed; an assessment of dendritic branching complexity. Output from the Sholl analysis was also utilized to evaluate synaptic connectivity by examining the number of dendritic spines between each successive radii.

Morphological characteristics of dendritic spines were examined using three parameters, including volume (μm^3), backbone length (μm), and head diameter (μm). Volume served as the primarily morphological parameter given that it encapsulates both backbone length and head diameter. Spine parameters were defined using well-accepted previously published results [i.e., volume, 0.05 to 0.85 μm: Hering & Sheng, 2001;

backbone length, 0.4 to 4.0 µm: Ruszcycki et al., 2012; head diameter, 0 to 1.2 µm: Konur et al., 2003].

Statistical Analysis

Data were statistically analyzed by conducting ANOVA and regression techniques (SAS/STAT Software 9.4, SAS Institute, Inc., Cary, NC; SPSS Statistics 26, IBM Corp., Somer, NY; GraphPad Software, Inc., La Jolla, CA). An alpha criterion of $p \leq 0.05$ was established for statistical significance.

Regression analyses (GraphPad Software, Inc., La Jolla, CA) were utilized to assess measures of neuronal morphology, including total dendrite length, area under the Sholl curve, and the total number of dendritic branches. Additionally, the area under the Sholl curve, the total number of dendritic branches, and the total number of dendritic spines were analyzed using a repeated-measures ANOVA (SPSS Statistics 26, IBM Corp., Somer, NY). Between subjects' factors included genotype (HIV-1 Tg vs control), biological sex (Male vs. Female), and age (PD 30, PD 60, PD 90, PD 120, and PD 180). The number of intersections at each radii (Sholl) or the number of dendrites at branch orders on through ten (Branch Order) served as the dependent variable.

Measures of synaptic dysfunction included the total number of dendritic spines, an assessment of synaptic connectivity, and dendritic spine morphological parameters. The total number of dendritic spines was examined using both regression analyses (GraphPad Software, Inc., La Jolla, CA) and a univariate ANOVA. A generalized linear mixed effects model with a Poisson distribution and an unstructured covariance pattern (SAS/STAT Software 9.4, SAS Institute, Inc., Cary, NC) was utilized to assess synaptic connectivity, by evaluating the total number of dendritic spines between each radius, and dendritic spine

volume, by examining the number of dendritic spines in each bin. Additionally, the median dendritic spine volume, dendritic spine backbone length, and dendritic spine head diameter were calculated for each animal to evaluate how dendritic spine morphology changes across time. Regression analyses (GraphPad Software, Inc., La Jolla, CA) and univariate ANOVAs were conducted on the median dendritic spine volume, dendritic spine backbone length, and dendritic spine head diameter.

RESULTS

Sholl Analysis

Total dendrite length was examined as one measure of neuronal morphology. Regression analyses revealed a differential dendrite development across time (Figure 7.1). Independent of genotype, a segmental linear regression provided a well-described fit for total dendrite length across age. In HIV-1 Tg animals ($R^2 \geq 0.91$), there was no significant growth from PD 30 to PD 120. However, HIV-1 Tg animals exhibited a linear increase in total dendrite length from PD 120 to PD 180. In control animals ($R^2 \geq 0.75$), a linear decrease in total dendrite length was observed from PD 30 to PD 60, followed by no additional changes in total dendrite length from PD 60 to PD 180. HIV-1 Tg animals, therefore, displayed a differential developmental growth trajectory for total dendrite length in pyramidal neurons from layers II-III of the mPFC.

The classical Sholl analysis was conducted to evaluate change in dendritic arbor complexity. To investigate if and/or how dendritic arbor complexity changes across time, the area under the Sholl curve was calculated for each animal. HIV-1 Tg animals, independent of biological sex, exhibited a differential development of dendritic arbor complexity relative to control animals (Figure 7.1; Genotype x Age interaction, [$F(5, 183)=2.8$, $p \leq 0.020$, $\eta_p^2=0.070$]). In HIV-1 Tg animals, a segmental linear regression

provided a well-described fit for the progression of area under the Sholl curve ($R^2 \geq 0.93$). Specifically, there was no evidence for increase in area under the Sholl curve from PD 30 to PD 120, but a linear increase in area under the Sholl curve from PD 120 to PD 180. In control animals, the progression of area under the Sholl curve was also best fit using a segmental linear regression ($R^2 \geq 0.76$), whereby a linear decrease in area under the Sholl curve was observed from PD 30 to PD 60, followed by a plateau.

Observations revealed by examining the area under the Sholl curve were confirmed by conducting a repeated-measures ANOVA on the number of intersections per radii, a more traditional statistical approach for Sholl analysis. Specifically, a statistically significant genotype x age interaction [$F(5, 183)=2.8$, $p \leq 0.019$, $\eta_p^2=0.070$) was also observed when utilizing a more traditional statistical approach for Sholl analysis. Although a statistically significant main effect of radius [$F(24, 4392)=225.1$, $p \leq 0.001$, $\eta_p^2=0.552$], there were no two-way or higher-order interactions with radius.

Branch Order

A centrifugal branch ordering method was utilized, whereby sophisticated neuronal reconstruction software counts assigns each dendrite with a branch order based on the number of segments traversed, to assess dendritic branching complexity. Branch orders one through ten were evaluated in the present study. Consistent with observations in Sholl analysis, HIV-1 Tg animals exhibited a differential development of dendritic branching complexity relative to control animals (Figure 7.1; Genotype x Age interaction, [$F(5,183)=3.3$, $p \leq 0.006$, $\eta_p^2=0.084$]). Specifically, in HIV-1 Tg animals, the total number of dendritic branches across time was well-described by a segmental linear regression, whereby, a plateau was observed from PD 30 to PD 120, followed by a subsequent linear increase in branches ($R^2 \geq 0.98$). A segmental linear regression also afforded the best fit for

control animals evidenced by a plateau from PD 30 to PD 90, followed by a linear decrease in branches ($R^2 \geq 0.86$).

Most critically, however, a prominent shift in the distribution of dendritic branches at each branch order was also observed (Genotype x Age x Branch interaction, [$F(45,1647)=1.9$, $p_{GG} \leq 0.013$, $\eta_p^2=0.049$]); results which are illustrated at PD 30 and PD 180. At PD 30 (Figure 7.1), HIV-1 Tg animals exhibited an increased relative frequency of dendrites on lower-order branches relative to control animals. However, at PD 180 (Figure 7.1), a prominent shift was observed whereby HIV-1 Tg animals displayed an increased relative frequency of dendrites on higher-order branches relative to control animals. Taken together, results support a differential development of dendritic branching complexity which may indicate alterations in dendritic pruning.

Excitatory Synapses

The dendritic spine head typically contains a single type 1 asymmetric synapse, thereby the total number of dendritic spines may serve as a surrogate for the approximate number of excitatory synapses on a neuron. Investigations of the average total number of spines revealed a differential progression of spine development across time (Figure 7.2; Genotype x Age interaction, [$F(5, 183)=4.8$, $p \leq 0.001$]). HIV-1 Tg animals exhibited a linear increase in the total number of spines across age, well-described by a first-order polynomial ($R^2 \geq 0.71$). In contrast, control animals displayed the greatest number of dendritic spines at PD 30, followed by a subsequent plateau; a pattern which was best fit by a segmental linear regression ($R^2 \geq 0.68$).

Further evidence for alterations in synaptic connectivity is afforded by examining the distribution of dendritic spines on pyramidal neurons from the mPFC. HIV-1 Tg animals displayed a prominent shift in the distribution of dendritic spines dependent upon

biological sex and age (Genotype x Age x Sex x Radii interaction, [$F(5,4944)=131.0$, $p \leq 0.001$]); results which are illustrated, dependent upon biological sex, at PD 30 (Figure 7.2) and PD 180 (Figure 7.2). At both PD 30 and PD 180, HIV-1 Tg animals exhibited an increased relative frequency of dendritic spines on more distal branches relative to control animals. Notably, the magnitude of the effect is dependent upon the factor of biological sex. Although HIV-1 Tg animals exhibited an increased number of dendritic spines across age, the distribution of dendritic spines was shifted towards distal branches supporting alterations in synaptic connectivity.

Dendritic Spine Morphology

Morphological characteristics of dendritic spines fall along a continuum (for review, Yuste, 2010) and may reflect functionality and capacity for structural change. Dendritic spine volume, encapsulating both backbone length and head diameter, was the primary morphological parameter investigated in the present study.

To investigate changes in dendritic spine volume across time, median volume (μm^3) was calculated for each animal. HIV-1 Tg animals, independent of biological sex, exhibited a differential progression of median dendritic spine volume relative to control animals (Figure 7.3; Genotype x Age interaction, [$F(5, 183)=29.8$, $p \leq 0.001$, $\eta_p^2=0.449$]). A linear decrease in median dendritic spine volume is observed in HIV-1 Tg animals across time ($R^2 \geq 0.83$). In sharp contrast, control animals exhibited a linear increase in median dendritic spine volume across time ($R^2 \geq 0.89$).

Examination of the distribution of dendritic spine volume in HIV-1 Tg and control animals as a function of age (Figure 7.3) confirmed these observations (Genotype x Age x Bin interaction, [$F(5,3288)=25.9$, $p \leq 0.001$]). At PD 30, PD 60, and PD 90, HIV-1 Tg

animals displayed a prominent population shift towards increased dendritic spine volume relative to control animals. However, at PD 120, PD 150, and PD 180, a prominent population shift towards decreased dendritic spine volume was observed in HIV-1 Tg animals relative to control animals. Notably, a statistically significant genotype x age x sex x bin interaction [$F(5, 3288)=19.7$, $p\leq0.001$] was also observed, reflecting a difference in the magnitude, but not pattern, of the shift in male and female HIV-1 Tg animals.

Dendritic spine backbone length and head diameter were also assessed as complementary measures of dendritic spine morphology. First, investigation of median dendritic spine backbone length revealed a differential progression in HIV-1 Tg and control animals, independent of biological sex (Figure 7.4; Genotype x Age interaction, [$F(5, 183)=4.7$, $p\leq0.001$, $\eta_p^2=0.114$]). A segmental linear regression provided a well-described fit for median backbone length in HIV-1 Tg animals ($R^2\geq0.96$), characterized by a linear decreased through PD 120, followed by a plateau. Median backbone length in control animals, however, is best fit using a first-order polynomial ($R^2\geq0.64$), illustrating the linear increase in median dendritic spine backbone length across time. Second, a differential progression of median dendritic spine head diameter was observed, independent of biological sex, in HIV-1 Tg animals relative to control animals (Figure 7.4; Genotype x Age interaction, [$F(5,183)=4.0$, $p\leq0.002$, $\eta_p^2=0.100$). HIV-1 Tg animals exhibited a linear decrease in median head diameter across time ($R^2\geq0.60$), whereas control animals displayed a linear increase in median head diameter across time ($R^2\geq0.63$). Thus, a differential progression in dendritic spine morphology, characterized by changes in volume, backbone length, and head diameter, were observed in HIV-1 animals relative to controls.

DISCUSSION

Prominent alterations in regressive (i.e., pruning) processes, as well as synaptic function, were observed, independent of biological sex, in pyramidal neurons from layers II-III of the mPFC in the HIV-1 Tg rat. Specifically, HIV-1 Tg animals exhibited a differential development of morphological parameters of pyramidal neurons, including total dendrite length, dendritic arbor complexity and dendritic branching complexity, relative to control animals; results which support an alteration in neurite pruning. Failure to effectively prune synapses was evidenced by a linear increase in the number of dendritic spines, a proxy for the number of excitatory synapses (Berry & Nedivi, 2017), in HIV-1 Tg animals across development. Furthermore, synaptic dysfunction was evidenced by profound alterations in synaptic connectivity and synaptic efficacy. Specifically, HIV-1 Tg animals exhibited an increased relative frequency of dendritic spines on more distal branches, supporting an alteration in synaptic connectivity. The linear decrease in dendritic spine volume, backbone length, and head diameter during development, observed in HIV-1 Tg animals relative to controls, may be associated with decreased synaptic efficacy. Understanding how the presence of HIV-1 viral proteins alters key progressive and regressive processes and synaptic function across time may afford a key target for the development of innovative therapeutics.

HIV-1 Tg animals, independent of biological sex, exhibited developmental alterations in dendritic pruning in pyramidal neurons from layers II-III of the mPFC (Figure 7.5). Specifically, an increase in total dendrite length, dendritic arbor complexity, and dendritic branching complexity was observed in HIV-1 Tg animals from PD 120 to PD 180; a developmental trajectory that was significantly different from control animals. In

sharp contrast, a cross-sectional study investigating neuronal morphology in HIV-1 Tg animals at an advanced age (i.e., approximately 20 months) failed to reveal a statistically significant alteration in either total dendrite length or dendritic arbor complexity (McLaurin et al., 2019b). However, at an advanced age, HIV-1 Tg animals displayed alterations in dendritic branching complexity characterized by an increased relative frequency of dendrites on lower-order branches. Advanced age and/or repeated neurocognitive testing may underlie differences in the inferences drawn from these two studies.

Synaptic pruning, a key regressive event that is important for the development of mature neuronal circuits (Riccomagno & Kolodkin, 2015), was altered in HIV-1 Tg animals. A linear increase in the total number of dendritic spines across time was observed in HIV-1 Tg animals. Observations in control animals, however, were consistent with the selective-elimination hypothesis, which suggests profound synaptic pruning during puberty (i.e., approximately PD 42 in the rat; Sengupta, 2013) that is completed by early adolescence (i.e., approximately PD 63 in the rat; Sengupta, 2013). Microglia, which serve as a viral reservoir for HIV-1 in the brain (e.g., Cosenza et al., 2002; Ko et al., 2019), may underlie deficits in synaptic pruning observed in the HIV-1 Tg rat. Specifically, during normal development, microglia engulf both the pre- and postsynaptic components of synapses (Paolicelli et al., 2011). Cx3cr1 (Paolicelli et al., 2011) and the classical complement cascade (e.g., Stevens et al., 2007; Schafer et al., 2012) are two signaling mechanisms which may guide microglia-dependent synaptic pruning. Notably, both Cx3cr1 (e.g., Duan et al., 2014) and complement receptor 3 (e.g., Mishra et al., 2018) are altered by HIV-1 viral proteins. Therefore, the presence of HIV-1 viral proteins leads to

activated microglia, as well as alterations in Cx3cr1 and complement receptor 3, which may underlie the failure to effectively prune synapses.

Profound deficits in synaptic connectivity were evidenced by a prominent rightward shift in the distribution of dendritic spines along the apical dendrite in HIV-1 Tg animals relative to controls. An increased relative frequency of dendritic spine on more distal dendrites, which extend from layers II-III of the mPFC into layer I, were observed in HIV-1 Tg animals relative to control animals. The PFC, which receives afferent projections from multiple brain regions (e.g., thalamic nuclei, the limbic system, hypothalamus; Fuster, 2008) and neurotransmitter systems (e.g., DA, NE, serotonin; Fuster, 2008), integrates and coordinates an extensive number of neural processes (Miller & Cohen, 2001). Examination of the predominant neurotransmitter receptors in each layer of the mPFC revealed DAergic, noradrenergic, and serotonergic receptors in layer II-III of the mPFC (Santana & Artigas, 2017). In sharp contrast, little receptor expression was observed in layer I of the mPFC (Santana & Artigas, 2017). The preponderance of dendritic spines on distal dendrites, which extend into layer I of the mPFC, supports a decreased number of monoamine receptors, and therefore neurotransmitter innervation, in HIV-1 Tg animals; a result which is consistent with neurotransmitter system alterations in HIV-1 seropositive individuals (e.g., Wang et al., 2004; Kumar et al., 2009) and biological systems utilized to model HIV-1 (e.g., Denton et al., 2019).

Progressive synaptic dysfunction, evidenced by profound alterations in the morphological parameters of dendritic spines, was also observed in HIV-1 Tg animals. Specifically, HIV-1 Tg animals displayed a linear decrease in dendritic spine volume across time, whereas control animals exhibited a linear increase in dendritic spine volume

throughout development. The continuous decline in dendritic spine volume supports an age-dependent decrease in PSD (Freire, 1978; Arellano et al., 2007), which may result in decreased synaptic efficacy, in the HIV-1 Tg rat. The PSD, which is a protein rich region located at the tip of postsynaptic dendritic spines, is a primary characteristic of glutamatergic excitatory synapses (for review, Boeckers, 2006). Notably, the down-regulation of the PSD and profound alterations in glutamate receptors (e.g., Haughey et al., 2001; Aksenov et al., 2012; Atluri et al., 2013), resulting from HIV-1 viral proteins, support functional alterations in the PSD.

Furthermore, the linear decrease in backbone length, which plateaus at PD 120, and the linear decrease in head diameter, support a morphological shift towards parameters consistent with a 'stubby' spine (Peters & Kaiserman-Abramof, 1970). 'Stubby' spines, which are prevalent during early, but not late, development, reflect an immature spine phenotype relative to other classical (i.e., 'thin' or 'mushroom') spine types (Harris et al., 1992). Morphologically, 'stubby' spines are characterized by the absence of a dendritic spine neck, an approximately equal head to neck ratio, and a smaller PSD (Peters & Kaiserman-Abramof, 1970; Schmidt & Eilers, 2009); parameters which suggest poor neurotransmitter innervation. Specifically, excitatory synapses, which receive neurotransmitter signals (Lodish et al., 2000), are primarily located on the head (e.g., Gray, 1959), but also the neck (Yuste, 2010), of dendritic spines (Figure 7.5). Thus, the morphological parameters of dendritic spines support prominent synaptic dysfunction, which likely results in deficits in synaptic connectivity.

In conclusion, the present study reveals profound alterations in dendrite and synaptic pruning, as well as progressive synaptic dysfunction, in the HIV-1 Tg rat. Given

evidence for decreased synaptic connectivity, weakened synapses, immature spines, the increase in dendritic spines throughout development may reflect an, albeit unsuccessful, compensatory mechanism. Notably, the factor of biological sex had no statistically significant effect on the pattern of results observed. However, there were differences in the magnitude, which deserves further consideration given sex differences in neurocognitive function (e.g., Maki et al., 2018; McLaurin et al., 2019b). Understanding how the presence of HIV-1 viral proteins alters key progressive and regressive processes and synaptic function across time may afford a key target for the development of innovative therapeutics.

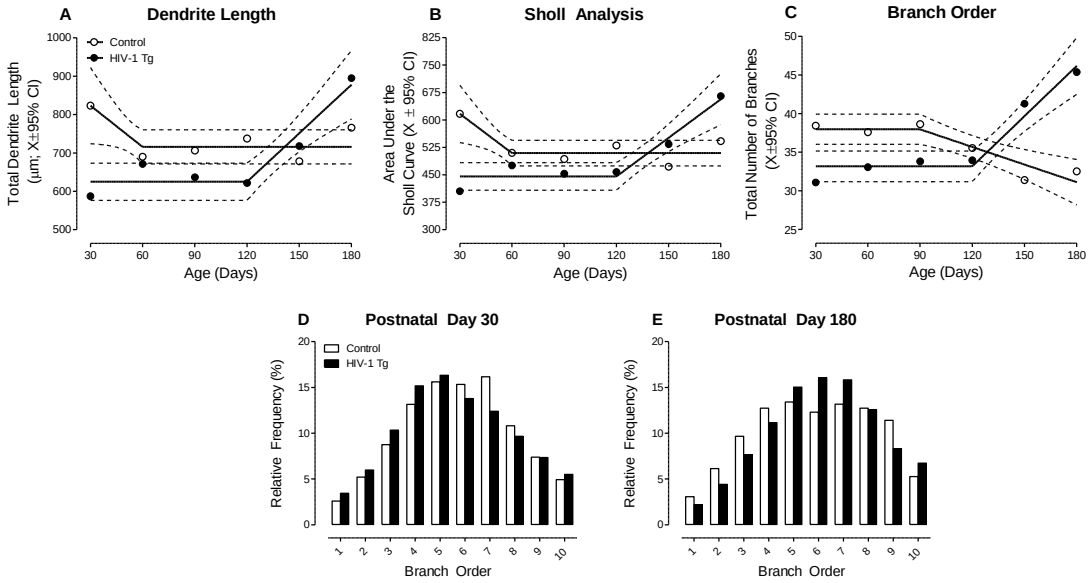

Figure 7.1 Progression of Neuronal Morphology. Morphological characteristics of pyramidal neurons from layers II-III of the mPFC were assessed using total dendrite length (**A**), Sholl analysis (**B**), and branch order (**C**). HIV-1 Tg animals exhibited a differential developmental trajectory of dendritic pruning evidenced by the increased dendrite length, area under the Sholl curve, and total number of branches between PD 120 and PD 180; a trajectory that was significantly different from control animals. Furthermore, a shift in the relative frequency of dendritic branches was observed as a function of age (i.e., PD 30 (**D**), PD 180 (**E**)). Specifically, at PD 30, HIV-1 Tg animals exhibited an increased relative frequency of dendritic branches at lower branch orders relative to controls. At PD 180, however, an increased relative frequency of dendritic branches was observed at higher order branches in HIV-1 Tg animals relative to controls.

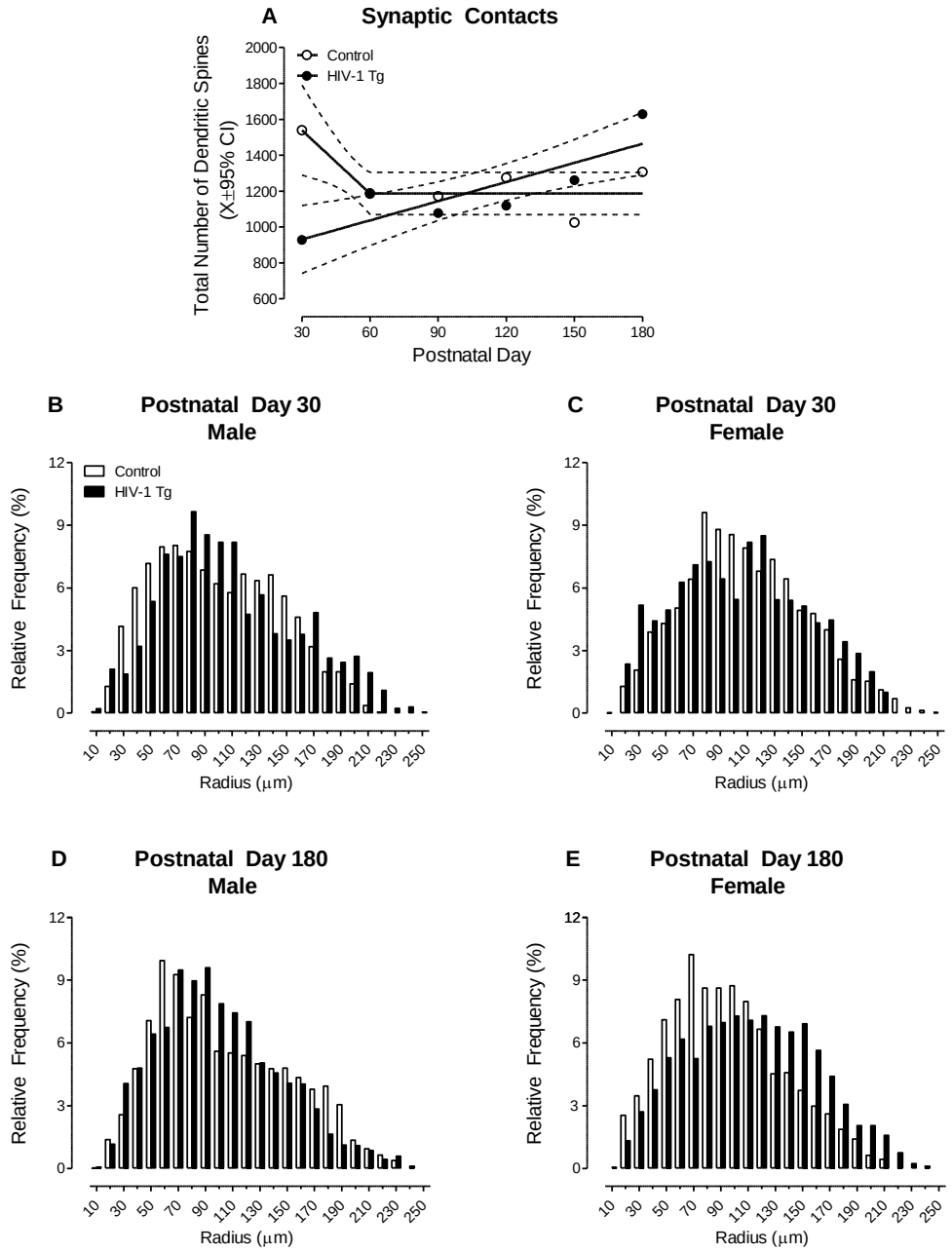

Figure 7.2 Excitatory Synapses. (**A**) A prominent alteration in synaptic pruning was observed in HIV-1 Tg animals, evidenced by the linear increase in total dendritic spines across time. Furthermore, at both PD 30 (**B**, **C**) and PD 180 (**D,E**), HIV-1 Tg animals exhibited a rightward shift in the distribution of dendritic spines, relative to control animals; the magnitude of which was dependent upon the factor of biological sex. HIV-1 Tg animals displayed an increased relative frequency of dendritic spines on more distal branches, supporting an alteration in synaptic connectivity, relative to control animals.

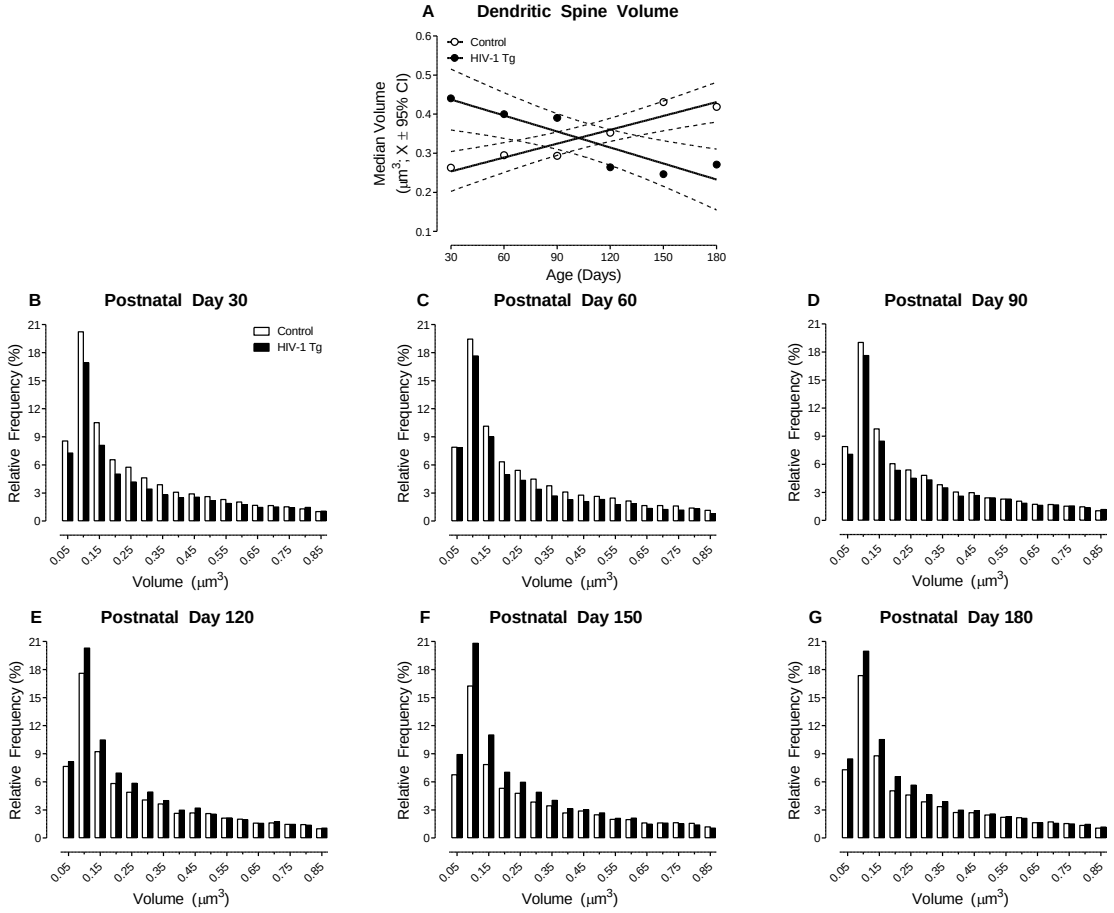

Figure 7.3 Dendritic Spine Volume. Dendritic spine volume, which encapsulates dendritic spine backbone length, head diameter, and neck diameter, was examined as a key morphological parameters of dendritic spines. (**A**) HIV-1 Tg animals exhibited a linear decrease in median dendritic spine volume, while control animals displayed a linear increase in median dendritic spine volume, across time; results which support profound alterations in synaptic function. (**B-G**) Examination of the distribution of dendritic spine volume in HIV-1 Tg and control animals as a function of age confirmed the observations inferred from median dendritic spine volume. Specifically, at PD 30, PD 60, and PD 90, HIV-1 Tg animals exhibited a distributional shift towards increased dendritic spine volume relative to control animals. However, at PD 120, PD 150, and PD 180, HIV-1 Tg animals displayed a distributional shift towards decreased dendritic spine volume relative to control animals.

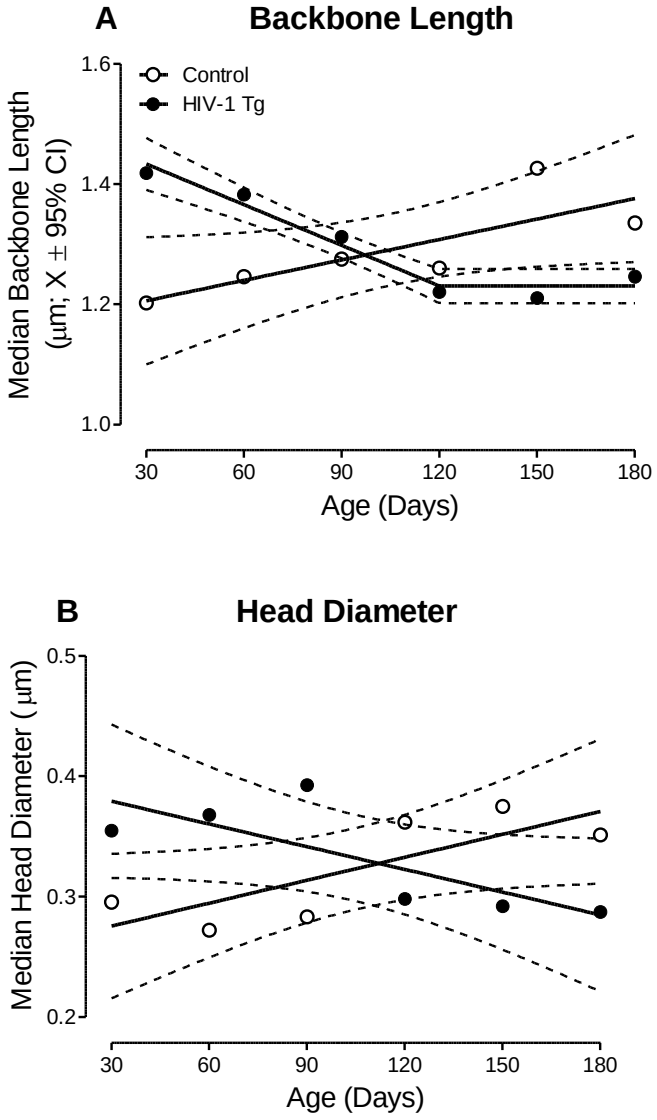

Figure 7.4 Morphology of Dendritic Spines. Median dendritic spine backbone length (**A**) and head diameter (**B**) were examined as additional morphological parameters. HIV-1 Tg animals exhibited a the linear decrease in backbone length, which plateaus at PD 120, and a linear decrease in head diameter across time; results which support a morphological shift towards parameters consistent with a 'stubby' spine. In sharp contrast, a linear increase in both backbone length and head diameter throughout development.

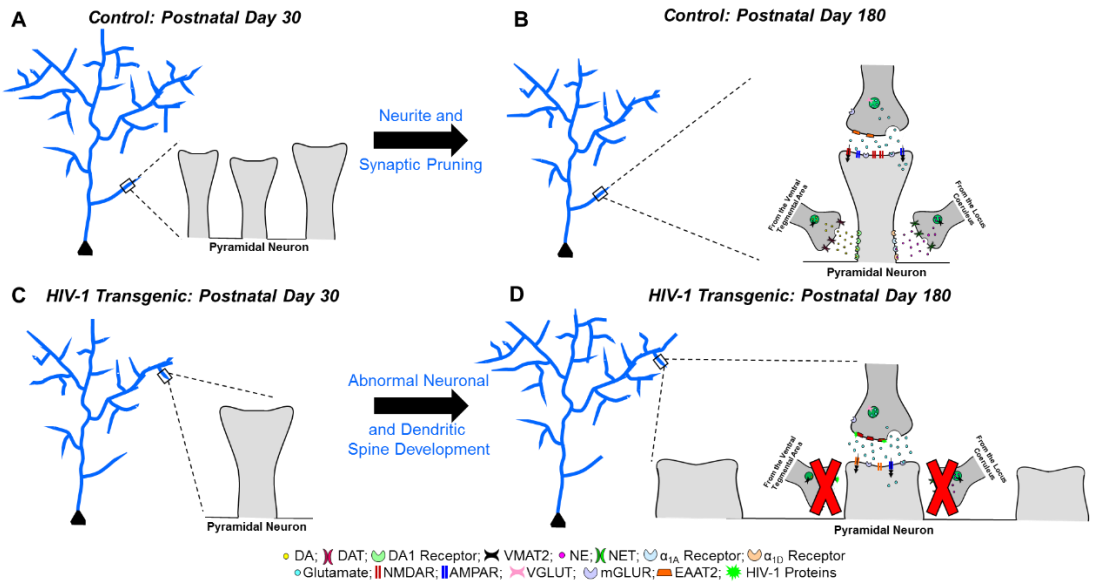

Figure 7.5 Age Related Change in Pyramidal Neurons. Pyramidal neurons from layers II-III of the mPFC are illustrated at PD 30 (**A**, **C**) and PD 180 (**B**, **D**) dependent upon genotype (Control (**A**,**B**), HIV-1 Tg (**C**, **D**)). Control animals exhibited an overproduction of dendritic branches and dendritic spines during early development (i.e., PD 30); an overproduction which was pruned during puberty consistent with normal development (Elston et al., 2009). At PD 180, control animals exhibited longer dendritic spines with increased volume and head diameter that were predominantly located on more proximal dendrites supporting the reception of DAergic afferents from the VTA and noradrenergic afferents from the LC. In sharp contrast, HIV-1 Tg animals exhibited a shorter total dendrite length and decreased total number of dendritic spines during early development (i.e., PD 30). HIV-1 Tg animals exhibited abnormal neuronal and dendritic spine development, whereby at PD 180, they displayed a greater total dendrite length and increased number of dendritic spines. Furthermore, HIV-1 Tg animals displayed shorter dendritic spines with decreased volume and head diameter, consistent with a 'stubby' phenotype, that were located on more distal dendrites; results which suggest poor reception of DAergic and/or noradrenergic afferents. Abbreviations: DA: Dopamine, DAT: Dopamine Transporter, DA1 Receptor: Dopamine Receptor D1, VMAT2: Vesicular Monoamine Transporter 2, NE: Norepinephrine, NET: Norepinephrine Transporter, α_{1A} Receptor: Alpha-1A Adrenergic Receptor, α_{1D} Receptor: Alpha-1D Adrenergic Receptor, NMDAR: NMDA Receptor, AMPAR: AMPA Receptor, VGLUT: Vesicular Glutamate Transporter, mGLUR: Metabotropic Glutamate Receptor, EAAT2: Excitatory Amino Acid Transporter 2. (Adapted from McLaurin et al., 2019b).

CHAPTER 8

GENERAL DISCUSSION

The HIV-1 Tg rat, resembling HIV-1 seropositive individual on lifelong cART, exhibits age-related progressive NCI in the absence of sensory or motor system deficits and comorbidities. Specifically, independent of biological sex, the HIV-1 Tg rat exhibits a differential progression of long-term episodic memory, temporal processing, stimulus-reinforcement learning, sustained attention, and flexibility and inhibition relative to controls. Prominent developmental alterations in regressive (i.e., pruning) processes, as well as synaptic function, were observed, independent of biological sex, in pyramidal neurons from layers II-III of the mPFC in the HIV-1 Tg rat, supporting a key neural mechanism underlying HAND. Critically testing the therapeutic efficacy of SE in the HIV-1 Tg rat revealed an innovative therapeutic approach for the prevention of NCI in HAND; a therapeutic that, at least partially, restored the developmental trajectory of neurocognitive function. Mechanistically, SE remodels neuronal circuitry at the synaptic level, evidenced by profound long-term modifications in neuronal morphology and dendritic spines in pyramidal neurons from layers II-III of the mPFC. Taken together, the present studies have defined HAND as a neurodegenerative disease characterized by progressive NCI and synaptic dysfunction; a disease trajectory that can be modified by therapeutics (i.e., SE) that mechanistically target synaptic dysfunction.

Neurocognitive assessments (e.g., PPI, locomotor activity, signal detection) conducted throughout the present studies evaluated the perception of time, which has been implicated as an elemental dimension of HAND (e.g., Chao et al., 2004; Moran et al., 2013a; McLaurin et al., 2019a), across a continuum of time interval manipulations (i.e., from milliseconds to days). Prominent deficits in timing, observed in the HIV-1 Tg rat, generalized across the factor of biological sex, age, neurocognitive assessment and time

interval manipulation. Treatment with SE prevented the development of alterations in the perception of time in preattentive processes (Moran et al., 2019), the temporal components of sustained attention, as well as the temporal components of reversal and flexibility. Therefore, the generalizability and sensitivity of temporal processing deficits supports a key target for the development of a diagnostic and/or prognostic biomarker for HAND.

Current diagnostic tools for milder forms of HAND lack both sensitivity and specificity (e.g., Haddow et al., 2013; Sakamoto et al., 2013; Zipursky et al., 2013), which has led to a quest for an innovative biomarker for HAND in the post-cART era. A series of studies have proposed PPI, an assessment of temporal processing, as a novel diagnostic and/or prognostic biomarker for HAND (for review, McLaurin et al., 2019c). The diagnostic utility of PPI was critically tested using DFA (e.g., McLaurin et al., 2016b; McLaurin et al., 2017c) and receiver operator characteristic curves (for review, McLaurin et al., 2019c). PPI accurately diagnoses (i.e., 86.7-97.1%) the presence of the HIV-1 transgene with high sensitivity (i.e., 89.3-100%) and high specificity (i.e., 79.5-94.1%).

Additional utilization of advanced statistical techniques, including regression and statistical mediation, have further tested the potential utility of PPI. Specifically, early alterations in PPI are predictive of later NCIs in a sex-dependent manner (i.e., Males: Sustained Attention; Females: Flexiblity and Inhibition); results which support its utility as a prognostic biomarker for HAND. Furthermore, statistical mediation analyses also revealed that preattentive processes, indexed using PPI, partially mediate alterations in higher-order cognitive processes supporting a causal neurobehavioral mechanism underlying HAND (McLaurin et al., 2019e). In addition to the strong statistical evidence supporting PPI, its brevity (i.e., approximately 15-25 minutes; Fournier & Hebert, 2013;

Minassian et al., 2013), ease of administration and test-retest reliability (e.g., Braff et al., 1978) make it an attractive biomarker for HAND in the post-cART era.

The factor of biological sex was an integral component of the experimental design for the studies presented herein. Women, who account for approximately 51% of HIV-1 seropositive individuals worldwide (UNAIDS, 2016) are inadequately represented in studies investigating HAND (Maki & Martin-Thormeyer, 2009). There remains, therefore, a critical need to directly compare neurocognitive function in males and females to address this knowledge gap (Maki et al., 2015). Investigation of sex differences in neurocognitive function have revealed greater NCI in HIV-1 seropositive females relative to HIV-1 seropositive males (e.g., Hestad et al., 2012; Royal et al., 2016; Maki et al., 2018); results which were translationally modeled in the HIV-1 Tg rat. Specifically, as demonstrated in the present study, female HIV-1 Tg animals exhibited greater NCI relative to male HIV-1 Tg animals in assessments of temporal processing, sustained attention, and flexibility and inhibition (Chapters 2, 3, 4). Critically, however, SE served as a efficacious therapeutic for NCI in both male and female HIV-1 Tg animals.

Notably, the neural mechanisms underlying HAND may also be influenced by the factor of biological sex. Cross-sectional studies in the HIV-1 Tg rat revealed sex differences in dendritic spine morphology with male HIV-1 Tg animals exhibiting a population shift towards shorter dendritic spines relative to their control counterparts (Chapter 4, 5). In sharp contrast, female HIV-1 Tg animals displayed a population shift towards longer dendritic spines (Chapter 4, 5). A longitudinal examination of pyramidal neurons from layers II-III of the mPFC, however, revealed no prominent effect of

biological sex on the pattern of neuronal and spine alterations (Chapter 7); an effect that may be due to age and/or the absence of neurocognitive testing.

In conclusion, the present study demonstrated progressive, age-related NCI and synaptic dysfunction in the HIV-1 Tg rat, in the absence of sensory or motor system functions and comorbidities. Treatment with SE, targeting alterations in synaptic dysfunction, selectively precludes the development of NCI, independent of biological sex. Most critically, SE restores, at least partially, the developmental trajectory of preattentive processes supporting an innovative therapeutic that modifies disease progression. Taken together, the present studies have defined HAND as a neurodegenerative disease characterized by age-related, progression neurocognitive impairments and synaptic dysfunction; a disease which can be modified by therapeutics (i.e., SE) that mechanistically target synaptic dysfunction.

REFERENCE LIST

Aarts, E., Verhage, M., Veenvliet, J.V., Dolan, C.V., & van der Sluis, A solution to dependency: Using multilevel analysis to accommodate nested data. *Nat Neurosci, 17,* 491-496.

Abbondanzo, S.J., & Chang, S.L. (2014). HIV-1 transgenic rats display alterations in immunophenotype and cellular responses associated with aging. *PloS one, 9,* e105256.

Abel, K., Waikar, M., Pedro, B., Hemsley, D., & Geyer, M. (1998). Repeated testing of prepulse inhibition and habituation of the startle reflex: A study in healthy human controls. *J. Psychopharmacol, 12,* 330-337.

Adler, L.E., Pachtman, E., Franks, R.D., Pecevich, M., Waldo, M.C., & Freedman, R. (1982). Neurophysiological evidence for a defect in neuronal mechanisms involved in sensory gating in schizophrenia. *Biol Psychiatry, 17,* 639-654.

Akaza, H. (2012). Prostate cancer chemoprevention by soy isoflavones: Role of intestinal bacteria as the "second human genome". *Cancer Sci, 103,* 969-975.

Aksenov, M.Y., Aksenova, M.V., Mactutus, C.F., & Booze, R.M. (2012). D1/NMDA receptors and concurrent methamphetamine+ HIV-1 Tat neurotoxicity. *J Neuroimmune Pharmacol, 7,* 599-608.

Aksenova, M.V., Aksenov, M.Y., Adams, S.M., Mactutus, C.F., & Booze, R.M. (2009). Neuronal survival and resistance to HIV-1 Tat toxicity in the primary culture of rat fetal neurons. *Exp Neurol, 215,* 253-263.

Alexander, G.E., DeLong, M.R., & Strick, P.L. (1986). Parallel organization of functionally segregated circuits linking basal ganglia and cortex. *Annu Rev Neurosci, 9,* 357-381.

Alexander, G.E., & Crutcher, M.D. (1990). Functional architecture of basal ganglia circuits: neural substrates of parallel processing. *Trends Neurosci, 13,* 266-271.

Alexander, G.E. (1994). Basal ganglia-thalamocortical circuits: Their role in control of movements. *J Clin Neurophysiol, 11,* 420-431.

Araya, R., Vogels, T.P., & Yuste, R. (2014). Activity-dependent dendritic spine neck changes are correlated with synaptic strength. *Proc Natl Acad Sci USA, 111,* E2895-E2904.

Arellano, J.I., Benavides-Piccione, R., Defelipe, J., & Yuste, R. (2007). Ultrastructure of dendritic spines: Correlation between synaptic and spine morphologies. *Front Neurosci, 1,* 131-143.

Atluri, V.S.R., Kanthikeel, S.P., Reddy, P.V.B., Yndart, A., & Nair, M.P.N. (2013). Human synaptic plasticity gene expression profile and dendritic spine density changes in HIV-infected human CNS cells: Role in HIV-1 associated neurocognitive disorders (HAND). *PLoS One, 8,* e61399.

Bagheri, M., Joghataei, M.T., Mohseni, S., & Roghani, M. (2011). Genistein ameliorates learning and memory deficits in amyloid β(1-40) rat model of Alzheimer's disease. *Neurobiol Learn Mem, 95,* 270-276.

Bangirana, P., Ruel, T.D., Boivin, M.J., Pillai, S.K., Giron, L.B., Sikorskii, A., et al. (2017). Absence of neurocognitive disadvantage associated with paediatric HIV subtype A infection in children on antiretroviral therapy. *J Int AIDS Soc, 20.*

Barchet, T.M., & Amiji, M.M. (2009). Challenges and opportunities in CNS delivery of therapeutics for neurodegenerative diseases. *Exper Opin Drug Deliv, 6,* 211-226.

Barker, G.R.I., Bird, F., Alexander, V., & Warburton, E.C. (2007). Recognition memory for objects, place, and temporal order: A disconnection analysis of the role of the medial prefrontal cortex and perirhinal cortex. *J Neurosci, 27,* 2948-2957.

Berry, K.P., & Nedivi, E. (2017). Spine dynamics: Are they all the same? *Neuron, 96,* 43-55.

Bertrand, S.J., Mactutus, C.F., Harrod, S.B., Morgan, A.J., & Booze, R.M. (2013). HIV-1 transgenic rat: Altered internal motivational state for natural rewards [Abstract]. *J Neurovirol, 19,* S12.

Bertrand, S.J., Mactutus, C.F., Aksenova, M.V., Espensen-Sturges, T.D., & Booze, R.M. (2014). Synaptodendritic recovery following HIV Tat exposure: Neurorestoration by phytoestrogens. *J Neurochem, 128,* 140-151.

Bertrand, S.J., Hu, C., Aksenova, M.V., Mactutus, C.F., & Booze, R.M. (2015). HIV-1 Tat and cocaine mediated synaptopathy in cortical and midbrain neurons is prevented by the isoflavone Equol. *Front Microbiol, 6,* 894.

Bertrand, S.J., Mactutus, C.F., Harrod, S.B., Moran, L.M., & Booze, R.M. (2018). HIV-1 proteins dysregulate motivational processes and dopamine circuitry. *Sci Rep, 8,* 7869.

Bethus, I., Tse, D., Morris, R.G. (2010). Dopamine and memory: modulation of the persistence of memory for novel hippocampal NMDA receptor-dependent paired associates. *J Neurosci, 30,* 1610-1618.

Boeckers, T.M. (2006). The postsynaptic density. *Cell Tissue Res, 326,* 409-422.

Bonelli, R.M., & Cummings, J.L. (2007). Frontal-subcortical circuitry and behavior. *Dialogues Clin Neurosci, 9,* 141-151.

Booze, R.M., & Mactutus, C.F. (1990). Developmental exposure to organic lead causes permanent hippocampal damage in Fischer-344 rats. *Experientia, 46,* 292-297.

Booze, R.M., Wood, M.L., Welch, M.A., Berry, S., & Mactutus, C.F. (1999). Estrous cyclicity and behavioral sensitization in female rats following repeated intravenous cocaine administration. *Pharmacol Biochem Behav, 64,* 605-610.

Bourgeois, J.P., Goldman-Rakic, P.S., & Rakic, P. (1994). Synaptogenesis in the prefrontal cortex of rhesus monkeys. *Cereb Cortex, 4,* 78-96.

Boska, M.D., Dash, P.K., Knibbe, J., Epstein, A.A., Akhter, S.P., Fields, N., et al. (2014). Associations between brain microstructures, metabolites, and cognitive deficits during chronic HIV-1 infection of humanized mice. *Mol Neurodegener, 9,* 58.

Braff, D., Stone, C., Callaway, E., Geyer, M., Click, I., & Bali, L. (1978). Prestimulus effects on human startle reflex in normal and schizophrenics. *Psychophysiology, 15,* 339-343.

Button, K.S., Ioannidis, J.P., Mokrysz, C., Nosek, B.A., Flint, J., Robinson, E.S., et al. (2013). Power failure: Why small sample size undermines the reliability of neuroscience. *Nat Rev Neurosci, 14,* 365-376.

Carlsson, S.G. (1972). Effects of apomorphine on exploration. *Physiol Behav, 9,* 127–129.

Carey, A.N., Sypek, E.I., Singh, H.D., Kaufman, M.J., & McLaughlin, J.P. (2012). Expression of HIV-Tat protein is associated with learning and memory deficits in the mouse. *Behav Brain Res, 229,* 48-56.

Casanova, M., You, L., Gaido, K.W., Archibeque-Engle, S., Janszen, D.B., & Heck, H.A. (1999). Developmental effects of dietary phytoestorgens in sprague-dawley rats and interactions of genistein and daidzein with rat estrogen receptors α and β in vitro. *Toxicol Sci, 51,* 236-244.

Casas, R., Muthusamy, S., Wakim, P.G., Sinharay, S., Lentz, M.R., Reid, W.C., et al. (2017). MR brain volumetric measurements are predictive of neurobehavioral impairment in the HIV-1 transgenic rat. *Neuroimage Clin, 17,* 659-666.

Castello, E., Baroni, N., & Pallestrini E. (1998). Neurotological and auditory brain stem response findings in human immunodeficiency virus-positive patients without neurologic manifestations. *Ann Otol Rhinol Laryngol, 107,* 1054–1060.

Centers for Disease Control and Prevention. (2013). *Diagnosis of HIV infection in the United States and Dependent Areas* (25). Available at: http://www.cdc.gov/hiv/pdf/g-l/hiv_surveillance_ report_vol_25.pdf.

Chan, P., & Brew, B.J. (2014). HIV associated neurocognitive disorders in the moder antiviral treatment era: Prevalence, characteristics, biomarkers, and effects of treatment. *Curr HIV/AIDS Rep, 11,* 317-324.

Chang, S.L., & Vigorito, M. (2006). Role of HIV-1 infection in addictive behavior: A study of the HIV-1 transgenic rat model. *Am J Infect Diseases, 2,* 98-106.

Changeau, J.P., & Danchin, A. (1976). Selective stabilization of developing synapses as a mechanism for the specification of neuronal networks. *Nature, 264,* 705-712.

Chao, L.L., Lindgren, J.A., Flenniken, D.L., & Weiner, M.W. (2004). ERP evidence of impaired central nervous system function in virally suppressed HIV patients on antiretroviral therapy. *Clin Neurophysiol, 115,* 1583-1591.

Chao, O.Y., Huston, J.P., Li, J.S., Wang, A.L., & de Souza Silva, M.A. (2016). The medial prefrontal cortex—lateral entorhinal cortex circuit is essential for episodic-like memory and associative object-recognition. *Hippocampus, 26,* 633-645.

Ciesla, J.A., & Roberts, J.E. (2001). Meta-analysis of the relationship between HIV infection and risk for depressive disorders. *Am J Psychiatry, 158,* 725-730.

Cohen, J., Cohen, P., West, S.G., & Aiken, L.S. (2003). *Applied multiple regression/correlation analysis for the behavioral sciences* (3rd ed.). Mahwah, NJ: Erlbaum.

Cohen, R.A., Seider, T.R., & Navia, B. (2015). HIV effects on age-associated neurocognitive dysfunction: Premature cognitive aging or neurodegenerative disease? *Alzheimers Res Ther, 7,* 37.

Cole, M.A., Castellon, S.A., Perkins, A.C., Ureno, O.S., Robinet, M.B., Reinhard, M.J., et al. (2007). Relationship between psychiatric status and frontal-subcortical systems in HIV-infected individuals. *J Int Neuropsychol Soc, 13,* 549-554.

Coleman, P.D. (2004). How old is old? Editorial. *Neurobiol Aging, 25,* 1 (Original work published 1989).

Collins, F.S., & Tabak, L.A. (2014). Policy: NIH plans to enhance reproducibility. *Nature, 505,* 612-613.

Cosenza, M. A., Zhao, M.-L., Si, Q., & Lee, S. C. (2002). Human brain parenchymal microglia express CD14 and CD45 and are productively infected by HIV-1 in HIV-1 encephalitis. *Brain Pathol, 12,* 442–455.

Crofton, K.M., & Sheets, L.P. (1989). Evaluation of sensory system function using reflex modification of the startle response. *J Am Coll Toxicol, 8,* 199-211.

Crowell, C.S., Malee, K.M., Yogev, R., & Muller, W.J. (2014). Neurologic disease in HIV-infected children and the impact of combination antiretroviral therapy. *Rev Med Virol, 24,* 316-331.

Crowell, C.S., Huo, Y., Tassiopoulos, K., Malee, K.M., Yogev, R., Hazra, R., et al. (2015). Early viral suppression improves neurocognitive outcomes in HIV-infected children. *AIDS, 29,* 295-304.

Cysique, L.A., Maruff, P., & Brew, B.J. (2004). Prevalence and pattern of neuropsychological impairment in human immunodeficiency virus infected/acquired immunodeficiency syndrome (HIV/AIDS) patients across pre and post-highly active antiretroviral therapy eras: a combined study of two cohorts. *J Neurovirol, 10,* 350-357.

Dalley, J.W., Cardinal, R.N., & Robbins, T.W. (2004). Prefrontal executive and cognitive functions in rodents: Neural and neurochemical substrates. *Neurosci Biobehav Rev, 28,* 771-784.

Dean, K.F., Sheets, L.P., Crofton, K.M., & Reiter, L.W. (1990). The effect of age and experience on inhibition of the acoustic startle response by gaps in background noise. *Psychobiology, 18,* 89-95.

Dehmel, S., Eisinger, D., & Shore, S. E. (2012). Gap prepulse inhibition and auditory brainstem-evoked potentials as objective measures for tinnitus in guinea pigs. *Front Systems Neurosci, 6,* 1-15.

Denenberg, V.H. (1984). Some statistical and experimental considerations in the use of the analysis-of-variance procedure. *Am J Physiol-Reg, I 246,* R403-R408.

Denton, A.R., Samaranayake, S.A., Kirchner, K.N., Roscoe, R.F., Berger, S.N., Harrod, S.B., et al. (2019). Selective monoaminergic and histaminergic circuit dysregulation following long-term HIV-1 protein exposure. *J Neurovirol, 25,* 540-550.

Desplats, P., Dumaop, W., Smith, D., Adame, A., Everall, I., Letendre, S., et al. (2013). Molecular and pathologic insights from latent HIV-1 infection in the human brain. *Neurology, 80,* 1415-1423.

Di Rocco, A., Bottiglieri, T., Dorfman, D., Werner, P., Morrison, C., & Simpson, D. (2000). Decreased homovanilic acid in cerebrospinal fluid correlates with impaired neuropsychologic function in HIV-1-infected patients. *Clin Neuropharmacol, 23,* 190-194.

Drzewiecki, C.M., Willing, J., & Juraska, J.M. (2016). Synaptic number changes in the medial prefrontal cortex across adolescence in male and female rats: A role for pubertal onset. *Synapse, 70,* 361-368.

Duan, M., Yao, H., Cai, Y., Liao, K., Seth, P., & Buch, S. (2014). HIV-1 Tat disrupts CX3CL1-CX3CR1 axis in microglia via the NF-KBYY1 pathway. *Curr HIV Res, 12,* 189-200.

Duffy, R., Wiseman, H., & File, S.E. (2003). Improved cognitive function in postmenopausal women after 12 weeks of consumption of a soya extract containing isoflavones. *Phamacol Biochem Behav, 75,* 721-729.

Eacott, M.J., Easton, A., & Zinkivskay, A. (2005). Recollection in an episodic-like memory task in the rat. *Learn Mem, 12,* 221–223.

Ellenbroek, B.A., Budde, S., & Cools, A.R. (1996). Prepulse inhibition and latent inhibition: the role of dopamine in the medial prefrontal cortex. *Neuroscience, 75,* 535-542.

Ellis, R., Langford, D., & Masliah, E. (2007). HIV and antiretroviral therapy in the brain: neuronal injury and repair. *Nat Rev Neurosci, 8,* 33-44.

Elston, G.N., Oga, T., & Fujita, I. (2009). Spinogenesis and pruning scales across functional hierarchies. *J Neurosci, 29,* 3271-3275.

European Collaborative Study. (2002). Level and patter of HIV-1 RNA viral load over age: Differences between girls and boys? *AIDS, 16,* 97-104.

Fazeli, P.L., Crowe, M., Ross, L.A., Wadley, V., Ball, K., & Vance, D.E. (2014). Cognitive functioning in adults aging with HIV: A cross-sectional analysis of cognitive subtypes and influential factors. *J Clin Res HIV AIDS Prev, 1,* 155-169.

Fendt, M., Koch, M., & Schnitzler, H.U. (1994). Sensorimotor gating deficit after lesions of the superior colliculus. *NeuroReport, 5,* 1725-1738.

Fendt, M., Li, L., & Yeomans, J.S. (2001). Brain stem circuits mediating prepulse inhibition of the startle reflex. *Psychopharmacology, 156,* 216-224.

Fennema-Notestine, C., Jernigan, T.L., Wong, J., Grant, I., & CHARTER Group. (2010). HIV-associated neurocognitive disorders persist in the era of potent antiretroviral therapy CHARTER study. *Neurology, 75,* 2087-2096.

Ferré, S., Fuxe, K., von Euler, G., Johansson, B., & Fredholm, B.B. (1992). Adenosine-dopamine interactions in the brain. *Neuroscience, 51,* 501-512.

Festa, L., Gutoskey, C.J., Graziano, A., Waterhouse, B.D., & Meucci, O. (2015). Induction of Interleukin-1β by human immunodeficiency virus-1 viral proteins leads to increased levels of neuronal ferritin heavy chain, synaptic injury, and deficits in flexible attention. *J Neurosci, 35,* 10550-10561.

Festa, L., Tian, Y., Platt, B., Floresco, S., & Meucci, O. (2017). In vivo manipulation of the CXCL12/CXCR4 signaling axis increases dendritic spine density and enhances cognitive flexibility in wild-type and HIV-Tg rats via the Rac1/PAK pathway. *J Neuroimmune Pharmacol, 12,* S25.

File, S.E., Jarrett, N., Fluck, E., Duffy, R., Casey, K., & Wiseman, H. (2001). Eating soya improves human memory. *Psychopharmacology (Berl), 157,* 430-436.

File, S.E., Hartley, D.E., Elsabagh, S., Duffy, R., & Wiseman, H. (2005). Cognitive improvement after 6 weeks of soy supplements in postmenopausal women is limited to frontal lobe function. *Menopause, 12,* 193-201.

Fitch, R.H., Threlkeld, S.W., McClure, M.M., & Peiffer, A.M. (2008). Use of a modified prepulse inhibition paradigm to assess complex auditory discrimination in rodents. *Brain Res Bull, 76,* 1-7.

Fitting, S., Booze, R.M., & Mactutus, C.F. (2006a). Neonatal hippocampal Tat injections: Developmental effects on prepulse inhibition (PPI) of the auditory startle response. *Int J Dev Neurosci, 24,* 275-283.

Fitting, S., Booze, R.M., & Mactutus, C.F. (2006b). Neonatal intrahippocampal glycoprotein 120 injection: The role of dopaminergic alteration in prepulse inhibition in adult rats. *J Pharmacol Exp Ther, 318,*1352-1358.

Fitting, S., Booze, R.M., & Mactutus, C.F. (2008a). Neonatal intrahippocampal injection of the HIV-1 proteins gp120 and Tat: Differential effects on behavior and the relationship to stereological hippocampal measures. *Brain Res, 1232,* 139-154.

Fitting, S., Booze, R.M., Hasselrot, U., & Mactutus, C.F. (2008b). Differential long-term neurotoxicity of HIV-1 proteins in the rat hippocampal formation: A design-based stereological study. *Hippocampus, 18,* 135-147.

Fitting, S., Booze, R.M., Hasselrot, U., & Mactutus, C.F. (2010). Dose-dependent long-term effects of Tat in the rat hippocampal formation: A design-based stereological study. *Hippocampus, 20,* 469-480.

Fitting, S., Ignatowska-Jankowska, B.M., Bull, C., Skoff, R.P., Lichtman, A.H., Wise, L.E., et al. (2013). Synaptic dysfunction in the hippocampus accompanies learning and memory deficits in human immunodeficiency virus type-1 Tat transgenic mice. *Biol Psychiatry, 73,* 443-453.

Fitting, S., Booze, R.M., & Mactutus, C.F. (2015). HIV-1 proteins, Tat and gp120, target the developing dopamine system. *Curr HIV Res, 13,* 21-42.

Foca, M., Moye, J., Chu, C., Matthews, Y., Rich, K., Handelsman, E., et al. (2006). Gender differences in lymphocyte populations, plasma HIV RNA levels, and disease progression in a cohort of children born to women infected with HIV. *Pediatrics, 118,* 146-155.

Fournier, P., & Hebert, S. (2013). Gap detection deficits in humans with tinnitus as assessed with the acoustic startle paradigm: Does tinnitus fill in the gap? *Hear Res, 295,* 16-23.

Franklin, S., Lim, H.J., Rennie, K. M., Eastwood, D., Cuene, B., & Havens, P.L. (2005). Longitudinal intellectual assessment of children with HIV infection. *J Clin Psychol Med Settings, 12,* 367-376.

Freire, M. (1978). Effects of dark rearing on dendritic spines in layer IV of the mouse visual cortex. A quantitative electron microscopical study. *J Anat, 126,* 193-201.

Freund, T.F., Powell, J.F., & Smith, A.D. (1984). Tyrosine hydroxylase-immunoreactive boutons in synaptic contact with identified striatonigral neurons, with particular reference to dendritic spines. *Neuroscience, 13,* 1189-1215.

Friedman, J.T., Peiffer, A.M., Clark, M.G., Benasich A., & Fitch R.H. (2004). Age and experience-related improvements in gap detection in the rat. *Dev Brain Res, 152,* 83-91.

Fuster, J.M. (2008). The Prefrontal Cortex (4th Ed). Academic Press.

Gao, H.M., Kotzbauer, P.T., Uryu, K., Leight, S., Trojanowski, J.Q., & Lee, V.M. (2008). Neuroinflammation and oxidation/nitration of α-synuclein linked to dopaminergic neurodegeration. *J Neurosci, 28,* 7687-7698.

Garvey, L.J., Yerrakalva, D., & Winston, A. (2009). Correlations between computerized battery testing and a memory questionnaire for identification of neurocognitive impairment in HIV type 1-infected subjects on stable antiretroviral therapy. *AIDS Res Hum Retroviruses, 25,* 765-769.

GBD 2016 Parkinson's Disease Collaborators. (2018). Global, regional and national burden of Parkinson's disease, 1990-2016: A systematic analysis for the global burden of disease study 2016. *Lancet Neurol, 17,* 939-953.

GBD 2016 Dementia Collaborators. (2019). Global, regional, and national burden of Alzheimer's disease and other dementias, 1990-2016: A systematic analysis for the global burden of disease study 2016. *Lancet Neurol, 18,* 88-106.

Gelman, B.B., & Nguyen, T.P. (2010). Synaptic proteins linked to HIV-1 infection and immunoproteasome induction: proteomic analysis of human synaptosomes. *J Neuroimmune Pharmacol, 5,* 92-102.

Gelman, B.B., Lisinicchia, J.G., Chen, T., Johnson, K.M., Jennings, K., Freeman, D.H., et al. (2012). Prefrontal dopaminergic and enkephalinergic synaptic accommodation in HIV-associated neurocognitive disorders and encephalitis. *J Neuroimmune Pharmacol, 7,* 686-700.

Geyer, M.A., Krebs-Thomson, K., Braff, D.L., & Swerdlow, N.R. (2001). Pharmacological studies of prepulse inhibition models of sensorimotor gating deficits in schizophrenia: a decade in review. *Psychopharmacology, 156,* 117-154.

Gimenez, F., Fernandez, C., & Mabondzo, A. (2004). Transport of HIV protease inhibitors through the blood-brain barrier and interactions with the efflux proteins, P-glycoprotein and multidrug resistance proteins. *J Acquir Immune Defic Syndr, 36,* 649-658.

Giros, B., Jaber, M., Jones, S.R., Wightman, R.M., & Caron, M.G. (1996). Hyperlocomotion and indifference to cocaine and amphetamine in mice lacking the dopamine transporter. *Nature, 379,* 606-612.

Glazier, M.G., & Bowman, M.A. (2001). A review of the evidence for the use of phytoestrogens as a replacement for traditional estrogen replacement therapy. *Arch Intern Med, 161,* 1161-1172.

Gonzalez, M., Cabrera-Socorro, A., Perez Garcia, C.G., Fraser, J.D., Lopez, F.J., Alonso, R., et al. (2007). Distribution patterns of estrogen receptor alpha and beta in the human cortex and hippocampus during development and adulthood. *J Comp Neurol, 503,* 790-802.

Gott, C., Gates, T., Dermody, N., Brew, B.J., & Cysique, L.A. (2017). Cognitive change trajectories in virally suppressed HIV-infected individuals indicate high prevalence of disease activity. *PLoS One, 12,* e171887.

Grant, I., Franklin, D.R., Deutsch, R., Woods, S.P., Vaida, F., Ellis, R.J., et al. (2014). Asymptomatic HIV-associated neurocognitive impairment increases risk for symptomatic decline. *Neurology, 82,* 2055-2062.

Gray, E.G. (1959). Electron microscopy of synaptic contacts on dendritic spines of the cerebral cortex. *Nature, 183,* 1592-1594.

Greenhouse, S.W., & Geisser, S. (1959). On methods in the analysis of profile data. *Psychometrika, 24,* 95-112.

Gupta, S., Knight, A.G., Gupta, S., Knapp, P.E., Hauser, K.F., Keller, J.N., et al. (2010). HIV-Tat elicits microglial glutamate release: Role of NAPDH oxidase and the cysteine-glutamate antiporter. *Neurosci Lett, 485,* 233-236.

Haas, K., Li, J., & Cline, H.T. (2006). AMPA receptors regulate experience-dependent dendritic arbor growth in vivo. *Proc Natl Acad Sci USA, 103,* 12127-12131.

Haddow, L.J., Floyd, S., Copas, A., & Gilson, R.J. (2013). A systematic review of the screening accuracy of the HIV Dementia Scale and International HIV Dementia Scale. *PLoS One, 8,* e61826.

Hanh, Y.K., Podhaizer, E.M., Farris, S.P., Miles, M.F., Hauser, K.F., & Knapp, P.E. (2015). Effects of chronic HIV-1 Tat exposure in the CNS: heightened vulnerability of males versus females to changes in cell numbers, synaptic integrity, and behavior. *Brain Struct Funct, 220,* 605-623.

Hao, J., Rapp, P.R., Leffler, A.E., Leffler, S.R., Janssen, W.G., Lou, W., et al. (2006). Estrogen alters spine number and morphology in prefrontal cortex of aged female rhesus monkeys. *J Neurosci, 26,* 2571-2578.

Harris, J.D. (1943). Habituatory response decrement in the intact organism. *Psychol Bull, 40,* 385-422.

Harris, K.M., & Stevens, J.K. (1988). Dendritic spines of rat cerebellar purkinje cells: Serial electron microscopy with reference to their biophysical characteristics. *J Neurosci, 8,* 4455-4469.

Harris, K.M., & Stevens, J.K. (1989). Dendritic spines of CA 1 pyramidal cells in the rat hippocampus: Serial electron microscopy with reference to their biophysical characteristics. *J Neurosci, 9,* 2982-2997.

Harris, K.M., Jensen, F.E., & Tsao, B. (1992). Three-dimensional structure of dendritic spines and synapses in rat hippocampus (CA1) at postnatal day 15 and adult ages: Implications for the maturation of synaptic physiology and long-term potentiation. *J Neurosci, 12,* 2685-2705.

Haseman, J.K., & Hogan, M.D. (1975). Selection of the experimental unit in teratology studies. *Teratology, 12,* 165-171.

Hauber, W., & Koch, M. (1997). Adenosine A_{2a} receptors in the nucleus accumbens modulate prepulse inhibition of the startle response. *NeuroReport, 8,* 1515-1518.

Haughey, N.J., Nath, A., Mattson, M.P., Slevin, J.T., & Geiger, J.D. (2001). HIV-1 Tat through phosphorylation of NMDA receptors potentiates glutamate excitotoxicity. *J Neurochem, 78,* 457-467.

Hayashi, Y., & Majewska, A.K. (2005). Dendritic spine geometry: Functional implication and regulation. *Neuron, 46,* 529-532.

Heaton, R.K., Clifford, D.B., Franklin, D.R., Woods, S.P., Ake, C., Vaida, F., et al. (2010). HIV-associated neurocognitive disorders persist in the era of potent antiretroviral therapy CHARTER study. *Neurology, 75,* 2087-2096.

Heaton, R.K., Franklin, D.R., Ellis, R.J., McCutchan, J.A., Letendre, S.L., Leblanc, S., et al. (2011). HIV-associated neurocognitive disorders before and during the era of combination antiretroviral therapy: differences in rates, nature, and predictors. *J Neurovirol, 17,* 3-16.

Heaton, R.K., Franklin, D.R., Deutsch, R., Letendre, S., Ellis, R.J., Casaletto, K., et al. (2015). Neurocognitive change in the era of HIV combination antiretroviral therapy: The longitudinal CHARTER study. *Clinical Infectious Disease, 60,* 473-480.

Henderson, V.W., St. John, J.A., Hodis, H.N., Kono, N., McCleary, C.A.Franke, A.A., et al. (2012). Long-term soy isoflavone supplementation and cognition in women: A randomized, controlled trial. *Neurology, 78,* 1841-1848.

Henry, B.L., Geyer, M.A., Buell, M.R., Perry, W., Young, J.W., Minassian, A., et al. (2014). Prepulse inhibition in HIV-1 gp120 transgenic mice after withdrawal from chronic methamphetamine. *Behav Pharmacol, 25,* 12-22.

Hering, H., & Sheng, M. (2001). Dendritic spines: Structure, dynamics and regulation. *Nat Rev Neurosci, 2,* 880-888.

Hersch, S.M., & White, E.L. (1981). Quantification of synapses formed with apical dendrites of golgi-impregnated pyramidal cells: Variability in thalamocortical inputs, but consistency in the ratios of asymmetrical to symmetrical synapses. *Neuroscience, 6,* 1043-1051.

Hestad, K.A., Menon, J.A., Silalukey-Ngoma, M., Franklin, D.R., Imasiku, M.L., Kalima, K., et al. (2012). Sex differences in neuropsychological performance as an effect of human immunodeficiency virus infection: A pilot study in Zambia, Africa. *J Nerv Ment Dis, 200,* 336-342.

Hoffman, H.S., & Searle, J.L. (1965). Acoustic variables in modification of startle reaction in rat. *J Comp Physiol Psychol, 60,* 53-58.

Hoffman, H.S., & Ison, J.R. (1980). Reflex modification in the domain of startle: I. Some empirical findings and their implications for how the nervous system processes sensory input. *Psychol Rev, 87,* 175-189.

Holson, R.R., & Pearce, B. (1992). Principles and pitfalls in the analysis of prenatal treatment effects in multiparous species. *Neurotoxicol Teratol, 14,* 221-228.

Huitron-Resendiz, S., De Rozieres, S., Sanchez-Alavez, M., Buhler, B., Lin, Y.C., Lerner, D.L., et al. (2004). Resolution and prevention of feline immunodeficiency virus-induced neurological deficits by treatment with the protease inhibitor TL-3. *J Virol, 78,* 4525-4532.

Huttenlocher, P.R. (1979). Synaptic density in human frontal cortex-Developmental changes and effects of aging. *Brain Res, 163,* 195-205.

Huttenlocher, P.R., & Dabholkar, A.S. (1997). Regional differences in synaptogenesis in human cerebral cortex. *J Comp Neurol, 387,* 167-178.

Ison, J.R., & Hammond, G.R. (1971). Modification of startle reflex in rat by changes in auditory and visual environments. *J Comp Physiol Psychol, 75,* 435-452.

Ison, J.R. (1984). Reflex modification as an objective test for sensory processing following toxicant exposure. *Neurobehav Toxicol Teratol, 6,* 437-445.

Ison, J. R., Agrawal, P., Pak, J., & Vaughn, W. J. (1998). Changes in temporal acuity with age and with hearing impairment in the mouse: a study of the acoustic startle reflex and its inhibition by brief decrements in noise level. *J Acoust Soc Am, 104,* 1696-1704.

Israel, S.M., Hassanzadeh-Behbahani, S., Turkeltaub, P.E., Moore, D.J., Ellis, R.J., & Jiang, X. (2019). Different roles of frontal versus striatal atrophy in HIV-associated neurocognitive disorders. *Hum Brain Mapp, 40,* 3010-3026.

Jacome, L.F., Gautreaux, C., Inagaki, T., Mohan, G., Alves, S., Lubbers, L.S., et al. (2010). Estradiol and ERβ agonists enhance recognition memory, and DPN, an ERβ agonist, alters brain monoamines. *Neurobiol Learn Mem, 94,* 488-498.

Japha, K., & Koch, M. (1999). Picrotoxin in the medial prefrontal cortex impairs sensorimotor gating in rats: Reversal by haloperidol. *Psychopharmacology (Berl), 144,* 347-354.

Javadi-Paydar, M., Roscoe, R.F., Denton, A.R., Mactutus, C.F., & Booze, R.M. (2017). HIV-1 and cocaine disrupt dopamine reuptake and medium spiny neurons in female rat striatum. *PLoS One, 12,* e0188404.

Jensen, E.V. (1962). On the mechanism of estrogen action. *Perspect Biol Med, 6,* 47-54.

June, H.L., Yang, A.R.S.T., Bryant, J.L., Jones, O., & Royal, W. (2009). Vitamin A deficiency and behavioral and motor deficits in the HIV-1 transgenic rat. *J Neurovirol, 15,* 380-389.

Kam, J.W.Y., Solbakk, A.K., Endestad, T., Meling, T.R., & Knight, R.T. (2018). Lateral prefrontal cortex lesion impairs regulation of internally and externally directed attention. *Neuroimage, 175,* 91-99.

Kamat, R., Woods, S.P., Marcotte, T.D., Ellis, R.J., Grant, I., & HIV Neurobehavioral Research Program (HNRP) Group. (2012). Implications of apathy for everyday functioning outcomes in persons living with HIV infection. *Arch Clin Neuropsychol, 27,* 520-531.

Kasai, H., Matsuzaki, M., Noguchi, J., Yasumatsu, N., & Nakahara, H. (2003). Structure-stability-function relationships of dendritic spines. *Trend Neurosci, 26,* 360-368.

Katsuno, M., Sahashi, K., Iguchi, Y., & Hashizume, A. (2018). Preclinical progression of neurodegenerative diseases. *Nagoya J Med Sci, 80,* 289-298.

Kendall, S.L., Anderson, C.F., Nath, A., Turchan-Cholewo, J., Land, C.L., Mactutus, C.F., et al. (2005). Gonadal steroids differentially modulate neurotoxicity of HIV and cocaine: Testosterone and ICI 182,780 sensitive mechanism. *BMC Neurosci, 6,* 40.

Kellogg, C., Ison, J.R., & Miller, R.K. (1983). Prenatal diazepam exposure: Effects on auditory temporal resolution in rats. *Psychopharmacology, 79,* 332-337.

Kesner, R.P. (2000). Subregional analysis of mnemonic functions of the prefrontal cortex in the rat. *Psychobiology, 28,* 219-228.

Khan, M.M., Dhandapani, K.M., Zhang, Q.G., & Brann, D.W. (2013). Estrogen regulation of spine density and excitatory synapses in rat prefrontal and somatosensory cerebral cortex. *Steroids, 78,* 614-623.

Kim, H., Ahrlund-Richter, S., Wang, X., Deisseroth, K., & Carlen, M. (2016). Prefrontal parvalbumin neurons in control of attention. *Cell, 14,* 208-218.

Ko, A., Kang, G., Hattler, J.B., Galadima, H.I., Zhang, J., Li, Q., et al. (2019). Macrophages but not Astrocytes Harbor HIV DNA in the Brains of HIV-1-Infected Aviremic Individuals on Suppressive Antiretroviral Therapy. *J Neuroimmune Pharmacol, 14,* 110-119.

Koch, M., Kungel, M., & Herbert, H. (1993). Cholinergic neurons in the pedunculopontine tegmental nucleus are involved in the mediation of prepulse inhibition of the acoustic startle response in the rat. *Exp Brain Res, 97,* 71-82.

Koch, M., & Schnitzler, H.U. (1997). The acoustic startle response in rats: Circuits mediating evocation, inhibition and potentiation. *Behav Brain Res, 89,* 35-49.

Koch, M. (1999). The neurobiology of startle. *Prog Neurobiol, 59,* 107-128.

Koekkoek, S., de Sonneville, L.M., Wolfs, T.F., Licht, R., & Geelen, S.P. (2008). Neurocognitive function profile in HIV-infected school-age children. *Eur J Paediatr Neurol, 12,* 290-297.

Konur, S., Rabinowitz, D., Fenstermaker, V.L., & Yuste, R. (2003). Systematic regulation of spine sizes and densities in pyramidal neurons. *J Neurobiol, 56,* 95-112.

Kraemer, H.C., Yesavage, J.A., Taylor, J.L., & Kupfer, D. (2000). How can be learn about developmental processes from cross-sectional studies, or can we? *Am J Psychiatry, 157,* 163-171.

Kritzer M.F., & Kohama S.G. (1998). Ovarian hormones influence morphology, distribution and density of tyrosine hydroxylase immunoreactive axons in the dorsolateral prefrontal cortex of adult rhesus monkeys. *J Comp Neurol, 395,* 1–17.

Kritzer, M. (2000). Effects of acute and chronic gonadectomy on the catecholamine innervation of the cerebral cortex in adult male rats: insensitivity of axons immunoreactive for dopamine-beta-hydroxylase to gonadal steroids, and differential sensitivity of axons immunoreactive for tyrosine hydroxylase to ovarian and testicular hormones. *J Comp Neurol, 427,* 617-633.

Kuiper, G.G., Enmark, E., Pelto-Huikko, M., Nilsson, S., & Gustafsson, J.A. (1996). Cloning of a novel receptor expressed in rat prostate and ovary. *Proc Natl Acad Sci USA, 93,* 5925-5930.

Kuiper, G.G., Carlsson, B., Grandien, K., Enmark, E., Häggblad, J., Nilsson, S., et al. (1997). Comparison of the ligna binding specificity and transcript tissue distribution of estrogen receptors alpha and beta. *Endocrinology, 138,* 863-870.

Kuiper, G.G., Lemmen, J.G., Carlsson, B., Corton, J.C., Safe, S.H., van der Saag, P.T., et al. (1998). Interaction of estrogenic chemicals and phytoestrogens with estrogen receptor beta. *Endocrinology, 139* 4252-4253.

Kumar, A.M., Fernandez, J.B., Singer, E.J., Commins, D., Waldrop-Valverde, D., Ownby, R.L., et al. (2009). Human immunodeficiency virus type 1 in the central nervous system leads to decreased dopamine in different regions of postmortem human brains. *J Neurovirol, 15,* 257-274.

Kumar, A.M., Ownby, R.L., Waldrop-Valverde, D., Fernandez, B., & Kumar, M. (2011). Human immunodeficiency virus infection in the CNS and decreased dopamine availability: Relationship with neuropsychological performance. *J Neurovirol, 17,* 26-40.

Kumari, V., Aasen, I., & Sharma, T. (2004). Sex differences in prepulse inhibition deficits in chronic schizophrenia. *Schiozophrenia Research, 69,* 219-235.

Lai, K.O., & Ip, N.Y. (2013). Structural plasticity of dendritic spines: The underlying mechanisms and its dysregulation in brain disorders. *Biochim Biophys Acta, 1832,* 2257-2263.

Lambert M.P., Barlow, A.K., Chromy, B.A., Edwards, C., Freed, R., Liosatos, M., et al. (1998). Diffusible, nonfibrillar ligands derived from Abeta 1-42 are potent central nervous system neurotoxins. *Proc Natl Acad Sci USA, 95,* 6448-6453.

Lashomb, A.L., Vigorito, M., Chang, S.L. (2009). Further characterization of the spatial learning deficit in the human immunodeficiency virus-1 transgenic rat. *J Neurovirol, 15,* 14-24.

Laughton, B., Cornell, M., Grove, D., Kidd, M., Springer, P.E., Dobbels, E., et al. (2012). Early antiretroviral therapy improves neurodevelopmental outcomes in infants. *AIDS, 26,* 1685-1690.

Lawson, M.A., Kelley, K.W., & Dantzer, R. (2011). Intracerebroventricular administration of HIV-1 Tat induces brain cytokine and indoleamine 2,3-dioxygenase expression: A possible mechanism for AIDS comorbid depression. *Brain Behav Immun, 25,* 1569-1575.

Lee, D.E., Reid, W.C., Ibrahim, W.G., Peterson, K.L., Lentz, M.R., Maric, D. et al. (2014). Imaging dopaminergic dysfunction as a surrogate marker of neuropathology in a small-animal model of HIV. *Mol Imaging, 13,* 1-10.

Lee, D.E., Yue, X., Ibrahim, W.G., Lentz, M.R., Peterson, K.L., Jagoda, E.M., et al. (2015). Lack of neuroinflammation in the HIV-1 transgenic rat: an [(18)F]-DPA714 PET imaging study. *J Neuroinflammation, 12,* 171.

Leitner, D.S., & Cohen, M.E. (1985). Role of the inferior colliculus in the inhibition of acoustic startle in the rat. *Physiol Behav, 34,* 65-70.

Leitner, D.S., Hammond, G.R., Springer, C.P., Ingham, K.M., Mekilo, A.M., Bodison, P.R., et al. (1993). Parameters affecting gap detection in the rat. *Percept Psychophys, 54,* 395-405.

Letendre, S., Marquie-Beck, J., Capparelli, E., Best, B., Clifford, D., Collier, A.C., et al. (2008). Validation of the CNS penetration-effectiveness rank for quantifying antiretroviral prenetration into the central nervous system. *Arch Neurol, 65,* 65-70.

Letendre, S.L., Ellis, R.J., Ances, B.M., & McCutchan, J.A. (2010). Neurologic complications of HIV disease and their treatment. *Top HIV Med, 18,* 45-55.

Leussis, M.P., & Bolivar, V.J. (2006). Habituation in rodents: A review of behavior, neurobiology, and genetics. *Neurosci Biobehav Rev, 30,* 1045-1064.

Li, H., Illenberger, J.M., McLaurin, K.A., Mactutus, C.F., & Booze, R.M. (2018). Identification of dopamine D1-alpha receptor within rodent nucleus accumbens by an innovative RNA in situ detection technology. *J Vis Exp, 133*.

Li, H., McLaurin, K.A., Mactutus, C.F., & Booze, R.M. (2020). Ballistic labeling of pyramidal neurons in brain slices and in primary cell culture. *J Vis Exp,* [In Press].

Li, L., Priebe, P.M., & Yeomans, J.S. (1998). Prepulse inhibition of acoustic or trigeminal startle of rats by unilateral electrical stimulation of the inferior colliculus. *Behav Neurosci, 112,* 1187-1198.

Li, L., & Yeomans, J.S. (2000). Using intracranial electrical stimulation to study the timing of prepulse inhibition of the startle reflex. *Brain Res Protoc, 5,* 67-74.

Li, X., Schwartz, P.E., & Rissman, E.F. (1997). Distribution of estrogen receptor-beta-like immunoreactivity in rat forebrain. *Neuroendocrinology, 66,* 63-67.

Lisman, J.E., & Grace, A.A. (2005). The hippocampal-VTA loop: controlling the entry of information into long-term memory. *Neuron, 46,* 703-713.

Livak, K.J., & Schmittgen, T.D. (2001). Analysis of relative gene expression data using real-time quantitative PCR and the 2(-Delta Delta C(T)) Method. *Methods, 25,* 402-408.

Lodish, H., Berk, A., Zipursky, S.L., Matsudaira, P., Baltimore, D., & Darnell, J. (2000). Neurotransmitters, Synapses, and Impulse Transmission. In: Molecular Cell Biology, 4th edition. New York: W. H. Freeman.

Lowick, S., Sawry, S., & Meyers, T. (2012). Neurodevelopmental delay among HIV-infected preschool children receiving antiretroviral therapy and healthy preschool children in Soweto, South Africa. *Psychol Health Med, 17,* 599-610.

Lund, T.D., Rhees, R.W., Setchell, K.D., & Lephart, E.D. (2001). Altered sexually dimorphic nucleus of the preoptic area (SDN-POA) volume in adult Long-Evans rats by dietary soy phytoestrogens. *Brain Res, 914,* 92-99.

Maki, P.M., & Martin-Thormeyer, E. (2009). HIV, Cognition and Women. *Neuropsychol Rev, 19,* 204-214.

Maki, P.M., Rubin, L.H., Valcour, V., Martin, E., Crystal, H., Young, M., et al. (2015). Cognitive function in women with HIV: Findings from the Women's Interagency HIV study. *Neurology, 84,* 231-240.

Maki, P.M., Rubin, L.H., Springer, G., Seaberg, E.C., Sacktor, N., Miller, E.N., et al. (2018). Differences in cognitive function between women and men with HIV. *J Acquir Immune Defic Syndr, 79,* 101-107.

Mansbach, R.S., Geyer, M.A., & Braff, D.L. (1998). Dopaminergic stimulation disrupts sensorimotor gating in the rat. *Psychopharmacology, 94,* 507-514.

Marcondes, F.K., Bianchi, F.J., & Tanno, A.P. (2002). Determination of the estrous cycle phases of rats: Some helpful considerations. *Braz J Biol, 62,* 609-614.

Markowitz, M., Saag, M., Powderly, W.G., Hurley, A.M., Hsu, A. Valdes, J.M., et al. (1995). A preliminary study of ritonavir, an inhibitor of HIV-1 protease, to treat HIV-1 infection. *N Engl J Med, 333,* 1534-1539.

Marks, W.D., Paris, J.J., Schier, C.J., Denton, M.D., Fitting, S., McQuiston, A.R., et al. (2016). HIV-1 Tat causes cognitive deficits and selective loss of parvalbumin, somatostatin, and neuronal nitric oxide synthase expressing hippocampal CA1 interneuron subpopulations. *J Neurovirol, 22,* 747-762.

Matas, C.G., Silva, S.M., Marcon Bde A., & Goncalves, I.C. (2010). Electrophysiological manifestations in adults with HIV/AIDS submitted and not submitted to antiretroviral therapy. *Pro Fono, 22,* 107-113.

McAlonan, K., & Brown, V.J. (2003). Orbital prefrontal cortex mediates reversal learning and not attentional set shifting in the rat. *Behav Brain Res, 146,* 97-103.

McArthur, J.C., Steiner, J., Sacktor, N., & Nath, A. (2010). Human immunodeficiency virus-associated neurocognitive disorders: Mind the gap. *Ann Neurol, 67,* 699-714.

McGaughy, J., & Sarter, M. (1995). Behavioral vigilance in rats: task validation and effects of age, amphetamine, and benzodiazepine receptor ligands. *Psychopharmacology, 117,* 340-357.

McLaughlin, J.P., Paris, J.J., Mintzopoulos, D., Hymel, K.A., Kim, J.K., Cirino, T.J., et al. (2017). Conditional human immunodeficiency virus transactivator of transcription protein expression induces depression-like effects and oxidative stress. *Biol Psychiatry Cogn Neurosci Neuroimaging, 2,* 599-609.

McLaurin, K.A., Booze, R.M., Moran, L.M., Li, H., & Mactutus, C.F. (2016a). Minding the gap: Progression of temporal processing deficits in the HIV-1 transgenic rat [abstract]. In: *Society for Neuroimmune Pharmacology*, Abstract nr W28.

McLaurin, K.A., Booze, R.M., & Mactutus, C.F. (2016b). Progression of temporal processing deficits in the HIV-1 transgenic rat. *Sci Rep, 6,* 32831.

McLaurin, K.A., Booze, R.M., & Mactutus, C.F. (2017a). Temporal processing demands in the HIV-1 transgenic rat: Amodal gating and implications for diagnostics. *Int J Dev Neurosci, 57,* 12-20.

McLaurin, K.A., Moran, L.M., Li, H., Booze, R.M., & Mactutus, C.F. (2017b). A gap in time: Extending our knowledge of temporal processing deficits in the HIV-1 transgenic rat. *J Neuroimmune Pharmacol, 12,* 171-179.

McLaurin, K.A., Booze, R.M., & Mactutus, C.F. (2017c). Selective developmental alterations in the HIV-1 transgenic rat: Opportunities for diagnosis of pediatric HIV-1. *J Neurovirol, 23,* 87-98.

McLaurin, K.A., Booze, R.M., Mactutus, C.F., & Fairchild, A.J. (2017d). Sex matters: Robust sex differences in signal detection in the HIV-1 transgenic rat. *Front Behav Neurosci, 11,* 212.

McLaurin, K.A., Li, H., Booze, R.M., Fairchild, A.J., & Mactutus, C.F. (2018a). Unraveling individual differences in the HIV-1 transgenic rat: Therapeutic efficacy of methylphenidate. *Sci Rep, 8,* 136.

McLaurin, K.A., Booze, R.M., & Mactutus, C.F. (2018b). Evolution of the HIV-1 transgenic rat: Utility in assessing the progression of HIV-1 associated neurocognitive disorders. *J Neurovirol, 24,* 229-245.

McLaurin, K.A., Cook, A.K., Li, H., League, A.F., Mactutus, C.F., & Booze, R.M. (2018c). Synaptic connectivity in medium spiny neurons of the nucleus accumbens: A sex-dependent mechanism underlying apathy in the HIV-1 transgenic rat. *Front Behav Neurosci, 12,* 285.

McLaurin, K.A., Moran, L.M., Booze, R.M., & Mactutus, C.F. (2019a). Selective estrogen receptor β agonists: A therapeutic approach for HIV-1 associated neurocognitive disorders. *J Neuroimmune Pharmacol.* [Epub ahead of print].

McLaurin, K.A., Li, H., Booze, R.M., & Mactutus, C.F. (2019b). Disruption of timing: NeuroHIV progression in the post-cART era. *Sci Rep, 9,* 827.

McLaurin, K.A., Booze, R.M., & Mactutus, C.F. (2019c). Diagnostic and prognostic biomarkers for HAND. *J Neurovirol, 25,* 686-701.

McLaurin, K.A., Moran, L.M., Li, H., Booze, R.M., & Mactutus, C.F. (2019d). The power of interstimulus interval for the assessment of temporal processing in rodents. *J Vis Exp, 146.*

McLaurin, K.A., Mactutus, C.F., Booze, R.M., & Fairchild, A.J. (2019e). An empirical mediation analysis of mechanisms underlying HIV-1 associated neurocognitive disorders. *Brain Res, 1724,* 146436.

Melendez, R.I., Roman, C., Capo-Velez, C.M., & Lasalde-Dominicci, J.A. (2016). Decreased glial and synaptic glutamate uptake in the striatum of HIV-1 gp120 transgenic mice. *J Neurovirol, 22,* 358-365.

Mersereau, J.E., Levy, N., Staub, R.E., Baggett, S., Zogric, T., Chow, S., et al. (2008). Liquiritigenin is a plant-derived highly selective estrogen receptor β agonist. *Mol Cell Endocrinol, 283,* 49-57.

Miller, E.K., & Cohen, J.D. (2001). An integrative theory of prefrontal cortex function. *Annu Rev Neurosci, 24,* 167-202.

Minassian, A., Henry, B.L., Woods, S.P., Vaida, F., Grant, I., Geyer, M.A., et al. (2013). Prepulse inhibition in HIV-Associated Neurocognitive Disorders. *J Int Neuropsychol Soc, 19,* 709-717.

Mintz, M. (1996). Levodopa therapy improves motor function in HIV-infected children with extrapyramidal syndromes. *Neurol, 47,* 1583-1585.

Mishra, N., Mohata, M., Aggarwal, H., Chaudhary, O., Das, B.K., Sinha, S., et al. (2018). Expression of complement receptor 3 (CR3) and regulatory protein CD46 on dendritic cells of antiretroviral naïve and treated HIV-1 infected individuals: Correlation with immune activation status. *Mol Immunol, 96,* 83-87.

Moran, L.M., Mactutus, C.F., & Booze, R.M. (2009). Generality of disruption of prepulse inhibition by the dopamine agonist apomorphine. http://www.cpdd.vcu.edu/Pages/Meetings/CPDD09AbstractBook.pdf.

Moran, L.M., Aksenov, M.Y., Booze, R.M., Webb, K.M., & Mactutus, C.F. (2012). Adolescent HIV-1 transgenic rats: evidence for dopaminergic alterations in behavior and neurochemistry revealed by methamphetamine challenge. *Curr HIV-1 Res, 10,* 415-424.

Moran, L.M., Booze, R.M., & Mactutus, C.F. (2013a). Time and time again: temporal processing demands implicate perceptual and gating deficits in the HIV-1 transgenic rat. *J Neuroimmune Pharmacol, 8,* 988-97.

Moran, L.M., Booze, R.M., Webb, K.M., & Mactutus, C.F. (2013b). Neurobehavioral alterations in HIV-1 transgenic rats: Evidence for dopaminergic dysfunction. *Exp Neurol, 239,* 139-147.

Moran, L.M., Booze, R.M., & Mactutus, C.F. (2014a). Modeling deficits in attention, inhibition, and flexibility in HAND. *J Neuroimmune Pharmacol, 9,* 508-521.

Moran, L.M., Fitting, S., Booze, R.M., Webb, K.M., & Mactutus, C.F. (2014b). Neonatal intrahippocampal HIV-1 protein Tat(1-86) injection: neurobehavioral alterations in the absence of increase inflammatory cytokine activation. *Int J Dev Neurosci, 38,* 195-203.

Moran, L.M., McLaurin, K.A., Booze, R.M., & Mactutus, C.F. (2019). Neurorestoration of sustained attention in a model of HIV-1 associated neurocognitive disorders. *Front Behav Neurosci, 13,* 169.

Moreno-Paublete, R., Canlon, B., & Cederroth, C.R. (2017). Differential neural responses underlying the inhibition of the startle response by prepulses or gaps in mice. *Front Cell Neurosci, 11,* 19.

Mueller, S.O., Simon, S., Chae, K., Metzler, M., & Korach, K.S. (2004). Phytoestrogens and their human metabolites show distinct agonistic and antagonistic properties on estrogen receptor alpha (ERalpha) and ERbeta in human cells. *Toxicol Sci, 80,* 14-25.

Mukherjee, J., Cardarelli, R.A., Cantaut-Belarif, Y., Deeb, T.Z., Srivastava, D.P., Tyagaranjan, S.K., et al. (2017). Estradiol modulates the efficacy of synaptic inhibition by decreasing the dwell time of $GABA_A$ receptors at inhibitory synapses. *Proc Natl Acad Sci U S A, 114,* 11763-11768.

Murphy, P.A., Farmakalidis, E., & Johnson, L.D. (1982). Isoflavone content of soya-based laboratory animal diets. *Food Chem Toxicol, 20,* 315-317.

Nemeth, C.L., Glasper, E.R., Harrell, C.S., Malviya, S.A., Otis, J.S., & Neigh, G.N. (2014). Meloxicam blocks neuroinflammation, but not depressive-like behaviors, in HIV-1 transgenic female rats. *PLoS One, 9,* e108399.

O'Brien, J.A., & Lummis, S.C.R. (2007). Diolistics: Incorporating fluorescent dyes into biological samples using a gene gun. *Trends Biotechnol, 25,* 530-534.

Ornitz, E.M., Guthrie, D., Sadeghpour, M., & Sugiyama, T. (1991). Maturation of prestimulation-induced startle modulation in girls. *Psychophysiology, 28,* 11-20.

Paolicelli, R.C., Bolasco, G., Pagani, F., Maggi, L., Scianni, M., Panzanelli, P., et al. (2011). Synaptic pruning by microglia is necessary for normal brain development. *Science, 333,* 1456-1458.

Paramesparan, Y. (2010). High rates of asymptomatic neurocognitive impairment in vertically acquired HIV-1-infected adolescents surviving into adulthood. *J Acquir Immune Defic Syndr, 55,* 134-136.

Paris, J.J,. Singh, H.D., Carey, A.N., & McLaughlin, J.P. (2015). Exposure to HIV-1 Tat in brain impairs sensorimotor gating and activates microglia in limbic and extralimbic brain regions of male mice. *Behav Brain Res, 291,* 209-218.

Paterni, I., Granchi, C., Katzenellenbogen, J.A., & Minutolo, F. (2014). Estrogen receptors alpha (ERα) and Beta (ERβ): Subtype-selective ligands and clinical potential. *Steroids, 90,* 13-29.

Patton, H.K., Zhou, Z.H., Bubien, J.K., Benveniste, E.N., & Benos, D.J. (2000). Gp120-induced alterations of human astrocyte function: Na(+)/H(+) exchange, K(+) conductance, and glutamate flux. *Am J Physiol Cell Physiol, 279,* C700-C708.

Paxinos, G., & Watson, C. (2014). The rat brain in stereotaxic coordinates. 7th ed. Elsevier Academic Press; Burlington.

Peng, J., Vigorito, M., Liu, X., Zhou, D., Wu, X., & Chang, S.L. (2010). The HIV-1 transgenic rat as a model for HIV-1 infected individuals on HAART. *J Neuroimmunol, 218,* 94-101.

Peris, J., Coleman-Hardee, M., Millard, W.J. (1992). Cocaine in utero enhances the behavioral response to cocaine in adult rats. *Pharmacol Biochem Behav, 42,* 509-515.

Petanjeck, Z., Judas, M., Simic, G., Rasin, M.R., Uylings, H.B.M., Rakic, P., et al. (2011). Extraordinary neoteny of synaptic spines in the human prefrontal cortex. *Proc Natl Acad Sci USA, 108,* 13281-13286.

Peters, A., & Kaiserman-Abramof, I.R. (1970). The small pyramidal neuron of the rat cerebral cortex. The perikaryon, dendrites and spines. *Am J Anat, 127,* 321-355.

Phan, J.A., Stokholm, K., Zareba-Paslawska, J., Jakobsen, S., Vang, K., Gjedde, A. et al. (2017). Early synaptic dysfunction induced by α-synuclein in a rat model of Parkinson's disease. *Sci Rep, 7,* 6363.

Phipps, A.J., Hayes, K.A., Buck, W.R., Podell, M., & Mathes, L.E. (2000). Neurophysiologic and immunologic abnormalities associated with feline immunodeficiency virus molecular clone FIV-PPR DNA inoculation. *J Acquir Immune Defic Syndr, 23,* 8-16.

Pierce, R.C., & Kalivas, P.W. (2007). Locomotor behavior. *Curr Protoc Neurosci,* 8.1.1-8.1.9.

Piotrowska, E., Jakobkiewicz-Banecka, J., Tylki-Szymanska, A., Liberek, A., Maryniak, A., Malinowska, M., et al. (2008). Genistin-rich soy isoflavone extract in substrate reduction therapy for Sanfilippo syndrome: An open-label, pilot study in 10 pediatric patients. *Curr Ther Res Clin Exp, 69,* 166-179.

Pothuizen, H.H.J., Jongen-Relo, A.L., & Feldon, J. (2005). The effects of temporary inactivation of the core and the shell subregions of the nucleus accumbens on prepulse inhibition of the acoustic startle reflect and activity in rats. *Neuropsychopharmacology, 30,* 683-696.

Price, R.W., Brew, B., Sidtis, J., Rosenblum, M., Scheck, A.C., & Cleary, P. (1988). The brain in AIDS: Central nervous system HIV-1 infection and AIDS dementia complex. *Science, 239,* 4840.

Prospero-Garcia, O., Huitron-Resendiz, S., Casalman, S.C., Sanchez-Alavez, Diaz-Ruiz, O., Navarro, L., et al. (1999). Feline immunodeficiency virus envelope protein (FIVgp120) causes electophysiological alterations in rats. *Brain Res, 836,* 203-209.

Rajan, I., & Cline, H.T. (1998). Glutamate receptor activity is required for normal development of tectal cell dendrites in vivo. *J Neurosci, 18,* 7836-7846.

Rankin, C.H., Abrams, T., Barry, R.J., Bhatnagar, S., Clayton, D., Colombo, J., et al. (2009) Habituation revisited: An updated and revised description of the behavioral characteristics of habituation. *Neurobiol Learn Mem, 92,* 135-138.

Rao, J.S., Kim, H.W., Kellom, M., Greenstein, D., Chen, M., Kraft, A.D., et al. (2011). Increased neuroinflammatory and arachidonic acid cascade markers, and reduced synaptic proteins, in brain of HIV-1 transgenic rats. *J Neuroinflammation, 8,* 101.

Raymond, L.A., Wallace, D., Berman, N.E., Marcario, J., Foresman, L., Joag, S.V., et al. (1998). Auditory brainstem responses in a Rhesus Macaque model of neuro-AIDS. *J Neurovirol, 4,* 512-520.

Reid, W., Sadowska, M., Denaro, F., Rao, S., Foulke, J., Hayes, N., et al. (2001). An HIV-1 transgenic rat that develops HIV-related pathology and immunologic dysfunction. *Proc Natl Acad Sci USA, 98,* 9271-9276.

Reid, W.C., Ibrahim, W.G., Kim, S.J., Denaro, F., Casas, R., Lee, D.E., et al. (2016a). Characterization of neuropathology in the HIV-1 transgenic rat at different ages. *J Neuroimmunol, 292,* 116-125.

Reid, W.C., Casas, R., Papadakis, G.Z., Muthusamy, S., Lee, D.E., Ibrahim, W.G., et al. (2016b). Neurobehavioral abnormalities in the HIV-1 transgenic rat do not correspond to neuronal hypometabolism on ^{18}F-FDG-PET. *PLoS One, 11,* e0152265.

Repunte-Canonigo, V., Lefebvre, C., George, O., Kawamura, T., Morales, M., Koob, G.F., et al. (2014). Gene expression changes consistent with neuroAIDS and impaired working memory in HIV-1 transgenic rats. *Mol Neurodegener, 9,* 26.

Riccomagno, M.M., & Kolodkin, A.L. (2015). Sculpting neural circuits by axon and dendrite pruning. *Annu Rev Cell Dev Biol, 31,* 779-805.

Robbins, T.W. (1977). A critique of the methods available for the measurement of spontaneous motor activity. In: Iversen LL, Iversen SD, Snyder SH (Eds) Handbook of Psychopharmacology, Volume 7. Plenum Press, NY, pp 37-82.

Robbins, T.W., & Arnsten, A.F. (2009). The neuropsychopharmacology of fronto-executive function: Monoaminergic modulation. *Annu Rev Neurosci, 32,* 267-287.

Rodriguez, A., Ehlenberger, D.B., Dickstein, D.L., Hof, P.R., & Wearne, S.L. (2008). Automated three-dimensional detection and shape classification of dendritic spines from fluorescence microscopy images. *PLoS One, 3,* e1997.

Rolls, E.T. (2004). The functions of the orbitofrontal cortex. *Brain Cogn, 55,* 11-29.

Romley, J.A., Juday, T., Solomon, M.D., Seekins, D., Brookmeyer, R., & Goldman, D.P. (2014). Early HIV treatment led to life expectancy gains valued at $80 billion for people infected in 1996-2009. *Health Aff (Millwood), 33,* 370-377.

Roscoe, R.F., Mactutus, C.F., & Booze, R.M. (2014). HIV-1 Transgenic female rat: synaptodendritic alterations of medium spiny neurons in the nucleus accumbens. *J Neuroimmune Pharmacol, 9,* 642-653.

Rose, J.E., & Woolsey, C.N. (1948). The orbitofrontal cortex and its connections with the mediodorsal nucleus in rabbit, sheep and cat. *Res Publ Assoc Nerv Ment Dis, 27,* 210-232.

Rowland, I.R., Wiseman, H., Sanders, T.A., Adlercreutz, H., Bowey, E.A. (2000). Interindividual variation in metabolism of soy isoflavones and lignans: influence of habitual diet on equol production by the gut microflora. *Nutr Cancer, 36,* 27-32.

Rowson, S.A., Harrell, C.S., Bekhbat, M., Gangavelli, A., Wu, M.J., Kelly, S.D., et al. (2016). Neuroinflammation and behavior in HIV-1 transgenic rats exposed to chronic adolescent stress. *Front Psychiatry, 7,* 102.

Royal, W., Zhang, L., Guo, M., Jones, O., Davis, H., & Bryant, J.L. (2012). Immune activation, viral gene product expression and neurotoxicity in the HIV-1 transgenic rat. *J Neuroimmunol, 247,* 16-24.

Royal, W., Cherner, M., Burdo, T.H., Umlauf, A., Letendre, S.L., Jumare, J. et al. (2016). Associations between cognition, gender and monocyte activation among HIV infected individuals in Nigeria. *PLoS One, 11,* e0147182.

Rubin, L.H., Maki, P.M., Springer, G., Benning, L., Anastos, K., Gustafson, D., Villacres, M.C., et al. (2017). Cognitive trajectories over 4 years among HIV-infected women with optimal viral suppression. *Neurology, 89,* 1594-1603.

Ruel, T.D., Zanoni, B.C., Ssewanyana, I., Cao, H., Havlir, D.V., Kamya, M., et al. (2011). Sex differences in HIV RNA level and CD4 cell percentage during childhood. *Clin Infect Dis, 53,* 592-599.

Ruel, T.D., Boivin, M.J., Boal, H.E., Bangirana, P., Charlebois, E., Havlir, D.V., et al. (2012). Neurocognitive and motor deficits in HIV-infected Ugandan children with high CD4 cell counts. *Clin Infect Dis, 54,* 1001-1009.

Ruszczycki, B., Szepesi, Z., Wilczynski, G.M., Bijata, M., Kalita, K., Kaczmarek, L., et al. (2012). Sampling issues in quantitative analysis of dendritic spines morphology. *BMC Bioinformatics, 13,* 213.

Sachana, M., Flaskos, J., Hargreaves, A.J. (2017). *Chapter 15-In vitro biomarkers of developmental neurotoxicity.* In: Reproductive and Developmental Toxicology (Second Edition). Academic Press. 255-288.

Sacktor, N., Skolasky, R.L., Seaberg, E., Munro, C., Becker, J.T., Martin, E., Ragin, A., Levine, A., & Miller, E. (2016). Prevalence of HIV-associated neurocognitive disorders in the Multicenter AIDS Cohort Study. *Neurology*, *86*, 334-340.

Sakamoto, M., Marcotte, T.D., Umlauf, A., Franklin, D., Heaton, R.K., Ellis, R.J., et al. (2013). Concurrent classification accuracy of the HIV dementia scale for HIV-associated neurocognitive disorders in the CHARTER cohort. *J Acquir Immune Defic Syndr, 62,* 36–42.

Santana, N., & Artigas, F. (2017). Laminar and cellular distribution of monoamine receptors in rat medial prefrontal cortex. *Front Neuroanat, 11,* 87.

Schikorski, T., & Stevens, C. (1999). Quantitative fine-structural analysis of olfactory cortical synapses. *Proc Natl Acad Sci USA, 96,* 4107-4112.

Schafer, D.P., Lehrman, E.K., Kautzman, A.G., Koyama, R., Mardinly, A.R., Yamasaki, R., et al. (2012). Microglia sculpt postnatal neural circuits in an activity and complement-dependent manner. *Neuron, 74,* 691-705.

Schmidt, H., & Eilers, J. (2009). Spine neck geometry determines spino-dendritic cross-talk in the presence of mobile endogenous calcium binding proteins. *J Comput Neurosci, 27,* 229-243.

Schofield, B.R., & Motts, S.D. (2009) Projections from auditory cortex to cholinergic cells in the midbrain tegmentum of guinea pigs. *Brain Res Bull, 80,* 163-170.

Schwarzkopf, S.B., McCoy, L., Smith, D.A., & Boutros, N.N. (1993). Test-retest reliability of prepulse inhibition of the acoustic startle response. *Biol Psychiatry, 34,* 896-900.

Seabold, G.K., Daunais, J.B., Rau, A., Grant, K.A., & Alvarez, V.A. (2010). DiOLISTIC labeling of neurons from rodent and non-human primate brain slices. *J Vis Exp, 41,* 2081.

Seamans, J.K., Lapish, C.C., & Durstewitz, D. (2008). Comparing the prefrontal cortex of rats and primates: Insights from electrophysiology. *Neurotox Res, 14,* 249-262.

Selemon, L.D. (2013). A role for synaptic plasticity in the adolescent development of executive function. *Transl Psychiatry, 3,* e238.

Sengupta, P. (2013). The laboratory rat: Relating its age with human's. *Int J Prev Med, 4,* 624-630.

Setchell, K.D., Borriello, S.P., Hulme, P., Kirk, D.N., & Axelson, M. (1984). Nonsteroidal estrogens of dietary origin: possible roles in hormone-dependent disease. *Am J Clin Nutr, 40,* 569-578.

Setchell, K.D. (1998). Phytoestrogens: The biochemistry, physiology, and implications for human health of soy isoflavones. *Am J Clin Nutr, 68(6 Suppl),* 1333S-13246S.

Setchell, K.D., Clerici, C., Lephart, E.D., Cole, S.J., Heenan, C., Castellani, D., et al. (2005). S-Equol, a potent ligand for estrogen receptor β, is the exclusive enantiomeric form of the soy isoflavone metabolite produced by human intestinal bacterial flora. *Am J Clin Nutr, 81,* 1072-1079.

Setchell, K.D., & Cole, S.J. (2006). Method of defining equol-producer status and its frequency among vegetarians. *J Nutr, 136,* 2188–93.

Setchell, K.D.R., & Clerici, C. (2010). Equol: Pharmacokinetics and biological actions. *J Nutr, 140,* 1363S-1368S.

Sheng, M., & Hoogenraad, C.C. (2007). The postsynaptic architecture of excitatory synapses: A more quantitative view. *Annu Rev Biochem, 76,* 823-847.

Sheppard, D.P., Iudicello, J.E., Bondi, M.W., Doyle, K.L., Morgan, E.E., Massman, P.J., et al. (2015). Elevated rates of mild cognitive impairment in HIV disease. *J Neurovirol, 21,* 576-584.

Sholl, D.A. (1953). Dendritic organization in the neurons of the visual and motor cortices of the cat. *J Anat, 87,* 387-406.

Shughrue, P.J., Lane, M.V., & Merchenthaler, I. (1997). Comparative distribution of estrogen receptor-alpha and –beta mRNA in the rat central nervous system. *J Comp Neurol, 388,* 507-525.

Siddiqui, S.V., Chatterjee, U., Kumar, D., Siddiqui, A., & Goyal, N. (2008). Neuropsychology of prefrontal cortex. *Indian J Psychiatry, 50,* 202-208.

Sin, W.C., Haas, K., Ruthazer, E.S., & Cline, H.T. (2002). Dendrite growth increased by visual activity requires NMDA receptor and Rho GTPases. *Nature, 419,* 475-480.

Sinharay, S., Lee, D., Shah, S., Muthusamy, S., Papadakis, G.Z., Zhang, X., et al. (2017). Cross-sectional and longitudinal small animal PET shows pre and post-synaptic striatal dopaminergic deficits in an animal model of HIV. *Nucl Med Biol, 55,* 27-33.

Smit, M., Binkman, K., Geerlings, S., Smit, C., Thyagarajan, K., Sighem, A.V., et al. (2015). Future challenges for clinical care of an ageing population infected with HIV: A modelling study. *Lancet Infect Dis, 15,* 810-818.

Smith, R., & Wilkins, M. (2015). Perinatally acquired HIV infection: long-term neuropsychological consequences and challenges ahead. *Child Neuropsychol, 21,* 234-268.

Spruston, N. (2008). Pyramidal neurons: dendritic structure and synaptic integration. *Nature Reviews Neuroscience, 9,* 206-221.

Stevens, B., Allen, N.J., Vazquez, L.E., Howell, G.R., Christopherson, K.S., Nouri, N., et al. (2007). The classical complement cascade mediates CNS synapse elimination. *Cell, 131,* 1164–1178

Sun, W., Doolittle, L., Flowers, E., Zhang, C., & Wang, Q. (2014). High doses of salicylate causes prepulse facilitation of onset-gap induced acoustic startle response. *Behav Brain Res, 258,* 187-192.

Sweatt, J.D. (2004). Hippocampal function in cognition. *Psychopharmacology (Berl), 174,* 99-110.

Swerdlow, N.R., Caine, S.B., Braff, D.L., & Geyer, M.A. (1992). The neural substrates of sensorimotor gating of the startle reflex: a review of recent findings and their implications. *J Psychopharmacol, 6,* 176-190.

Taber, M.T., & Fibiger, H.C. (1995). Electrical stimulation of the prefrontal cortex increases dopamine release in the nucleus accumbens of the rat: modulation by metabotropic glutamate receptors. *J Neurosci, 15,* 3896-3904.

Takahashi, K., Nagai, T., Kamei, H., Maeda, K., Matsuya, T., Arai, S., et al. (2007). Neural circuits containing pallidotegmental GABAergic neurons are involved in the prepulse inhibition of the startle reflex in mice. *Biol. Psychiatry, 62,* 148–157.

Tansey, M.G., & Goldberg, M.S. (2010). Neuroinflammation in Parkinson's disease: its role in neuronal death and implications for therapeutic intervention. *Neurobiol Dis, 37,* 510-518.

Teeraananchai, S., Kerr, S.J., Amin, J., Ruxrungtham, K., & Law, M.G. (2017). Life expectancy of HIV-positive people after starting combination antiretroviral therapy: A meta-analysis. *HIV Med, 18,* 256-266.

Thompson, P.M., Dutton, R.A., Hayashi, K.M., Toga, A.W., Lopez, O.L., Aizenstein, H.J., et al. (2005) Thinning of the cerebral cortex visualized in HIV/AIDS reflect CD4(+) T lymphocyte decline. *Proc Natl Acad Sci USA, 102,* 15647-15652.

Thompson, R.F., & Spencer, W.A. (1966). Habituation: A model phenomenon for the study of neuronal substrates of behavior. *Psychol Rev, 73,* 16-43.

Threlkeld, S.W., Hill, C.A., Rosen, G.D., & Fitch, R.H. (2009). Early acoustic discrimination experience ameliorates auditory processing deficits in male rats with cortical developmental disruption. *Int J Dev Neurosci, 27,* 321-328.

Turner, J.G., Brozoski, T.J., Bauer, C.A., Parrish, J.L., Myers, K., Hughes, L.F., et al. (2006). Gap detection deficits in rats with tinnitus: A potential novel screening tool. *Behav Neurosci, 120,* 188-195.

Turner, J.G., & Parrish, J.L. (2008). Gap detection methods for assessing salicylate-induced tinnitus and hyperacusis in rats. *Am J Audiol, 17,* 185-192.

Tuscher, J.J., Luine, V., Frankfurt, M., & Frick, K.M. (2016). Estradiol-mediated spine changes in the dorsal hippocampus and medial prefrontal cortex of ovariectomized female mice depend on ERK and mTOR activation in the dorsal hippocampus. *J Neurosci, 36,* 1483-1489.

Uchizono, K. (1965). Characteristics of excitatory and inhibitory synapses in the central nervous system of the cat. *Nature, 207,* 642-643.

Ulyings, H.B.M., & Van Eden, C.G. (1990). Qualitative and quantitative comparison of the prefrontal cortex in rat and in primates, including humans. *Prog Brain Res, 85,* 31-62.

Ulyings, H.B.M., Groenewegen, H.J., & Kolb, B. (2003). Do rats have a prefrontal cortex. *Behav Brain Res, 146,* 3-17.

UNAIDS. (2013). *HIV and Aging*. (2013). Available online at: http://www.unaids.org/sites/ default/files/media_asset 20131101_JC2563_hiv-and-aging_en_0.pdf.

UNAIDS. (2016). AIDS by the numbers. Available online at: https://www.unaids.org /sites/default/files/media_asset/AIDS-by-the-numbers-2016_en.pdf

UNAIDS. (2017). *Fact Sheet*. Available online at: http://www.unaids.org/sites/default/files /media_asset/ UNAIDS_FactSheet_en.pdf.

UNAIDS. (2019). Global HIV & AIDS statistics-2019 fact sheet. Available online at: https://www.unaids.org/en/resources/fact-sheet

Valcour, V., Shikuma, C., Shiramizu, B., Watters, M., Poff, P., Selnes, O., et al. (2004) Higher frequency of dementia in older HIV-1 individuals: The Hawaii aging with HIV-1 cohort. *Neurology, 63,* 822-827.

Valcour, V., Chalermchai, T., Sailasuta, N., Marovich, M., Lerdlum, S., Suttichom, D., et al. (2012). Central nervous system viral invasion and inflammation during acute HIV infection. *J Infect Dis, 206,* 275-282.

Vigorito, M., LaShomb, A.L., & Chang, S.L. (2007). Spatial learning and memory in HIV-1 transgenic rats. *J Neuroimmune Pharmacol, 2,* 319-328.

Vigorito, M., Connaghan, K.P., & Chang, S.L. (2015). The HIV-1 transgenic rat model of neuroHIV. *Brain Behav Immun, 48,* 336-349.

Wallace, D.R., Dodson, S., Nath, A., & Booze, R.M. (2006). Estrogen attenuates gp120- and tat1-72-induced oxidative stress and prevents loss of dopamine transporter function. *Synapse, 59,* 51-60.

Wang, Z., Pekarskaya, O., Bencheikh, M., Chao, W., Gelbard, H.A., Ghorpade, A., et al. (2003). Reduced expression of glutamate transporter EAAT2 and impaired glutamate transport in human primary astrocytes exposed to HIV-1 or gp120. *Virology, 312,* 60-73.

Wang, G.J., Chang, L., Volkow, N.D., Telang, F., Logan, J., Ernst, T., et al. (2004). Decreased brain dopaminergic transporters in HIV-associated dementia patients. *Brain, 127,* 2452-2458.

Wang, S., Zhu, J., & Xu, T. (2018). 17β-estradiol (E2) promotes growth and stability of new dendritic spines via estrogen receptor β pathway in intact mouse cortex. *Brain Res Bull, 137,* 241-248.

Waynforth, H.B., & Flecknell, P.A. (1992). Experimental and surgical techniques in the rat. Elsevier Science: New York.

Wears, R.L. 2002). (Advanced statistics: statistical methods for analyzing cluster and cluster-randomized data. *Acad Emerg Med, 9,* 330-341.

Webb, K.M., Aksenov, M.Y., Mactutus, C.F., & Booze, R.M. (2010). Evidence for developmental dopaminergic alterations in the human immunodeficiency virus-1 transgenic rat. *J Neurovirol, 16,* 168-173.

Wecker, J.R., Ison, J.R., & Foss, J.A. (1985). Reflex modification as a test for sensory function. *Neurobehav Toxicol Teratol, 7,* 733-738.

Wecker, J.R., & Ison, J.R. (1986). Visual function measured by reflex modification in rats with inherited retinal dystrophy. *Behav Neurosci, 100,* 679-684.

Weed, M.R., Gold, L.H., Polis, I., Koob, G.F., Fox, H.S., & Taffe, M.A. (2004). Imparied performance on a rhesus monkey neuropsychological testing battery following simian immunodeficiency virus infection. *AIDS Res Hum Retroviruses, 20,* 77-89.

West, S.G., Biesanz, J.C., & Kwok, O.M. (2004). Within-subject and longitudinal experiments: Design and analysis issues. In Sansone C, Morf C, Panter AT (Eds), The SAGE handbook of methods in social psychology. Sage Publications, Thousand Oaks, CA, pp 287-312.

Westwood, F.R. (2008). The female rat reproductive cycle: a practical histological guide to staging. *Toxicol Pathol, 36,* 375–384.

WHO [No authors listed]. (1988). Animal models for HIV infection and AIDS: memorandum from a WHO meeting. *Bull World Health Organ, 66,* 561-74.

Wilson, M.D., Sethi, S., Lein, P.J., & Keil, K.P. (2017). Valid statistical approaches for analyzing sholl data: Mixed effects versus simple linear models. *J Neurosci Methods, 279,* 33-43.

Winer, B.J. (1971). *Statistical Principles in Experimental Design* (2nd ed.) New York: McGraw-Hill (1971).

Wong, J.Y.F., Clifford, J.J., Massalas, J.S., Kinsella, A., Waddington. J.L., & Drago, J. (2003). Essential conservation of D_1 mutant phenotype at the level of individual topographies of behaviour in mice lacking both D_1 and D_3 dopamine receptors. *Psychopharmacology, 167,* 167-173.

Young, J.S., & Fechter, L.D. (1983). Reflex inhibition procedures for animal audiometry: A technique for assessing ototoxicity. *J Acoust Soc Am, 73,* 1686-1693.

Yuste, R. (2010). Dendritic Spines. Cambridge: Massachusetts Institutes of Technology.

Zgalijardic, D.J., Borod, J.C., Foldi, N.S., Mattis, P.J., Gordon, M.F., Feigin, A., et al. (2006). An examination of executive dysfunction associated with frontostriatal circuitry in Parkinson's disease. *J Clin Exp Neuropschol, 28,* 1127-1144.

Zhang, J.Q., Cai, W.Q., Zhou, D.S., & Su, B.Y. (2002). Distribution and differences of estrogen receptor beta immunoreactivity in the brain of adult male and female rats. *Brain Res, 935,* 73-80.

Zhang, J., Forkstam, C., Engel, J.A., & Svensson, L. (2000). Role of dopamine in prepulse inhibition of acoustic startle. *Psychopharmacology, 149,* 181-188.

Zhao, H., Li, X., Wu, W., Li, Z., Qian, L., Li, S., et al. (2015). Atrophic patterns of the frontal-subcortical circuits in patients with mild cognitive impairment and Alzheimer's disease. *PLoS One, 10,* e0130017.

Zipursky, A.R., Gogolishvili, D., Rueda, S., Brunetta, J., Carvalhal, A., McCombe, J.A., et al. (2013). Evaluation of brief screening tools for neurocognitive impairment in HIV/AIDS: A systematic review of the literature. *AIDS, 27,* 2385–2401.

APPENDIX A

SUPPLEMENTARY FIGURE FOR CHAPTER 3[4]

[4] KA McLaurin, RM Booze, CF Mactutus. 2018. *Journal of Neurovirology*. 24(2):229-245. Reprinted here with permission of publisher.

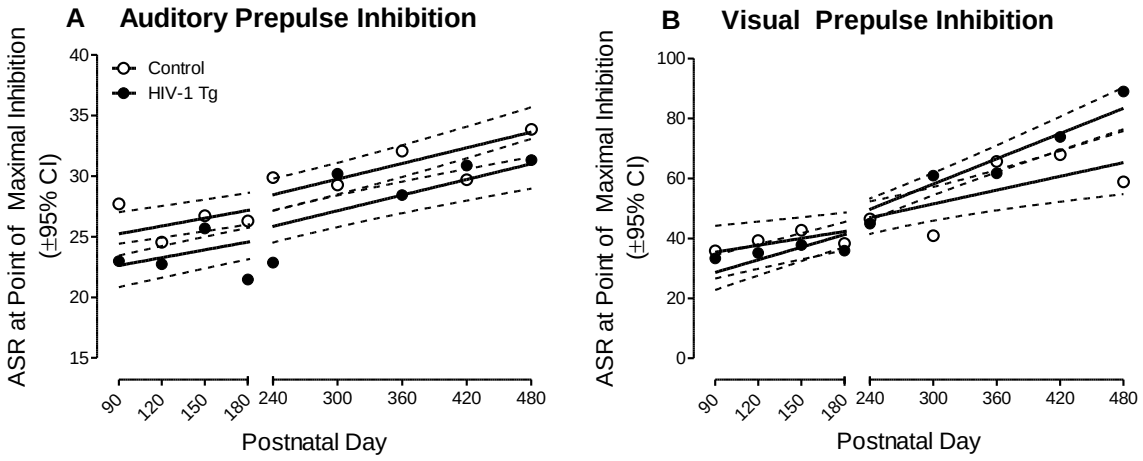

Figure A.1 Point of Maximal Inhibition. The ASR at the point of maximal inhibition is illustrated for auditory (**A**) and visual (**B**) prepulse inhibition (PPI) as a function of genotype (HIV-1 Tg, control) and age (±95% CI). (**A**) In auditory PPI, a linear increase in ASR at the point of maximal inhibition was observed in both HIV-1 Tg and control animals as a function of age. A global first-order polynomial was the best fit for both HIV-1 Tg and control animals; no significant differences in the rate of increase in ASR at the point of maximal inhibition was observed between genotypes [$F(2,14) = 3.2$, $p \geq 0.05$]. (**B**) In visual PPI, both HIV-1 Tg and control animals displayed a linear increase in the ASR at the point of maximal inhibition as a function of age. Although the ASR at the point of maximal inhibition increased significantly faster in HIV-1 Tg animals relative to controls [$F(1,14)=14.5$, $p \leq 0.002$], robust inhibition to the visual prestimulus was observed at all test sessions.

APPENDIX B

SUPPLEMENTARY INFORMATION FOR CHAPTER 4[5]

[5] KA McLaurin, H Li, RM Booze, CF Mactutus. 2019. *Scientific Reports.* 9(1):827. Reprinted here with permission of publisher.

Phase 1: Original Acquisition

Signal Detection

The signal detection test sessions, which began with a 5-minute habituation period, were conducted during the light-cycle in a darkened operant chamber. After each trial began, two retractable levers were extended for 2 sec and remained extended for 6 sec for the animal to make a response. A variable ITI of 9±3 sec was present, during which time the levers were retracted. Approximately half of the animals were trained to press the left lever during signal trials and the right lever during non-signal trials (hits and correct rejections, respectively). The other half of the subjects were trained using the reverse set of rules. A correct response, including hits and correct rejections, was rewarded with a sucrose pellet. Incorrect responses, including misses and false alarms, were not rewarded. Animals were trained on each vigilance program until meeting criteria of at least 70% accuracy for 5 consecutive or 7 non-consecutive test sessions, at which point they were promoted to the next program. Percent accuracy was calculated as follows: (Total Number of Hits and Correct Rejections)/(Total Number of Correct and Incorrect Responses x 100).

Statistical Analysis

The temporal process of learning (i.e., the number of days to meet criterion) during original acquisition, as a function of retest assessment, and during reversal acquisition was analyzed using a generalized linear mixed effects model with a Poisson distribution and an unstructured covariance pattern (SAS/STAT Software 9.4, SAS Institute, Inc., Cary, NC). Genotype (HIV-1 Tg vs. control) and sex (male vs. female) were included as between-subject's factors. For reversal acquisition, only the animals with at least 60 days to complete the task were included in the figures and analysis (Control: *N*=17 litters; male, *n*=24, female, *n*=24; HIV-1 Tg: *N*=18 litters; male *n*=17; female, *n*=21).

The number of days meeting criterion during 18 month acquisition, to directly assess functional form, was analyzed using a curve-fitting analysis and fit with a 95% CI (GraphPad Software, Inc., La Jolla, CA, USA).

Signal duration data during original acquisition, as a function of retest assessment, during the 18 month acquisition, and the reversal task was analyzed using a mixed-factor ANOVA (SPSS Statistics 24, IBM Corp., Somer, NY) with genotype (HIV-1 Tg vs. control) and sex (male vs. female) serving as between-subject's factors. Response type (hits vs. misses), signal duration (e.g., 1000, 500, 100 msec) and retest assessment served as the within-subject's factors, as appropriate. During original acquisition and retest assessments, signal detection data was analyzed for the first 5 consecutive or 7 non-consecutive days that an animal achieved 70% accuracy. For the 18-month acquisition assessment, all 5 days were included in the analysis. For the reversal task, when an animal met criteria, the first 5 consecutive or 7 non-consecutive days that an animal achieved 70% accuracy were included. In the reversal assessment, if an animal failed to meet criteria, but had 60 days or had completed 45 days by approximately 20 months of age, the 7 days with the highest percent accuracy were included in the analysis. To illustrate the profound genotype differences in the progression of sustained attention across retest assessments, data in Figure 4.4 were statistically extrapolated to 10 msec; the 10 msec point was not included in the statistical analysis. The factor of retest assessment was included in the statistical analysis of the 18-month challenge and reversal task, thus only the animals that completed both assessments were included in the statistical analysis; figures represent all animals that completed a given assessment.

Censored data, either due to euthanization, an equipment malfunction, or failure to complete the retest assessment was handled using the mean series imputation method (Retest Assessment 3: HIV-1 Tg female, *n*=2; Retest Assessment 4: control female, *n*=1; Retest Assessment 5: control female, *n*=1, control male, *n*=1, HIV-1 Tg female, *n*=4, HIV-1 Tg male, *n*=2; 18 Month Challenge: control female, *n*=1, control male, *n*=1, HIV-1 Tg female, *n*=1; Reversal Assessment: control male, *n*=3, HIV-1 Tg female, *n*=1).

Neuronal morphology was assessed using two measures, including the number of segments at each branch order and the number of intersections at successive radii (i.e., Sholl analysis). The number of segments at each branch order were analyzed using a generalized linear mixed effects model with a Poisson distribution and an unstructured covariance pattern (SAS/STAT Software 9.4, SAS Institute, Inc., Cary, NC) with genotype (HIV-1 Tg vs. control), sex (male vs. female) and branch order (Branches 1 – 10) included as factors in the analysis. The number of intersections at successive radii was analyzed using a mixed-design ANOVA, restricted maximum likelihood estimation model parameters, a variance components covariance structure (Wilson et al., 2017), and a random intercept and random slope (i.e., Radius; SAS/STAT Software 9.4, SAS Institute, Inc., Cary, NC).

Dendritic spine connectivity was evaluated using the number of dendritic spines, dependent upon spine type (i.e., thin, stubby, mushroom), between each radii. Dendritic spine backbone length, head diameter, and volume were examined as assessments of dendritic spine morphology. A generalized linear mixed effects model with a Poisson distribution and an unstructured covariance pattern was conducted using PROC GLIMMIX (SAS/STAT Software 9.4, SAS Institute, Inc., Cary, NC) for both dendritic spine

connectivity and dendritic spine morphology. Analyses were conducted on the number of dendritic spines between each successive radii or the number of dendritic spines within each bin. Between-subject's factors included genotype (HIV-1 Tg vs. Control) and biological sex (male vs. female).

The gene expression of each neuroinflammatory marker was analyzed individually using a two-way ANOVA, with genotype (HIV-1 Tg vs. control) and biological sex (male vs. female), serving as the between-subject's factors.

A DFA was utilized to examine the utility of neurocognitive impairments across the lifespan or dendritic spine alterations to correctly classify animals based on their genotype (SPSS Statistics 24, IBM Corp., Somer, NY).

Table B.1 Primers for Neuroinflammatory Markers.

Rat genes	Forward (5'-3')	Reverse (5'-3')	GenBank Identifiers
TNF-α	ACCACGCTCTT CTGTCTACTG	CTTGGTGGTTT GCTACGAC	NM 013693.3
IL-1β	GCAATGGTCGG GACATAGTT	AGACCTGACT TGGCAGAGGA	NM 031512.2
IL-6	GCCCTTGCTGG TGGATGTT	GAGAGGGAGT GCTGCTTGGA	NM 010559.3
β-Actin	AAGTCCCTCAC CCTCCCAAAAG	AAGCAATGCT GTCACCTTCCC	NM 007393.5

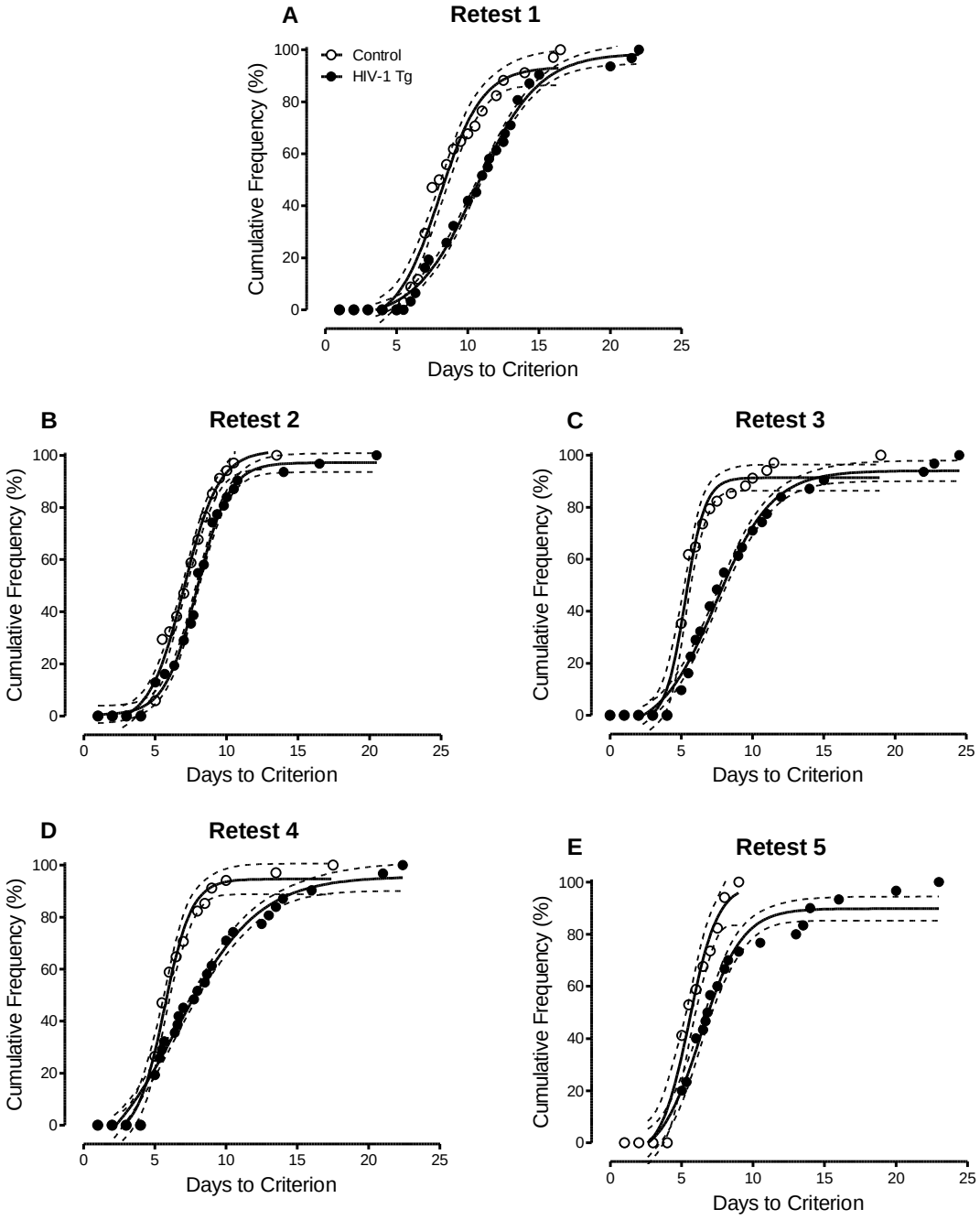

Figure B.1 Cumulative Frequencies of Acquisition. Temporal process of acquisition as a function of retest session (*N*=17-20 litters per genotype). At each individual retest session (i.e., Retest 1: **A**, Retest 2: **B**, Retest 3: **C**, Retest 4: **D**, Retest 5: **E**) HIV-1 Tg animals, independent of biological sex, took a significantly greater number of days to acquire the signal detection task ($p \leq 0.05$); an impairment which progressed as a function of retest session. Data are presented as cumulative frequencies with 95% confidence intervals fit to the curve.

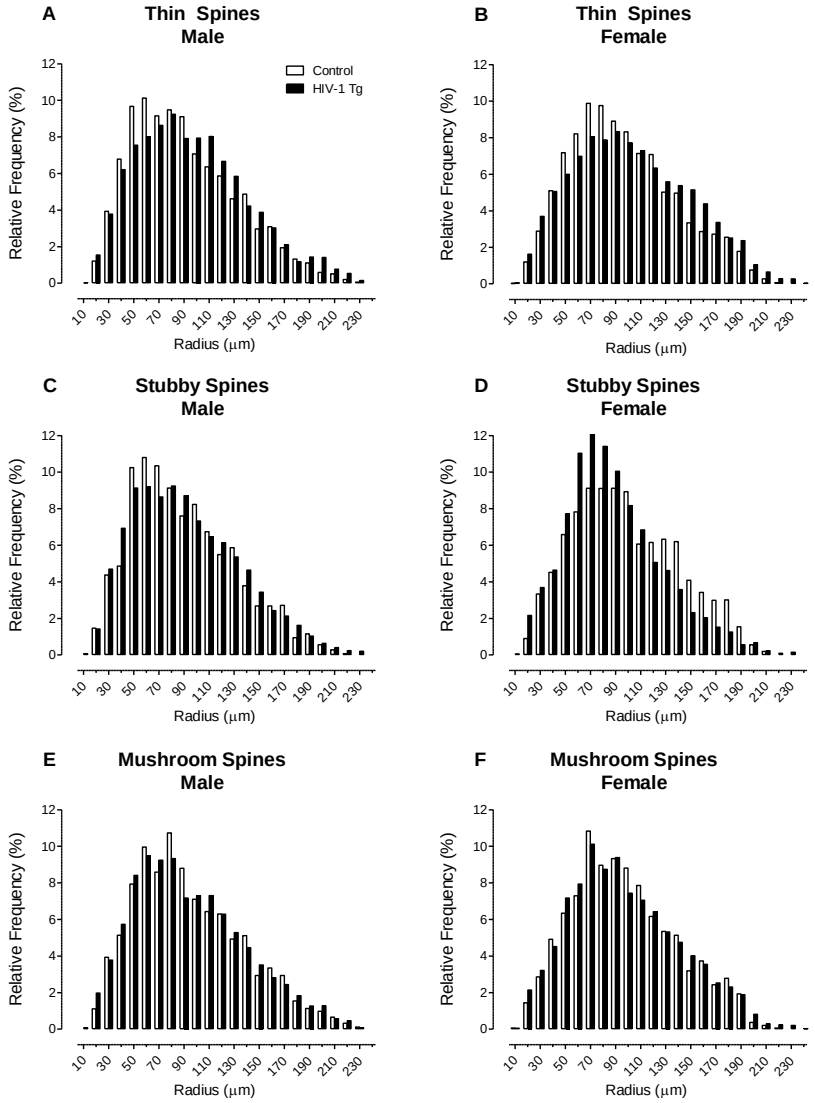

Figure B.2 Synaptic Connectivity: Biological Sex: The distribution of dendritic spines on successive radii is illustrated as a function of spine type (i.e., Thin Spines (**A**,**B**), Stubby Spines (**C**,**D**), and Mushroom Spines (**E**,**F**)) and biological sex (i.e., Male (**A**,**C**,**E**), Female (**B**,**D**,**F**)) (*N*=16-19 litters). HIV-1 Tg animals exhibited an increased relative frequency of thin dendritic spines on more distal branches relative to controls; the magnitude of which was influenced by the factor of biological sex. In sharp contrast, an assessment of stubby dendritic spines revealed a population shift with an increased relative frequency on more proximal branches in HIV-1 Tg animals relative to controls; an effect influenced by the factor of biological sex. No significant differences in the distribution of mushroom dendritic spines were observed.

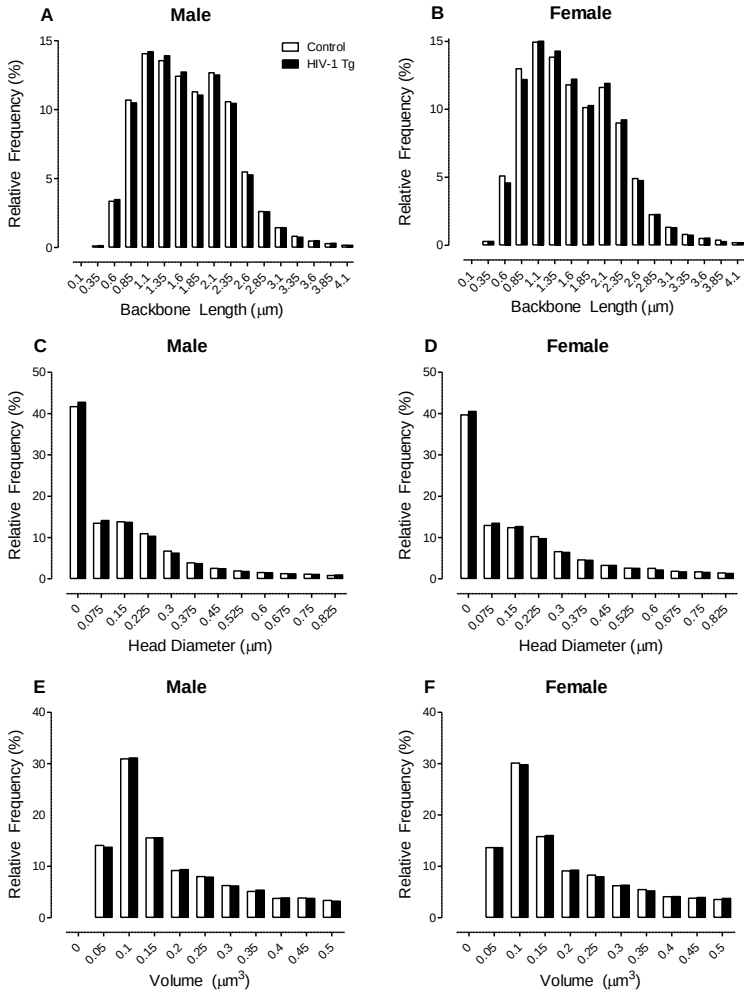

Figure B.3 Dendritic Spine Morphology. Presence of the HIV-1 transgene and the factor of biological sex influenced dendritic spine morphology. Male HIV-1 Tg animals exhibited a distributional shift towards shorter dendritic spines (**A**) relative to male control animals; no significant alterations in dendritic spine head diameter (**C**) or volume (**E**) were observed in male HIV-1 Tg animals. Female HIV-1 Tg animals displayed a distributional shift towards longer dendritic spines (**B**) with increased head diameter (**D**) relative to female control animals; no significant alterations in dendritic spine volume (**F**) were observed in female HIV-1 Tg animals. A generalized linear mixed effects model with a Poisson distribution confirmed these observations, revealing a significant genotype x sex x bin interaction for both backbone length [$F(1,1659)=37.2$, $p\leq0.001$] and head diameter [$F(1,1154)=68.2$, $p\leq0.001$]; an effect not observed for dendritic spine volume ($p>0.05$). Data are illustrated as relative frequencies.

APPENDIX C

PERMISSION TO REPRINT

Journalpermissions <journalpermissions@springernature.com>
Tue 2/18/2020 6:47 AM
MCLAURIN, KRISTEN

Dear Kristen,

Thank you for your recent Springer Nature permissions request. These works are licensed under the Creative Commons Attribution 4.0 International License, which permits unrestricted use, distribution, modification, and reproduction in any medium, provided you:

1) give appropriate acknowledgment to the original author(s) including the publication source,
2) provide a link to the Creative Commons license/include a notice of the CC license in legend and reference, and indicate if changes were made.

You are not required to obtain permission to reuse these articles, but you must follow the above two requirements.

Images or other third party material included in the article are encompassed under the Creative Commons license, unless indicated otherwise in the credit line. If the material is not included under the Creative Commons license, users will need to obtain permission from the license holder to reproduce the material.

To view a copy of the Creative Commons license, please visit http://creativecommons.org/licenses/by/4.0/

Please let me know if you have any questions.

Best wishes,
Oda

Oda Sigveland
Rights Executive

SpringerNature
The Campus, 4 Crinan Street, London N1 9XW,
United Kingdom
T +44 (0) 207 014 6851

http://www.nature.com
http://www.springer.com
http://www.palgrave.com

Header

Thank you for your order!

Dear Kristen McLaurin,

Thank you for placing your order through Copyright Clearance Center's RightsLink® service.

Order Summary

Licensee:	University of South Carolina
Order Date:	Feb 17, 2020
Order Number:	4771600424267
Publication:	Journal of NeuroVirology
Title:	Evolution of the HIV-1 transgenic rat: utility in assessing the progression of HIV-1-associated neurocognitive disorders
Type of Use:	Thesis/Dissertation
Order Total:	0.00 USD

View or print complete details of your order and the publisher's terms and conditions.

Sincerely,

Copyright Clearance Center

Tel: +1-855-239-3415 / +1-978-646-2777
customercare@copyright.com
https://myaccount.copyright.com